



UNIVERSITY OF
LEICESTER

**AN ENVIRONMENTAL STUDY OF THE FACTORS
CONTRIBUTING TO THE CONTROL OF *ARTHROSPIRA*
SPP. IN EAST AFRICAN SODA LAKES (LAKE
BOGORIA, KENYA)**

Thesis submitted for the degree of

Doctor of Philosophy

at the University of Leicester

By

Aisha Salah Emhemed Amer, B.Sc. and M.Sc.

Department of Infection, Immunity and Inflammation

University of Leicester

Leicester

UK

March, 2019

FACTORS CONTRIBUTING TO THE CONTROL OF *ARTHROSPIRA* SPP. IN EAST AFRICAN SODA LAKES (LAKE BOGORIA, KENYA)

Aisha Salah Emhemed Amer

Abstract

East Africa's Central Rift Valley has the largest population of lesser flamingos (*Phoeniconaias minor*) in the world. The lesser flamingos diet consists almost entirely of *Arthrospira* spp. Occasionally, unexpected crashes in the *Arthrospira* density occur. The main aim of this study was to investigate whether cyanobacteriophages contribute to this, and if they can regulate *Arthrospira* spp. biomass in Lake Bogoria.

Limnological studies of the lake showed that pH levels were stable, only changing 0.11 units over the study period. All other parameters were lower than previously reported. Conductivity was 41.7 mS cm⁻¹ at the beginning of the study and 63.7 at the end. The total nitrogen concentration explains 14 % of the variance in Chl-a.

The analysis of three *Arthrospira* morphotypes (S, C and H) revealed that the S-morphotype was dominant (47.67%) followed by the C-morphotype (40.65%) and H-morphotype (11.69%). Genetic analysis of these morphotypes found that they are the same *Arthrospira* species; most likely *Arthrospira maxima*.

A severe collapse in the *Arthrospira*'s population was observed in July 2016 and this was accompanied by the presence of virus-like particles (VLPs) within *Arthrospira* samples that were examined following sectioning. There was a strong negative correlation between VLPs concentration and Chl-a content ($r_s = -0.629$). Cell lysis in the form of trichome fragmentation was only observed once, and occurred in the S-morphotype. The largest increase in VLPs concentration occurred within five days of incubation at an OD₅₆₀ of ~0.3. Three incomplete prophages were detected; one was integrated into the H-morphotype and two into the S-morphotype genome. Metagenomic analysis revealed no known cyanophages in lake's waters. The VLPs count using NanoSight was positively associated with their count using epifluorescence microscopy ($r_s = 0.728$). Cyanophages could thus play a vital role in controlling the *Arthrospira* biomass in such extreme environments.

Acknowledgements

I thank Allah, the Almighty for giving me the strength, grace, good health and provision to carry on this project until the end.

Despite the difficulties I have experienced over the past four years, the support I have received has been very influential and has contributed greatly to overcoming them. I have many people to thank, some of whom I may forget to mention but to whom I am very grateful, and I would like to say that I could never have completed this work without you:

In Leicester:

First and foremost, I would like to seize this opportunity to express my deepest regards and gratitude to my supervisors Prof. Martha Clokie and Prof. David Harper for their guidance, supervision, constructive feedback and support given to me over the course of my PhD. I sincerely thank my annual review panel members, Dr. Primrose Freestone and Dr. Sinead Drea for their excellent advice and guidance throughout my research. I thank Dr. Emma Tebbs for providing me with remote sensing data. I also thank Natalie Allcock, Anna Straatman-Iwanowska and Dr. Ir K.R. Straatman for their technical support with TEM and epifluorescence microscope. I would also like to express my sincere thanks to Dr. Nathan Brown for his help with Bioinformatics. A special thanks to Dr. Andrew Millard for his essential scientific advice. Furthermore, my appreciation also goes to Sophie Clough for providing me with her metagenomics data. I would also like to take the opportunity to thank my colleagues in Lab230 for their support and encouragement at all times. Finally, I acknowledge my friends Amal Alyamani and Samand Yaqub.

In Kenya:

A huge thanks to Ezekiel Chebii for collecting the samples for the entire study period and I hope that he achieves his dream of obtaining the degree that he seeks.

In Libya:

There are not enough words to express my gratitude to my wonderful mum, thank you for being my motivation, showing me unwavering support and immeasurable love and for helping me to find the self-belief to complete this thesis, and for your patience in my absence throughout my study. Thank you to all my brothers, sisters and relatives. A special thanks to Dr. Abdulmagid Elazhari who supported me a lot over this long journey. Finally, I want to thank my country (Libya), as represented by the Ministry of Higher Education for giving me this opportunity in the form of financial support to complete this study.

Dedication

“To the spirit of my dear father, Salah. Your presence was a great incentive and your absence added more responsibility to achieve this dream”

Publications

Amer, A. S., Clokie, M. J., Junaideen, M. I., Tebbs, E. J., Chebii, E., Pacini, N., Harper, D. M., 2018. Towards understanding Lesser Flamingo unpredictability in East Africa; what might cause crashes in their major food item at a lake? *Flamingo*, Journal of the IUCN SSC WI Flamingo Specialist Group.

Table of Contents

Abstract.....	i
Acknowledgements.....	ii
Dedication.....	iv
Publications (accepted).....	v
List of Figures.....	xii
List of Tables.....	xx
Abbreviations.....	xxiv
Chapter 1 Introduction.....	1
1.1 East African Rift Valley soda lakes (EASLs).....	2
1.1.1 Overview.....	2
1.1.2 Kenyan Rift Valley soda lakes.....	3
1.1.3 Lake Bogoria.....	5
1.2 Cyanobacteria.....	6
1.2.1 Definition.....	6
1.2.2 Biodiversity of cyanobacteria in Kenyan alkaline-saline lakes, with particular reference to Lake Bogoria.....	7
1.2.3 <i>Arthrospira</i> features and its diversity in Kenyan soda lakes.....	7
1.2.3.1 Distribution.....	8
1.2.3.2 Morphology.....	9
1.2.3.3 Life cycle.....	9
1.2.3.4 Taxonomy.....	10
1.2.3.5 <i>Arthrospira</i> as an alkaliphile.....	11
1.2.3.6 <i>Arthrospira</i> and light adaptation.....	12
1.2.3.7 Crashes of <i>Arthrospira</i> biomass in Kenyan soda lakes and theories behind it.....	13
1.2.3.8 Theories behind the decline of the lesser flamingo.....	16
1.3 Bacteriophages.....	20
1.3.1 Definition.....	20
1.3.2 Phage life cycle.....	22
1.3.3 Cyanophages.....	23

1.3.4	Cyanophages and cyanobacteria interaction.....	24
1.3.5	Cyanophages and <i>Arthrospira</i> in Kenyan soda lakes.....	25
1.3.6	Cyanobacterial defence mechanisms against exogenous DNA uptake.....	25
1.4	Thesis aim and Justification.....	28
1.5	Objectives.....	28
1.6	Research questions.....	29
1.7	Study hypotheses.....	29
1.8	Thesis layout.....	30
Chapter 2	General materials and methods.....	31
2.1	Study area and site description.....	31
2.2	Sampling design.....	32
2.3	General materials and methods.....	34
2.3.1	Medium preparation.....	35
2.3.2	Culture conditions.....	35
Chapter 3	Limnological features of Lake Bogoria (between May 2015 to March 2017).....	36
3.1	Introduction.....	36
3.1.1	Aim and chapter questions.....	37
3.2	Materials and methods.....	38
3.2.1	pH.....	38
3.2.2	Electrical Conductivity (EC).....	38
3.2.3	Salinity.....	38
3.2.4	Chl- a Content.....	39
3.2.4.1	The Acetone extraction method (on water samples).....	39
3.2.4.2	Remote Sensing method.....	40
3.2.5	Total nitrogen and total phosphorus measurements.....	40
3.2.6	Statistical analyses.....	42
3.2.7	Overview.....	43
3.3	Results.....	44
3.3.1	Variability in Properties of Lake Bogoria.....	44
3.3.1.1	Variability in conductivity and salinity of Lake Bogoria.....	44
3.3.1.2	Variability in pH of Lake Bogoria.....	46

3.3.1.3	Variability in major nutrients concentration (total N and total P) of Lake Bogoria	47
3.3.1.4	Variability in Chl-a content of Lake Bogoria.....	49
3.3.2	Time series forecasting of Chl-a content of Lake Bogoria	51
3.3.3	The relationship between physico-chemical and biological properties of Lake Bogoria.....	53
3.4	Discussion.....	56
3.5	Conclusion and future work.....	60
Chapter 4	<i>Arthrospira</i> morphology and physiology	61
4.1	Introduction	61
4.1.1	Aim and objectives	63
4.2	Materials and methods.....	63
4.2.1	Axenic Culture production	63
4.2.1.1	<i>Arthrospira</i> isolation	64
4.2.1.2	<i>Arthrospira</i> purification	65
4.2.2	Long-term preservation of cultures	69
4.2.2.1	Cryopreservation.....	69
4.2.2.2	Preservation at low temperature	70
4.2.3	<i>Arthrospira</i> abundance in Lake Bogoria	70
4.2.4	Comparison of trichome characteristics between three morphotypes.....	71
4.2.5	Morphological changes of trichomes	72
4.2.6	Motility assay.....	73
4.2.7	Electron microscopic analysis	73
4.2.7.1	Transmission Electron Microscopy (TEM).....	73
4.2.7.2	Scanning Electron Microscopy (SEM).....	75
4.2.8	Statistical analyses	76
4.2.9	Overview	77
4.3	Results.....	78
4.3.1	Production of clonal, axenic cultures of <i>Arthrospira</i> spp. of Lake Bogoria.....	78
4.3.2	Long-term preservation of <i>Arthrospira</i> cultures	80
4.3.3	<i>Arthrospira</i> population	81
4.3.3.1	Changes in <i>Arthrospira</i> population	81

4.3.3.2	The relationship between <i>Arthrospira</i> abundance and phytoplankton biomass.....	88
4.3.3.3	The relations between the abundance of three <i>Arthrospira</i> morphotypes and the properties of the lake	88
4.3.3.4	Comparison of trichome characters between three morphotypes.....	90
4.3.4	The change in trichome helicity of <i>Arthrospira</i> spp.....	93
4.3.5	Motility of <i>Arthrospira</i> spp.....	95
4.3.6	Ultrastructure of <i>Arthrospira</i> spp.....	97
4.3.7	Absence of gas vacuoles and sinking velocity of <i>Arthrospira</i> spp.....	103
4.4	Discussion.....	105
4.5	Conclusion and future work.....	115
Chapter 5 Comparative genomic analysis of <i>Arthrospira</i> of Lake Bogoria.....		116
5.1	Introduction	116
5.2	Material and methods.....	119
5.2.1	DNA extraction of <i>Arthrospira</i> of Lake Bogoria	119
5.2.2	PCR amplification and sequencing.....	121
5.2.2.1	PCR amplification.....	121
5.2.2.2	Phylogenetic analysis.....	122
5.2.3	Whole DNA sequencing and analysis.....	123
5.2.3.1	Whole genome sequencing.....	123
5.2.3.2	Genome assembly and annotation.....	124
5.2.3.3	Comparative genome analysis	124
5.2.3.4	Gliding motility genes	127
5.2.4	Overview	127
5.3	Results.....	127
5.3.1	PCR amplification.....	127
5.3.2	Marker genes sequences and Phylogenetic analyses.....	128
5.3.3	Whole genome sequencing, assembly and annotation	133
5.3.4	Phylogenetic and comparative genomics analyses of <i>Arthrospira</i> from Lake Bogoria	135

5.3.4.1	General genomic features of two <i>Arthrospira</i> morphotypes (H and S).....	135
5.3.4.2	Phylogenetic analysis of whole genome of <i>Arthrospira</i>	141
5.3.4.3	Comparative genome analysis	144
5.3.5	Gliding motility genes	155
5.4	Discussion.....	156
5.5	Conclusion and future work.....	159
Chapter 6	<i>Arthrospira</i> phage investigation	161
6.1	Introduction	161
6.1.1	Aim and objectives	162
6.2	Material and methods.....	162
6.2.1	Cyanophage Isolation (well assay)	162
6.2.2	Screening the <i>Arthrospira</i> samples for cyanophage infection (TEM analysis)	163
6.2.3	NanoSight Technology assay.....	163
6.2.4	Phycocyanin fluorescence intensity assay	164
6.2.5	Epifluorescence microscopy examination.....	165
6.2.6	Protein profile of Lake Bogoria	168
6.2.7	Metagenomics work.....	170
6.2.8	Prophage detection	172
6.2.9	Genome protection (CRISPR identification)	172
6.2.10	Statistical analyses.....	173
6.2.11	Overview	175
6.3	Results.....	175
6.3.1	Cyanophage isolation (well assay)	175
6.3.2	Screening the <i>Arthrospira</i> samples for cyanophage infection (TEM analysis)	178
6.3.3	VLP concentrations using NanoSight	180
6.3.3.1	Variability in VLPs concentration of Lake Bogoria.....	180
6.3.3.2	The relationship between the VLPs concentration and the limnological properties of Lake Bogoria.....	181
6.3.3.3	The variability in VLP concentrations between control and incubated culture with water sample of Lake Bogoria	182
6.3.4	The variability in phycocyanin fluorescence	184

6.3.5	The variability in VLPs concentration using Epifluorescence microscopy	188
6.3.6	Protein profile of Lake Bogoria	191
6.3.7	Metagenomics analysis	192
6.3.8	Prophage identification	197
6.3.9	CRISPR identification	202
6.3.10	Microzooplankton and <i>Arthrospira</i>	208
6.4	Discussion.....	209
6.5	Conclusion and future work.....	215
Chapter 7	Overall discussion and recommendations	216
7.1	Key findings of the limnological features of Lake Bogoria and their relationship with the <i>Arthrospira</i> population	216
7.2	Phenotypic and genetic analyses of morphotypes.	218
7.3	The role of cyanophage infection in the breakdown of <i>Arthrospira</i> spp. in Lake Bogoria.....	220
7.4	A summary of the evidence for cyanophage-caused collapse of blooms.....	223
7.5	A summary of this project's contribution to overall understanding of EASLs.....	225
7.6	Recommendations for Future Work	225
Chapter 8	Appendices.....	227
8.1	Appendix 1: Medium, Buffers and Solutions	227
8.1.1	Zarrouk's medium.....	227
8.1.2	Solutions.....	228
8.1.3	Buffers	237
8.2	Appendix 2: Supplementary Data	240
Bibliography	264

List of Figures

Figure 1.1: Chemical concentrations of different lakes.....	1
Figure: 1.2 Gregory Rift Valley, taken from (McCall, 2010).....	3
Figure 1.3: <i>Arthrospira</i> life cycle.....	10
Figure 1.4: Filter-feeding system of lesser flamingos.....	17
Figure 1.5: Schematic illustration of the main phage families.	21
Figure 1.6: A model structure of T4 phage, modified from (Tokarz-Deptuła <i>et al.</i> , 2011).....	21
Figure 1.7: Life cycles of a bacteriophage.....	22
Figure 1.8: Barriers against the transmission of exogenous DNA into cyanobacteria, taken from (Stucken <i>et al.</i> , 2013).....	27
Figure 2.1: Map of Lake Bogoria and its location within the East African Rift Valley; from (Tebbs <i>et al.</i> , 2013).	31
Figure 2.2: Views across the lake.	32
Figure 2.3: Images of sample collection.....	33
Figure 2.4: Sample taken subsurface to avoid floating Cyanobacterial scum.	33
Figure 3.1: Digestion Unit structure.....	41
Figure 3.2: Schematic diagram of the limnological features analysis of Lake Bogoria.....	43
Figure 3.3: The variation in Bogoria's conductivity (EC) and salinity during the period of May 2015-Mar 2017.	45
Figure 3.4: The variation in Bogoria's pH over the period of study (May 2015-Mar 2017).....	47
Figure 3.5: The variation in Bogoria's total N and total P concentrations over the period of study (May 2015-Mar 2017).	48
Figure 3.6: The variation in biomass of Chl-a ($\mu\text{g L}^{-1}$) of Lake Bogoria over the period of study, acetone extraction method.	50
Figure 3.7: Chl-a concentration in Lake Bogoria for the period (1999-2017)....	50
Figure 3.8: The variation in biomass of chl-a ($\mu\text{g L}^{-1}$) in Lake Bogoria over the period (May2015-Feb2017), remote sensing method.	51
Figure 3.9: Forecasting and real values of Chl-a content of Lake Bogoria (2000-2018).....	52

Figure 3.10: Autocorrelation function (ACF) and Partial Autocorrelation function (PACF) for first order differencing of monthly Chl-a content data of Lake Bogoria.....	52
Figure 3.11: Scatter plots showing the relationships between Lake Bogoria properties over the period from May 2015 to Mar 2017.	54
Figure 3.12: Regression line describing the relationship between total N and Chl-a concentration (phytoplankton biomass) for Lake Bogoria.	55
Figure 4.1: The use of a phototactic movement on the scratched agar plate to purify <i>Arthrospira</i> spp.	66
Figure 4.2: Trichome morphological characteristics of <i>Arthrospira</i>	71
Figure 4.3: Digital image showing the motility assay procedure.....	73
Figure 4.4: Schematic diagram of the sample treatment.	77
Figure 4.5: Light and SEM images of clonal trichomes of three <i>Arthrospira</i> morphotypes (S, C and H) from Lake Bogoria.	78
Figure 4.6: Cell lysis of three <i>Arthrospira</i> morphotypes after cycloheximide treatment.	79
Figure 4.7: Contamination of <i>Arthrospira</i> 's culture with heterotrophic bacteria after streaking the culture on enriched Zarrouk's medium plate, incubated for 72 hours.	80
Figure 4.8: Cultures of <i>Arthrospira</i> after freezing and thawing.	80
Figure 4.9: <i>Arthrospira</i> spp. cultures after being incubated at 4 °C in the dark for approximately two weeks.	81
Figure 4.10: Mean values comparison of three <i>Arthrospira</i> morphotypes abundance (C, S and H) (trichome mL ⁻¹) of Lake Bogoria from Aug2015 to Mar 2017.	82
Figure 4.11: The relationship between phytoplankton biomass (Chl-a content) and <i>Arthrospira</i> abundance at Lake Bogoria.	88
Figure 4.12: The significant relationships between the three <i>Arthrospira</i> morphotypes populations and Lake Bogoria characteristics during the period between August 2015 and Mar 2017, n = 36.	89
Figure 4.13: Comparison of mean and median (coils per trichome) values of morphological parameters of three morphotypes of <i>Arthrospira</i> spp. in Lake Bogoria.....	91
Figure 4.14: Morphological changes of <i>Arthrospira</i> of Lake Bogoria.....	93

Figure 4.15: Light micrographs of morphological changes of three <i>Arthrospira</i> spp. morphotypes isolated from Lake Bogoria.	94
Figure 4.16: Micro images of <i>Arthrospira</i> S-morphotype plated on low strength agar (0.6%) of Zarrouk's medium showing the gliding motility of its filaments. .	95
Figure 4.17: Micro images of <i>Arthrospira</i> C-morphotype plated on low strength agar (0.6%) of Zarrouk's medium showing no gliding motility of its filaments. .	96
Figure 4.18: Micro images of <i>Arthrospira</i> H-morphotype plated on low strength agar (0.6%) of Zarrouk's medium showing no gliding motility of its filaments. .	96
Figure 4.19: Scanning electron image of <i>Arthrospira</i> spp. from Lake Bogoria with a part of trichome in continual spiral coil.	97
Figure 4.20: Electron micrograph of a longitudinal section of <i>Arthrospira</i> spp. from Lake Bogoria.	98
Figure 4.21: Electron micrograph of an <i>Arthrospira</i> 's section, showing four layers of the cell wall (LI, LII, LIII and LIV).	98
Figure 4.22: Electron micrographs of <i>Arthrospira</i> cellular architecture in cross-sections.	99
Figure 4.23: Ultrastructure of <i>Arthrospira</i> from Lake Bogoria showing gas vacuoles.	100
Figure 4.24: Electron micrographs of <i>Arthrospira</i> sections showing the photosynthetic lamellae (thylakoids).	100
Figure 4.25: Electron micrographs of <i>Arthrospira</i> sections showing the circular arrangement of thylakoids in the S-morphotype.	101
Figure 4.26: Electron micrographs of the cross and longitudinal sections of <i>Arthrospira</i> from Lake Bogoria showing the thylakoid membranes arrangement in C and H morphotypes (A and B respectively).	101
Figure 4.27: Electron micrograph of an <i>Arthrospira</i> section showing polyhedral bodies (carboxysomes) with a polygonal profile and cylindrical bodies.	102
Figure 4.28: Ultrastructure of <i>Arthrospira</i> from Lake Bogoria showing a mesosome.	103
Figure 4.29: Ultrastructure of <i>Arthrospira</i> showing a new, unknown structure.	103
Figure 4.30: Macrographs of cyanobacterium <i>Arthrospira</i> cultures (H-morphotype) illustrating the different behaviour after sub culturing them in Zarrouk's medium.	104

Figure 4.31: Macrographs of cyanobacterium <i>Arthrospira</i> cultures (S-morphotype) illustrating the presence of inclusions that look like gas vacuoles.	105
Figure 5.1: Schematic diagram of <i>Arthrospira</i> genome analysis pathway.....	127
Figure 5.2: Gel Electrophoresis on 1% agarose gel of the PCR products of three <i>Arthrospira</i> marker genes for three <i>Arthrospira</i> morphotypes (S, C and H) from Lake Bogoria.....	128
Figure 5.3: Molecular Phylogenetic analysis of <i>Arthrospira</i> strains made based on the alignment of ITS region sequences of 53 <i>Arthrospira</i> strains, as inferred with the Geneious software.....	131
Figure 5.4: Molecular Phylogenetic analysis of <i>Arthrospira</i> strains made on the basis of the alignment of the phycocyanin locus (PC-IGS) sequences of 41 <i>Arthrospira</i> strains, as inferred with the Geneious software.....	132
Figure 5.5: Phylogenetic tree of <i>Arthrospira</i> strains based on the alignment of 16S rRNA gene sequences of 28 <i>Arthrospira</i> strains as inferred by the Geneious software.....	133
Figure 5.6: Circle plot showing the whole-genome schematic comparison of two <i>Arthrospira</i> morphotype S and H genomes.....	139
Figure 5.7: Subsystem statistics diagram of S-morphotype.....	140
Figure 5.8: Subsystem statistics diagram of H-morphotype.....	140
Figure 5.9: <i>Arthrospira</i> tree of eight strains, six of which are available in the NCBI database and the two Bogoria isolates (H and S) concatenated 27 conserved genes.....	141
Figure 5.10: A rooted phylogenetic tree based on the aligned sequences of the core genes of nine <i>Arthrospira</i> strains that were produced by the Roary tool.	142
Figure 5.11: RAxML Rooted phylogenetic tree based on the aligned sequences of the core genes of the nine <i>Arthrospira</i> strains produced by the LS-BSR tool.	143
Figure 5.12: Neighbour-joining phylogeny based on the alignment of the orthologous and xenologous sequences regions of nine <i>Arthrospira</i> strains, as generated by the Mauve tool.....	144
Figure 5.13: Frequency chart showing the frequency of genes for the <i>Arthrospira</i> genomes analysed.....	145

Figure 5.14: A heat map generated by Roary plots showing the tree compared to a matrix in the presence and absence of core and accessory genes.	145
Figure 5.15: Pie chart showing the distribution of different categories of genes and the number of isolates they are present.	146
Figure 5.16: Pan-genome plots, showing how the pan genome changes with the addition of a new genome (arranged in random order).	147
Figure 5.17: Progressive Mauve alignment shows an alignment of the two Bogoria <i>Arthrospira</i> morphotypes (H and S).	148
Figure 5.18: A Mauve alignment of five <i>Arthrospira</i> strains including Bogoria morphotypes.	148
Figure 5.19: Blast dot plots of tow <i>Arthrospira</i> morphotypes (H and S) with more identical complete genomes in the NCBI database using RAST tool.	150
Figure 5.20: Genome alignment of the representative <i>Arthrospira</i> (S-morphotype) of Lake Bogoria with the reference genomes using Mauve tool.	152
Figure 5.21: Blast dot plot of <i>Arthrospira</i> from Lake Bogoria (<i>Arthrospira</i> Bogoria S) against <i>Arthrospira</i> platensis C1 after reordering the contigs.	153
Figure 5.22: Genome comparison of <i>Arthrospira</i> Bogoria S and the reference genome of <i>Arthrospira</i> platensis C1.	154
Figure 5.23: Graphical circular map of <i>Arthrospira maxima</i> var. <i>Bogoriensis</i> genome.	155
Figure 6.1: The filtration unit structure.	167
Figure 6.2: Schematic pathway for the <i>Arthrospira</i> phage investigation.	175
Figure 6.3: Lysis of S-morphotype filaments that were incubated with water samples from Lake Bogoria.	176
Figure 6.4: Lysis of S-morphotype filaments that were incubated with water samples from Lake Bogoria.	177
Figure 6.5: Electron micrographs of 0.2 µm filtered <i>Arthrospira</i> cultures showing the phage morphology.	178
Figure 6.6: TEM images of the <i>Arthrospira</i> sections for the entire period of study.	179
Figure 6.7: Electron micrographs of <i>Arthrospira</i> sections from Lake Bogoria (Jul 2016).	179
Figure 6.8: The variation in VLPs concentrations during the period May 2015-Mar 2017.	180

Figure 6.9: Scatterplots of the relationships between Lake Bogoria properties and VLPs concentration (E8 VLP mL ⁻¹) over the period of the study.	182
Figure 6.10: Box-plots of differences in VLPs concentrations of the incubated S-morphotype of the <i>Arthrospira</i> culture with and without water sample of Jul 2016 for 19 days.	183
Figure 6.11: Comparisons of phycocyanin fluorescence intensity of cyanobacterium <i>Arthrospira</i> between the C-morphotype (incubated with water samples from Lake Bogoria (May 2015-Mar 2017) and the control culture (without water sample).	185
Figure 6.12: Comparisons of phycocyanin fluorescence intensity between the S-morphotype of cyanobacterium <i>Arthrospira</i> that was incubated with water samples from Lake Bogoria (May 2015-Mar 2017) and the control culture (<i>Arthrospira</i> without water sample).....	187
Figure 6.13: Epifluorescence microscopy images of S-morphotype of <i>Arthrospira</i> cultures.	189
Figure 6.14: Comparison of median values of VLPs count between different S-morphotype <i>Arthrospira</i> cultures incubated with the Lake Bogoria water sample (Jul 2016).	190
Figure 6.15: The correlation between the mean values of the E8 VLP mL ⁻¹ by using two different techniques, NanoSight and Epifluorescence microscopy.	191
Figure 6.16: Protein profile of Lake Bogoria.	192
Figure 6.17: Taxonomic spectrum of metagenome reads for Sep 2014 water sample visualised with Krona.	193
Figure 6.18: Krona Classification plot of metagenome data of May 2015 water sample.	194
Figure 6.19: Krona Classification plot of metagenome data of Jul 2015 water sample.	195
Figure 6.20: Taxonomic spectrum of metagenome reads for Sep 2015 water sample visualized with Krona.	196
Figure 6.21: Heatmap comparison of the species abundance between four metagenomics samples.	197
Figure 6.22: Linear genome view of the incomplete prophage integrated within H-morphotype genome of <i>Arthrospira</i> from Lake Bogoria.	199

Figure 6.23: Linear genome view of the first incomplete prophage integrated within the S-morphotype genome of <i>Arthrospira</i> from Lake Bogoria.	200
Figure 6.24: Linear genome view of the second incomplete prophage found in the S-morphotype genome of the <i>Arthrospira</i> from Lake Bogoria.	201
Figure 6.25: Electron micrographs of Lake Bogoria sample (Dec 2016).	208
Figure 6.26: Micrograph of <i>Arthrospira</i> sections from Lake Bogoria (Dec 2016).	208
Figure 7.1: Schematic diagram of my research contribution to the overall lesser flamingo lakes ecosystem in East Africa.	225
Figure 8.1: Multiple sequence alignment of 16S rRNA consensus sequences of three <i>Arthrospira</i> morphotypes (S, C and H) from Lake Bogoria, using Geneious software.	244
Figure 8.2: Multiple sequence alignment of ITS consensus sequences of three <i>Arthrospira</i> morphotypes (S, C and H) from Lake Bogoria, using Geneious software.	245
Figure 8.3: Multiple sequence alignment of PC-IGS locus consensus sequences of three <i>Arthrospira</i> morphotypes (S, C and H) from Lake Bogoria, using Geneious software.	246
Figure 8.4: Box plot of the number of new genes of nine <i>Arthrospira</i> genomes produced pan genome pipeline of Roary.	247
Figure 8.5: Box plot of the number of conserved genes of nine <i>Arthrospira</i> genomes produced pan genome pipeline of Roary.	247
Figure 8.6: Box plot of the number of nine genomes produced pan genome pipeline of Roary.	248
Figure 8.7: Pairwise amino acid sequences alignment of pilQ consensus sequences of two <i>Arthrospira</i> morphotypes (H and S) from Lake Bogoria using Muscle tool.	249
Figure 8.8: Pairwise amino acid alignment of pilT-1 consensus sequences of two <i>Arthrospira</i> morphotypes (H and S) from Lake Bogoria using Muscle tool.	250
Figure 8.9: Pairwise amino acid sequences alignment of pilT-2 consensus sequences of two <i>Arthrospira</i> morphotypes (H and S) from Lake Bogoria using Muscle tool.	250

Figure 8.10: Pairwise amino acid sequences alignment of pilT-3 consensus sequences of two <i>Arthrospira</i> morphotypes (H and S) from Lake Bogoria using Muscle tool.....	251
Figure 8.11: Details of incomplete prophage region, which is integrated within the H-morphotype of <i>Arthrospira</i> genome from Lake Bogoria.....	261
Figure 8.12: Details of the first incomplete prophage region that is integrated within the S-morphotype of <i>Arthrospira</i> genome from Lake Bogoria.....	262
Figure 8.13: Details of the second incomplete prophage region that is integrated within the S-morphotype of <i>Arthrospira</i> genome from Lake Bogoria.....	263

List of Tables

Table 1.1: Some examples of <i>Arthrospira</i> global distribution.	8
Table 1.2: <i>Arthrospira</i> collapses in Kenyan alkaline-saline lakes.	14
Table 1.3: Reported lesser flamingo die-offs in the Rift Valley Lakes, Nakuru and Bogoria from 1991 to 2009.	18
Table 2.1: Geographical and Morphometric characteristics of Lake Bogoria. .	32
Table 3.1: Descriptive analysis results of limnological parameters of Lake Bogoria for the entire study period (May 2015-Mar 2017).	44
Table 3.2: The significant results of Bonferroni post hoc tests for pairwise comparisons in conductivity of Lake Bogoria (May 2015-Mar 2017).	46
Table 3.3: The significant results of Bonferroni post hoc tests for pairwise comparisons in salinity of Lake Bogoria (May 2015-Mar 2017).	46
Table 3.4: The significant results of Bonferroni post hoc tests for pairwise comparisons in pH of Lake Bogoria (May 2015-Mar 2017).	47
Table 3.5: The significant results of Bonferroni post hoc tests for pairwise comparisons in total N of Lake Bogoria (May 2015-Mar 2017).	49
Table 3.6: The significant results of Bonferroni post hoc tests for pairwise comparisons in total P of Lake Bogoria (May 2015-Mar 2017).	49
Table 3.7: Estimates of the model parameters.	51
Table 3.8: ARIMA fit results of Chl- a time series (May 2015-Mar 2017).	53
Table 3.9: Forecasting time series data of Chl-a content ($\mu\text{g L}^{-1}$) of Lake Bogoria (Jun 2017-Dec 2018).	53
Table 3.10: Summary statistics of the linear regression model.	55
Table 3.11: Summary of the salinity and conductivity data of Lake Bogoria (Mach 1974- May 2017).	57
Table 4.1: Cryopreservation agents and their concentration.	70
Table 4.2: Composition of the ethanoic resin solution and incubation time.	74
Table 4.3: Dehydration agent concentrations and incubation time.	75
Table 4.4: Results of the Bonferroni post hoc tests of the main effect of time on <i>Arthrospira</i> 's population.	83
Table 4.5: Paired-samples t-test results of <i>Arthrospira</i> abundance for the entire period of study.	84

Table 4.6: Description of three <i>Arthrospira</i> morphotypes based on their morphological characteristics.	90
Table 5.1: Details of primers used in the present study.	122
Table 5.2: Nucleotide identity of the consensus sequences of the ITS region of three <i>Arthrospira</i> morphotypes from Lake Bogoria.....	128
Table 5.3: Nucleotide identity of the consensus sequences of PC-IGS locus of the three <i>Arthrospira</i> morphotypes from Lake Bogoria.....	129
Table 5.4: Nucleotide identity of the consensus sequences of 16S rRNA gene of the three <i>Arthrospira</i> morphotypes from Lake Bogoria.....	129
Table 5.5: Nucleotide identity of ITS region of the three <i>Arthrospira</i> morphotypes from Lake Bogoria to the close relative species present in GenBank.	129
Table 5.6: Nucleotide identity of PC-IGS locus of the three <i>Arthrospira</i> morphotypes from Lake Bogoria to the close relative species present in GenBank.	129
Table 5.7: Nucleotide identity of 16S rRNA of the three <i>Arthrospira</i> morphotypes from Lake Bogoria to the close relative species present in GenBank.	130
Table 5.8: Canu assembly results of two <i>Arthrospira</i> morphotypes from Lake Bogoria.....	134
Table 5.9: The average of contig properties for two <i>Arthrospira</i> morphotypes from Lake Bogoria.....	134
Table 5.10: Annotation details of two <i>Arthrospira</i> morphotypes from Lake Bogoria.....	135
Table 5.11: Genome feature comparison among <i>Arthrospira</i> species.	136
Table 5.12: Calculated amino acid sequences identity (%) of 27 conserved genes between nine <i>Arthrospira</i> strains.	137
Table 5.13: The contig number, start and end position of each contig before and after rearrangement the contigs.	154
Table 6.1: The quality and quantity of DNA for four water samples from Lake Bogoria.....	172
Table 6.2: Description of the phages based on their morphological parameters.	178
Table 6.3: Descriptive analysis results for VLPs concentrations for Lake Bogoria samples for the entire study period (May 2015-Mar 2017).	180

Table 6.4: The significant results of the Bonferroni post hoc tests for pairwise comparisons in the VLPs concentration from Lake Bogoria (May 2015- Mar 2017).....	181
Table 6.5: Independent-Sample Man-Whitney U Test for the differences in VLPs concentration between the control and incubated <i>Arthrospira</i> culture.....	183
Table 6.6: The median values and test statistic for the significant time points of phycocyanin fluorescence of the control and C-morphotype incubated cultures with water samples from the lake over the period of the study.....	186
Table 6.7: The median values and test statistic for the significant time points of phycocyanin fluorescence of the control and S-morphotype incubated cultures with water samples from the lake over the period of the study.....	188
Table 6.8: Illumina sequencing results for four metagenomics of Lake Bogoria water samples.....	192
Table 6.9: Total prophages detected within two <i>Arthrospira</i> genomes of Lake Bogoria using the PHASTER tool.....	199
Table 6.10: Details of identified CRISPRs in the H-morphotype of <i>Arthrospira</i> genome from Lake Bogoria.....	203
Table 6.11: Details of identified CRISPRs in S-morphotype of the <i>Arthrospira</i> genome from Lake Bogoria.....	204
Table 6.12: Comparison of number of CRISPR arrays between <i>Arthrospira</i> strains.....	205
Table 6.13: Features of matching regions between the CRISPRs of the two <i>Arthrospira</i> morphotypes (H and S) and metagenomic data of four samples – Sep 2014, May 2015, Jul 2015 and Sep 2015.....	206
Table 8.1: Normality test result of lake characteristics (EC, pH, total N, total P, salinity and chl-a content using acetone extraction method and remote sensing method.....	240
Table 8.2: Normality test of Chl-a content using remote sensing.....	242
Table 8.3: Model Summary of linear regression.....	242
Table 8.4: ANOVA Summary of linear regression.....	242
Table 8.5: Normality test of two-way ANOVA of <i>Arthrospira</i> spp. abundance during the period of study.....	243
Table 8.6: NanoSight NTA 2.0 software settings.....	252
Table 8.7: Epifluorescence microscopy settings.....	252

Table 8.8: Normality test of VLPs concentration using NanoSight technique for the entire period of study (May2015-March2017).....	253
Table 8.9: Normality test results of VLPs concentration in control culture and incubated culture with water sample of Jul-2016 for 19 days.	253
Table 8.10: Levene's Test for Equality of Variance results for VLPs concentration in the control and incubated cultures with water sample of Jul-2016 for 19 days.	254
Table 8.11: The homogeneity of variance test result of the VLPs concentration between different treatments.....	254
Table 8.12: Non-significant results of Mann-Whitney U test for phycocyanin fluorescence intensity assay(C-morphotype).	254
Table 8.13: Non-significant results of Mann-Whitney U test for phycocyanin fluorescence intensity assay (S- morphotype).....	256
Table 8.14: Bacteria composition and abundance in Sep 2014 water sample, which constitute 100% of the total.....	257
Table 8.15: Bacteria composition and abundance in May 2015 water sample, which constitute 93.28% of the total.....	258
Table 8.16: Viruses composition and abundance in May 2015 water sample, which constitute 6.72 % of the total.....	259
Table 8.17: Bacteria composition and abundance in Jul 2015 water sample, which constitute 100% of the total.....	259
Table 8.18: Bacteria composition and abundance in Sep 2015 water sample, which constitute 77.53 % of the total.....	260
Table 8.19: Viruses composition and abundance in Sep 2015 water sample, which constitute 22.47% of the total.....	260

Abbreviations

Symbol	Definition
A	<i>Arthrospira</i>
Abs	Absorption
ACF	Autocorrelation function
ANOVA	Analysis of variance
APS	Ammonium persulfate
ARIMA	Auto Regression Integrated Moving Average
ATC	Automatic temperature compensation
BHI	Brain heart infusion
BIC	Bayesian Information Criterion
a.u	Arbitrary unit
BLAST	Basic local alignment search tool
Blastn	nucleotide BLAST
Ca	Calcium
CFU	colony-forming unit
CO ₂	Carbon dioxide
CO ₃ ²⁻	Carbonate
CaCl ₂ .6H ₂ O	Calcium chloride hexahydrate
CRISPRs	Clustered Regularly Interspaced Short Palindromic Repeats
CDS	Coding sequence
Chl- <i>a</i>	Chlorophyll <i>a</i>
Cl	Chloride
cm	Centimetre
Coa	Coat protein
CTAB	Cetrimonium bromide
CuSO ₄ .5H ₂ O	Copper (II) sulfate
dH ₂ O	Distilled water
DMSO	Dimethyl sulfoxide
DNA	Deoxyribonucleic Acid
dsDNA	double stranded DNA
dsRNA	double stranded ribonucleic acid
dATP	deoxyadenosine triphosphate
dCTP	deoxycytosine triphosphate
dGTP	deoxyguanine triphosphate
dNTPs	deoxyribonucleotide triphosphate
DLS	dynamic laser scattering
DR	Direct repeat
EASL	East African saline alkaline lakes, East African soda lakes
dTTP	deoxythymidine triphosphate
EC	Electrical Conductivity
EDTA	Ethylenediaminetetraacetic acid
EDTA-Na ₂	Ethylene Diamine Tetraacetic Acid DiSodium
F	Forward
F ⁻	Fluoride
FAB	Fastidious Anaerobe Broth
FeCl ₃	Ferric chloride
FeSO ₄ .7H ₂ O	Ferrous sulfate
FGS	First-Generation Sequencing
g	Gram

Continued on next page

Continued from previous page.

Symbol	Definition
GC content	Guanine-cytosine content
H ₃ BO ₃	Boric acid
HCl	Hydrochloric acid
HCO ₃ ⁻	Bicarbonate
HGAP3	Hierarchical Genome Assembly Process
HMDS	Hexamethyldisilazane
H ₂ SO ₄	Sulfuric acid
H ₂ S	Hydrogen Sulfide
H ₂ O	Water
Hyp	Hypothetical protein
jp	junctional pores
Kb	Kilobases
K	Potassium
KCl	Potassium chloride
K ₂ HPO ₄	Dipotassium hydrogenphosphate
K ₂ PO ₄	Potassium phosphate
kV	Kilo Voltage
kPa	Kilo pascal
Indels	An insertion or deletion of bases in the genome
ITCZ	Inter-Tropical Convergence Zone
ITS	Internal transcribed spacer of ribosomal genes
IUCN	International Union for Conservation of Nature
L	Litre
LCB	locally collinear block
LCL	Lower confidence intervals for forecasts
LS-BSR	large-scale blast score ratio pipeline
Ma	Million Years
MAE	Mean Absolute Error
MAPE	Mean Absolute Percentage Error
MaxAE	Maximum Absolute Error
MaxAPE	Maximum Absolute Percentage Error
Mb	Megabases
Mdn	Median
MEGA	Molecular Evolutionary Genetics Analysis
Mg	Magnesium
MgCl ₂	Magnesium (II) chloride
MgSO ₄ ·7H ₂ O	Magnesium sulfate heptahydrate
mS	Milli Siemens
N	Nitrogen
n	Sample size
Na	Sodium
NaCl	Sodium chloride
NaHCO ₃	Sodium bicarbonate
NaNO ₃	Sodium nitrate
Na ₂ HPO ₄	Disodium hydrogen phosphate
NaOH	Sodium hydroxide
NCBI	National centre for biotechnology information
NiSO ₄ ·7H ₂ O	Nickel (II) sulfate heptahydrate
(NH ₄) ₆ Mo ₇ O ₂₄	Ammonium heptamolybdate
nm	Nanometre

Continued on next page

Continued from previous page.

Symbol	Definition
nr	Non-redundant
NTA	Nanoparticle Tracking Analysis
OD ₅₆₀	(OD ₅₆₀ nm) Optical density at 560 nm wave length
P	Phosphorus
<i>P</i>	<i>Phoenicianaias</i>
PacBio	Pacific Bioscience
PACF	Partial Autocorrelation
PFD	photon flux densities
PHASTER	phage search tool – enhanced release
PBS	Phosphate buffered saline
PCR	Polymerase chain length polymorphism
PC-IGS	Phycocyanin intergenic spacer
PLP	Phage-like-protein
Pla	Plate protein
PS I	Photosystem I
PSII	Photosystem II
<i>r</i>	Effect size
R	Reverse
RAST	Rapid Annotations Subsystems Technology
RNA	Ribonucleic acid
RMSE	Root Mean Square Error
rpm	Revolution per minute
rRNA	ribosomal RNA
<i>r_s</i>	Spearman's rank correlation coefficients
SD	Standard deviation
SDS-PAGE	Polyacrylamide Gel Electrophoresis
SDS	Sodium dodecyl sulfate
SEM	Scan electron microscopy
SGS	Second-Generation Sequencing
Sh	Slime sheath
Sha	Tail shaft
Si ⁴⁺	Silicon
SMRT	Single molecule real time sequencing
ssDNA	single stranded DNA
ssRNA	single stranded RNA
SO ₄ ²⁻	Sodium sulfate
TAE	Tris-acetate-EDTA
TE	Tris-EDTA
TEM	Transmission electron microscopy
TEMED	Tetramethylethylenediamine
TGS	Third-Generation Sequencing
TN	Total nitrogen
TP	Total phosphorus
tRNA	Transfer RNA
tmRNA	Transfer-messenger RNA
UCL	Upper confidence intervals for forecasts
μm	Micrometre
UPH ₂ O	Ultra-pure water
VLPs	Virus Like Particles
ZnSO ₄ ·7H ₂ O	Zinc sulfate heptahydrate
η ²	Partial eta squares
α	(Alpha) statistical Significant level

Nucleotide Base and amino acid Codes.

Symbol	Full name
Nucleotide Bases	
A	adenine
C	cytosine
G	guanine
T	thymine
Amino Acid Codes	
A	Alanine
R	Arginine
N	Asparagine
D	Aspartic acid
C	Cysteine
Q	Glutamine
E	Glutamic acid
G	Glycine
H	Histidine
I	Isoleucine
L	Leucine
K	Lysine
M	Methionine
F	Phenylalanine
P	Proline
O	Pyrrolysine
S	Serine
U	Selenocysteine
T	Threonine
W	Tryptophan
Y	Tyrosine
V	Valine
B	Aspartic acid or Asparagine
Z	Glutamic acid or Glutamine
X	Any amino acid
J	Leucine or Isoleucine

Chapter 1 Introduction

Saline lakes are found throughout the world, lying in arid and semiarid areas with 25-200 mm and 200-500 mm annual precipitation respectively, usually where tectonics have moulded their hydrology and morphometry (Schagerl and Oduor, 2008). Most of these lakes are closed basins (endorheic), in that they have few if any, surface outlets such as rivers, so the only way for them to lose their water is via evaporation (Street-Perrott and Roberts, 1983, Olaka *et al.*, 2010). They thus become highly saline and alkaline with the dominance of sodium (Na^+) and carbonate and bicarbonate (CO_3^{2-} , HCO_3^-) ions and a pH higher than 9.0. This type of lake is called a soda lake (Schagerl and Renaut, 2016) but more precisely, an alkaline-saline lake (Vareschi, 1978); in this thesis, the terms are used interchangeably. Such lake waters also have high levels of chloride (Cl^-), fluoride (F^-) ions and aqueous silica (H_4SiO_4), whereas the concentrations of magnesium (Mg^{2+}) and calcium (Ca^{2+}) cations are lower (Figure 1.1).

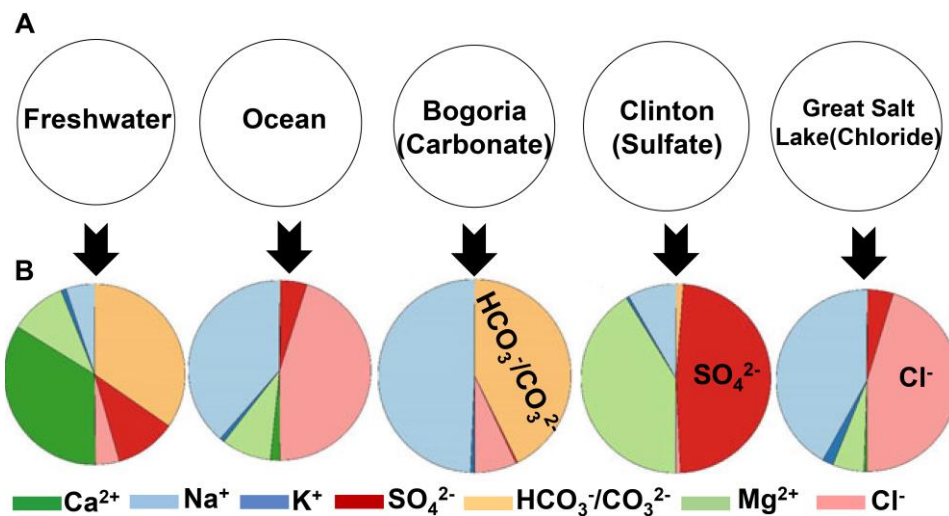


Figure 1.1: Chemical concentrations of different lakes.

(A) The five range from freshwater to high saline lake water, (B) Ions label basis meq L^{-1} , taken from (Schagerl and Renaut, 2016).

Soda lakes are situated on different continents, especially in areas with a volcanic background such as eastern parts of the East African Rift Valley and many of the lakes in the western region of North America (Schagerl and Renaut, 2016).

1.1 East African Rift Valley soda lakes (EASLs)

1.1.1 Overview

The East African Rift Valley (Afro-Arabian Rift Valley) is one of the longest rifts in the world, extending from Jordan, across the eastern part of Africa to Mozambique and Botswana over more than 3000 km, 40-70 km wide (Melack, 1981). This trough was likely formed during the Cenozoic era (roughly 40 million years ago), and consists of the two branches, the eastern and western (Trauth *et al.*, 2005). The complex geological and historical difference between two arms has influenced lake development and characteristics; thus, their basins are morphometrically varied. Previous volcanic and tectonic activity has played a vital role in the formation of their morphological and hydrological features (Schlüter, 1997, Oduor and Schagerl, 2007b). The oldest and deepest lakes on the earth are found within the western rift, which runs from Uganda to Botswana (Burgis and Morris (1987) cited in Schagerl and Renaut (2016)). The Eastern (Gregory) limb is the most active continental zone on the earth's surface and extends along the whole eastern side of the African continent, from Ethiopia through Kenya to Tanzania (Dawson, 2008). It has a variety of lakes of varying ages and characteristics ranging from freshwater lakes to soda lakes, only three of its 14 lakes are freshwater (*ibid*).

Soda lakes have been received much less attention than freshwater lakes in the literature because the latter have an economic value for people through agricultural, fishery and tourist activities (Harper *et al.*, 2011). Moreover, freshwater lakes are generally known for their high biodiversity, in contrast to alkaline-saline lakes that tend to be more productive but have considerably lower species biodiversity. This stems from the pH and salinities that prevent the growth of many species, but those species that do survive can grow without competition, resulting in a high abundance. The most obvious are the alkaliphilic cyanobacteria (Oduor and Schagerl, 2007b). Kenya contains several such endorheic eastern rift lakes (Jirsa *et al.*, 2013).

1.1.2 Kenyan Rift Valley soda lakes

The Eastern Rift Valley in Kenya is wider at northern Kenya at Lake Turkana, then crosses the equator and continues southwards to northern regions of Tanzania in Lake Natron. It contains a series of lakes including two freshwater lakes – Baringo and Naivasha and six saline–alkaline lakes, Turkana, Logipi, Bogoria, Nakuru, Elmenteita, and Magadi (Britton and Harper, 2006). Figure 1.2 shows the Gregory Rift Valley and its Kenyan lakes.

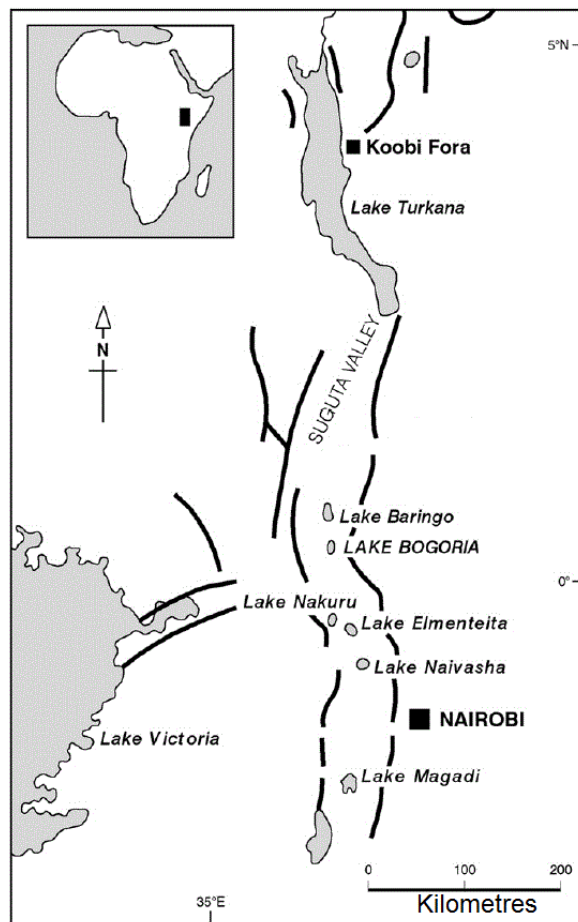


Figure: 1.2 Gregory Rift Valley, taken from (McCall, 2010).

The formation of the lakes basins has been estimated to have occurred around the Mio-Pleistocene era (Tiercelin and Lezzar, 2002). Their geological background reflects their topological and morphometric characteristics (Ring, 2014), as mentioned above (1.1.1) due to the climate and tectonic activities involved in their formation and hydrology (Clarke, 1990, Bergner *et al.*, 2009, Olago *et al.*, 2009).

These sensitive aquatic ecosystems, as all closed lakes, are quite varied in terms of their size and chemical, hence limnological properties (Harper *et al.*, 2003, Jirsa *et al.*, 2013). They have a high temperature and limited light penetration, besides having high salinity levels of more than 3 g L⁻¹ and high pH levels of up to 11 (Oduor and Schagerl, 2007b), with the mean annual rainfall of 535 mm (Philip-Heinemann (1991) cited in Matagi (2004)). The high salinity arises as a consequence of the chemical erosion of the surrounding volcanic rocks into the basins through a process called silicate hydrolysis (Deocampo and Renaut, 2016), followed by concentration by evaporation. They also have higher temperatures than expected because of the volcanic centres that supply heat to the system from hot springs and geysers below the lake beds (Dawson, 2008, Abbate *et al.*, 2015).

These environmental conditions are unsuitable for most phytoplankton species, so the species diversity that is found in these lakes as a consequence is generally very poor (Oduor and Schagerl, 2007b). Haloalkaliphiles that use high sodium concentrations to balance osmotic pressure are called natronophiles. Ideal examples of that are *Arthrospira* spp. (Voronichin, Koma'rek and Lund) that dominate Kenyan soda lakes with massive relative biomasses (average chlorophyll-a content (Chl-a): Lake Bogoria 388 µg L⁻¹, Lake Nakuru 646 µg L⁻¹ and Lake Elmenteita 267 µg L⁻¹ (Schlesinger *et al.*, 1996, Oduor and Schagerl, 2007a). All soda lakes have a high sensitivity to change in climatic conditions and water levels therefore these green turbid biomasses are highly dependent on seasonality and are occasionally substituted by eualgae such as diatoms, nanoplankton such as *Picocystis salinarum* (Schagerl and Oduor, 2008, Schagerl *et al.*, 2015), and unicellular cyanobacteria, *Synechococcus* sp. (Jones and Grant, 2000). In addition, other alkaliphilic aerobic organotrophic bacteria are present in high numbers; for instance, (Mwatha, 1991) showed that the total bacteria count (CFU) in three Kenyan soda lakes – lakes Elmenteita, Bogoria, and Nakuru was 10⁷-10⁸ mL⁻¹.

Filamentous cyanobacteria species of the genus *Arthrospira* are the preferred diet of lesser flamingos (*Phoeniconaias minor* Geoffroy); in this thesis, both common and scientific names are used interchangeably. Flocks dominate these

waterbodies, in numbers that exceed 75% of the world's population, moving between the lakes in an unpredictable manner looking for food (Childress *et al.*, 2007a). They attract hundreds of thousands of tourists to the lakes to see the stunning spectacle; this, contributes substantially to Kenya's national income (Harper *et al.*, 2003). Lake Bogoria is a typical example of such a spectacle in Kenya's Great Rift Valley.

1.1.3 Lake Bogoria

Lake Bogoria (previously called Lake Hannington) is an extreme alkaline-saline lake, with a volcanic origin, is a stratified lake (De Cort *et al.*, 2013). It is climatically located within the Inter-Tropical Convergence Zone (ITCZ) and characterised by erratic and irregular rainfall (Oduor and Schagerl, 2007b, Kaggwa *et al.*, 2013b). This has led to an erosion of the vegetative cover around the lake and washing of dissolved inorganic elements from the catchment. There is a gradual decrease in salinity from the south to the north basin, which receives most of the river inputs (McCall, 2010).

The water budget of the lake comes (in order of magnitude) from the catchment to the south and east parts of the lake whose rivers flow into the northern end, from many fumaroles, boiling springs, and geysers and from direct precipitation (Harper *et al.*, 2003, Ballot *et al.*, 2004b, McCall, 2010). Its rainfall pattern has two main periods, Apr-May and Oct-Nov; in addition, there is another small peak in Jul-Aug (Davies *et al.*, 1985, LaVigne and Ashley, 2001), with an annual rainfall (500-1000 mm). This area of the eastern part of the East African Rift Valley has a naturally low level of humidity, and thus a high level of evaporation (Oduor and Schagerl, 2007b), estimated to be higher than 2500 mm per year (Renaut *et al.*, 2008).

The chemical composition of the lake is stable and dominated by a high level of sodium carbonate and bicarbonate. Research conducted between 1974 and 2000 found that the strong evaporation and the inflows from adjacent springs resulted in the lake conductivity remaining relatively steady at between 72 mS cm⁻¹ and 77 mS cm⁻¹, an alkalinity of 1500 meq L⁻¹, a pH of 10.2-10.3 and a salinity of > 40‰ (Harper *et al.*, 2003, McCall, 2010).

Despite this extreme environment, Lake Bogoria is a rich home for a large number of species of microorganisms and their viruses, and it is famous for a high biomass of phytoplankton of more than several hundred $\mu\text{g L}^{-1}$ of Chl-*a* which underpins the presence of lesser flamingos. The lake's productivity is commensurate with tropical forests' productivity, owing to the high temperatures, low-light penetration and high inputs of CO_2 through HCO_3^- , CO_3^{2-} and CO_2 interaction; thus, it is considered one of the most productive ecosystems in the world (Talling *et al.*, 1973, Melack and Kilham, 1974, Oduor and Schagerl, 2007b). Ballot *et al.* (2004b) showed that this simple aquatic system is dominated by only one primary producer; the filamentous cyanobacterium *Arthrospira fusiformis*, which forms a massive monospecific population, accounting for more than 97% of the whole biomass. More recently, this population dropped only to 80% of the total, with other cyanobacteria species such as *Synechocystis* sp. and chlorophyte of *Keratococcus* sp. began to contribute to the remaining phytoplankton biomass (Schagerl and Oduor, 2008). There are no aquatic macrophytes in this, or other, alkaline-saline lakes; littoral species such as grasses that are tolerant of these extreme conditions occur (Harper *et al.*, 2003).

The lake is one of the six Ramsar sites in Kenya, and has a particular commercial importance to the local economy, primarily because this stunning ecosystem is one of the most enthralling wildlife scenes of the world. Hundreds of thousands of tourists visit it annually to see the natural spectacles of the hot springs and flamingos (Harper *et al.*, 2003, Ndetei and Muhandiki, 2005, Straubinger-Gansberger *et al.*, 2014).

1.2 Cyanobacteria

1.2.1 Definition

Cyanobacteria are Gram-negative and photoautotrophic prokaryotic organisms (sometimes mistakenly called blue-green algae) (Schopf, 2000). They are considered to be the oldest primary producers in the world, generating about 45% of world productivity (Field *et al.*, 1998), with 3×10^{14} g C universal biomass (Garcia-Pichel *et al.*, 2003). Even though microalgae are aerobic phototrophic

prokaryotes, some of them can use H₂S instead of H₂O as an hydrogen donor during anaerobic photosynthesis conditions (Cohen *et al.*, 1986).

All cyanobacteria have a chlorophyll pigment (Scheer, 2006) that combines with other accessory pigments, which include carotenoids in most of them (Takaichi and Mochimaru, 2007), and phycobilin, where the inclusion of phycocyanin is reflected in the blue-green colour, or allophycocyanin and phycoerythrin that reflects the red colour, of some species (Cornejo and Beale, 1997). Nitrogen (N) and phosphorus (P) elements play a major role in limiting and controlling cyanobacteria growth (Ryther and Dunstan, 1971).

This taxon of bacteria is widespread, diverse and cosmopolitan in terms of its morphology and physiology. Species can tolerate and adapt to a varied range of environments; their habitats include numerous aquatic, terrestrial and extreme habitats such as hot springs and alkaline-saline lakes (Helbling *et al.*, 2006)

1.2.2 Biodiversity of cyanobacteria in Kenyan alkaline-saline lakes, with particular reference to Lake Bogoria

The alkaline-saline lakes in the East African Rift Valley are also known as *Arthrospira*-lakes, because of the dominance of this species within them. However, this is not always the case, and indeed only a few lakes such as Chitu (Ethiopia), Bogoria (Kenya) and Big Momela (Tanzania) are predominantly populated by *Arthrospira* spp. depending on climatic conditions and water levels. These *Arthrospira* blooms share their environment with or are even replaced by other cyanobacteria such as *Anabaenopsis*, *Cyanospira*, *Synechococcus* or *Chroococcus* (Jones and Grant, 2000, Krienitz *et al.*, 2016a)

Lake Bogoria, like many Kenyan soda lakes, is a hyperautotrophic lake with a more than 10 gC m⁻² day⁻¹ primary production, which has been positively correlated with the high density of cyanobacteria biomass (Whittaker and Likens, 1973, Melack and Kilham, 1974, Oduor and Schagerl, 2007b).

1.2.3 *Arthrospira* features and its diversity in Kenyan soda lakes

The *Arthrospira* genus (formerly known as *Spirulina*) is filamentous, non-heterocystous, motile, oxygenic and photosynthetic cyanobacteria. *Arthrospira* belongs to the class Cyanophyceae, subclass Oscillatoriophyceae, order

Oscillatoriales and family *Microcoleaceae* (Dadheech *et al.*, 2010, Sili *et al.*, 2012). Furthermore, phycocyanin pigment is the most significant pigment along with carotenoid and chlorophyll (Muthulakshmi *et al.*, 2012). *Arthrospira* is rich in crude protein, 60% of its dry weight (DW), which together with substantial fatty acids, vitamins and iron (Ciferri, 1983), give it high nutritional and pharmaceutical value to humans (Belay *et al.*, 1993, Yin *et al.*, 2017).

1.2.3.1 Distribution

Arthrospira is the major phytoplankton feature of soda lakes (Table 1.1), but its members live in a broad range of environmental conditions, from freshwater-saline to soda lakes, hypersaline lakes (Ciferri, 1983, Dadheech *et al.*, 2010).

Table 1.1: Some examples of *Arthrospira* global distribution.

Continent	Country	Lake	Reference
Africa	Kenya	Bogoria, Nakuru, Sonachi, Simbi, Oloidien, Elmenteita	(Melack and Kilham, 1974, Melack, 1979, Melack, 1981, Vareschi, 1982, Melack, 1988)
		Magadi	(Melack, 1996, Ballot <i>et al.</i> , 2005)
	Ethiopia	Abijatta, Arenguade, Chitu, Kilotes	(Schagerl and Oduor, 2008, Melack, 2009, Krienitz and Kotut, 2010)
		Tanzania	Natron, Eyasi, Big Momella, Magad, Manyara, Reshitani, Tulusia
	Uganda	Katwe, Masehe	(Melack and Kilham, 1974, Tuite, 1981)
	Sudan	Dariba	(Mungoma, 1990)
Asia	Turkey	Van	(Fott and Karim, 1973)
	India	Shambhar, Mansagar	(Hammer, 1986)
Central America	Mexico	Texoco	(Dadheech <i>et al.</i> , 2010)
Europe	Sebria	salty puddles (Baranda)	(Ciferri, 1981, Dadheech <i>et al.</i> , 2010)
			(Fužinato <i>et al.</i> , 2010)

1.2.3.2 Morphology

This genus of cyanobacteria was first studied in by Stizenberger (1852) who described it as a filamentous and helical trichome (in this thesis, two terms, trichome and filament are used interchangeably). The trichome architecture (such as its arrangement and size) is varied, with the trichome width 2.5-16 μm , helix pitch 0-80 μm and coil diameter 15-60 μm (Li *et al.*, 2001, Kaggwa *et al.*, 2013a). The characterisation of the orientation and morphology of the *Arthrospira* trichome is essentially determined by growth conditions. Much has been written about the effect of climatic conditions and water level on the helicity of *Arthrospira* trichome. For example, Krienitz *et al.* (2013) noticed that low salinity levels were positively correlated with a small morphotype of *Arthrospira*. Whilst in the same year Kaggwa *et al.* (2013a) suggested that the loose morphotype dominated the phytoplankton population in lakes Nakuru and Bogoria during favourable conditions, whereas the large and tight trichome thrived under biological stress such as zooplankton grazing or virus infections. Much morphological and molecular work is still needed to investigate the morphology, abundance and dominance in the presence of environmental stresses.

1.2.3.3 Life cycle

The life cycle of *Arthrospira* is very simple, as indeed are all the life cycles of *Microcoleaceae* family members (Figure 1.3). Asexual reproduction is by fragmentation – a technique to multiply the trichome and cause the new and young trichomes to elongate by binary fission (Tomaselli *et al.*, 1981). The process starts by breaking up the terminal part of the trichome into small chunks called necridia. Those pieces are colourless and biconcave because they lose their pigments during the lysis. The process produces new motile specialized cells (a few cells long) called hormogonia, whose cytoplasm has a lesser degree of granulation and whose cell colour appears very light blue-green. A short chain of the cells leave the mother trichome and elongate by binary fission; consequently, a new trichome is produced (Figure 1.3). After that, the accessory pigment of phycocyanin starts working by giving the cells the blue-green colour and the cell cytoplasm becomes more granulated.

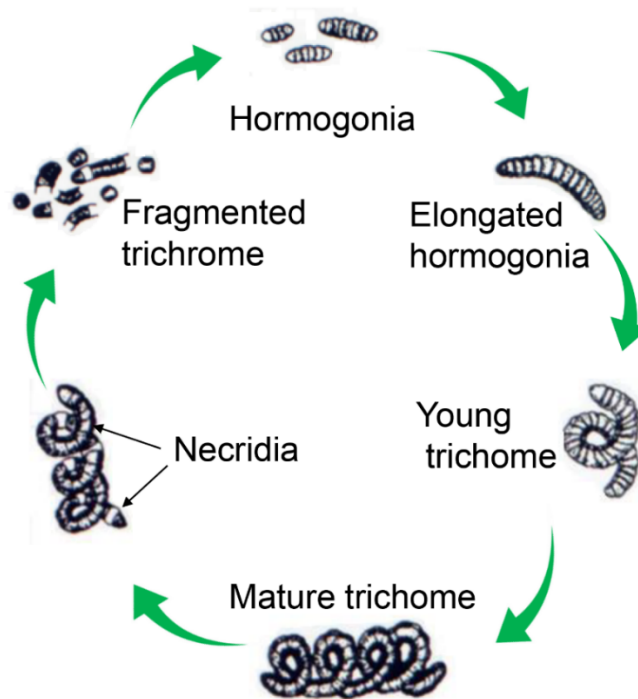


Figure 1.3: *Arthrospira* life cycle.

The figure shows hormogonia cells and how they release from the original trichome, leaving beyond a colourless sheath, modified from (Muhling, 2000).

1.2.3.4 Taxonomy

Since the end of the last century, two filamentous cyanobacteria (genera, *Arthrospira* and *Spirulina*) have been subjected to intense taxonomical and nomenclatural debate. The root of this argument is the morphological similarity between them. The first observation (Wittrock and Nordstedt, 1884) described the filaments as “ *Spirulina jeneri* f. *platensis* ” without considering the presence or absence of septa within the trichome. Eight years later Gomont (1892) confirmed the presence of septa in the Oscillatoriaceae family; thus, a new genus was established under the name of *Arthrospira*. After an extensive debate between taxonomists, the trichome helicity was finally considered to be the defining morphological taxonomical feature (Komárek and Anagnostidis, 2005), and six years later Komarek and Hauer (2011) suggested *Spirulina* as the commercial name of this helical cyanobacterium, replacing its scientific and taxonomic name with *Arthrospira*. Scientists subsequently concluded that *Arthrospira* has two behavioural forms, one being planktonic where all its members are able to float on the surface of the alkaline-saline lakes in tropical and subtropical regions such as East Africa and South Asia, and named two

species, *Arthrospira maxima* and *A. fusiformis*. The other is benthic where its members are not able to float on the surface of the water bodies because of their lack of gas vacuoles. Rather, these latter forms thrive in freshwater; for example, in America, and are named *Arthrospira platensis* and *Arthrospira jenneri*. Komárek *et al.* (2014) recently considered *Arthrospira* to be a different genus from *Spirulina* and they listed *Arthrospira* under order Oscillatoriales, whereas *Spirulina* is classified as being under order Spirulinales.

After the genomic revolution, a purely morphological taxonomic tool was no longer sufficient; molecular investigations were undertaken; phycologists have started using independent culture methods to achieve these ends. Most scientists began to use genetic markers to distinguish between *Arthrospira* and *Spirulina*; Scheldeman *et al.* (1999) used ITS (Internal Transcribed Spacer), whilst Manen and Falquet (2002) used the phycocyanin locus (*cpcB-cpcA*). The authors confirmed that *Arthrospira* and *Spirulina* are distantly related genera. Some years later, Dadheech *et al.* (2010) used ITS and (*cpcB-cpcA*) to distinguish between 53 *Arthrospira* strains from three different continents – Asia, Africa and Latin America. However, genes such as 16 rRNA are highly conservative, so they are not good tools by which to identify a strain at the species level. They showed a high similarity between most of the strains, even those that belong to different species. Currently, a new molecular technique has been developed, called whole genome sequencing and more than one platform has been used so far to produce high-quality analyses. My study used this approach to identify the *Arthrospira* Bogoria species.

1.2.3.5 *Arthrospira* as an alkaliphile

Arthrospira thrives in alkaline and saline water bodies, which are rich in sodium carbonate-bicarbonate and are at elevated pH levels. Studies have been conducted to investigate the optimal pH for a maximum growth; for example, Belkin and Boussiba (1991) determined the most favourable pH for *Arthrospira* growth to be in a range between 9.5-9.8; in addition, pH 7.0 affected *Arthrospira* negatively and the growth rate reduced to only 20% of optimal growth. Those authors also studied *Arthrospira*'s ability to cope with differences in pH through the whole plasma membrane, where they found that when the pH outside the

cell was in the region between 10.0 and 11.5, the pH inside the cell was maintained at 8.0 and 8.5 respectively. To answer the question as to how *Arthrospira* maintains its low internal pH, a large and growing body of literature reports investigations into other alkaliphilic cyanobacteria where it was demonstrated that the Na⁺/H⁺ antiporter is the most important requirement (Miller *et al.*, 1984, Espie *et al.*, 1988). Any deficiency in sodium supply is a – dramatic inhibiting factor on growth and the photosynthesis process in *Arthrospira*, through the inhibition of photosystem II (PSII) and degradation of the phycocyanin pigment (Schlesinger *et al.*, 1996). The optimal Na⁺ concentration should not be less than 50 mM, pH in the range 9.5-11.5 and sodium concentrations around 150-250 mM; a high alkalinity would be more effective still when combined with optimal temperature and salinity levels (32-35 C° and 20-70 gL⁻¹ respectively) (Ciferri, 1983).

1.2.3.6 *Arthrospira* and light adaptation

The effect of light-stress on the cultivation of *Arthrospira* indoors has been intensively studied, as light-stress is potentially the most significant environmental factor to influence the light-harvesting antennae (phycobilisomes). For example, Bocci *et al.* (1980) found that *Arthrospira* growth was fully light-saturated at intensities between 150 and 200 $\mu\text{mol photon m}^{-2} \text{s}^{-1}$. About thirty years later, Danesi *et al.* (2011) showed that optimal *A. fusiformis* growth, with a cell productivity of approximately 95 mg L d⁻¹, was achieved at an intensity of 24 $\mu\text{mol photons m}^{-2} \text{s}^{-1}$. This value is considerably lower than that typically recorded outdoors in the tropical environments of EASLs. The hyper-productivity of these extreme environments is attributed to high ambient temperatures, high light intensities and a limitless supply of CO₂, with an average of approximately 12 hours of daylight and light intensity that exceeds 2,000 $\mu\text{mol photon m}^{-2} \text{s}^{-1}$ (Krienitz and Schagerl, 2016).

The loss of photosynthetic capacity, also referred to as photoinhibition, has been investigated in many *Arthrospira* strains in terms of damage to photosystem II (PSII). This damage as a result of exceeding optimal photon flux densities (PFD) and over saturating photosynthesis. For example, in *A. fusiformis* strain P4P photoinhibition was expressed as a decrease in the D1

protein, which is an essential component of PSII (Sili *et al.*, 2012). In the *A. fusiformis* strain M2, the initial slope of the P/I curve was reduced by 48% compared to a control after the cells were exposed to high light (Torzillo and Vonshak, 1994). Light regulation was also found to have a strong effect on the phycobilisome structure in *A. platensis* C1, after it was grown under low (50 $\mu\text{mol photons m}^{-2} \text{s}^{-1}$) and high (500 $\mu\text{mol photons m}^{-2} \text{s}^{-1}$) light intensities. The polypeptide linker which has a molecular weight of 33 kDa and that is normally present under low light conditions, disappeared under high light intensities, which led to smaller phycobilisomes. The decrease in the number of light-harvesting antennae is associated with the reduction in phycocyanin and allophycocyanin content from cells exposed to low light to cells were exposed to high light (Nomsawai *et al.*, 1999).

1.2.3.7 Crashes of *Arthrospira* biomass in Kenyan soda lakes and theories behind it

As mentioned earlier, *Arthrospira* dominates the phytoplankton of EASLs such as Lake Bogoria (Harper *et al.*, 2003, Kaggwa *et al.*, 2013a), Nakuru (Vareschi, 1978, Krienitz and Kotut, 2010), Elmenteita (Ballot *et al.*, 2004b, Schagerl and Oduor, 2008) and others (Table 1.1). Under strong alkaline conditions such as in Bogoria and Elmenteita, productivity has reached roughly 20 $\text{gC m}^{-2} \text{day}^{-1}$. However, these high populations have recently been observed to fluctuate over time points. Table 1.2 shows *Arthrospira* population crashes in Kenyan alkaline-saline lakes.

Table 1.2: *Arthrospira* collapses in Kenyan alkaline-saline lakes.

Date of crash	Lake	Reference
1971	Elmenteita	(Melack and Kilham, 1974)
1973 (Mar-Sep)	Bogoria	(Melack, 1977)
1973-1974	Elmenteita	(Espie <i>et al.</i> , 1988)
1974	Nakuru	(Vareschi, 1982)
1974 and 1976	Elmenteita	(Tuite, 1981)
1974 (Jan-Mar)	Nakuru	(Tuite, 2000)
Late 1999/ early 2000	Bogoria	(Tebbs <i>et al.</i> , 2013)
2001 (Jun)	Nakuru	(Ballot <i>et al.</i> , 2004b)
2001 (Oct)	Bogoria	(Harper <i>et al.</i> , 2003)
2002 (Sep)	Elmenteita	(Ballot <i>et al.</i> , 2004b)
2004	Bogoria	(Tebbs <i>et al.</i> , 2013)
2004 (Jul-Oct)	Bogoria	(Schagerl and Oduor, 2008)
2006	Bogoria	(Krienitz and Kotut, 2010)
2008 (Dec)-2009 (Apr) and 2009 (Sep-Oct)	Nakuru	(Kaggwa <i>et al.</i> , 2013b)
19-27 Apr 2010	Bogoria	(Tebbs, 2014)
2011	Elmenteita	(Krienitz <i>et al.</i> , 2013)
2012	Nakuru	(Krienitz <i>et al.</i> , 2013)
2013-2015	Bogoria	(Krienitz <i>et al.</i> , 2016a)

Recently, due to the importance of this cyanobacterium as the diet for lesser flamingos, researchers have investigated the causes behind the mystery of *Arthrospira* spp. population collapses in EASLs. Cloern (1996) reviewed the several environmental variables that can influence phytoplankton population dynamics, including physical (water level and light attenuation), chemical (nutrients supply) and biological (lifestyle) factors. The causes are speculative and far from being completely understood for *Arthrospira*, but several have been suggested as potential factors.

The first possible cause comes from the distinct nature of soda lakes, as described above. These lakes are sensitive to climatic changes such as periodic droughts, they can become shallower and so gain a higher surface-to-volume ratio which can affect the lake properties negatively, The pronounced changes in water level, salinity and nutrient concentrations and their effect on algal biomass have been observed (Schagerl and Oduor, 2008, Krienitz and Kotut, 2010). Schagerl and Oduor (2008) found that phytoplankton species diversity decreased as a consequence of the increase in conductivity and water temperature in Bogoria, Nakuru and Elmenteita. They also showed that the distributions of *A. fusiformis* and *A. platensis* were mainly influenced by both

light attenuation and elevated nitrate concentrations. However, the physical differences between Lake Bogoria and the other two lakes should not be overlooked when comparing. MacIntyre and Melack (1982) reported the effect of lake topology on the water column of lake Sonachi, demonstrating that the lake morphometry plays a vital role in maintaining the meromixis of the lake as a consequence of the effect of wind, affecting the distribution and supply of nutrients. Schagerl *et al.* (2015), argue in a detailed study however, that physical and chemical factors control algal biomass. These authors described an irregular shift in phytoplankton population in Lake Nakuru after a severe drought causing a drastic decrease in water level. They illustrated that a variable salinity was the most significant driving force shifting the phytoplankton community. Harper *et al.* (2003) showed that Lake Bogoria is much deeper than other lakes, with a maximum of around 10.2 m, and thus, is a more stable aquatic system than others. *Arthrospira* breakdown, therefore, is more likely to be caused by biological factors, rather than physical factors in this lake.

The second potential cause underlying such unpredictable collapses in the *Arthrospira* population is grazing pressure by microzooplankton. These grazers have been noted as a shaping factor in phytoplankton diversity in other aquatic bodies (Salmaso and Padisák, 2007). However, there are relatively few studies that describe the role of microzooplankton in structuring primary producers in EASLs. Kaggwa *et al.* (2013a) and Kaggwa *et al.* (2013b) correlated the availability of the tight morphotype of *Arthrospira* with the growth of microzooplankton population such as rotifers and ciliates. In contrast, Burian *et al.* (2013) argue that the abundance of microzooplankton is too low to affect the *Arthrospira* density in Lake Bogoria. One year later the same authors, Burian *et al.* (2014) added that the only possible influence that microzooplankton can have is during the period of low densities of *Arthrospira* and overwhelming numbers of microzooplankton.

Cyanophage infections are the third suggested cause for irregular and an unforeseeable decline in *Arthrospira* biomass (Jacquet *et al.*, 2013). These attacks and their effects on the breakdown of *Arthrospira* could then result in a significant reduction in lesser flamingo density (Peduzzi *et al.*, 2014).

1.2.3.8 Theories behind the decline of the lesser flamingo

The East African Rift Valley is famous for richness in biodiversity and numbers of avifauna that use the soda lakes as havens. In Lake Bogoria about 223 species have been recorded (Harper *et al.*, 2003). Two species of flamingos are present, the lesser flamingo, *P. minor* (the dominant species, making up 90 % of the entire flamingo population) and the greater flamingo *Phoenicopterus roseus* Pallas making up the remainder (Vareschi, 1978). Both are specialised feeders and there is no competition between them, because the lesser flamingo feeds on cyanobacteria and algae (Krienitz *et al.*, 2016b), the greater flamingo feeds on tiny invertebrates (Ridley *et al.*, 1955, Jenkin, 1957).

Lesser flamingos are itinerant birds, which commute between the lakes sporadically looking for the best feeding (Ndetei and Muhandiki, 2005, Krienitz and Kotut, 2010). The highest distribution of populations of lesser flamingos is in East Africa, with about 1.5-2.0 million birds. Kenya sometimes has the largest proportion, with a fluctuating population that has sometimes reached 1.5 million (Childress *et al.*, 2007b); for example, Owino *et al.* (2001) showed that the lesser flamingo's population in Lake Bogoria at times accounted for 98.8% of the Central Rift Valley population. This reflects the quite specific and harsh conditions of the lake that encourage *Arthrospira* spp. growth as lesser flamingo's main diet, though alternatively, they can feed on benthic diatoms (Krienitz and Kotut, 2010). Ridley *et al.* (1955) cited in Ciferri (1983) showed that *Arthrospira* was the only food in lesser flamingos' stomachs. Their food preference is a result of the structure of the filter lamella, which provides 20-40 cm⁻² tiny edging platelets (Jenkin, 1957).

A bird when feeding submerges its head slightly under the water and moves it from side to side, taking in water through the pumping action of the tongue. Food particles are filtered through lamellae, which retain food particles (Krienitz and Kotut, 2010, Kaggwa *et al.*, 2013b, Krienitz *et al.*, 2016a) (Figure1.4). Consequently, authors consider them the environmental indicator of the food web of the EASLs where *Arthrospira* is dominant (ibid). Breeding of lesser flamingos, only at Lake Natron, is very unpredictable but when it occurs is

between October and December, when nests can be constructed on salt islands (Krienitz *et al.*, 2016b).

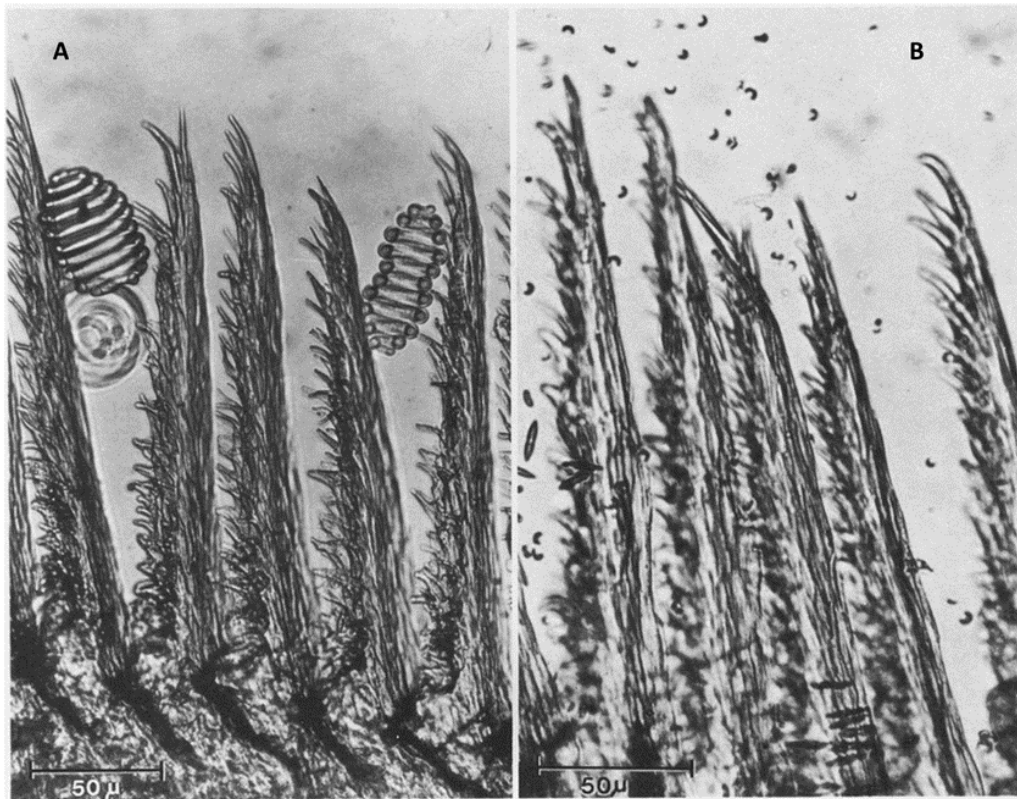


Figure 1.4: Filter-feeding system of lesser flamingos.

The platelets of this apparatus are well designed to catch the *Arthrospira* spp. trichomes (A) instead of unicellular cyanobacteria (B), taken from (Vareschi, 1978).

An irregular occurrence of mortality amongst lesser flamingos in the Kenyan Rift Valley has been noticed since 1928 (Ndetei and Muhandiki, 2005), but an increased increase in lesser flamingo die-offs have been suggested since 1990 (Straubinger-Gansberger *et al.*, 2014). Table 1.3 displays the reported number of dead lesser flamingos in Lakes Nakuru and Bogoria from 1991 to 2009.

Table 1.3: Reported lesser flamingo die-offs in the Rift Valley Lakes, Nakuru and Bogoria from 1991 to 2009.

Year	No. of carcasses	Season	Lake	References
1991	40,000		Bogoria and Nakuru	unpublished data
1993	18,500	Sept-Nov	Bogoria and Nakuru	(Kock <i>et al.</i> , 1999, Ndetei and Muhandiki, 2005),
1995/1996	50,000		Bogoria and Nakuru	(Krienitz <i>et al.</i> , 2005a)
1999/2000	200,000	20 months	Bogoria	(Harper <i>et al.</i> , 2003)
1999/2000	30,000		Bogoria	(Krienitz <i>et al.</i> , 2003)
2006	35,000	July, Aug	Nakuru	(Krienitz and Kotut, 2010)
2008	30,000	July	Bogoria	(Krienitz and Kotut, 2010, Straubinger-Gansberger <i>et al.</i> , 2014)
2009	2,000	March, Aug	Bogoria	(Straubinger-Gansberger <i>et al.</i> , 2014)

Adapted from (Straubinger-Gansberger *et al.*, 2014).

The causes of these deaths are the source of considerable debate amongst researchers and environmental conservation organisations. To date, there have been three hypotheses.

The most probable cause is the decline in food, as a consequence of damage and to their habitats by factors such as drought or inundation (Childress *et al.*, 2007b), contamination of lakes from farming and urbanisation (Childress *et al.*, 2006). Both can result in alterations in the primary producer's biomass (Ndetei and Muhandiki, 2005, Krienitz and Kotut, 2010). Krienitz and Kotut (2010) suggested that the collapse of *Arthrospira* spp. and their subsequent replacement with *Anabaenopsis* could indirectly influence the lesser flamingos because the diameter of this replacement diet was between 300 and 2000 μm , which is larger than the holes in the lamellae gaps in the lesser flamingo bill (50 μm). Thus, this would block the gaps in their filters, which would prevent food intake. In addition, *Anabaenopsis* is a low-nutritional value diet source, which could cause malnutrition, which would lead to immunodeficiency that could result in the infection of the lesser flamingos by different types of mycobacteriosis (Ballot *et al.*, 2004b). For example, *Mycobacterium avium*, which causes Avian mycobacteriosis, has been detected in lesser flamingos at

different points in time (Kaliner and Cooper, 1973, Cooper *et al.*, 1975, Sileo *et al.*, 1979, Kock *et al.*, 1999, Oaks *et al.*, 2006).

The dense flocks of lesser flamingos allow this infectious agent to spread very quickly (Cooper *et al.*, 2014). However, Harper *et al.* (2003) showed that during the high level of lesser flamingos die-offs in 2000-2001, the food supply (phytoplankton biomass) was more than sufficient, which suggests that birds might arrive at a food-rich lake already weakened by starvation in the lake from whence they came. Kaggwa *et al.* (2013b) noticed about 10 years later that, even though the dominance of *Arthrospira* exceeded 80%, there were still significant lesser flamingo mortalities. These observations indicate that whilst food quality and quantity is an important factor, a greater understanding of conditions in other lakes might play a major role in lesser flamingos' mortalities.

Another suggested cause of these mortalities has been cyanotoxins, but this currently remains the subject of debate. Microcystin and anatoxin-a have been found in phytoplankton in several Kenyan lakes (Ballot *et al.*, 2004b, Ballot *et al.*, 2005, Ndetei and Muhandiki, 2005). These were detected in different regions of the soda lakes such as hot springs and sediments (Krienitz *et al.*, 2003, Krienitz *et al.*, 2005b, Dadheech *et al.*, 2009), at Lake Bogoria and Lake Nakuru between 2001 and 2003 (Krienitz *et al.*, 2005a). The neurotoxin was detected in lesser flamingo feathers (Metcalf *et al.*, 2013), and hepatoin microcystin-YR was found in the stomach, intestine and faecal matter of lesser flamingos (Krienitz *et al.*, 2003). Some researchers, however, have argued that *A. fusiformis* and *A. maxima* are not toxic. For example, Mussagy *et al.* (2006) tried to detect *Arthrospira* toxins, but ultimately were unable to determine their presence. Straubinger-Gansberger *et al.* (2014) investigated the presence of cyanotoxins in phytoplankton in Lake Nakuru and Lake Bogoria for almost a year (Jul 2008 – Nov 2009), but even during the lesser flamingo mortality outbreak, they were not able to detect any cyanotoxins in lesser flamingo tissues. Ballot *et al.* (2005) however, found cyanotoxins such as anatoxin-a; in a separate experiment, *Arthrospira* extract was toxic to mice (Lugomela *et al.*, 2006).

Another potential toxic factor is the possible pollution by pesticides and heavy metals such as Cobalt (Co), Cadmium (Cd), Copper (Cu), Lead (Pb), Nickel (Ni) and Zinc (Zn), which are derived from various industrial and agricultural activities (Koeman *et al.*, 1972, Greichus *et al.*, 1978, Kairu, 1996, Ndetei and Muhandiki, 2005). Heavy metals concentrations were found to be greater than admissible levels in drinking water (HDL, WHO) in Lake Bogoria, Lake Nakuru and Lake Elmenteita (Ochieng *et al.*, 2007).

The last and most recently proposed cause of lesser flamingo mortality is starvation after bacteriophage (virus) infection of *Arthrospira* spp. Cyanophages (viruses that infect the cyanobacteria) have the ability to infect species and removal flamingo food (Peduzzi *et al.*, 2014), forcing them either to disperse to available food areas or face starvation and weakness.

1.3 Bacteriophages

1.3.1 Definition

The obligate intercellular parasitic viruses, which infect bacteria, are known as bacteriophages, or phages for short. The discovery of what is referred to as those that “eat bacteria” was found by two scientists, Frederick Twort (1915) in England and Felix d’Herelle (1919) at the Pasteur Institute in France (Duckworth, 1976). Viruses are the most abundant biological entities on the planet, and there is now an appreciation of the considerable influence they have on bacterial abundance, species composition, biogeochemical cycling and horizontal gene transfer in ecosystems (Bratbak *et al.*, 1989, Fuhrman and Proctor, 1990, Fuhrman, 1999).

There are small phage groups with single-stranded deoxyribonucleic acid (ssDNA), single-stranded ribonucleic acid (ssRNA), or double-stranded ribonucleic acid (ds RNA), but more than 96% of phages contain double-stranded deoxyribonucleic acid (dsDNA) (Ackermann, 2007). The cyanobacterial phage group belongs to the so-called ‘tailed phages’ (Ackermann, 2007, Hagens and Loessner, 2007). All tailed phages are classified under order Caudovirales, which includes three families *Myoviridae*, *Siphoviridae* and *Podoviridae* (ibid) (Figure 1.5).

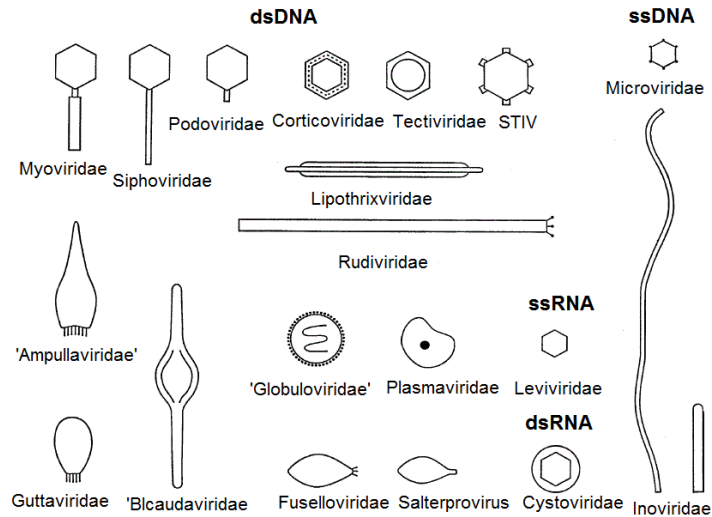


Figure 1.5: Schematic illustration of the main phage families.

The four nucleic acid phage groups (dsDNA, ssDNA, dsRNA and ssRNA) are shown, taken from (Ackermann, 2006).

Myoviruses have long contractile tails and a wide variety of host ranges. In contrast, siphoviruses characterized by long non-contractile tails and have a much lower host range. Finally, podoviruses have short non-contractile tails and have the narrowest host range (Suttle, 2005). The phage genetic material (either DNA or RNA) is surrounded by a protein coating called a capsid (Clark and March, 2006), which is connected to a tail that contains fibres (Haq *et al.*, 2012) (Figure 1.6).

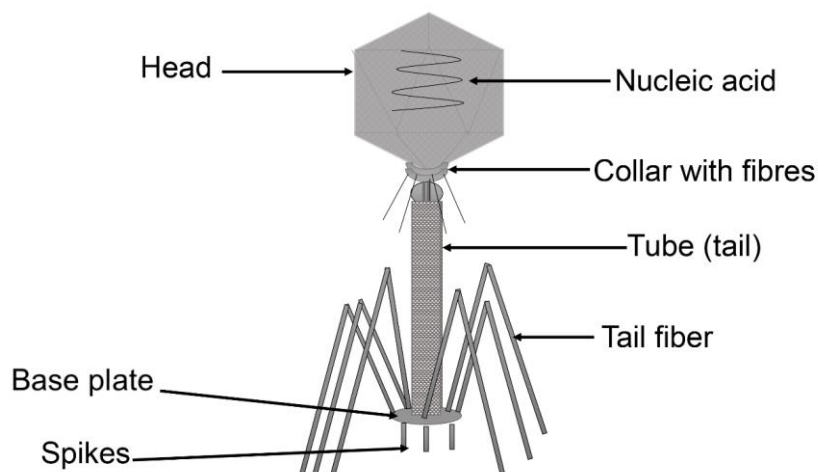


Figure 1.6: A model structure of T4 phage, modified from (Tokarz-Deptuła *et al.*, 2011).

1.3.2 Phage life cycle

The phage life cycle has been reviewed in considerable depth. Hanlon (2007), Haq *et al.* (2012) and Mann and Clokie (2012) showed that phages propagate through two different life cycles, which are the lytic or lysogenic, and the pseudolysogenic life cycle (Abedon, 2009). Figure 1.7 illustrates a phage life cycles.

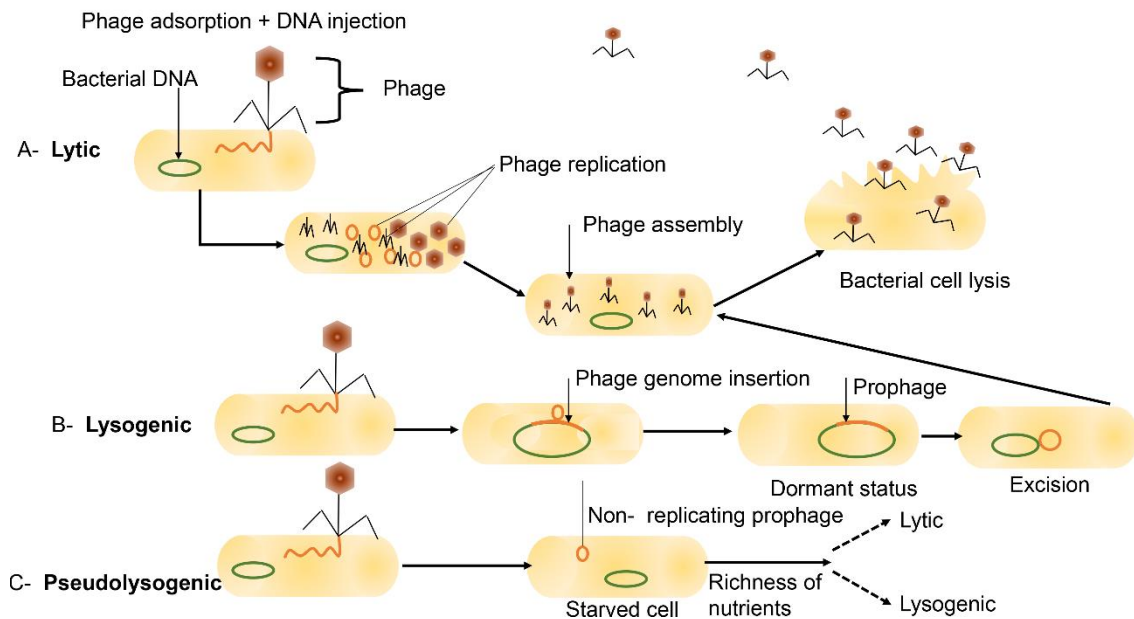


Figure 1.7: Life cycles of a bacteriophage.

Two life cycles types (lytic and lysogenic) and the dormant state (pseudolysogenic) are shown, modified from (Feiner *et al.*, 2015).

The first type is the obligatory lytic phage (virulent phage) which is able to kill the target cell after infection, consequently releasing the progeny phages. This type of phage life cycle has specific terms according to the stage of infection, which are -

- 1- Eclipse period, which refers to the time after entering the target cell and before phage assembly.
- 2- Latent period, which is defined as the time between entering the phage genome into the cell and releasing the new phage.
- 3- Burst size, which is the number of new phages that yielded per infected cell.

The second type, temperate phage, can either kill its host or integrate its genome into the host and replicate with the host for several generations as a prophage.

Pseudolysogeny is an inactive and temporary stage of the phage life cycle that occurs when the ideal infection cannot be completed. This dormant state only occurs under specific conditions, which include when the target cells face physiological or environmental stresses. Wilson *et al.* (1996) found that when *Synechococcus* cultures suffered a shortage in phosphate supply in the media and were infected with compulsory lytic phage S-PM2, the progenies were reduced by 80%. This means the most of the phage's genome could not be expressed. There is a general thought that during any period of low host density, phages tend to be temperate, while a high host density encourages the occurrence of lytic phages (Stewart and Levin, 1984).

1.3.3 Cyanophages

Cyanophages are viral agents that particularly infect cyanobacteria. Before cyanobacteria were classified separately from algae, these viruses had been known as phycoviruses (Schneider *et al.*, 1964) and algophages (Safferman and Morris, 1964). Despite the fact that the first isolation of cyanophages was from freshwater habitats (Safferman and Morris, 1963), the majority of research conducted to date has been on marine cyanophages (Fuhrman, 1999, Suttle, 2005). In addition, the majority of cyanophages that have been discovered and identified belong to order Caudovirales with dsDNA (Ackermann, 1987). Of the 13 families of this order, cyanophages belong to three (*Myoviridae*, *Siphoviridae* and *Podoviridae*) (ibid). Scientists use the terms *cyanomyoviridae*, *cyanosiphoviridae* and *cyanopodoviridae* to describe the three morphological different families. Other morphological shapes have been confirmed; for instance, three filamentous cyanophages have been isolated as *Microcystis*, *Anabaena* and possible *Planktothrix* cyanophages (Deng and Hayes, 2008). The majority of cyanopodoviruses and cyanosiphoviruses have been isolated from freshwater, whereas the majority of cyanomyviruses have been isolated from marine water (Hambly *et al.*, 2001). Cyanomyoviruses and

cyanosiphoviruses are mostly virulent phages, but cyanopodoviruses have a tendency to be lysogenic (Suttle, 2005).

1.3.4 Cyanophages and cyanobacteria interaction

It has been confirmed that cyanophages play a significant role in the breakdown of cyanobacteria blooms in freshwater ecosystems (Deng and Hayes, 2008). Manage *et al.* (2001) reported that there was a relationship between the crash of *Microcystis aeruginosa* bloom and the rate of cyanophage infections in Japanese hypertrophic ponds. The collapse of a *M. aeruginosa* population has been attributed to viral agents in Australian subtropical lakes (Tucker and Pollard, 2005). Cyanophages have been also shown to be responsible for removing approximately 3% of the total population of marine *Synechococcus* sp. on a daily basis (Suttle, 2007a).

The well-documented cyanophages that infect filamentous cyanobacteria of the *Lyngbya*, *Plectonema* and *Phormidium* (LPP) genera, are classed together as the LPP phage-group (Johnson and Potts, 1985). Since then, many viral infections of filamentous cyanobacteria have been found, such as the near-complete lysis of *Limnothrix* sp. and *Prochlorothrix hollandica*, recorded in Lake Loosdrecht in the Netherlands; TEM analysis showed virus-like particles (VLPs) within the filament sections, supported by an increased presence of extracellular VLPs (Van Hannen *et al.*, 1999). Another study, conducted in the same lake found that viral infections accounted for 84-97% mortality of the primary producers (*Limnothrix* and *Pseudanabaena*) between Dec 2004 and Jan 2005 (Tijdens *et al.*, 2008a). It has recently been observed that a virus belonging to the *Siphoviridae* family has the ability to split the cyanobacterium *Cylindrospermopsis raciborskii* filament into small visible fragments in a freshwater lake in Australia (Pollard and Young, 2010).

All these impacts of the phage on its host and vice versa are considered from the perspective of phage/host interaction concepts. Many studies in the literature describe phage/host interactions in detail and from different perspectives. The review by Levin and Bull (2004) is one of the most important reviews indicating the importance of considering the various phage/host interaction concepts. The authors illustrate some of the most important

questions that must be answered to understand the conditions required to obtain the ideal lytic infection. For example, what is the adsorption rate? Is the phage able to produce a prolific infection? Do the host properties affect phage features? What are the rates of host decline and phage increase? What is the burst size, latent period and the density of the phage and its host?

Another important term that should be introduced for lytic phage is the “proliferation threshold”, where this kind of phage cannot propagate properly due to a cut-off limit (Mann, 2003), estimated for heterotrophic bacteria as 10^4 cells mL⁻¹ (Wiggins and Alexander, 1985), although this value is affected by other obligatory lytic phage parameters such as burst size, the same value has been confirmed for the unicellular cyanobacterium of *Synechococcus* (Rodda, 1996), cited in (Suttle, 2007a). Gons *et al.* (2006) estimated that a burst size of more than 200-400 is more likely to eliminate the *Limnothrix* sp. host.

1.3.5 Cyanophages and *Arthrospira* in Kenyan soda lakes

The correlation between cyanophages and the collapse of cyanobacteria blooms has been studied in detail, but the role of these viral agents in causing *Arthrospira* populations in general and those in EASLs in particular to crash has received considerably less attention. Only two pieces of research have reported these infections. (Jacquet *et al.*, 2013) isolated a new cyanopodovirus that infects *A. platensis* in certain French pools. Peduzzi *et al.* (2014), using an epifluorescence microscope and electronic microscope (TEM), suggested that cyanophage infections on *A. fusiformis* biomass may have a considerable influence on increasing lesser flamingo mortalities.

1.3.6 Cyanobacterial defence mechanisms against exogenous DNA uptake

The defence mechanisms of bacteria in general, and cyanobacteria in particular against foreign DNA uptake include physical, chemical and genetic barriers (Stucken *et al.*, 2013). Over the last two decades, there has been a growing consideration of how these barriers can be broken by viral attack and the impact that on regulating and shaping phytoplankton blooms. Physical barriers include the natural competence of cyanobacteria, such as certain proteins involved in the formation of the type IV pili (T4P); these proteins also make up the short

type II secretion system (T2SS) found in gram-negative bacteria. In addition to this and to the role played in mobility of pili (see chapter 5, section 5.4.5), these proteins bind foreign DNA at the cell surface, transfer the DNA to the cytoplasm, and then convert it into a single strand, and finally protect it from restriction endonucleases (Chen and Dubnau, 2004). Disruption of these proteins could affect the protection of the foreign DNA against endonucleases attack.

Another structural barrier is the unique arrangement of the exopolysaccharide (EPS) layer of cyanobacteria, this EPS layer is composed of the sheath, capsule and mucilage (Figure 6.1 A). The complex composition of the EPS around the cell forms a strong physical barrier against DNA uptake. The slime sheath that encapsulates the cyanobacteria contains metabolites, such as the UV-protective Scytonemin (Proteau *et al.*, 1993). Non-covalently attached proteins containing non-specific extracellular nucleases that break down foreign DNA are also within the EPS layer (Wolk and Kraus, 1982, Soper and Reddy, 1994, Takahashi *et al.*, 1996); Chapter 4 (section 4.3.6) gives further details related to the slime sheath surrounding *Arthrospira* filaments.

The third major barrier to foreign DNA is a genetic-based mechanism, which includes restriction-modification (RM) systems (Arber and Linn, 1969) and the Clustered Regularly Interspaced Short Palindromic Repeats (CRISPR) system (Sorek *et al.*, 2013) (Figure 1.8 A and B). RM systems include a restriction endonuclease (REase) and a cognate methyltransferase (MTase) (Vasu and Nagaraja, 2013). REase recognizes foreign DNA and then breaks it down at a specific sequence motif, while MTase modifies DNA by the methylation of cytosine and adenine residues within the REase recognition sequence. This protects the host DNA against REase activity (Figure 1.8 A).

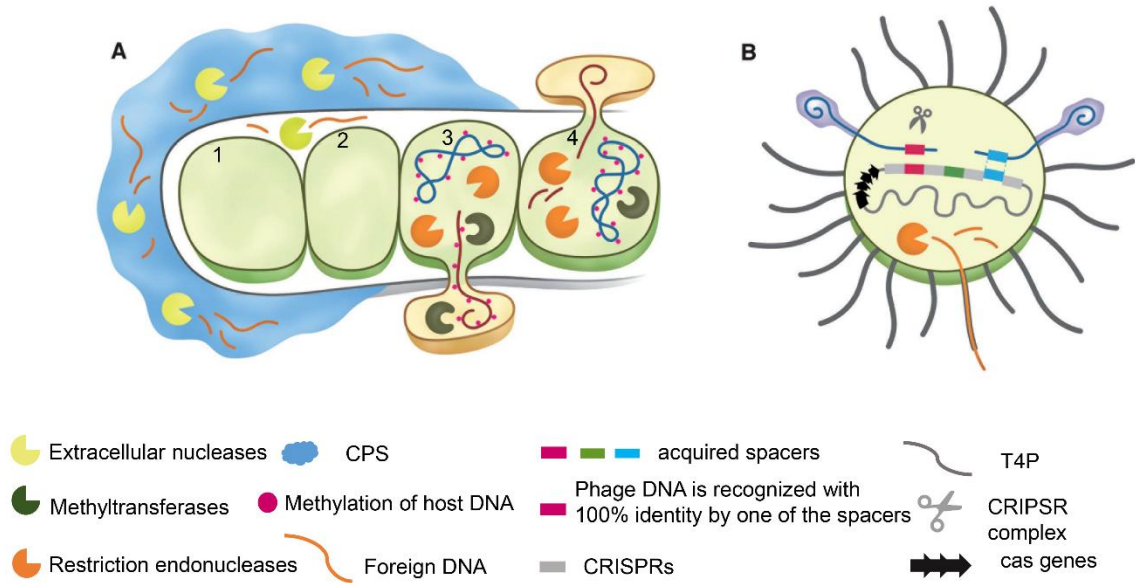


Figure 1.8: Barriers against the transmission of exogenous DNA into cyanobacteria, taken from (Stucken *et al.*, 2013).

(A) A thick EPS layer consisting of a capsular polysaccharide (CPS) and the sheath surrounding the cyanobacterial cell forms a physical barrier against foreign DNA transmission. Extracellular nucleases produced by the cell are immersed in the EPS matrix and break up the exogenous DNA on contact. This barrier might be bypassed either by filament breakage, enzymatic efficiency. For example, some phages have the ability to produce enzymes that degrade the polysaccharide (Labrie *et al.*, 2010), decomposed chemically, or might be thin enough so that it allows cells to contact with each other and therefore allow the foreign DNA to enter the cell by conjugation (third and fourth cell in part A of the figure) or transduction. RM systems can distinguish between the exogenous DNA and cyanobacterial DNA through methylation of the cell DNA by MTases. REases recognize and break the unmethylated DNA (third cell in part A of the figure). Foreign DNA can escape degradation by this mechanism through premethylation of DNA by active enzymes within the cell or by the random premethylation of the DNA with *dam* or *dcm* methylases (Fourth cell in 6.1 A). B shows CRISPR systems which are made up of *Cas* genes, CRISPRs and acquired spacers. The growth of type four of pili (T4P) has only been observed for unicellular cyanobacteria (Stucken *et al.*, 2013).

RM systems are categorized into four categories (I-IV) based on their recognition location, split position, subunit formation and cofactor requirements (Roberts *et al.*, 2003). Most cyanobacterial restriction enzymes belong to the Type II RM systems, these include the enzymes Avall, Aval and Asull, which are the most naturally recurring enzymes (Lyra *et al.*, 2000). The first RM system detected in unicellular cyanobacteria were from the colonial *Microcystis* and *Cyanothece* genera (Soper and Reddy, 1994, Takahashi *et al.*, 1996), but most of the RM systems detected have been from filamentous cyanobacteria

(Wolk and Kraus, 1982, Lyra *et al.*, 2000). More restriction barriers appear to exist in filamentous cyanobacteria, ranging from *Arthrospira* and *Oscillatoria*, as well as unicellular *Cyanothece* and all Pleurocapsales strains. The largest recognition site distributions have been detected in the genomes of *M. aeruginosa* NIES-843 (40 motifs), *A. maxima* CS-328 (37 motifs), *Calothrix* sp. PCC 7103 (34 motifs) and *Nodularia spumigena* CCY9414 (28 motifs) (Stucken *et al.*, 2013).

Another genetic barrier against foreign DNA invasion, which is a signature of a previous phage infection, is the CRISPR loci (Stern *et al.*, 2012). It consists of an array of repeated sequences, separated by differentiated sequence spacers of lengths and structures that are flanked by CRISPR-associated (*Cas*) genes (Barrangou *et al.*, 2007) (Figure 1.8 B).

1.4 Thesis aim and Justification

EASLs are important ecosystems, as described above; particularly economic importance for the Kenyan people (Harper *et al.*, 2003, Krienitz and Kotut, 2010). Lake Bogoria is an ideal example of such lakes. In these aquatic environments unpredictable episodes of lesser flamingo mortalities have been reported (Vareschi, 1978, Codd *et al.*, 2003, Krienitz and Kotut, 2010). Although many reasons have been suggested as potential causes for these periodic mortalities, to date there are few studies of whether cyanophage infections could be a factor in the crash of the principal diet of the lesser flamingo (*Arthrospira* spp.). Therefore, there is a pressing need to investigate whether cyanophages are responsible for mediating a bottom-up cascade (*Arthrospira* disappearance), as proposed by Peduzzi *et al.* (2014). The aim of this study was to determine the role of viruses in the food web structure in one EASLs (Lake Bogoria).

1.5 Objectives

The aim was pursued through the following objectives:

- 1- To measure the key limnological features of Lake Bogoria (electrical conductivity, Chl-a content, pH, salinity and total Nitrogen and Phosphorus

concentration) continuously over the study period in order to produce a complete picture of the lake and correlate this with the virus availability.

2- To perform microscopy and genetic studies on samples of *Arthrospira* from Lake Bogoria in Kenya to establish the specific species and strain diversity.

3- To culture, the *Arthrospira* strains found in the lake and characterise their physiology.

4- To establish the conditions needed to isolate viruses that infect *Arthrospira*.

5- Use culture-independent methods to determine the diversity of the viruses associated with Lake Bogoria.

6- To conclude from any combination of results, whether cyanophages might cause *Arthrospira* spp. populations to crash.

1.6 Research questions

1. How can the diversity of cyanobacteria species and strains in EASLs be established, using samples from Lake Bogoria?

2. How can cyanophages be isolated?

3. How can cyanobacteria be infected by cyanophages?

4. To what extent are cyanophages responsible for the crash of the cyanobacterium *Arthrospira* population?

1.7 Study hypotheses

This study hypothesizes that the crash of a mono-specific bloom of *Arthrospira* in an alkaline-saline lake of East Africa is caused by cyanophage infections.

I further hypothesise that different strains of the species occur after the crash than before.

1.8 Thesis layout

This thesis has been organised in seven chapters as follows

Chapter 1 introduction of this study (literature review), including a description of its aim and objectives.

Chapter 2 the general methodology used in this study.

Chapter 3 reports the variation in certain limnological properties of Lake Bogoria (pH, electrical conductivity, Chl-*a* content, salinity and total of nitrogen and phosphorus content) and then consider the correlations between these features to give the complete picture of the lake between May 2015 and Mar 2017.

Chapter 4 is a study of *Arthrospira*, including isolation, morphology, abundance, ultrastructure, and behaviour.

Chapter 5 gives the genetic identification of Lake Bogoria *Arthrospira* with the other available *Arthrospira* species in the NCBI database.

Chapter 6 describes the isolated cyanobacterium used to investigate the presence of its cyanophages in Lake Bogoria's water.

Chapter 7 draws all information together to re-examine the idea of postulated by Peduzzi *et al.* (2014) as an overall discussion. Specific predictions are presented and tested on a chapter by chapter basis and the findings of the thesis discussed in the context of existing knowledge and the current theories regarding EASLs and their dominant primary producer (*Arthrospira* cyanobacterium).

Chapter 2 General materials and methods

2.1 Study area and site description

This study was conducted on Lake Bogoria, one of the EASLs. It lies in a semi-arid area on the floor of the Gregory Rift Valley in North West Kenya, about 240 km north of Nairobi (Harper *et al.*, 2003, Hickley *et al.*, 2003). It consists of three basins, the North, Central and South (Figure 2.1). The location and morphometric properties of this lake are given in Table 2.1.

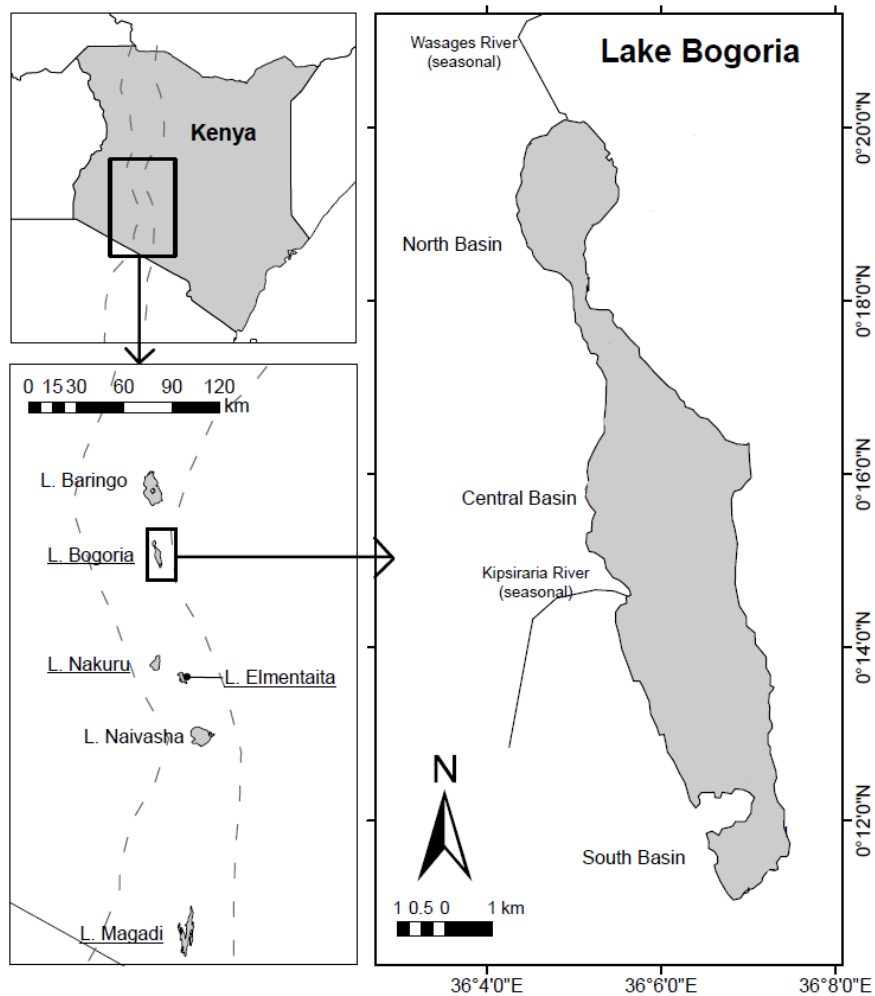


Figure 2.1: Map of Lake Bogoria and its location within the East African Rift Valley; from (Tebbs *et al.*, 2013).

Table 2.1: Geographical and Morphometric characteristics of Lake Bogoria.

Character	Measurement	Reference
Geographical location	00° 16' N and 36° 06' E	(Hickley <i>et al.</i> , 2003)
Altitude (a.s.l.) (m)	980	(Hickley <i>et al.</i> , 2003)
Surface area (km ²)	34	(Harper <i>et al.</i> , 2003)
Mean depth (m)	5.68	(Hickley <i>et al.</i> , 2003)
Maximum depth (m)	10 (5.9 North basin, 10.2 Central basin and 8.4 South basin)	(Hickley <i>et al.</i> , 2003)
Catchment area (km ²)	1500	(Oduor and Schagerl, 2007a)
Rainfall (mm year ⁻¹)	708	(Harper <i>et al.</i> , 2003)
Length (km)	17.25	(Hickley <i>et al.</i> , 2003)
Width (km)	1-4	(Harper <i>et al.</i> , 2003)
Area (ha)	3000	(Harper <i>et al.</i> , 2003)
Volume (m ³)	164 x10 ⁶ m ³	(Hickley <i>et al.</i> , 2003)
Shoreline length (km)	44.0	(Hickley <i>et al.</i> , 2003)

2.2 Sampling design

Lake Bogoria's central basin was used as the sample collection point for this study (Figure 2.2). Water samples from the shoreline were collected by Mr. Ezekiel Chebii (Kenya) at weekly intervals between May 2015 and Mar 2017, using a 1 litre jug, inverted and submerged by hand underneath the water surface, then slowly turned upright so as to fill with sub-surface water approximately 5 cm depth (Figure 2.3 and 2.4).

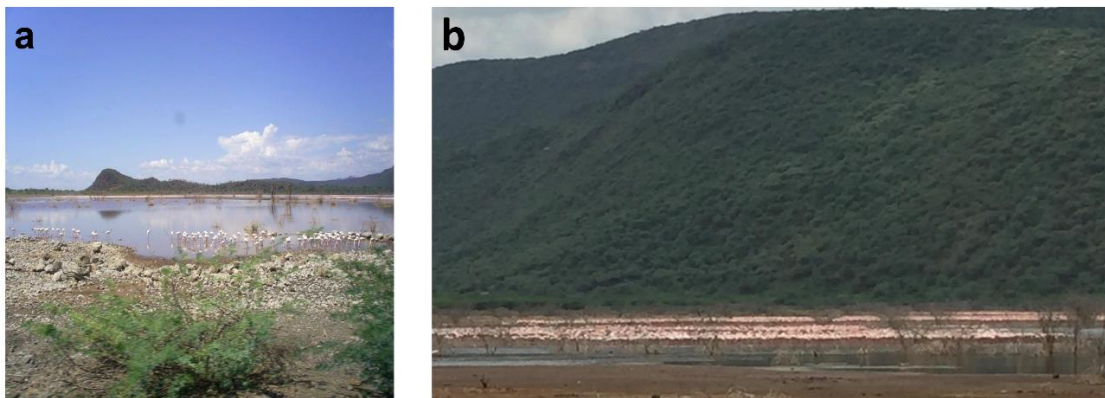


Figure 2.2: Views across the lake.

a) Northern end and b) neck between north and central basin, just to the north of the sample site.

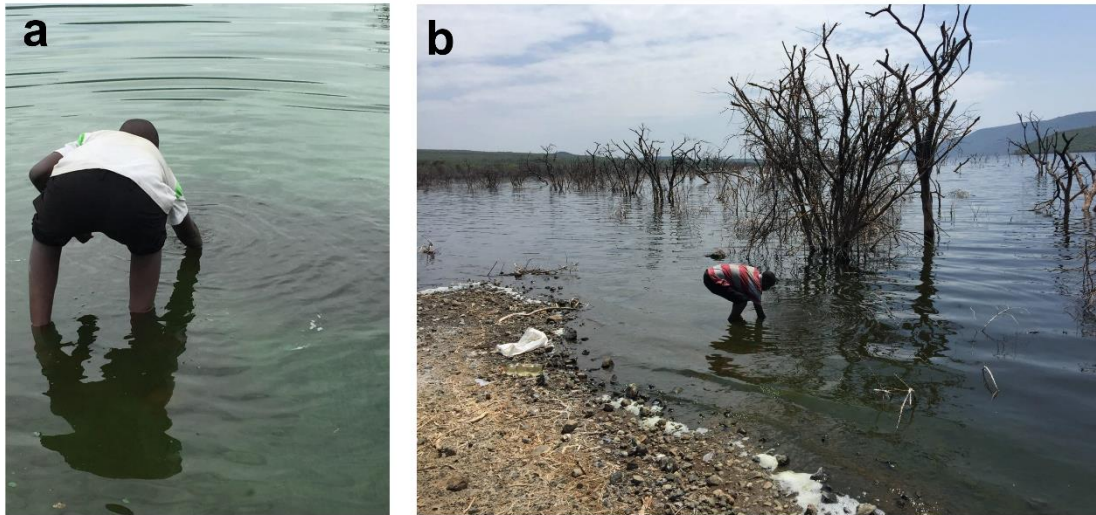


Figure 2.3: Images of sample collection.

a) Ezekiel taking a sample at the Central basin sample site, b) Another sample collection showing flooded trees that illustrate high lake water level (hence low conductivity due to freshwater input).

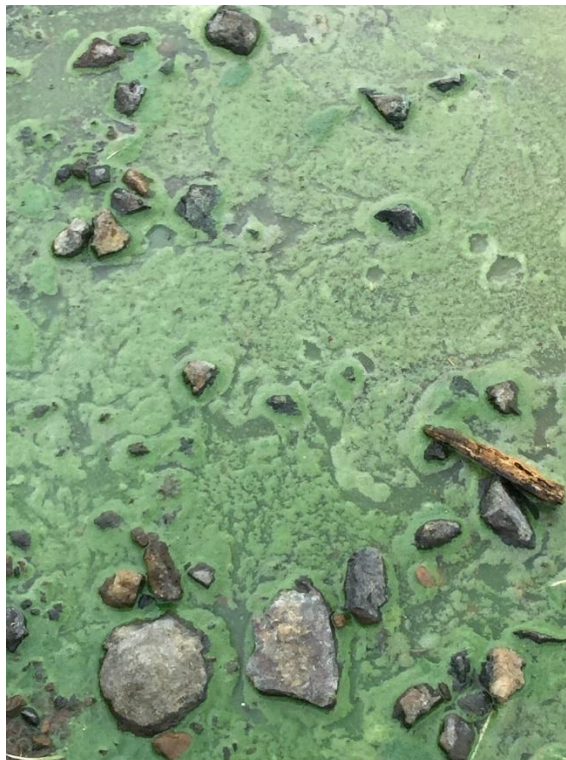


Figure 2.4: Sample taken subsurface to avoid floating Cyanobacterial scum.

Samples were taken at the edge of a flooded road, over a drain bridge so that the depth of water under the sample was approximately 1 metre. These water samples were filtered at the lakeside laboratory of the National Reserve, through 0.7µm glass microfiber papers (47 mm, Fisherbrand 11764083, Fisher Scientific, UK).

All the filtered water samples (330 mL up to 1 litre) were immediately stored in polypropylene closure plastic bottles (Thermo Fisher Scientific, 312105-0032, UK) and stored at 4°C until their transportation to the UK. The filter papers (three biological and technical repeats performed) with their retained filtrates containing the cyanobacteria were placed in individual self-seal polythene bags, within a flask in the dark at -20°C for Chl-a content analysis when returned to the UK. Water samples were taken by air as hold luggage in sealed cool boxes kept refrigerated with freezer blocks; filter papers in their bags were individually taken inside thermos flasks filled with ice, inside the cool boxes.

Fresh unfiltered water samples (1-3 litres) were also collected on every occasion that the accumulated weekly samples were taken to the UK, on the day before flying (Aug 2015, Mar 2016, May 2016, Jul 2016, Dec 2016 and Mar 2017). These fresh samples were used to conduct light-based and electron (transmission and scanning) microscopy (TEM and SEM) work. After samples arrived in Leicester, the water samples were immediately filtered through 0.2 µm filters (500 mL Bottle Top Filter, Filtropur BT50, USA) to eliminate bacteria and other debris, and then the filtrate stored in new polypropylene plastic bottles at 4°C. The filter papers with residue were stored at - 20°C. Remaining fresh unfiltered water samples were maintained at room temperature within the laboratory in sterilized Erlenmeyer flasks (Fisherbrand, Fisher Scientific, UK).

2.3 General materials and methods

All solutions, medium, glassware and other materials used for handling the cyanobacterium cultures had been autoclaved at 121 °C for 15 minutes. Sterile nuclease-free water (VWR, Life Science, UK) was used for any particularly sensitive work such as DNA extraction, Polymerase Chain Reaction (PCR) and Nanosight Technology, Ultrapure water (UPW) was used for general work such as a medium preparation. Heat sensitive material was sterilised by being

passed through 0.22 μm filters (Millex[®], Germany). All components of any solutions and buffers used in the present study are described in Appendix 8.1. All microscopy works were accomplished by working aseptically next to a Bunsen burner and on surfaces sterilized with 1000 ppm of Precept (Johnson & Johnson Company, UK).

2.3.1 Medium preparation

A modified Zarrouk's medium (Zarrouk, 1966) was the standard growth medium for all *Arthrospira* species (Mussagy *et al.*, 2006). The chemical components of this medium L⁻¹ of deionized distilled water (dH₂O) are listed in Appendix 8.1. All chemicals were firstly dissolved in 900 mL of dH₂O. Then, to enrich the medium with microelements, 1 mL of trace element solution (Appendix 8.1) was added. Thereafter, the solution was stirred for one hour and the pH was adjusted to 8.5 using 5 M NaOH before autoclaving. The pH was measured by meter (JENWAY 3310, UK), calibrated to pH 7.00 \pm 0.01 and 10.00 \pm 0.01 (Scientific Laboratory, Nottingham, UK). Afterwards, the volume of the medium was topped up to 1 L using dH₂O and was then sterilized at 121 °C for 15 minutes.

2.3.2 Culture conditions

Arthrospira isolated from Lake Bogoria were grown in sterilized Erlenmeyer flasks containing using volumes varying between 50 to 2000 mL volumes of Zarrouk's medium at 26°C, under continuous light produced using fluorescent lamps, with illumination at 13-15 $\mu\text{mol.m}^{-2} \text{s}^{-1}$ (Quantum Sensor, Skye, UK), without agitation, in a cyanobacterial incubator (Versatile Environmental Test Chamber, SANYO, Japan). Light filters (Neutral Density Filter 0.6 ND, LEE Filters, White Light, UK) were used to filter the irradiance. Cultures were also maintained in the laboratory at room temperature under a natural light-dark cycle. The cultures were hand shaken once a day and renewed according to the state of the cultures (generally every 50 days). To maintain the cyanobacterium cultures, they were sub-cultured by adding a 1:10 dilution of the stock into fresh Zarrouk's medium. A spectrophotometer (6715 UV/Vis JENWAY, UK) was used once a week to measure the growth of the culture by analysing samples using a wavelength of 750 nm OD₇₅₀.

Chapter 3 Limnological features of Lake Bogoria (between May 2015 to March 2017)

3.1 Introduction

Lake Bogoria was chosen as my study site as it is one of the most important flamingo feeding lakes in Kenya (Childress *et al.*, 2007a). They feed on the cyanobacterial species *Arthrospira* spp. which are the lake's dominant primary producers. Lake Bogoria has a larger catchment, is deeper, with a smaller surface to volume ratio and a continuous inflow from thermal springs (about 25% of inflow), all of which give it a greater chemical stability, compared to its neighbouring shallow lakes, such as Lake Nakuru. It has recently experienced prolonged rainfall however, starting in 2010, that diluted its salinity by over half to 31 mS cm⁻¹ in 2013 (Taylor, 2014) compared to its 'normal' earlier state of about 72 mS cm⁻¹ (Harper *et al.*, 2003).

In earlier years there was lower rainfall however and lake levels were declining. Several studies have shown the effects of such climatic variability on the characteristics of the lake. For example, during one year (August 2005 - August 2006), the lake water level decreased by about 30 cm (Renaut *et al.*, 2008). Another example can be seen from Jirsa *et al.* (2013) who monitored the water properties of lakes Bogoria and Nakuru over the period of August 2008 to October 2009; they suggested that the increase in salt concentration during this period was most likely due to the lakes' reduction in water level. The first decade of this century was one of drought throughout Kenya that resulted in the levels of Lake Naivasha, which is continuously monitored, falling to 1945 records (Harper *et al.*, 2011). Other lakes visually declined in the same way (Harper, pers. comm).

Any changes in lake properties can affect and shape phytoplankton diversity, a vital contributing cause (Melack, 1988). Therefore, there is an urgent need to shed light on the role of the lake's physico-chemical properties in controlling its phytoplankton biomass. Since the early decades of the 20th century, numerous studies into Lake Bogoria's basin have mainly focused on limnological or geological features, with little emphasis on changes in detailed biological properties, such as phytoplankton. The collapse of blooms, or unexpected shift

from one dominant phytoplankter (*Arthrospira*) to another, has been reported by several observers (Schagerl and Oduor, 2008, Krienitz and Kotut, 2010, Tebbs *et al.*, 2013). These bloom breakdown events remain a source of mystery because the factors that cause them are still uncertain and are just speculated upon (see chapter 1, section 1.2.3.6). There is also a potential role of climate change in water characteristics such as salinity and major nutrient availability.

3.1.1 Aim and chapter questions

The aim of this chapter was to investigate the changes in some of the physico-chemical conditions of Lake Bogoria that could affect the cyanobacteria (*Arthrospira*) population. This aim was achieved via the following objectives:

- 1- The Electrical Conductivity (EC), pH and salinity of water samples were measured in order to establish their levels and time-scale of any changes.
- 2- The changes in Chl-a content of the lake was determined, as an indicator of phytoplankton biomass and comparing with any changes in lake salinity.
- 3- The concentrations of major cyanobacterial nutrients – nitrogen and phosphorus – were measured to investigate their availability and correlate with phytoplankton biomass for the entire duration of the study.

The chapter thus seeks to address the following questions:

- 1- Do the limnological properties of Lake Bogoria change during the period of study (May 2015-Mar 2017) and if so, by how much?
- 2- Is there any relationship between physico-chemical properties and phytoplankton biomass in Lake Bogoria over this period?

The null hypotheses are:

- 1- There are no differences in the lake physico-chemical characteristics during the study period.
- 2- Physico-chemical properties are not responsible for phytoplankton biomass variation in Lake Bogoria.

3.2 Materials and methods

All the above-mentioned physical, chemical and biological properties of the water were measured on samples collected as described in chapter 2, section 2.2, at the University of Leicester (there were no samples for Nov 2016 due to technical loss, which has been considered in the analysis).

3.2.1 pH

pH is a measure of the hydrogen ion concentration ($\text{pH} = -\log[\text{H}^+]$) (Buck *et al.*, 2002). A Jenway 3310 pH Meter probe (Richmond Scientific, UK) was used. The instrument was calibrated as described in section 2.3.1, as it was known that the pH of the Bogoria water is over 9.0, with the automatic temperature compensation (ATC) set to 25°C.

3.2.2 Electrical Conductivity (EC)

EC is defined as the amount of electric current that water can carry, which is greater the more ions are dissolved in it (Moore *et al.*, 2008). A HI 98192 EC Hanna Meter (Hanna Instruments, UK) was used to measure this. Soda lakes are known for their high levels of conductivity, so the water samples were diluted 10-fold by deionized water and the instrument was calibrated according to the manufactory instructions with the ATC set to 25°C.

3.2.3 Salinity

Water salinity is the concentration of salt (NaCl) per unit mass of seawater. In salt of freshwater lakes, it includes the total concentration of all ions, not only that of NaCl (Williams and Sherwood, 1994). In light of this definition, there are two methods which can be used to measure salt lakes' salinity, one direct and the other indirect. The direct and accurate measurement can only be achieved by analyzing all ionic contents and adding their concentrations, which is time-consuming and expensive. This study, therefore, employed the indirect approach based on the relationship between conductivity and salinity as described in (Williams, 1986), with the equation:

$$S = 0.4665k^{1.0878} \quad (r^2 = 0.98799)$$

Where S is the salinity in g L^{-1} and k is the EC in mS cm^{-1} .

3.2.4 Chl- a Content

Chl-a concentration is commonly used (as here) as an indicator of phytoplankton biomass status. Over the period of the study, two methods were used to determine this parameter, as described below.

3.2.4.1 The Acetone extraction method (on water samples)

The pigment was extracted using a high concentration of acetone, then the absorbance measured at specific wavelengths before and after acidification. The 'Standard Methods' protocol of the APHA (Anon, 1992) based upon an earlier publication by Talling and Driver (1963) was followed here. All extraction steps were conducted in near-dark conditions and as soon as possible after sample receipt.

The frozen filter papers containing the retained phytoplankton as described in Chapter 2, section 2.2 were removed one by one to avoid any Chl-a degradation. Each was cut into small pieces then a pestle and mortar used to grind the sample in 2-3 mL of 90% aqueous acetone solution (Fisher Scientific, UK) (Appendix 8.1) with approximately 0.2 g glass beads (425-600 μm , Sigma-Life Science, UK) for 3-4 minutes. Once the grinding was complete, the mortar's contents were carefully transferred to a 15mL centrifuge tube. Any remaining residue was rinsed into the centrifuge tube which was then topped up to 10.1 mL volume with 90% aqueous acetone (the extra volume of 0.1 mL allows for the filter paper volume so gives 10.0 mL). To help the acetone steep the filtered slurry, the closed centrifuge tube was stored in the dark at 4 $^{\circ}\text{C}$ for 14-18 hours. Prior to processing the next sample, the mortar and pestle were rinsed with dH₂O and then 90% aqueous acetone. In this way, any remnants from the previous extraction were removed. The above extraction steps were repeated for all samples. The following morning the tubes were centrifuged at 500 g for 5 minutes using a Megafuge 16R centrifuge (Thermoscientific, USA) to precipitate all fibres. All the filtrate was transferred back to the refrigerator, while the spectrophotometer was set up and glass cuvettes were filled with 1 mL of each extract sample; one cuvette with 1 mL of 90% acetone as a blank to zero the machine at each measurement. The first readings were at the wavelengths of 664 nm and 750 nm. After running the whole set of samples (three readings per sample), 0.1 mL of 1N HCl (Appendix 8.1) was added to each sample

cuvette and carefully mixed for 90 seconds. This acidification step was followed by measuring the absorbance at 665 and 750 nm.

Once all samples were run as described above, the concentration of the Chl-a was calculated using the following equation:

$$\text{Chl-a } \mu\text{g L}^{-1} = \frac{26.7 (\text{corr.664} - \text{corr.665}) \times \text{volume of extract in L}}{\text{volume of sample in } \frac{\text{L}}{1000} \times 1 \text{ cm}}$$

Where:

Corr. 664 is the reading before acidification and 750 Abs reading subtraction.

Corr. 665 is the reading after acidification and 750 Abs reading subtraction (Talling and Driver, 1963).

3.2.4.2 Remote Sensing method

It is well-established that satellite data analysis is an important tool for the long-term monitoring of environmental phenomena. It has been shown to be a good investigation tool for monitoring cyanobacteria biomass as an indicator of eutrophication (Kutser, 2004, Kutser *et al.*, 2006, Matthews *et al.*, 2010) using measurements of water quality parameters such as Chl-a, chromophoric dissolved organic matter (CDOM), total dissolved solids (TSS) and Secchi disk depth (Mayo *et al.*, 1995, Brezonik *et al.*, 2005, Matthews *et al.*, 2010). There are a variety of satellite sensors and the Landsat Enhanced Thematic Mapper Plus (ETM⁺) was chosen by Dr. Emma Tebbs, (now King College London University), to study the Chl-a of Lake Bogoria in the first study of phytoplankton in a soda lake for her PhD (Tebbs, 2014). She provided me with the chlorophyll-a content of Bogoria obtained using her algorithm for calculating chlorophyll of soda lakes from satellite images (Tebbs *et al.*, 2013), from Oct 1999 up to May 2017.

3.2.5 Total nitrogen and total phosphorus measurements

Nutrient supply enhances phytoplankton thriving in aquatic bodies. Generally, two elements, phosphorus (P) and nitrogen (N), are the key to determining nutrients for aquatic phytoplankton growth (Lv *et al.*, 2011). Total concentrations

of these nutritional limiting factors were measured over the period of the current study. Total nitrogen-N and phosphorus-P were measured using Kjeldahl Digestion. Figure 3.1 shows the digestion unit structure, part of an automatic analyser (SEAL Analytical, Southampton, UK). The principle of this method is that all P and N are converted to ortho-phosphate and ammonia respectively, then their concentrations are measured (mg L^{-1}).



Figure 3.1: Digestion Unit structure.

All Bogoria's water samples were diluted 5-fold and the pH adjusted using 12N sulphuric acid to neutralise the water for analyses, as recommended by (Oduor and Schagerl, 2007b). Next, 25 mL of each diluted sample was added to a clean digestion tube, then, 5 mL of digestion solution (Appendix 8.1) added and mixed manually. Three tubes of 25 mL of deionized water were used as a blank. 4-5 boiling stones (Kjeldahl granules 500 g) were added to each digestion tube to avoid the solution boiling over during digestion. Before placing the tubes in the digestion block, the digestion cycle was set using the block digester operator system as follows: 160 °C for 40 min then 200 °C for 40 min finally 380 °C for 50 min. Tubes were left to cool for about 10 min after the completion of the digestion step and then diluted with 25 mL deionized water. For the colourimetric determination of ortho-phosphate and ammonia, Approximately 1.750 μL of each digested samples and blanks were transferred into 2 mL sample cups and then placed on the AQ2 discrete analyzer with two standards, one for N and another for P (Appendix 8.1). Two sets of 40 mL of N, P reagents

vessels (Appendix 8.1) were placed on the machine to calibrate it prior to the analyses.

3.2.6 Statistical analyses

Every two months were treated as a data point (time point) for all lake properties (EC, pH, Chl- *a* content (Acetone extraction method), salinity, total P, total N). Therefore, samples were classified into 11 time points ($n = 6$), except for remote sensing data, where the presence of the missing values led to a small sample size, therefore, every three months were treated as a data point ($n = 5$). Consequently, samples were classified into 7-time points.

All data were firstly tabulated in Microsoft Excel 2013, then imported into IBM SPSS Statistics version 24 software as repeated-measures design. The data for all parameters were approximately normally distributed, as assessed by the Shapiro-Wilk test and Kolmogorov-Smirnov^a tests ($p > 0.05$), except for two-time points for pH (Appendix 8.2, Tables 8.1 and 8.2). There were no outliers as assessed by the inspection of a boxplot. Moreover, Z-scores (Skewness/Std. Error and Kurtosis/Std. Error) for skewness and kurtosis were in the range of normally distributed data (± 2.58) for all variables (Appendix 8.2, Tables 8.1 and 8.2). However, the small sample size has affected the results of histograms, Q-Q plots and Mauchly's test of sphericity. Thus, nonparametric Friedman's ANOVA test was used and then followed by Pairwise comparisons with a Bonferroni correction for multiple comparisons (Statistics, 2012). Data are presented as medians.

Time series analysis was used to forecast and model the time series of monthly Chl-*a* content as an indicator of phytoplankton biomass of the lake for the period from Apr 2017 to Dec 2018. The remote sensing data ($n = 208$) were imported into the SPSS software as monthly means before being analysed using the expert modeller. A Chl-*a* sequence chart was built to detect the growth in the variance with time (non-stationarity); therefore, it was necessary to stabilize the variance (stationary time series). This was achieved by transforming the time series using a first difference transformation method. As a rule of thumb, time series should not include missing values. Thus, the mean of the entire time

series was used to replace the missing values, as described by (Arumugam and Saranya, 2018).

A Spearman's rank-order correlation was run to assess the association between the physico-chemical properties of the lake ($n = 66$). To determine the environmental variables significantly influencing Chl-a concentration (dependent variable), linear regression was performed. To do this, the data for each parameter ($n = 23$) were firstly checked for autocorrelation issues in the residuals using the Durbin Watson test. A first-order differencing transformation was used to remove them and transform the data into stationary time series data if any autocorrelations were detected. Data are represented as monthly means. Data management and analysis were performed using Excel 2013, SPSS (version 24) and GraphPad Prism 7.

3.2.7 Overview

Figure 3.2 illustrates the overall work flow for this chapter.

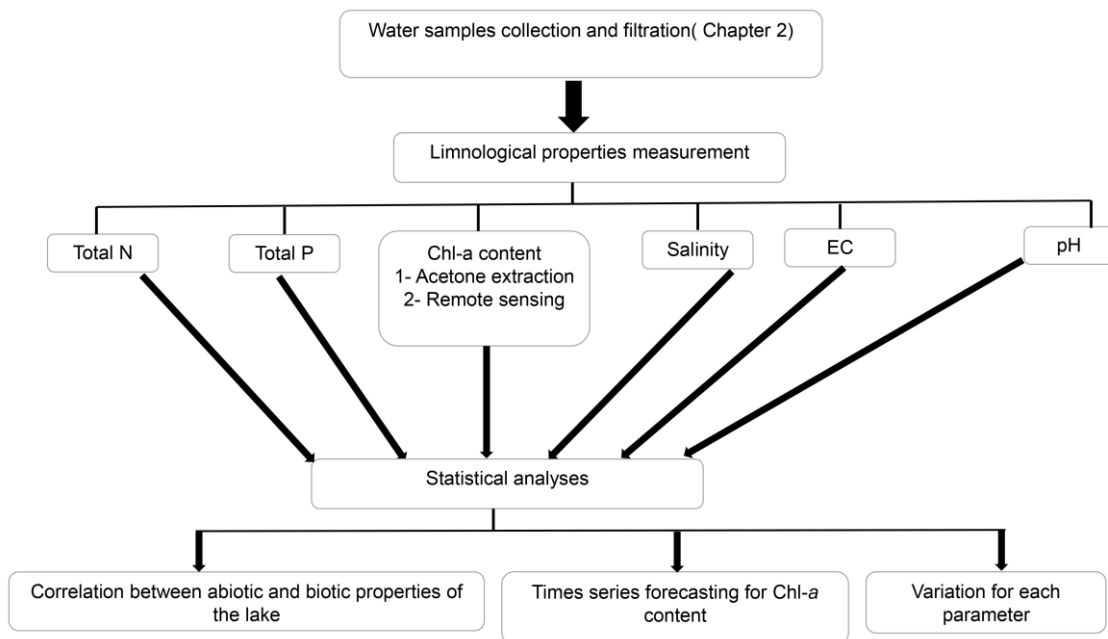


Figure 3.2: Schematic diagram of the limnological features analysis of Lake Bogoria.

3.3 Results

3.3.1 Variability in Properties of Lake Bogoria

Most of the lake water properties varied throughout the study (Table 3.1). The pH remained constant over the current study duration, other characteristics increased by an order of magnitude variation between time points. The parameters that changed most during the study; from 0.70 mg L⁻¹, 0.60 mg L⁻¹ to 2.35 mg L⁻¹, 4.43 mg L⁻¹ were the total P and N concentrations, respectively – major cyanobacterial nutrients.

Table 3.1: Descriptive analysis results of limnological parameters of Lake Bogoria for the entire study period (May 2015-Mar 2017).

Property	Min	Median	Max	Mean ± SD
pH	10.05	10.10	10.16	10.1 ± 0.26
Total N (mg L ⁻¹)	0.60	2.87	4.43	2.74 ± 0.88
Chl- a content (µg L ⁻¹)	49.84 ^a , 183 ^b	163.2 ^a , 266 ^b	380.20 ^a , 356 ^b	175 ^a ± 85.98 ^a 252.17 ^b ± 47.91 ^b
Salinity (g L ⁻¹)	28.43	30.10	43.97	33.71 ± 5.86
Total P (mg L ⁻¹)	0.70	1.49	2.35	1.44 ± 0.37
EC (mS cm ⁻¹)	40.9	46.10	65.30	51.10 ± 8.10

a = Chl-a content using acetone extraction method and b = chl-a content using remote sensing method, n = 66 except for= Chl-a content using remote sensing, n =35.

3.3.1.1 Variability in conductivity and salinity of Lake Bogoria

There was a clear trend of a gradually increasing conductivity of the lake from a median of 41.70 mS cm⁻¹ in May-Jun 2015 to 59.60 mS cm⁻¹ in May-Jun 2016. It then decreased for a short time (Jul-Oct 2016), after which it once again increased and levelled off at its highest value (63.70 mS cm⁻¹) at the end of the study period (Figure 3.3A).

Given that the lake's salinity was measured using Williams's equation (see section 3.2.3), its trend was similar to the conductivity pattern observed (Figure 3.3B), with the lowest value of 26.99 g L⁻¹ at the beginning of the study and highest value 42.79 g L⁻¹ at the end of the study.

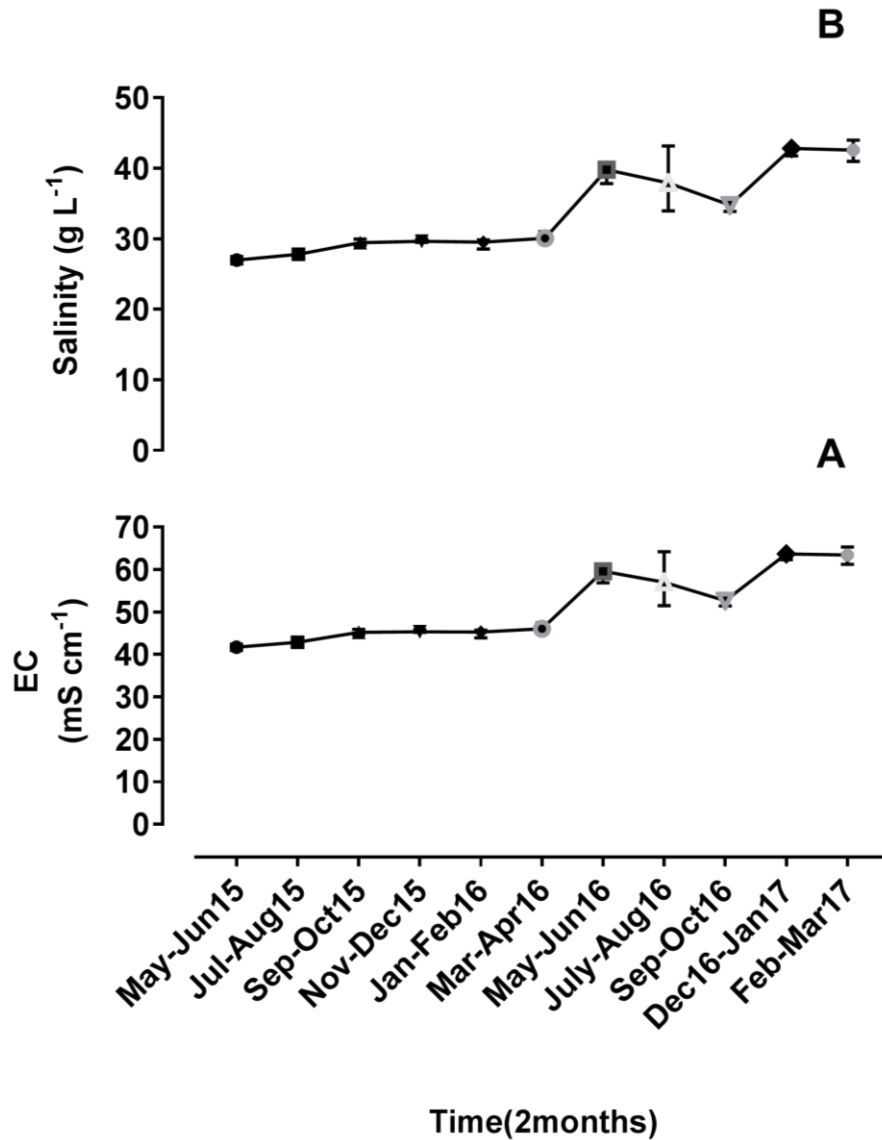


Figure 3.3: The variation in Bogoria's conductivity (EC) and salinity during the period of May 2015-Mar 2017.

A) Conductivity, (B) Salinity. Error bars represent 95% CI; n = 6.

The difference in conductivity and salinity between the time groups were statistically significant, $\chi^2(10) = 57.10$, $p < 0.0001$ (conductivity), $\chi^2(10) = 57.23$, $p < 0.0001$ (salinity). The results of the post-hoc analyses for multiple comparisons using the Bonferroni correction illustrated that 9 out of 55-time group companions were significantly different from each other for both parameters, as outlined in Tables 3.2 and 3.3 respectively.

Table 3.2: The significant results of Bonferroni post hoc tests for pairwise comparisons in conductivity of Lake Bogoria (May 2015-Mar 2017).

Pairwise	Test statistic	Adjusted <i>p</i> value	Effect size (<i>r</i>)
Jul-Aug15 vs. May-Jun16	- 6.50	0.038	0.63
Jul-Aug 15 vs. Dec16- Jan17	- 8.25	0.001	0.63
Jul-Aug15 vs. Feb-Mar17	-8.58	< 0.0001	0.63
Jan-Feb 16 vs. Feb-Mar17	-6.75	0.023	0.63
Jan-Feb 2016 vs. Dec-Jan 2016	-6.42	0.044	0.63
May-Jun15 vs. Feb-Mar17	-9.58	< 0.0001	0.63
May-Jun15 vs. May-Jun 16	-7.50	0.005	-0.63
May-Jun15 vs. Jul-Aug 16	-7.33	0.007	0.63
May-Jun15 vs. Dec16-Jan17	-9.25	< 0.0001	0.63

The significance level (α) is 0.05.

Table 3.3: The significant results of Bonferroni post hoc tests for pairwise comparisons in salinity of Lake Bogoria (May 2015-Mar 2017).

pairwise	Test statistic	Adjusted <i>p</i> value	Effect size (<i>r</i>)
Jul-Aug15 vs. May-Jun16	- 6.50	0.038	0.63
Jul-Aug 15 vs. Dec16- Jan17	- 8.25	0.001	0.63
Jul-Aug15 vs. Feb-Mar17	-8.58	< 0.001	0.63
Jan-Feb 16 vs. Feb-Mar17	-6.58	0.032	0.63
Jan-Feb 16 vs. Feb-Mar17	-6.92	0.017	0.63
May-Jun15 vs. Feb-Mar17	-9.58	< 0.001	0.63
May-Jun15 vs. May-Jun 16	-7.50	0.005	-0.63
May-Jun15 vs. Jul-Aug16	-7.33	0.007	0.63
May-Jun15 vs. Dec16-Jan17	-9.25	< 0.001	0.63

The significance level (α) is 0.05.

3.3.1.2 Variability in pH of Lake Bogoria

There was a relatively stable trend in the pH of the lake between 10.14 as the highest value in Dec 2016-Jan 2017 and 10.08 as the lowest value in Jan-Feb 2016 (thus variability was so low that error bars cannot be seen) (Figure 3.4). The differences between pH values in Lake Bogoria were statistically significant, $X^2(10) = 40.40$, $p < 0.0001$. A post hoc analysis test illustrated that 5 out of 55-time group companions were significantly different from each other, as shown in Table 3.4.

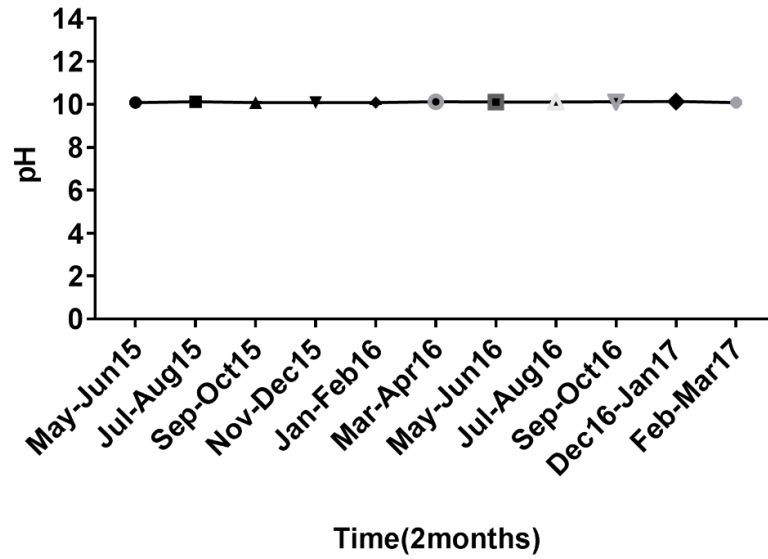


Figure 3.4: The variation in Bogoria’s pH over the period of study (May 2015-Mar 2017).

Error bars represent 95% CI; n = 6.

Table 3.4: The significant results of Bonferroni post hoc tests for pairwise comparisons in pH of Lake Bogoria (May 2015-Mar 2017).

Pairwise	Test statistic	Adjusted <i>p</i> value	Effect size (<i>r</i>)
Jan-Feb16 vs. Mar-Apr16	- 6.58	0.032	0.63
Jan-Feb16 vs. Sep-Oct16	- 8.17	0.001	0.63
May-Jun15 vs. Dec16-Jan17	-7.08	0.012	0.63
Nov-Dec15 vs. Dec16-Jan17	-7.08	0.012	0.63
Feb-Mar17 vs. Sep-Oct16	6.75	0.023	0.63

The significance level (α) is 0.05.

3.3.1.3 Variability in major nutrients concentration (total N and total P) of Lake Bogoria

There was a progressive rise in total N concentration from 1.39 mg L⁻¹ at the beginning of the study to 3.69 mg L⁻¹ in Nov-Dec 2015. After that, its concentration decreased gradually until it reached 2.38 mg L⁻¹ in Sep-Oct 2016, then again increased to 3.62 mg L⁻¹ at the end (Figure 3.5A). In the same time, there was an increasing trend in total P concentration of the lake from 1.01 mg L⁻¹ in May-Jun 2015 to 2.02 mg L⁻¹ at the end of the study, although the trend slightly fluctuated in the middle of the study (Figure 3.5B).

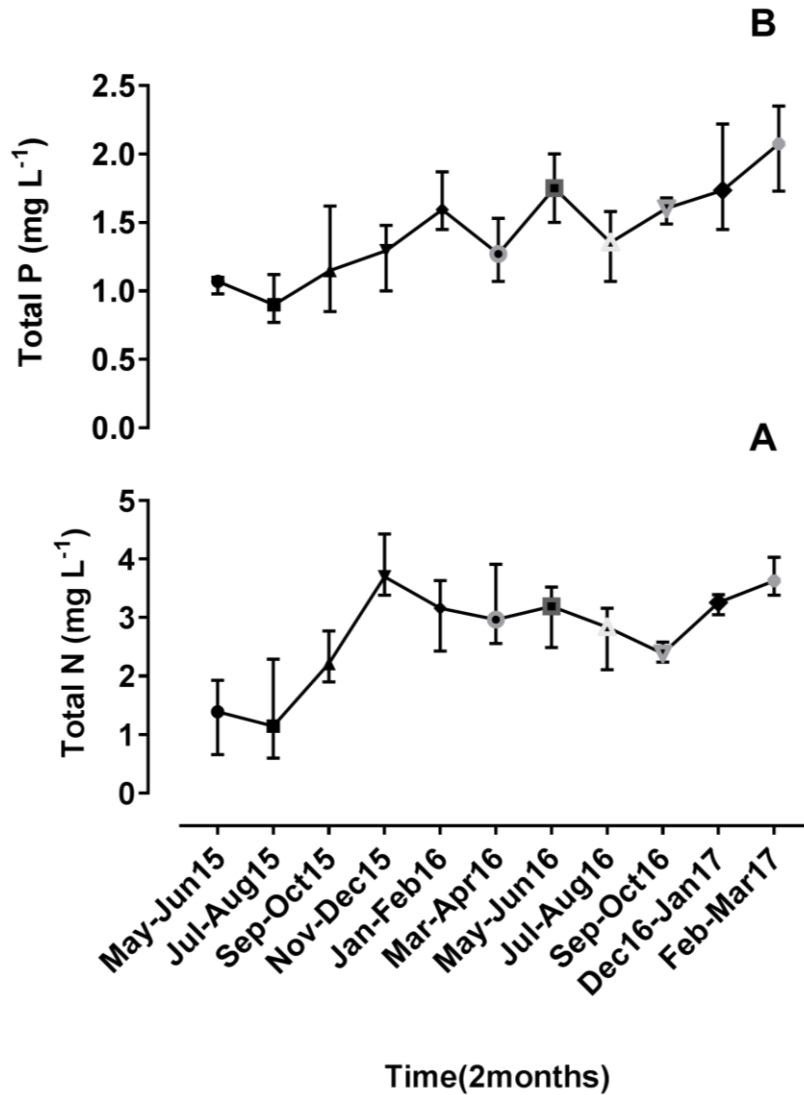


Figure 3.5: The variation in Bogoria's total N and total P concentrations over the period of study (May 2015-Mar 2017).

A) Total N, (B) Total P. Error bars represent 95% CI; n = 6.

There were statistical significant differences in total N and total P concentrations between time groups, $X^2(10) = 49.91$, $p < 0.0001$ (N), $X^2(10) = 48.60$, $p < 0.0001$ (P). The tables below (Tables 3.5 and 3.6) show the post hoc test results where 6 and 7 out of 55 pairwise comparisons were significantly different from each other for both parameters respectively.

Table 3.5: The significant results of Bonferroni post hoc tests for pairwise comparisons in total N of Lake Bogoria (May 2015-Mar 2017).

pairwise	Test statistic	Adjusted <i>p</i> value	Effect size (<i>r</i>)
May-Jun15 vs. Nov-Dec15	- 8.67	< 0.0001	0.63
May-Jun15 vs. Feb-Mar17	- 8.83	< 0.0001	0.63
Jul-Aug15 vs. Feb-Mar17	-8.50	< 0.001	0.63
Jul-Aug15 vs. Nov-Dec15	-8.33	0.001	0.63
Sep-Oct15 vs. Feb-Mar17	-6.83	0.020	0.64
Sep-Oct15 vs. Nov-Dec15	-6.67	0.027	0.64

The significance level (α) is 0.05.

Table 3.6: The significant results of Bonferroni post hoc tests for pairwise comparisons in total P of Lake Bogoria (May 2015-Mar 2017).

pairwise	Test statistic	Adjusted <i>p</i> value	Effect size (<i>r</i>)
Jul-Aug15 vs. May-Jun16	- 7.00	0.014	0.63
Jul-Aug15 vs. Dec16-Jan17	- 7.50	0.005	0.63
Jul-Aug15 vs. Feb-Mar17	-9.17	< 0.0001	0.63
May-Jun15 vs. Dec16-Jan17	-6.67	0.027	-0.63
May-Jun15 vs. Feb-Mar17	-8.33	0.001	0.63
Sep-Oct15 vs. Feb-Mar17	-7.17	0.010	-0.63
Nov-Dec15 vs. Feb-Mar17	-6.83	0.020	0.63

The significance level (α) is 0.05.

3.3.1.4 Variability in Chl-a content of Lake Bogoria

There was a sharp increase in the biomass of Chl-a from 161.08 $\mu\text{g L}^{-1}$ at the beginning of the study to 334.62 $\mu\text{g L}^{-1}$ in Sep-Oct 2015, then a progressive decrease with a slightly improving trend at the end of the study using acetone extraction method (Fig 3.6). The difference in Chl-a content between the time groups was statistically significant, $X^2(10) = 30.15$, $p < 0.001$. The post hoc tests results revealed that the Chl-a concentration in Jul-Aug 2016 was significantly lower than Jul-Aug 2015 and Sep-Oct 2015 (6.67, $p = 0.027$) and (9.00, $p < 0.0001$) respectively. It was also significantly lower in Sep-Oct 2016 than Sep-Oct 2015 (6.50, $p = 0.038$).

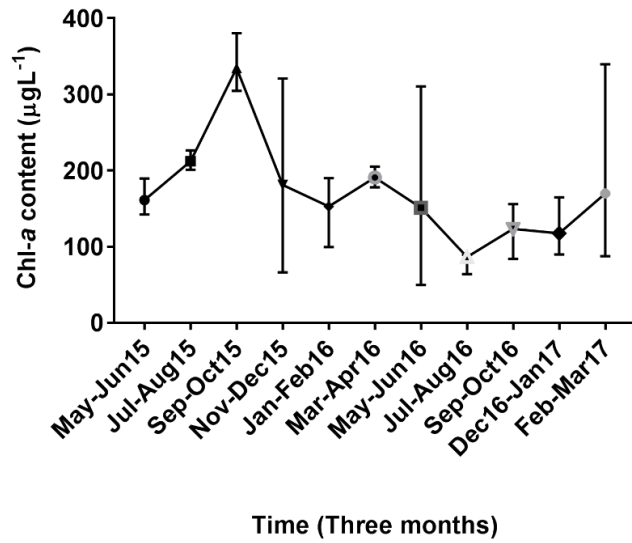


Figure 3.6: The variation in biomass of Chl-a ($\mu\text{g L}^{-1}$) of Lake Bogoria over the period of study, acetone extraction method.

Error bars represent 95% CI; n = 6.

Chl-a concentration from the ETM⁺ satellite sensor collected over 17 years, from 1999 to 2017, showed fluctuations with a slight decrease over the last five years (Figure 3.7).

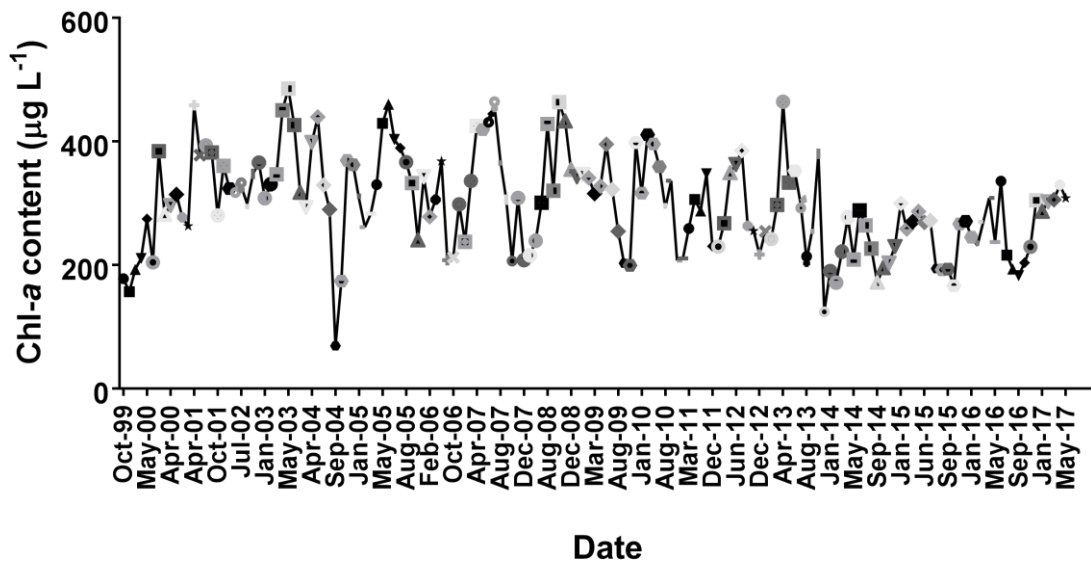


Figure 3.7: Chl-a concentration in Lake Bogoria for the period (1999-2017).

There was significant difference in Chl-a concentration between time groups (remote sensing method), $\chi^2(6) = 19.20$, $p = 0.004$. It was significantly lower in Aug-Oct 2015 and Aug-Oct 2016 than Dec 2016-Feb 2017, (-4.30 , $p = 0.035$) and (-4.50 , $p = 0.021$) respectively (Figure 3.8).

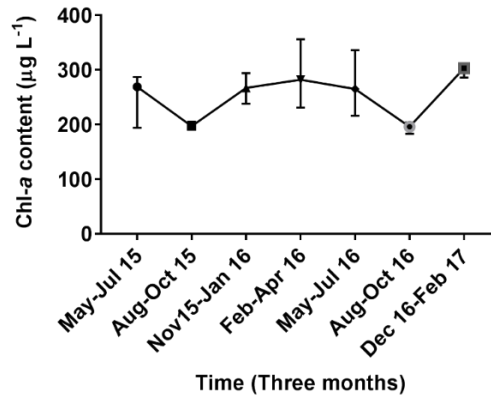


Figure 3.8: The variation in biomass of chl-a ($\mu\text{g L}^{-1}$) in Lake Bogoria over the period (May2015-Feb2017), remote sensing method.

Error bars represent 95% CI; $n = 5$.

3.3.2 Time series forecasting of Chl-a content of Lake Bogoria

The Auto Regression Integrated Moving Average (ARIMA) (0, 0, 1) (1, 0, 1) model was statistically significant for all parameters and so could be used to forecast the time series of Chl-a of Lake Bogoria, $p < 0.0001$ (Table 3.7). The forecasting plot (Figure 3.9) shows this result. Although a small amount of autocorrelation remained (Figure 3.10), the Durbin Watson test revealed that there were no autocorrelations between the residuals (test statistic = 2.52). Moreover, the residuals were random (Ljung-Box test Q-statistic (15) = 24.27, $p = 0.061$). Table 3.8 shows the model fit results. Therefore, and based on these results, future values were forecasted for the period of Jun 2017- Dec 2018, as shown in Table 3.9.

Table 3.7: Estimates of the model parameters.

		Estimate	SE	t	Sig (p)
MA	Lag 1	0.553	0.059	9.361	< 0.0001
AR, Seasonal	Lag 1	0.962	0.048	20.070	< 0.0001
MA, Seasonal	Lag 1	0.867	0.100	8.661	< 0.0001

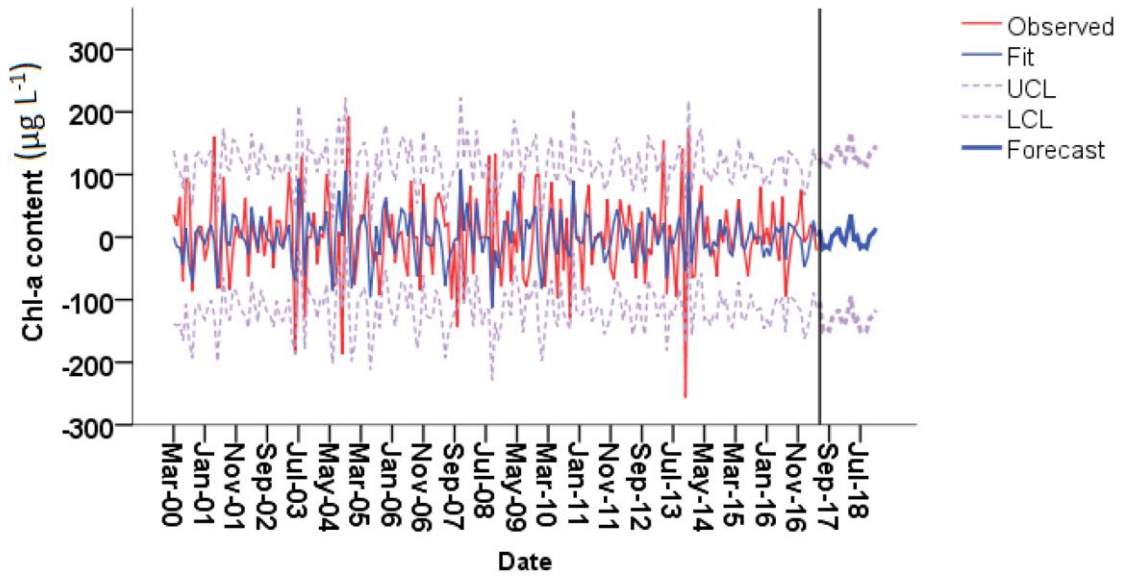


Figure 3.9: Forecasting and real values of Chl-a content of Lake Bogoria (2000-2018).

UCL and LCL are upper and lower confidence intervals for forecasts.

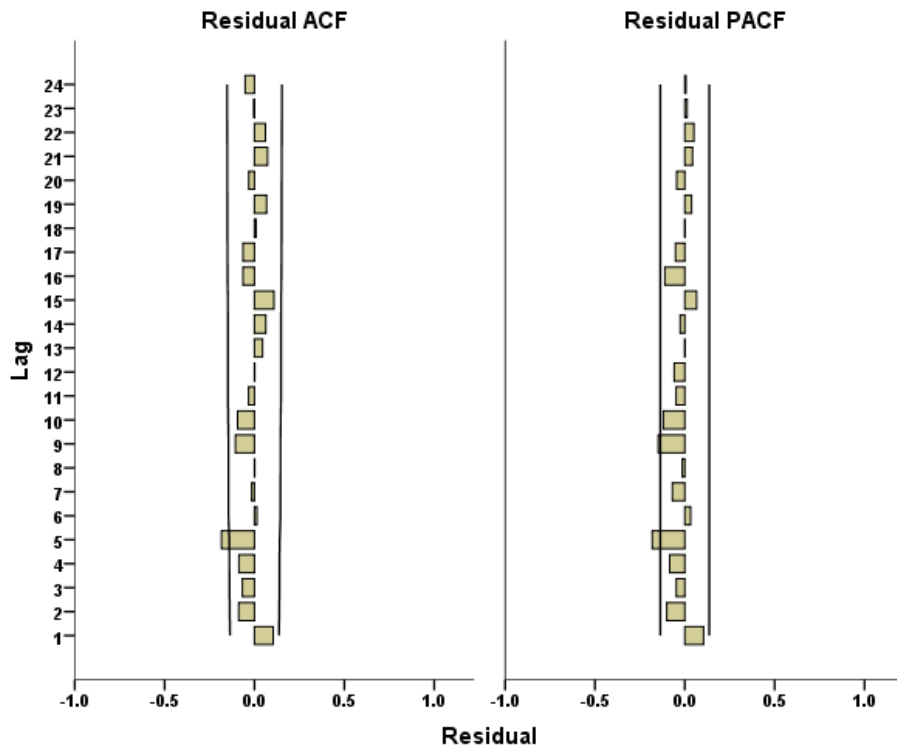


Figure 3.10: Autocorrelation function (ACF) and Partial Autocorrelation function (PACF) for first order differencing of monthly Chl-a content data of Lake Bogoria.

The graph shows an approximately random distribution of residuals.

Table 3.8: ARIMA fit results of Chl- a time series (May 2015-Mar 2017).

Fit Statistic	Mean
Stationary R-squared	0.197
R-squared	0.197
RMSE	58.88
MAPE	229.05
MaxAPE	7308.78
MAE	44.15
MaxAE	0.35
Normalized BIC	8.228
Number of outliers	0

Table 3.9: Forecasting time series data of Chl-a content ($\mu\text{g L}^{-1}$) of Lake Bogoria (Jun 2017-Dec 2018).

Date	Forecasted value ($\mu\text{g L}^{-1}$)	Date	Forecasted value	Date	Forecasted value ($\mu\text{g L}^{-1}$)
Jun-17	320	Feb-18	279	Oct-18	275
Jul-17	302	Mar-18	291	Nov-18	280
Aug-17	288	Apr-18	327	Dec-18	295
Sep-17	370	May-18	320		
Oct-17	272	Jun-18	320		
Nov-17	278	Jul-18	303		
Dec-17	293	Aug-18	290		
Jan-18	289	Sep-18	273		

3.3.3 The relationship between physico-chemical and biological properties of Lake Bogoria

As mentioned earlier in section 3.2.3, the salinity reflects the lake's conductivity; therefore, it was used only to study its correlation with other parameters of the lake. Preliminary analysis showed the relationship between physico-chemical characteristics to be monotonic between only pH & salinity, total N concentration & salinity, total P & salinity and total N & total P, as assessed by the visual inspection of a scatterplot (Figure 3.11).

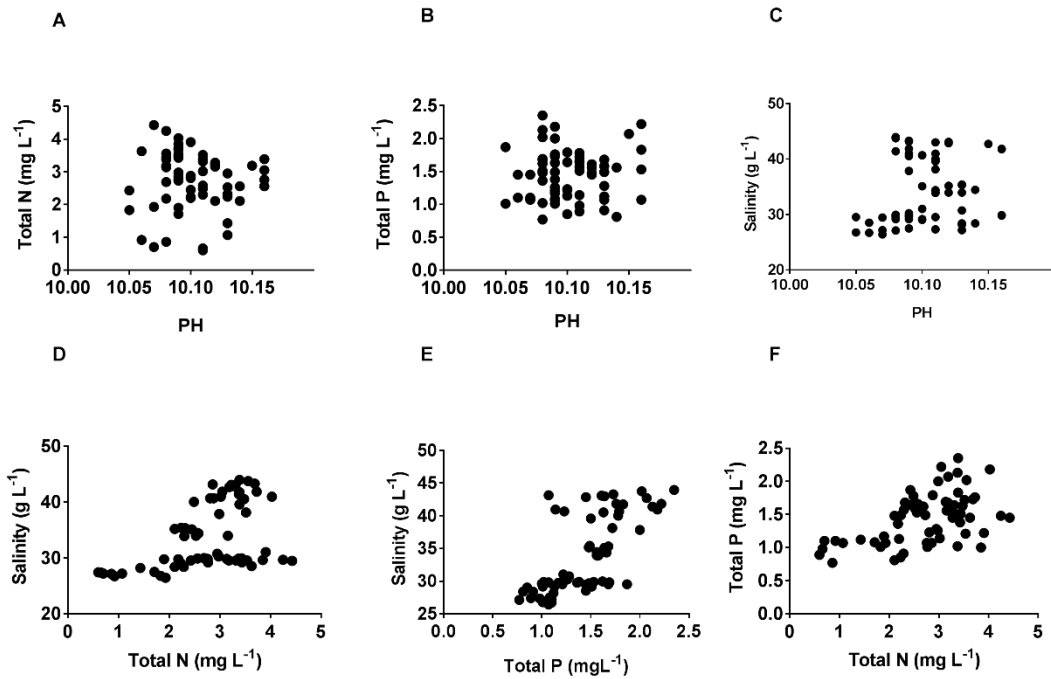


Figure 3.11: Scatter plots showing the relationships between Lake Bogoria properties over the period from May 2015 to Mar 2017.

A and B show non-monotonic relationship, whereas C, D, E and F represent monotonic positive association, $n = 66$.

There was a weak positive relationship between pH and salinity with Spearman's Rank correlation coefficient $r_s(64) = 0.283$, 95 % BCa CI [0.035, 0.518], $p = 0.021$. The total N concentration was moderately positively associated with an increase in salinity and total P concentration throughout the entire period of the study, $r_s(64) = 0.532$, 95 % BCa CI [0.319, 0.703], $p < 0.0001$; $r_s(64) = 0.482$, 95 % BCa CI [0.277, 0.646], $p < 0.0001$, respectively. Total P concentration showed a strong significant increase when salinity increased, $r_s(64) = 0.709$, 95 % BCa CI [0.547, 0.818], $p < 0.0001$.

The only significant predictor of Chl-*a* among the four predictors (salinity, pH, total N, total P) was total N, $F(1, 21) = 4.424$, adjusted $R^2 = 0.14$, $p < 0.048$ – 14 % of the variation in Chl-*a* content could explain by total N concentration. This result was only obtained when considering remote sensing data; with acetone extraction data, the test was not significant. The prediction equation was – Chl-*a* content = $-1.832 + 32.06 \times \text{total N concentration}$ (Table 3.10).

Table 3.10: Summary statistics of the linear regression model.

Model	Unstandardized Coefficients		Standardized Coefficients	t	Sig. (p)	95 % Confidence Interval for B	
	B	Std. Error	Beta			Lower Bound	Upper Bound
Constant	-1.832	8.614		-0.213	0.834	-19.801	16.137
Total N	32.065	15.244	0.426	2.103	0.048	0.266	63.863

This means that an extra mg L⁻¹ of total N leads to a 32.07 µg L⁻¹ increase in Chl-a concentration. A scatterplot of Chl-a concentration against the total N concentration with a superimposed regression line indicated a positive linear relationship between the variables, with a correlation coefficient (*r*) of 0.426 (Figure 3.12).

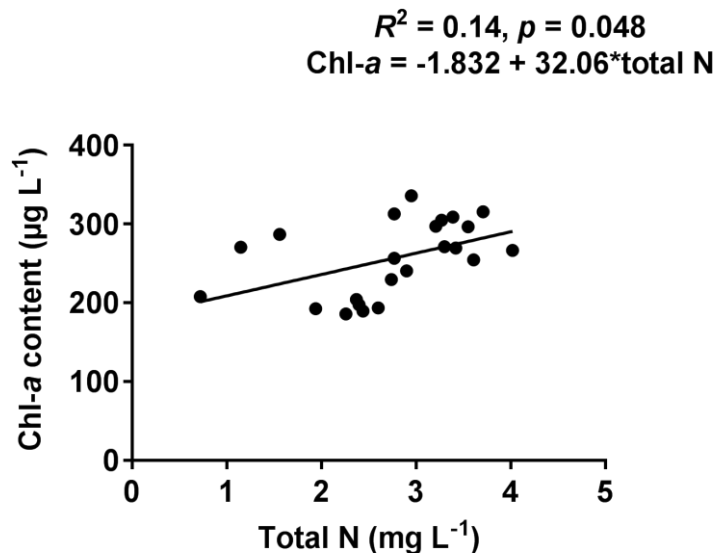


Figure 3.12: Regression line describing the relationship between total N and Chl-a concentration (phytoplankton biomass) for Lake Bogoria.

Data represent the monthly means of the period between May 2015 and Mar 2017, *n* = 23.

There was homoscedasticity and normality of the residuals as assessed by visual inspection of the plot of standardized residuals versus standardized predicted values, and a normal probability plot respectively. Moreover, there was the independence of residuals, as assessed by the Durbin-Watson statistic, of 2.141. Model summary and ANOVA test results are shown in Appendix 8.2 Table 8.3 and 8.4 respectively. Other physico-chemical lake properties were not

good predictors of Chl-a. This was because the regression model did not fit (ANOVA test was not significant, $p > 0.05$).

3.4 Discussion

Various factors limited the interpretation of the physico-chemical properties of Lake Bogoria during the period May 2015 to March 2017. The first is that all analyses were conducted in the UK (University of Leicester) and not at the study site. The major difficulty that this causes is the time difference between sample collection and analysis, which can impact measurements such as pH and nutrient concentration (N and P). The samples were often not shipped for three months post collection, although they were stored immediately in a lake-side freezer according to a standard method described in Chapter 2 until being shipped. To minimise errors however, the total concentration for each species was measured when analysing nutrient concentrations (N and P), so changes between forms were not relevant.

Lake Bogoria is physico-chemically stable, compared to its neighbouring lakes. It is deeper than most lakes, such as Lake Nakuru so is protected from sudden, significant and short-term changes in lake water properties. The pH was relatively stable, ranging from 0.11 units over the study period. This is consistent with other studies such as Harper *et al.* (2003) who showed that the pH of Bogoria changed by only 0.7 units over Intermittent intervals between 1972 and 2003. Schagerl *et al.* (2015) also found that the pH of Bogoria was stable at the range of 10.0 ± 0.2 over the period of Jul 2008 to Oct 2009. The stability of the lake's pH was also confirmed by the correlation between pH and total N, P parameters, where there was no relationship. The only relationship was between the pH and salinity parameters, which even then might, in fact, have no effect on pH, as it was a very weak association ($r_s = 0.283$, $p = 0.021$). Therefore, all the above observations reflect Melack (1981) original findings that the pH of Lake Bogoria is stable between 10.3 and 10.2. Similarly, the pH of other neighbouring lakes such as Lake Nakuru and Lake Elmenteita was approximately stable at a mean of 10.7 and 10.6 respectively over a whole year (October 1988 to September 1989), although the conductivity of both lakes was lower than Bogoria at a mean of 23.4 and 16.6 mS cm^{-1} respectively (Mwatha,

1991). It can thus be suggested that the lake water is well buffered against changes in other parameters.

Conductivity and salinity were varied and less stable over the study period indicating an upward trend. Their values were moderate and sometimes lower than those in previously reported observations, especially with regards to data obtained from the 1970s (Table 3.11). This also accords with (Clough, 2015), who showed that the conductivity of Bogoria waters has decreased compared to earlier records and there was a very high lake level indicating freshwater dilution.

Table 3.11: Summary of the salinity and conductivity data of Lake Bogoria (Mach 1974- May 2017).

Study period	EC ms cm ⁻¹	Salinity ppt	Reference
Mar-1974	77	-	(Vareschi, 1978)
13 Apr-1974	72	-	(Melack, 1981)
1975-7	59	-	(Harper <i>et al.</i> , 2003)
1978	44	-	(Harper <i>et al.</i> , 2003)
1988/9	36.8	-	(Harper <i>et al.</i> , 2003)
2000-3	74.2	-	(Harper <i>et al.</i> , 2003)
Jun2001-Sep2002	-	40-50	(Ballot <i>et al.</i> , 2004a)
Aug2008- Oct2009	67.0	43.10	(Jirsa <i>et al.</i> , 2013)
Jul2008 –Oct 2009	-	43.1	(Schagerl <i>et al.</i> , 2015)
2009-2013	25-50	-	Unpublished data (Robinson, 2015)
Sept 2014	29.40	-	Unpublished data (Clough, 2015)
May2015-Mar2017	46.10	30.1	Current study

It should be noted that the previous low measures of conductivity, recorded in 1978 and 1988/9, both corresponded with periods of “El Nino” heavy rainfall and maximum lake levels of the continuously-recorded Lake Naivasha to the south (Harper *et al.*, 2011). The most recent decrease in lake’s salinity and conductivity of my study was due to the abundant influx of freshwater during the beginning of the current decade, which led to the dilution of surface waters (see chapter 2, Figure 2.3 b) (Harper, Tebbs, pers. obs.) (Oduor and Kotut, 2016). Another possible cause, which could make a small difference in the results of determining the salinity and conductivity values of this type of water, is the measurement method itself, as described in sections 3.2.2 and 3.2.3. For example, if the conductivity was measured without water dilution the results (between 28.4 and 29.6 mS cm⁻¹) (Clough, 2015) would be lower than the

actual values, therefore, this type of water needs pre-treatment before proceeding with the measurements.

The decrease in conductivity did not have a significant impact on pH, but it appears to have had an impact on the disruption of the aquatic ecosystem, leading to a change in the availability of food (Arengo and Baldassarre, 1999, Oduor and Schagerl, 2007a, Hill *et al.*, 2013). Melack (1988) also suggested that the sudden change in salinity of the water body, which exceeds the physiological endurance of cyanobacteria, is likely to cause species changes. Cyanobacteria of the genus *Arthrospira* can withstand different levels of conductivity (salinity), and are found in lakes with high salinity and whose conductivity exceeds 60 mS cm⁻¹, as well as in low salinity aquatic environments, where the conductivity is about 6 mS cm⁻¹ (Fužinato *et al.*, 2010). Kebede (1997) tested the growth of *Arthrospira* under different conditions of salinity (with adding 13-88 g of NaHCO₃, NaCl or NaSO₄) and found that growth at the same extent decreased but did not stop completely. This wide range of the genus' salinity tolerance is supported by the finding of this study, where salinity varied between 28.43 and 43.97 g L⁻¹. *Arthrospira* is a well-adapted cyanoprokaryote which almost forms a unialgal biomass of this harsh environment.

The availability of essential nutrients, such as P and N, is an important factor in limiting and shaping phytoplankton blooms (Paerl, 1996, Oliver and Ganf, 2000). During my study period, the concentrations of both elements (Total N = 2.87 mgL⁻¹ and total P = 1.49 mgL⁻¹) were low compared to previous measurements. For example, Ballot *et al.* (2004b) recorded high mean of total P concentrations (2.1–14.4 mgL⁻¹) and a high mean of total N concentrations (2.8–5.6 mgL⁻¹) during the period from Jun 2001 to Sept 2002. Schagerl *et al.* (2015) reported levels of 3.371 mgL⁻¹ of total P and 4.7 mgL⁻¹ total N between Jul 2008 and Oct 2009. This gradual decrease in the concentrations of these two components may be due to the dilution by freshwater input that the lake has received since 2010.

In comparison, lakes in the surrounding area such Lake Nakuru and Lake Elmenteita showed much higher nutrient concentrations with values of 4.1, 4.4

mgL⁻¹ (Total N) and 2.5, 2.1 mgL⁻¹ (Total P) respectively in the late 1980s (Mwatha, 1991). In contrast to Lake Bogoria where almost no human activity exists, at Lake Nakuru and Lake Elmenteita, anthropogenic activities play an important role in nutrient supply. For instance, Lake Elmenteita's hot springs are used for the personal hygiene by the local people, while Lake Nakuru is the drain for the sewage of the city, which is considered as an important factor contributing to increase in nutrients in the lake (Ballot *et al.*, 2004b). Almost all a lake's N and P are present in inorganic soluble forms at high pH. The concentrations of these two nutrients were significantly positively associated with the salinity of the lake water. This finding is consistent with that of Jirsa *et al.* (2013), who reported that the conductivity of Lake Nakuru was strongly positively correlated with dissolved-bound nitrogen (DN). Moreover, the N and salinity correlation supports evidence from previous observations of Curtis and Adams (1995), who found that there was a strong positive correlation between dissolved organic matter (DOM) with an N-content characteristic of allochthonous DOM and conductivity of saline lakes in North America. Furthermore, another factor that should not be overlooked when comparing Lake Bogoria with a shallow lake such as Lake Nakuru is that Lake Bogoria is a chemically stratified lake (Renaut and Tiercelin, 1994). In other words, its water layers do not mix for long periods of time, unlike Lake Nakuru, where water layers mix daily. This, in turn, coincided with the high dilution of water (the vast quantities of fresh water that the lake received) could affect the distribution of the nutrients in different layers of the lake.

The two methods used in the current study to measure the concentration of Chl-*a* in the lake generally showed a progressive reduction in phytoplankton biomass during the study period (using the acetone extraction) or over the last five years (using remote sensing). This reduction in Chl-*a* reflected the increase in lake levels (higher surface area), which suggests that the inflow of freshwater had a negative effect on the phytoplankton communities. Robinson (2015) also found that the Chl-*a* concentration decreased between 2009 and 2013.

Environmental factors have been used as predictors for phytoplankton biomass in temperate lakes. In my study, among four repressors, only total N had a

correlation with Chl-a, 14 % of its variation was explained by total N. In fresh water, P is considered as a limiting nutrient rather than N. Talling and Talling (1965) suggested that N is more likely to be a major player in the phytoplankton-nutrient relationship in tropical African lakes because nitrate levels were often very low, whereas phosphate levels were relatively high. This is not always so, as Kalff (1983) demonstrated that the Sonachi and Oloidien lakes are highly P deficient (but Oloidien then was freshwater and Sonachi a small crater lake), and it was a short-term study. Therefore, this weak role that total N can play in controlling the phytoplankton biomass of Bogoria could suggest that this alkaline-saline water body is not nutrient limited hence there are other factors at work for collapse events of *Arthrospira*. There are likely to be biotic factors (grazers/ viruses) and the most logical explanation is to be cyanophages (Chapter 6).

The Chl-a concentration was used in this chapter as an indicator of the *Arthrospira* biomass because it is the dominant primary producer (more than 97% of the whole biomass) in this extreme water body (Ballot *et al.*, 2004b). However, the current study found it more suitable to use the *Arthrospira* population as an indicator of its status for the entire period of study. Therefore, besides the study into *Arthrospira* morphology and physiology, further study into changes in this taxon's population was carried out, as explained in the next chapter.

3.5 Conclusion and future work

Lake Bogoria is a well-buffered aquatic system in the East African Rift Valley. With the exception of pH, all other parameters were affected during the long and heavy rainfall that has taken place since 2010. These variations in lake parameters seem not to be the reason for the phytoplankton biomass reduction, however. Total N is more likely to have been responsible for phytoplankton biomass rather than total P, but this role that total N can play as a nutritional limiting factor is slight ($R^2 = 0.14$). This would be a fruitful area for further longitudinal research that would help us to establish a greater degree of understanding into the effects of the environmental factors in such an extreme environment.

Chapter 4 ***Arthrospira* morphology and physiology**

4.1 Introduction

The filamentous, non-heterocystous and helically-coiled cyanobacterium genus *Arthrospira* is the characteristic photosynthetic organism that dominates the phytoplankton of EASLs, particularly Lake Bogoria, sometimes forming thick cyanobacterial mats or scums (Kebede, 1997). It is also commercially renowned as ‘*Spirulina*’ and accounts for about 60% of the global cyanobacteria biomass production for human consumption, cultured in tropical countries (Depraetere *et al.*, 2015). Ten species have been listed by Sili *et al.* (2012), four of which are the most widespread and well-studied (Komárek and Lund, 1990); these are *A. fusiformis* (Voronichin) Komarek & Lund, *Arthrospira jenneri* Stizenberger ex Gomont, *A. maxima* Setchell & Gardner and *A. platensis* (Nordstedt) Gomont.

The genus is the main diet source for lesser flamingos, *Phoenicopterus minor* Geoffroy; a fully-grown adult lesser flamingo needs to consume up to 72 g dry weight (DW) of *Arthrospira* per day in these harsh environments (Vareschi, 1982). Birds rapidly move from one lake to another when the food level falls markedly below this (Harper *et al.*, 2016). There have been alarming periods of mortality of large fractions of the population of *P. minor* at some lakes in Kenya and Tanzania (Harper *et al.*, 2003, Harper *et al.*, 2016). Despite the many theories that have been suggested as causes for the death of these birds, the real reason remains unclear (see section 1.2.3.7). Nutrition is a key factor in the survival of all organisms and life in general, so studying the morphology and physiology of *Arthrospira* provides a good foundation in the search for an explanation of whether *Arthrospira* waxes and wanes may cause lesser flamingos to occasionally die in large numbers.

The morphology of the filaments found in *Arthrospira* is arranged as a multicellular, cylindrical and unbranched trichome enclosed in a thin sheath within an open helix. The filaments show little tightness at cross-walls that separate the trichome into the cells (Tomaselli, 1997). The helix geometry of the trichome can vary according to different species; these differences can be found in the trichome length, coil pitch, degree of coiling (helicity), colour, attenuation

and diameter. These parameters shape the trichome architecture into different morphotypes; they are also highly affected by physico-chemical growth conditions (Vonshak and Tomaselli, 2000). For example, reversible change of filament structure from coiled to spiral shape has been observed after transferring *Arthrospira* filaments from liquid to solid media (Van Eykelenburg and Fuchs, 1980).

The abundance of *Arthrospira* spp. is sometimes irregular (Schagerl and Oduor, 2008, Krienitz and Kotut, 2010). Environmental stresses have been suggested as the main factor for this (Schagerl and Oduor, 2008). Some reduction in *Arthrospira* abundance may be associated with its morphological changes, but very few thorough studies have so far been conducted into its morphological variability. Therefore, it is of great importance to observe and expand our knowledge of morphological aspects of *Arthrospira* in their natural habitats and in controlled culture systems.

Previous studies of the ultrastructure of *Arthrospira* strains have provided phycologists with vital evidence to differentiate between two genera, *Arthrospira* and *Spirulina* (Muhling, 2000). However, no studies thus far have investigated the ultrastructural of *Arthrospira* found in the EASLs, particularly Lake Bogoria. This study will thus contribute to the field by providing a deeper insight into the anatomy of *Arthrospira*, and differences between all morphotypes.

With the exception of *Synechococcus*, which is capable of swimming, all motile cyanobacteria are free floating and display-gliding motility, therefore, trichome motility has also been used as a taxonomic tool for *Arthrospira* species. Two forms of trichome, benthic and planktonic, have been observed around the world based on the possession of gas vacuoles. Komárek and Lund (1990) used this feature to classify *A. platensis* and *A. jenneri* as benthic species, meaning that they do not have gas vacuoles. On the other hand, *A. maxima* and *A. fusiformis* were classified as planktonic, as they possess gas vacuoles. Such taxonomic tools are the starting point of the *Arthrospira* spp. of Lake Bogoria, which has previously been named *A. fusiformis* by other authors without any careful examination.

4.1.1 Aim and objectives

The aims of this chapter were to:

- 1- Characterize the *Arthrospira* spp. of Lake Bogoria by their morphology and physiology.
- 2- Study the change in *Arthrospira* spp. abundance over the period of study.

These aims were achieved by the following objectives:

- 1- Isolating and purifying *Arthrospira* spp. collected from Lake Bogoria.
- 2- Performing microscopy on samples to establish the species of *Arthrospira*.
- 3- Monitoring morphological changes and the physiology of *Arthrospira* morphotypes to understand any differences between them.

This chapter tries to answer the following questions:

- 1- How many *Arthrospira* morphotypes are present in Lake Bogoria and which is/are dominant?
- 2- Is there any relationship between the lake environmental variables and *Arthrospira* abundance?
- 3- Is there any difference in the ultrastructure and physiology of *Arthrospira*'s morphotypes?

4.2 Materials and methods

4.2.1 Axenic Culture production

Axenic (pure) cultures are required for phage isolation (chapter 6) and genomic analysis (chapter 5), so all fresh samples of Lake Bogoria *Arthrospira* cyanobacteria were grown in the same selective medium (see chapter 2, section 2.3.1), to prevent and limit any contamination. The protocols for producing a pure culture of cyanobacteria have been improved to enable elimination of all bacterial contamination; considered a challenging task (Sena *et al.*, 2011). This project has used and sometimes modified most isolation and purification methods that have been used to isolate and purify the filamentous cyanobacteria, both physical and chemical methods of purification.

4.2.1.1 *Arthrospira* isolation

Fresh unfiltered water samples from Lake Bogoria were the starting point of isolation steps. The initial microscopic examination of the water samples showed three different morphotypes of *Arthrospira* in the lake; therefore, the objective was to isolate each morphotype separately. Zarrouk's medium is a selective medium that selects for *Arthrospira* species (Mussagy *et al.*, 2006), which was used to culture, isolate and purify the *Arthrospira* spp. for the entire duration of this study.

The first step of isolation was to wash by screening. About 50 mL of fresh water sample was filtered through sterile 106 and 71 μm sieves (Test Sieve, Endecotts Limited, UK), to decrease the population of microorganisms smaller than *Arthrospira* filaments. Filaments on the sieve were then washed with Zarrouk's medium. This step was repeated several times. Afterwards, filaments on the sieve were suspended in 50 mL fresh Zarrouk's medium.

The second step was to isolate each of the morphotypes. Three had been observed by microscopic examination, hereafter called S, H and C. The single cell isolation technique (Urmeneta *et al.*, 2003) was used with some modifications, using 250 μL of fresh Zarrouk's medium, added to each well of three, microtiter plates (Greiner bio-one, UK), labelled S, H and C. Then, 100 μL of the *Arthrospira* culture from the previous step was placed into the Petri dish under light microscope at 30x magnification (Digi-Steddy, CETI microscopes, UK) and one healthy and complete filament of the first morphotype (not a piece of filament) was transferred into the first well using a sterile needle (Myjector[®] 29G x 1/2"-0.33x12 mm, USA). The second filament was transferred into the second well and the third filament was transferred into the third well until the first plate was completed with only one morphotype, each well containing one filament. This was repeated for the second and third morphotype on the second and the third plates respectively. Needles were replaced between each plate to avoid any cross mixing between the morphotypes. Once all three plates were finished, they were incubated in the chamber, as described in section 2.3.2.

On the third day, three sterile microtitre plates were filled with 250 μL of fresh medium into each well. These plates were separated and labelled according to

the morphotype as before (S, H and C). To wash the filaments, 20 drops (20 μ L each) of fresh medium were placed on a sterile Petri dish, and the first incubated plate was placed on the microscope stage. After that, a single filament from the first well of the incubated plate was picked up with a sterile needle and transferred into the first drop of the medium. The filament was washed by mixing in the drop and then transferred to the second drop. This washing step was repeated until the filament was washed 20 times. Afterwards, this filament was transferred into the first well in the corresponding fresh-labelled plate. This entire washing step was repeated for each of the filaments present in the three plates. To ensure each well had only one filament and each plate had the same morphotype, a well was discarded and the procedure repeated if any different filament morphology was found within a well, or if a well had more than one filament. This method of isolation was repeated for approximately 3-4 months until it was ensured that each plate had only one morphotype and one filament in each well. These three plates were then incubated in the cyanobacterial chamber as described in section 2.3.2.

4.2.1.2 *Arthrospira* purification

Generally speaking, the purification of filamentous cyanobacteria from other bacterial contamination is more difficult and complex than purification of unicellular cyanobacteria. Consequently, and after a relatively long time of isolation, further physical and chemical techniques were needed in order to obtain axenic (free of contamination) *Arthrospira* cultures.

1- Physical purification techniques

Before starting with the first method of this approach, the cyanobacterium cultures from the last isolation step (section 4.2.1.1) were grown in plates for approximately two weeks, then transferred to 100 mL flasks containing 50 mL of fresh medium. To increase the probability of obtaining a good quality of morphotypes, only 10 of the 96 wells were chosen and transferred into 10 flasks for each morphotype; 10 samples were chosen that appeared the most healthy and least fragmented. Afterwards, three sets of flasks (10 flasks per morphotype) were incubated in the cyanobacterial chamber as described in section 2.3.2 for another two weeks.

The first method of physical purification used, described by Vaara *et al.* (1979), was designed based on the idea that most filamentous cyanobacteria have phototactic movement on a scratched agar plate. To test this method, 40 mL of each three morphotypes cultures were washed with fresh medium and pelleted using the sterile sieve. The remaining 10 mL of the cultures were subcultured by adding 40 mL of fresh medium into each flask and returned to the chamber. The pelleted filaments were then placed on the edge of 0.6 % scored cyanobacteria agar (Appendix 8.1). To ensure unidirectional light, the three plates were placed in foil, with lateral holes made to allow the light to pass through from one side (illustrated in Figure 4.1). The three plates labelled H, S and C were incubated under these conditions and checked for the gliding of filaments from the inoculum site every day for 3 days.

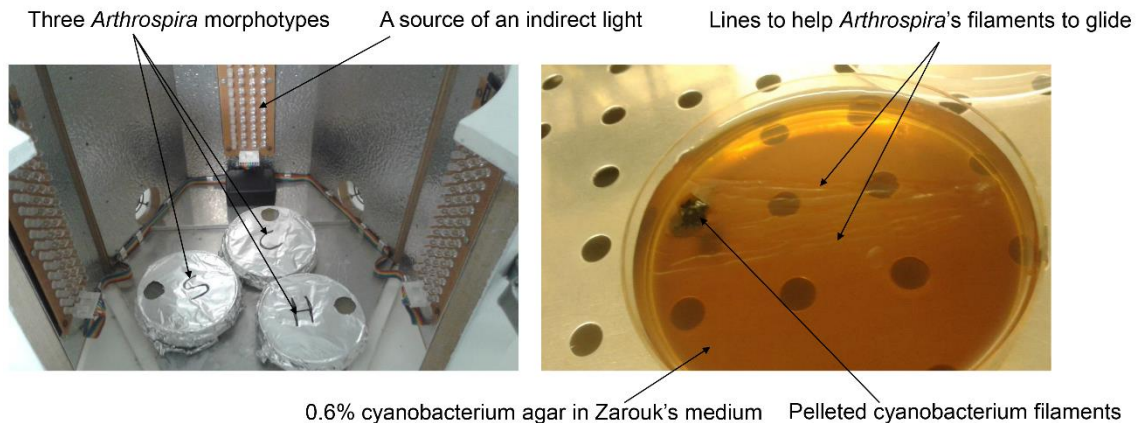


Figure 4.1: The use of a phototactic movement on the scratched agar plate to purify *Arthrospira* spp.

The second physical method of purification was based on the notion that, as the members of this cyanobacterium genus have a helical shape, this shape could increase the chance of contamination, as contaminants could lodge in these coils (e.g. eggs of rotifers). Consequently, the method used by Ciferri (1983) was adopted for the current study - a fragmentation of the trichome into single cells or short fragments containing a few cells each, followed by UV light irradiation. The three *Arthrospira* morphotypes that were successfully isolated separately were targeted for further purification. About 5 mL of each morphotype of *Arthrospira* cultures that had been incubated for two weeks were fragmented using sonication for 20 seconds (Soniprep 150 Plus Digital Ultrasonic Disintegrator, UK). The fragmented trichomes were then filtered

through sterile filter papers of 7 μm (WhatmanTM, UK), and then washed several times with fresh medium. These fragments were then washed off the filter papers and suspended in 25 mL of fresh medium. To be able to isolate these fragments, 20 μL of the fragmented filaments of each morphotype were placed onto a sterile glass slide, then using a light microscope a single fragment was picked up using a sterile needle. To increase the efficiency of this method, the fragment was as short as possible, and then transferred into the first well of a microtitre plate, with each well containing 250 μL of fresh medium. This step was repeated until the microtitre plate was filled with each morphotype, then repeated for the other two. To establish the cyanobacterial cultures, plates were incubated in the chamber as described in section 2.3.2, until filamentous growth was observed. Following the fragmentation step, researchers such as Ciferri (1983) used UV light irradiation to eliminate the contaminants. In this project, UV light treatment was avoided, as it is associated with a high risk of introducing mutations (Vass *et al.*, 2013).

2- Chemical purification techniques

The outputs of the physical techniques were followed by chemical treatments to ensure the elimination of contaminants that the previous methods might not have been able to remove. To prevent potential eukaryotic growth, such as grazers like *Branchionus* spp., different chemical treatments were used. The first widely used procedure was the treatment of *Arthrospira* cultures with cycloheximide (Ji Won *et al.*, 2010). This antibiotic was used to control eukaryotes such as yeast and fungi through protein synthesis inhibition.

Zarouk's medium is alkaline, which degrades cycloheximide and prevents antibiotic activity, therefore, cultures were first washed using autoclaved dH_2O . To do this, 50 mL of fresh cultures in triplicate for the three morphotypes were separately filtered and then washed several times with autoclaved dH_2O through the sieve. Afterwards, each pelleted filament on the sieve was transferred into a sterile flask containing 50 mL of autoclaved dH_2O . This step was repeated for each replicate of the three morphotypes. Before adding 20 $\mu\text{g mL}^{-1}$ of cycloheximide (Sigma Aldrich, UK) to each culture, an aliquot from each flask was used to ensure the culture was $\text{pH}\sim 7$. The treated cultures were

then incubated in the chamber, as described in section 2.3.2, for 72 hours. Once the incubation was completed, all cultures were examined under a microscope for the presence of microzooplankton, then washed using the sieve and re-cultured into Zarouk's medium.

The second method that was tested is a treatment of the cultures with a mixture of urea and ammonium bicarbonate. To do this, 25 mL of fresh cultures of the three morphotypes were incubated with a mixture of 60 mg L⁻¹ of urea (Fisher Scientific, UK) and 100 mg L⁻¹ of ammonium bicarbonate (Acros Organics, UK) (Appendix 8.1) for 72 hours in the chamber, as described above. Afterwards, the cultures were examined microscopically for any eukaryotic contamination.

After physical and eukaryotic purification steps, additional chemical purification was necessary to prevent the potential contamination by heterotrophic bacteria that may stick to the *Arthrospira* filaments. This purification consisted of antibiotic treatments. In this project, this step was carried out using two approaches. The first one was following the work of Sena *et al.* (2011), who suggested the elimination of bacterial contaminants found in *Arthrospira* cultures before determining the contaminants. This might be due to the extreme environment and relatively poor medium that is usually used for culturing these species; therefore, this treatment is related to particularly known contaminants. The antibiotic combination consisting of ampicillin 61.6 µg mL⁻¹, penicillin G 85.8 µg mL⁻¹ (Alfa Aesar®, UK), cefoxitin 76.6 µg mL⁻¹ (Cayman Chemical, USA) and meropenem 38.9 µg mL⁻¹ (Santa Cruz Biotechnology, USA) was prepared (Appendix 8.1). These antibiotics were applied to each morphotype in triplicate. The treated cultures were then incubated in *Arthrospira* chambers in the dark for 72 hours. Cultures were then washed several times with the fresh medium using a sterile sieve. Afterwards, the pellets were transferred to fresh Zarrouk's medium and incubated in the *Arthrospira* chamber until the green filaments of cyanobacterium were observed (approximately 20 days). To check for bacterial contamination, 10 µl of culture was then streaked onto nutrient cyanobacterial agar (Sigma, UK) that was supplemented with 1% glucose (VWR, Belgium), 0.3% yeast extract (Oxoid Ltd, Basingstoke, UK) and 0.5% peptone

(Bacteriological peptone, Oxoid Ltd, Basingstoke, UK) (Appendix 8.1) and incubated in the chamber in the dark for 72 hours.

The second chemical approach that was also used was since *Arthrospira* is a prokaryote; consequently, it is sensitive to antibiotics. Therefore, to avoid or reduce the effect of antibiotic treatment on this cyanobacterium, determining the contaminants before applying additional antibiotics might be a more powerful tool. To do this, PCR using universal 16s rRNA primers was performed. After identifying these contaminants by sequencing and analysing the PCR products, specific antibiotics treatments were also applied.

4.2.2 Long-term preservation of cultures

There is a lack of effective methods for the long-term storage of filamentous cyanobacteria. Furthermore, it is time-consuming to renew the cyanobacterial cultures by sub-culturing, as this can be the main source of contamination. Repeat sub-culturing is also more likely to increase the risk of genetic drifts that can contribute to different genotypes and phenotypes within the strains; to give an example, Muhling (2000) found that the helical shape of *Arthrospira* trichomes was lost in some strains after long-term sub-culturing under laboratory conditions. There is thus an urgent need to develop a reliable method for the long-time preservation of *Arthrospira* spp. This study tested two methods as described in (Muhling, 2000) and Shiraishi (2016) for preserving *Arthrospira* cultures.

4.2.2.1 Cryopreservation

The use of cryoprotectants is the most commonly employed method for bacterial preservation. In the current study, several cryopreservation agents were tested. Two methods of freezing were carried out, first was snap freezing using liquid nitrogen, and the second was to use a - 80 °C deep freeze. These two methods of freezing were used for all samples mentioned below. To do this, 25 mL of the exponential phase of three *Arthrospira* morphotypes were pelleted using a sterile sieve. Afterwards, the dense trichomes were transferred into 2 mL polypropylene screw-top tubes (Sigma-Aldrich®, UK) in triplicate for each morphotype. They have then filled to three quarters with the cryoprotectants accordingly. Besides the commercial cryoprotectant, another three were used.

These were Glycerol, Dimethyl sulfoxide (DMSO) and methanol; the respective concentrations are listed in Table 4.1. After that, the first set of tubes were frozen with the use of liquid nitrogen for 1 hour, and then stored at -80 °C for 24 hours. Another set of samples was frozen inside isopropyl alcohol-insulated cryopreservation containers (NalgeneMr. Frosty™ Cryo 1 °C Freezing Container, Nalge Nunc International Corp., New York) at -80 °C for 24 hours. On the second day, the cultures were regenerated from the frozen samples by thawing at room temperature and then transferred to approximately 30 mL of fresh medium. Subsequently, the cultures were incubated under the standard conditions.

Table 4.1: Cryopreservation agents and their concentration.

Chemical	Concentration (%)
Glycerol (ACROS, UK)	50
Dimethyl sulfoxide (DMSO) (Fisher Scientific, UK)	5, 10 and 30
Methanol (Fisher Scientific, UK)	10
Commercial cryoprotectant agent (Viabank)	

4.2.2.2 Preservation at low temperature

Three morphotypes were tested for long-term preservation under low-temperature conditions. To do this, two sets of flasks containing 25 mL of *Arthrospira* cultures were stored under different growth conditions. The first set was stored in the dark (cardboard box) in a cold room at 4 °C while another set was stored under low light at 4 °C. To evaluate the validity of this method, aliquots were taken every week and examined microscopically.

4.2.3 *Arthrospira* abundance in Lake Bogoria

Six fresh, unfiltered water samples (Aug 2015, Mar 2016, May 2016, July 2016, Dec 2016 and Mar 2017) from the central basin of the lake were preserved with 2.5% glutaraldehyde (Sigma Aldrich, UK) (Appendix 8.1) for qualitative and quantitative analysis of *Arthrospira*. The abundance of three morphotypes S, C and H of *Arthrospira* were counted under light microscope 100x magnification using a plastic Sedwick Rafter Slide (Pyser-Sgi, UK), as described in Harper *et al.* (2003). Fifteen replicates for each morphotype were carried out.

4.2.4 Comparison of trichome characteristics between three morphotypes

An unfiltered water sample that has been collected in May 2016 from the central basin was also used to perform the qualitative analysis of *Arthrospira* in order to characterize the morphological differences between the three morphotypes (H, C and S). One mL of the sample was placed onto the plastic Sedgwick Rafter slide, and then examined using light microscopy at 100 and 200 x magnifications without covering the slide to avoid diminishing the trichome helix with pressure. The following morphological trichome parameters were analysed – the number of coils (turns) per trichome, helix diameter in the middle, helix pitch (distance between coils), trichome length, helicity, colour and trichome end attenuation (Figure 4.2). Average values of parameters were determined after counting and measuring 40 trichomes of each morphotype.

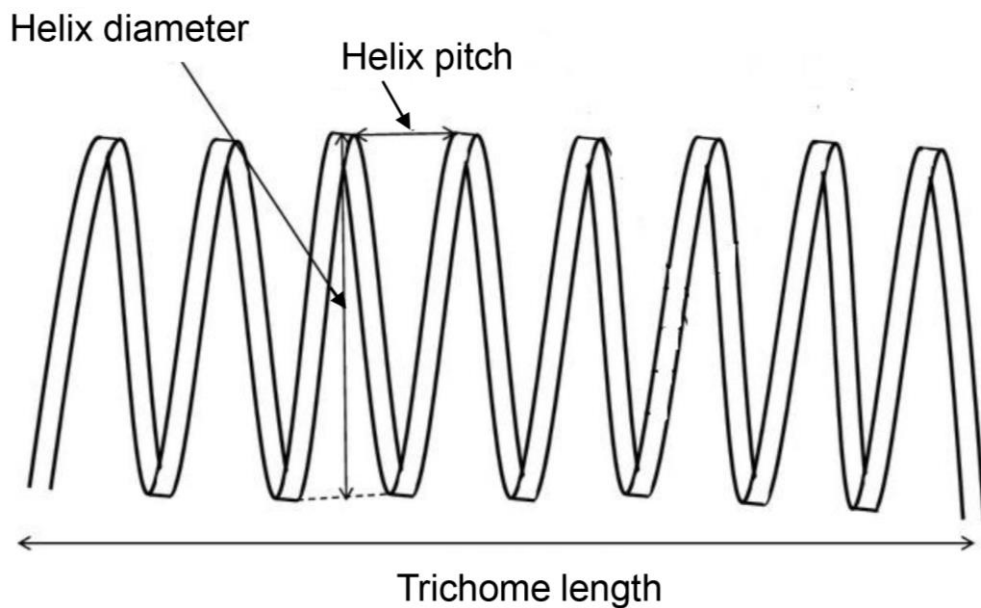


Figure 4.2: Trichome morphological characteristics of *Arthrospira*.

The diagram adapted from (Kaggwa *et al.*, 2013a).

4.2.5 Morphological changes of trichomes

Morphological changes are widespread phenomena amongst helical filamentous cyanobacteria. Studies over the past three decades have focused on the finding the reasons for changes in trichome helicity of *Arthrospira* spp., including medium, light and temperature or the combination of all growth conditions (Muhling, 2000).

This study has attempted to shed some light on the influence of a medium's pH on trichome helicity. To do this, an unfiltered water sample of the lake (May 2016) was firstly examined under a light microscope and the images were recorded with a CETi camera. Afterwards, cyanobacteria of this sample (25 mL) were filtered, washed several times with fresh medium and then cultured in a 25 mL fresh medium at standard conditions for over a month. During the incubation, aliquots were taken every 5 or 6 days and examined under a light microscope. After the incubation was complete, the culture was filtered, washed with filtered Lake Bogoria water and then incubated in a 25 mL water sample from the lake for over five months. To maintain the *Arthrospira*, 5 mL of filtered water sample was added weekly. To mimic the lake Bogoria water, only one condition was adjusted; the pH. There were two reasons for this. The first was the difference between the pH of the medium (pH 9.0) and Lake Bogoria (average pH 10.2). The second reason was that this study tried to use the selective and standard medium for this cyanobacterium (Zarrouk's medium), and the adjustments of other factors, such as nutrient components, is too extensive topic to investigate. Therefore, to evaluate the effect of pH on trichome helicity, two 1-litre bottles of Zarrouk's medium were prepared, one with a pH of 9.0 and another of 10.2, which was adjusted with 5 M NaOH. Three morphotypes of *Arthrospira* (S, H and C) were cultured in triplicate in 50 mL of two sets of flasks. The first set contained medium (pH 9.0) while the other set contained medium (pH 10.2). The flasks were incubated as described in section 2.3.2. The cultures were microscopically examined, and micro images were taken.

4.2.6 Motility assay

A simple definition of gliding motility can be described as the "self-propulsion across a solid or semi-solid material without the aid of any visible organ (i.e. flagellum) or apparent change in the shape of the organism" (Castenholz, 1982). Except for *Synechococcus*, all motile cyanobacteria glide. *Arthrospira* spp. are famous for gliding motility on a solid substrate (Urmeneta *et al.*, 2003). To test this for the Lake Bogoria isolated *Arthrospira*, 10 mL of its three morphotypes were concentrated separately using a sterile sieve. Afterwards, approximately 100 μ L of these dense cultures were inoculated on the centre of low strength Zarrouk's medium agar plates (0.6%) (Figure 4.3) (Appendix 8.1). Three plates per morphotype were prepared. Subsequently, the plates were incubated as described in section 2.3.2. The ability to glide was monitored for a week and microscopic images were taken.

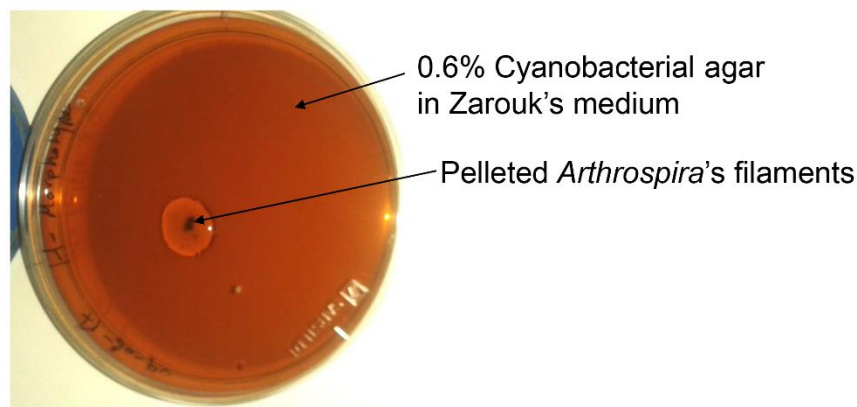


Figure 4.3: Digital image showing the motility assay procedure.

4.2.7 Electron microscopic analysis

4.2.7.1 Transmission Electron Microscopy (TEM)

TEM was used to identify and compare the ultrastructure of this cyanobacterium and examine for cyanophages within the cyanobacterium (see chapter 6, section 6.2.2).

Fixation and embedding

30 mL of the six unfiltered water samples from Lake Bogoria from six different collection times (Aug 2015, Mar 2016, May 2016, Dec 2016 and Mar 2017), and the three *Arthrospira* morphotypes (H, C and S) that were isolated from the lake

and cultured in the laboratory were fixed in glutaraldehyde in Zarrouk's medium (2.5 % final concentration) for 4 hours. The samples were then washed twice with a growth medium using a centrifuge. From this step, all processes were accomplished with a rotary mixer. The pelleted filaments were subsequently embedded in 3% agar. Afterwards, the agar embedded pellet was dissected into 1 mm³ blocks, suspended in the medium. Before fixing the blocks in 1% Osmium tetroxide/1.5% potassium ferricyanide (Appendix 8.1) in the medium for 1.5 hours, the excess medium was discarded. After the fixation step was completed, the samples were dehydrated in 70% ethanol for 30 min. The dehydration step was carried out overnight by replacing the ethanol with fresh 70% ethanol. The following day, further dehydration steps were performed by gradually increasing the ethanol concentration (90% once, then three times with 100%) for 30-minute durations. During the dehydration, the resin was prepared (Appendix 8.1). Subsequently, the dehydrated samples were then gradually embedded in the resin by increasing the Spurr's modified concentration. Table 4.2 shows the ratios of the analytical grade ethanol: Spurr's modified resin.

Table 4.2: Composition of the ethanoic resin solution and incubation time.

Analytical grade ethanol : Spurr's modified resin	Incubation time (min)
3: 1	60
1: 1	90
3: 1	90

Once the last incubation was completed, the resin solution was replaced with 100% of Spurr's modified resin for several durations; firstly for 30 min, secondly overnight, and lastly twice for 90 min. Before embedding and polymerising the samples into beam capsules for 16 hours at 60 °C, the resin was replaced with 100 % fresh resin.

Sectioning of embedded cyanobacterium samples

Polymerised samples were sectioned into 80 nm thick using a Leica Ultra cut E ultramicrotome. Prior to collecting the ultra-thin sections onto copper mesh grids, they were launched into a tank of water to avoid cracking. The grids were then stained with 1 % uranyl acetate 10 µL (divided into drops) for 5-10 sec. To

leave a thin film of the stain on the surface of the grid, Whatman filter papers were used to blot the excess stain. Subsequently, the grids were dried at room temperature into sterile Petri dishes. Specimens were then viewed using the JEOL 1400 TEM operated at 80 kV. Digital images were captured using an SIS Megaview III digital camera with attached software.

4.2.7.2 Scanning Electron Microscopy (SEM)

Images were taken using SEM after several pre-treatments to study the ultrastructure of the surface of *Arthrospira* filaments from Lake Bogoria. An unfiltered sample from Aug 2015 was preserved in glutaraldehyde, embedded in agar and then dissected as described in section 4.2.7.1. All mixing steps were done on a rotary mixer. The cyanobacterium blocks were then washed twice with the medium for 5 minutes. The sample was dehydrated afterwards, by gradually increasing the concentration of ethanol. Table 4.3 shows all dehydration conditions.

Table 4.3: Dehydration agent concentrations and incubation time.

Ethanol concentration (%)	Incubation time (min)
30	30
50	30
70	30
90	30
100	30
100 Analytic grade ethanol	Twice 30 min each

The sample was incubated in ethanol/hexamethyldisilazane (HMDS) twice for 30 minutes each after the dehydration steps were completed. Subsequently, it was incubated twice in 100 % of HMDS for 30 minutes each. The sample was prepared for gold coating by discarding all the liquid and the sample air-dried. It was then placed in aluminium stubs and sputter coated with gold. A VG Microtech SC7640 sputter coating unit was operated for 120 secs at 2.2 kV after mounting the sample. The images were taken using a Hitachi S3000h Scanning Microscope with an accelerating voltage of 10 kV.

4.2.8 Statistical analyses

A two-way repeated measures ANOVA was run to determine the effect of different morphology and time on *Arthrospira* abundance ($n = 15$). Analysis of the standardized residuals showed that there was normality, as assessed by the Shapiro-Wilk test and Kolmogorov-Smirnov^a of normality ($p > .05$) (Appendix 8.2, Table 8.5). There were no outliers, as assessed by examination of standardized residuals for values greater than ± 3 . There was sphericity for the main effect of morphotype as assessed by the Mauchly's test of sphericity, $\chi^2 (2) = 4.617$, $p = .099$. However, Mauchly's test of sphericity indicated that the assumption of sphericity had been violated for the main effect of the time and the two-way interaction between time and morphology effects, $\chi^2 (14) = 4.617$, $p < 0.0001$ and $\chi^2 (54) = 115.728$, $p < 0.0001$ respectively. Therefore, degrees of freedom were corrected using Greenhouse-Geisser correction estimates of sphericity (epsilon (ϵ) = 0.467) for the main effect of time and 0.306 two-way interaction between time and morphology effects, as recommended by Maxwell & Delaney (2004). Data are presented as mean \pm standard deviation unless otherwise stated. A paired-samples t-test was used to determine whether there was a statistically significant mean difference between all pairwise of interaction between time and morphology, the significant level was corrected to 0.003.

A Spearman's rank-order correlation (r_s) was performed to assess the relationship between the phytoplankton biomass and *Arthrospira* abundance, $n = 5$. The same test was also used to determine the association between the population of three morphotypes, C, S and H and lake properties (pH, total nitrogen, total phosphorus and salinity), $n = 36$.

The differences in morphological parameters among the three morphotypes were analysed. The data of the trichome length parameter were normally distributed for the three morphotypes, C, S and H, as assessed by the inspection of a Q-Q plot and Shapiro-Wilk test, $p > 0.05$. The helix diameter in the middle and helix pitch parameters were approximately normally distributed after transforming the data using reciprocal and square root transformations respectively, as assessed by Kolmogorov-Smirnov^a test, $p > 0.05$ for two

parameters. There were no outliers in three parameters, as assessed by inspection of a boxplot, and there was no homogeneity of variances, as assessed by Levene's test of homogeneity of variances ($p < 0.0001$); therefore, a one-way ANOVA with Welch Howell of F-ratio correction and Games-Howell test for post-hoc multiple comparisons was used, ($n = 40$). The number of coils per trichome parameter was not normally distributed even with data transformation; therefore, a non-parametric of Kruskal-Wallis H test with a Bonferroni correction for multiple comparisons was used ($n = 40$). Data management and analysis were performed using the statistical program SPSS (Version 24).

The Fiji software was used to process the images of the morphological features of the *Arthrospira*.

4.2.9 Overview

Figure 4.4 summarises the treatment of samples described here.

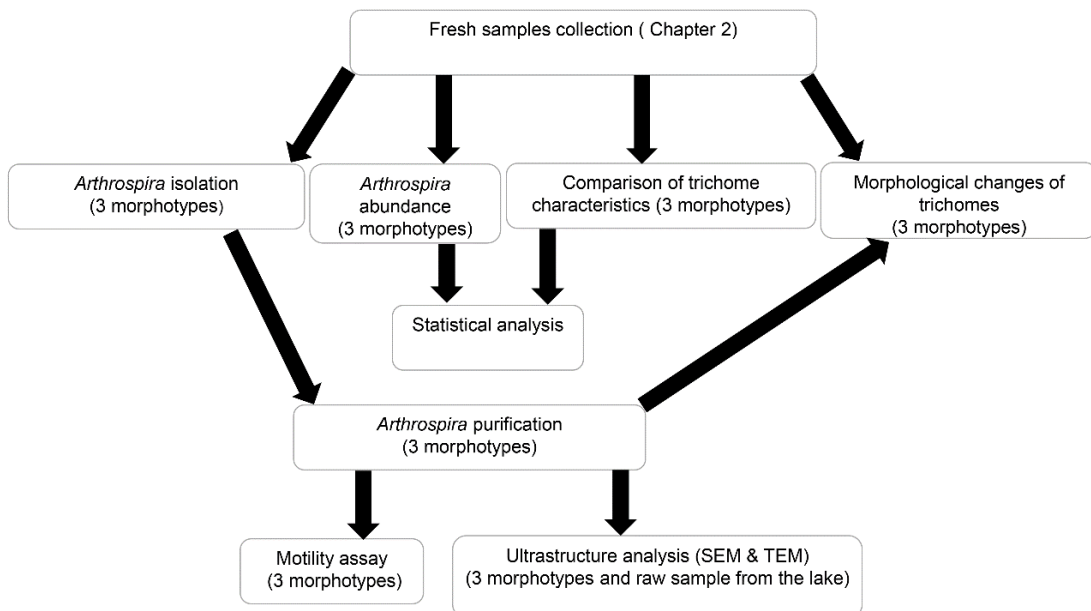


Figure 4.4: Schematic diagram of the sample treatment.

4.3 Results

4.3.1 Production of clonal, axenic cultures of *Arthrospira* spp. of Lake Bogoria

Three distinct *Arthrospira* spp. morphotypes, tightly coiled (H-morphotype), spiral or loosely coiled (S-morphotype), and intermediately coiled (C-morphotype) were observed and successfully isolated from Lake Bogoria's water (Figure 4.5).

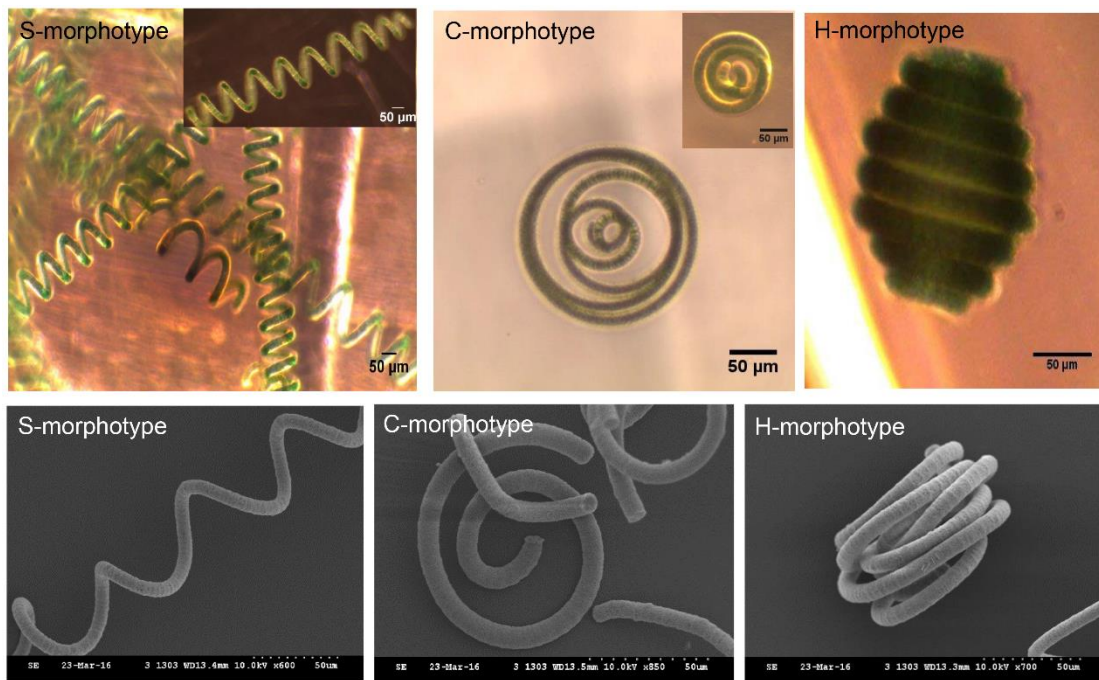


Figure 4.5: Light and SEM images of clonal trichomes of three *Arthrospira* morphotypes (S, C and H) from Lake Bogoria.

Note the variability in the trichome helicity between the three morphotypes. Scale bars = 50 µm.

The combination of two physical methods, a single cell isolation technique and fragmentation, was able to eliminate both microzooplankton and other cyanobacteria. The first chemical treatment that was used to eliminate any potentially remaining microzooplankton was the use of the antibiotic agent cycloheximide; however, this failed mid-experiment – following antibiotic treatment and the transfer of filaments back to normal Zarrouk's medium (pH ~ 9.0), the cells burst (Figure 4.6).

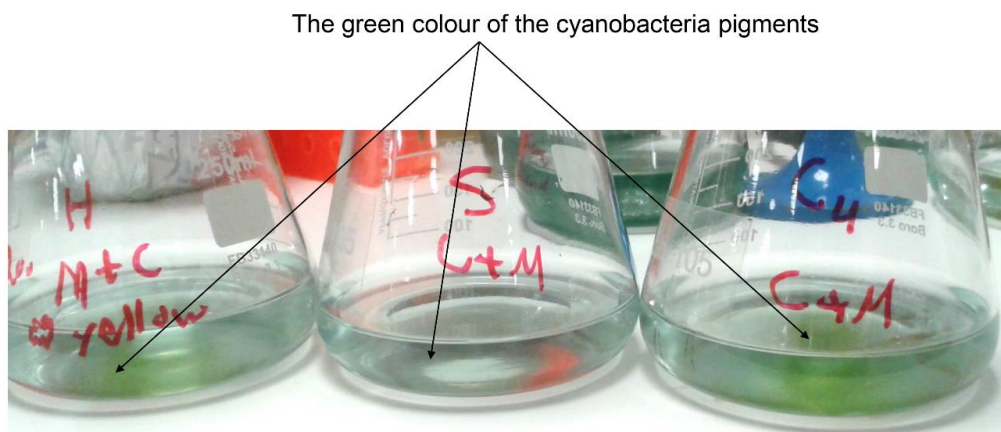


Figure 4.6: Cell lysis of three *Arthrospira* morphotypes after cycloheximide treatment.

The figure shows the spread of the green colour from the cyanobacterium pigments after transferring the filaments from adjusted Zarrouk's medium (pH 7.0) to Zarrouk's medium (pH 9.0).

The second approach was to treat the cultures with urea and ammonium bicarbonate. This seemed to be effective as no microzooplankton was detected post-treatment. In contrast, heterotrophic bacteria were detected again after the antibiotic treatment. Although the treatment of *Arthrospira* cultures with antibiotics significantly reduced the number of bacterial contaminations, it was not able to produce axenic cultures of *Arthrospira*, and this treatment also negatively affected the *Arthrospira* filaments.

The PCR targeting the universal 16S rRNA gene was able to identify the bacterial contaminants. They were *Pseudomonas* spp., *Burkholderia* spp. and other unculturable bacteria. *Pseudomonas* is famous for antibiotic resistance, but some antibiotics that are described as effective, such as gentamycin, imipenem, cefoxitin and meropenem, were used. Unfortunately, the treatment of *Arthrospira* cultures with these antibiotics affected the cyanobacterium itself and the bacterial contaminations were still present (Figure 4.7). Therefore, the *Arthrospira* cultures that were used throughout this study were not axenic cultures (free of bacteria).

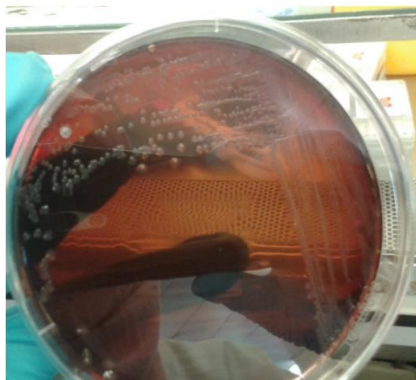


Figure 4.7: Contamination of *Arthrospira*'s culture with heterotrophic bacteria after streaking the culture on enriched Zarrouk's medium plate, incubated for 72 hours.

4.3.2 Long-term preservation of *Arthrospira* cultures

Unfortunately, no surviving cells were observed under all conditions tested and cells lysis was observed as judged by the presence of phycocyanin pigments in the samples (Figure 4.8 A, B and C). All cryoprotectants used were ineffective for *Arthrospira* cultures.

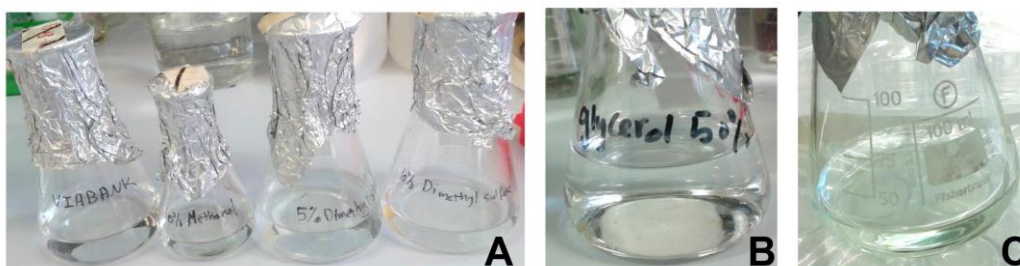


Figure 4.8: Cultures of *Arthrospira* after freezing and thawing.

A) *Arthrospira* cultures were frozen in the presence of various concentrations of cryopreservation agents; from left to right, Viabank, 10% Methanol, 5% DMSO and 10% DMSO. B) 50% glycerol. C) 30% DMSO, then frozen at a cooling rate of approximately $-1\text{ }^{\circ}\text{C min}^{-1}$ using an isopropyl alcohol-insulated cryopreservation container. The green colour was an indicator for cells lysis.

Long-term preservation was also tested by storing the cultures at $4\text{ }^{\circ}\text{C}$ in the dark. Although some *Arthrospira* trichomes still showed viability for approximately two weeks (Figure 4.9), none of the three filament morphotypes survived for more than two weeks under this condition. Most cultures lost their viability during the first month at this low temperature, as judged by the presence of phycocyanin pigment in the samples.

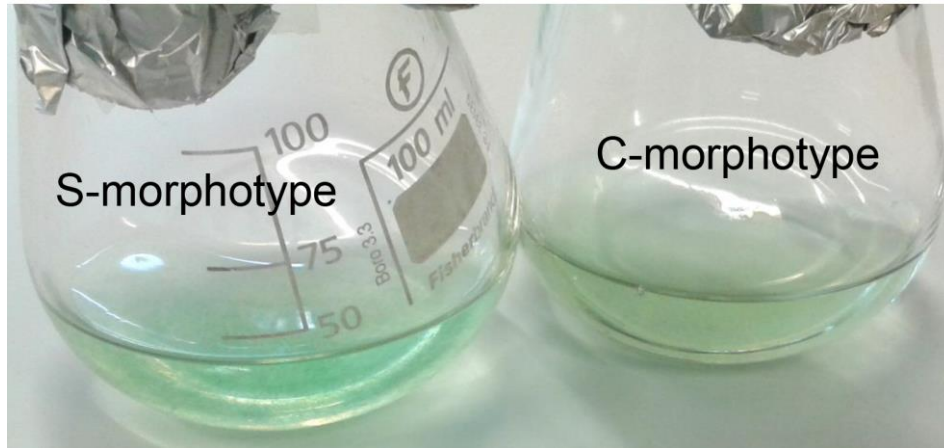


Figure 4.9: *Arthrospira* spp. cultures after being incubated at 4 °C in the dark for approximately two weeks.

Some trichomes still show some viability while the others were lysed, as detected by the spreading of the phycocyanin pigment in the cultures.

4.3.3 *Arthrospira* population

4.3.3.1 Changes in *Arthrospira* population

The three *Arthrospira* spp. morphotypes varied in abundance. The S-morphotype was the most dominant (47.67%) followed by the C-morphotype (40.65%), with the lowest being the H-morphotype (11.69%) (Figure 4.10). The highest population recorded was the S-morphotype (146.47 ± 4.84 trichome mL⁻¹) in Dec 2016. The three morphotypes (C, S and H) crashed during the study period in Jul 2016, to 3.20 ± 1.74 , 30.27 ± 1.75 , and 1.60 ± 1.40 trichome mL⁻¹, respectively.

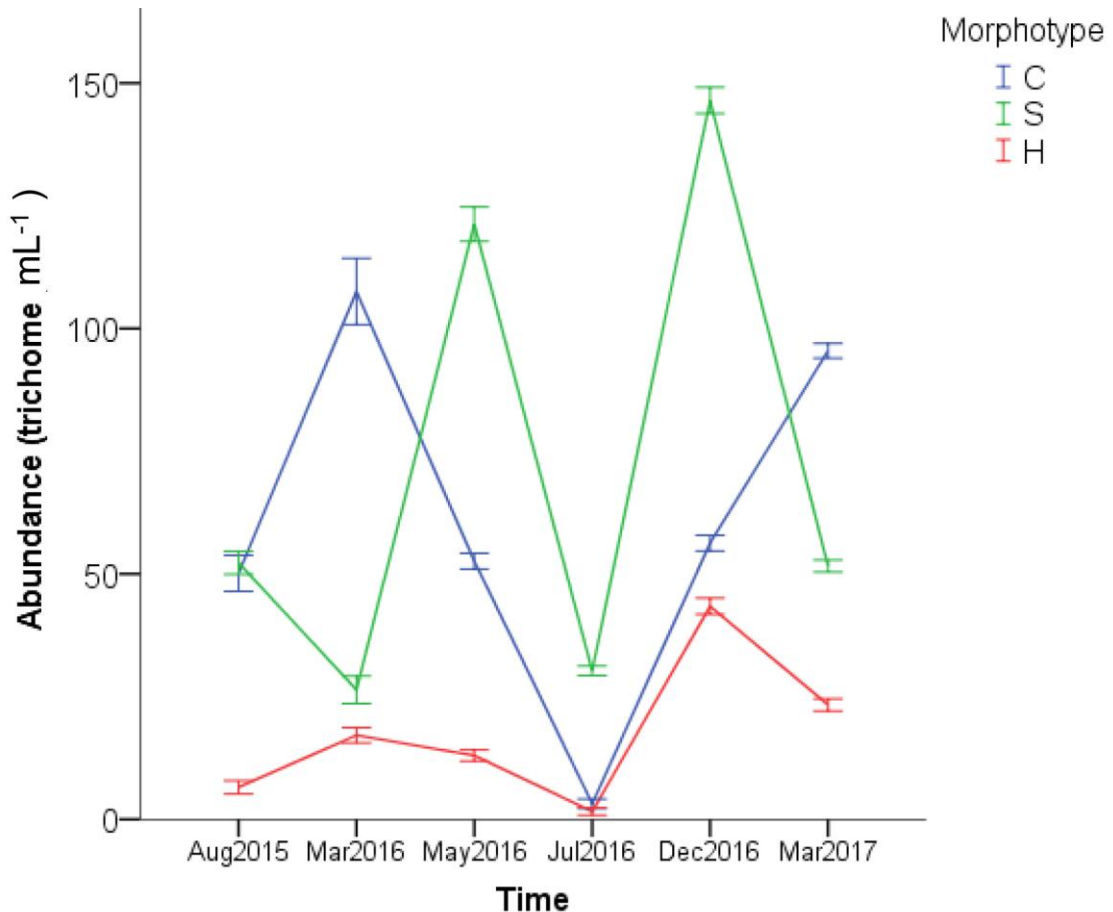


Figure 4.10: Mean values comparison of three *Arthrospira* morphotypes abundance (C, S and H) (trichome mL⁻¹) of Lake Bogoria from Aug2015 to Mar 2017.

n =15; error bars represent 95 % CI.

There was a significant effect of the morphotype on *Arthrospira*'s population, $F(2, 28) = 5702, p < 0.0001$, partial eta squared (η^2) = 0.998. The pairwise comparison revealed that the population was statistically significantly lower in C-morphotype (60.87 ± 8.30 trichome mL⁻¹) compared to the S-morphotype (71.38 ± 6.19 trichome mL⁻¹), $p < 0.0001$. However, the population of C-morphotype (60.87 ± 8.30 trichome mL⁻¹) was statistically significantly higher than the population of H-morphotype (17.50 ± 3.81 trichome mL⁻¹), $p < 0.0001$. Moreover, the population of S-morphotype (71.38 ± 6.19 trichome mL⁻¹) was statistically higher than the population of H-morphotype (17.50 ± 3.81 trichome mL⁻¹), $p < 0.0001$. There was also a significant main effect of time on the *Arthrospira*'s population, $F(2.34, 32.72) = 1031.14, p < 0.0001$, partial eta

squared (η^2) = 0.987. All pairwise comparison groups of the time were significantly different, $p < 0.05$, as shown in Table 4.4.

Table 4.4: Results of the Bonferroni post hoc tests of the main effect of time on *Arthrospira*'s population.

Pairwise comparison	Mean Difference
Aug15 vs. Mar16	-14.04 ^{****}
Aug15 vs. May16	-25.98 ^{****}
Aug15 vs. Jul16	24.62 ^{****}
Aug15 vs. Dec16	-45.73 ^{****}
Aug15 vs. Mar17	-20.49 ^{****}
Mar16 vs. May16	-11.93 ^{****}
Mar16 vs. Jul16	38.67 ^{****}
Mar16 vs. Dec16	-31.69 ^{****}
Mar16 vs. Mar17	-6.44 ^{***}
Jul16 vs. Dec16	-70.36 ^{****}
Jul16 vs. Mar17	-45.11 ^{****}
Dec16 vs. Mar17	-25.24 ^{****}
May16 vs. Jul16	50.60 ^{****}
May16 vs. Dec16	-19.76 ^{****}
May16 vs. Mar17	5.49 ^{****}

The mean difference is significant at the 0.05, significant differences indicated by asterisks. (**** $p < 0.0001$, *** $p < 0.001$).

A two-way interaction between morphotype and time on *Arthrospira* abundance was statistically significant, $F(3.06, 42.87) = 1463$, $p < 0.0001$, partial eta squared (η^2) = 0.991. Paired-samples t-tests revealed that only nine pairwise comparisons were not statistically different at an adjusted α level of 0.003 (Table 4.5).

Table 4.5: Paired-samples t-test results of *Arthrospira* abundance for the entire period of study.

Pairwise	Mean Difference	t	Pairwise	Mean Difference	t
Aug15 C vs. Aug15 S	-2.13	-1.79	Aug15 S vs. Jul16 H	50.67*	54.23
Aug15 C vs. Aug15 H	43.60*	31.93	Aug15 S vs. Dec16 C	-4.00	-3.03
Aug15 C vs. Mar16 C	-57.40*	-17.29	Aug15 S vs. Dec16 S	-94.20*	-60.78
Aug15 C vs. Mar16 S	23.73*	11.06	Aug15 S vs. Dec16 H	8.87*	7.91
Aug15 C vs. Mar16 H	33.00*	18.93	Aug15 S vs. Mar 17 C	-43.20*	-40.21
Aug15 C vs. May16 C	-2.47	-2.47	Aug15 S vs. Mar 17 S	0.67	0.61
Aug15 C vs. May16 S	-71.13*	-33.89	Aug15 S vs. Mar 17 H	28.93*	23.93
Aug15 C vs. May16 H	37.13*	22.66	Aug15 H vs. Mar16 C	-101.00*	-33.15
Aug15 C vs. Jul16 C	46.93*	31.89	Aug15 H vs. Mar16 S	-19.87*	-13.49
Aug15 C vs. Jul16 S	19.87*	12.17	Aug15 H vs. Mar16 H	-10.60*	-12.73
Aug15 C vs. Jul16 H	48.53*	31.21	Aug15H vs. May16 C	-46.07*	-69.25
Aug15 C vs. Dec16 C	-6.13	-3.55	Aug15 H vs. May16 S	-114.73*	-72.71
Aug15 C vs. Dec16 S	-96.33*	-49.94	Aug15 H vs. May16 H	-6.47*	-8.10
Aug15 C vs. Dec16 H	6.73*	4.43	Aug15 H vs. Jul16 C	3.33*	5.17
Aug15 C vs. Mar 17 C	-45.33*	-27.44	Aug15 H vs. Jul16 S	-23.73*	31.02
Aug15 C vs. Mar 17 S	-1.47	-0.96	Aug15 H vs. Jul16 H	4.93*	9.16
Aug15 C vs. Mar 17 H	26.80*	15.35	Aug15 H vs. Dec16 C	-49.73*	-50.59
Aug15 S vs. Aug15 H	45.73*	62.92	Aug15 H vs. Dec16 S	-139.93*	-117.29
Aug15 S vs. Mar16 C	-55.27*	-17.95	Aug15 H vs. Dec16 H	-36.87*	-45.87
Aug15 S vs. Mar16 S	25.87*	13.99	Aug15 H vs. Mar 17 C	-88.93*	-118.17
Aug15 S vs. Mar16 H	35.13*	32.09	Aug15 H vs. Mar 17 S	-45.07*	-70.86
Aug15 S vs. May16 C	-0.33	-0.46	Aug15 H vs. Mar 17 H	-16.80*	-22.96
Aug15 S vs. May16 S	-69.00*	-47.13	Mar 16 C vs. Mar16 S	81.13*	32.46
Aug15 S vs. May16 H	39.27*	37.77	Mar 16 C vs. Mar16 H	90.40*	31.87
Aug15 S vs. Jul16 C	49.07*	58.26	Mar 16 C vs. May16 C	54.93*	17.21

Continued on next page.

Table 4.5 continued from previous page.

Pairwise	Mean Difference	t	Pairwise	Mean Difference	t
Aug15 S vs. Jul16 S	22.00*	21.02	Mar 16 C vs. May16 S	-13.73*	-4.46
Mar 16 C vs. May16 H	94.53*	31.35	May 16 C vs. May16 S	-68.67*	-42.77
Mar 16 C vs. Jul16 C	104.33*	34.14	Mar16 C vs. Dec16 H	64.13*	20.89
Mar 16 C vs. Jul16 S	77.27*	25.72	Mar 16 C vs. Mar 17 C	12.07*	4.17
Mar 16 C vs. Jul16 H	105.93*	35.34	Mar 16 C vs. Mar 17 S	55.93*	17.26
Mar 16 C vs. Dec16 C	51.27*	17.03	Mar 16 C vs. Mar 17 H	84.20*	27.90
Mar 16 C vs. Dec16 S	-38.93*	-13.71	Mar 16 S vs. Mar 16 H	9.27*	6.71
Mar16 C vs. Dec16 H	64.13*	20.89	Mar 16 S vs. May16 C	-26.20*	-16.52
Mar 16 C vs. Mar 17 C	12.07*	4.17	Mar 16 S vs. May16 S	-94.87*	46.25
Mar 16 C vs. Mar 17 S	55.93*	17.26	Mar 16 S vs. May16 H	13.40*	10.13
Mar 16 C vs. Mar 17 H	84.20*	27.90	Mar 16 S vs. Jul16 C	23.20*	17.47
Mar 16 S vs. Mar 16 H	9.27*	6.71	Mar 16 S vs. Jul16 S	-3.87	-3.17
Mar 16 S vs. May16 C	-26.20*	-16.52	Mar 16 S vs. Jul16 H	24.80*	20.53
Mar 16 S vs. May16 S	-94.87*	-46.25	Mar 16 S vs. Dec16 C	-29.87*	-21.43
Mar 16 S vs. May16 H	13.40*	10.13	Mar 16 S vs. Dec16 S	-120.07*	-71.22
Mar 16 S vs. Jul16 C	23.20*	17.47	Mar 16 S vs. Dec16 H	-17.00*	-12.88
Mar 16 S vs. Jul16 S	-3.87	-3.17	Mar 16 S vs. Mar 17 C	-69.07*	-55.35
Mar 16 S vs. Jul16 H	24.80*	20.53	Mar 16 S vs. Mar 17 S	-25.20*	17.48
Mar 16 S vs. Dec16 C	-29.87*	-21.43	Mar 16 H vs. May16 C	-35.47*	-38.13
Mar 16 S vs. Dec16 S	-120.07*	-71.22	Mar 16 H vs. May16 S	-104.13*	-62.35
Mar 16 S vs. Dec16 H	-17.00*	-12.88	Mar 16 H vs. May16 H	4.13*	4.900
Mar 16 S vs. Mar 17 C	-69.07*	-55.35	Mar 16 H vs. Jul16 C	13.93*	18.21
Mar 16 S vs. Mar 17 S	-25.20*	-17.48	Mar 16 H vs. Jul16 S	-13.13*	-16.58
Mar 16 S vs. Mar 17 H	3.07	2.55	Mar 16 H vs. Jul16 H	15.53*	22.10
Mar 16 H vs. May16 C	-35.47*	-38.13	Mar 16 H vs. Dec16 C	-39.13*	-38.61
Mar 16 H vs. May16 S	-104.13*	-62.35	Mar 16 H vs. Dec16 S	-129.33*	-92.64
Mar 16 H vs. May16 H	4.13*	4.90	Mar 16 H vs. Dec16 H	-26.27*	-25.27
Mar 16 H vs. Jul16 C	13.93*	18.21	Mar 16 H vs. Mar 17 C	-78.33*	-74.00

Continued on next page.

Table 4.5 continued from previous page.

Pairwise	Mean Difference	t	Pairwise	Mean Difference	t
Mar 16 H vs. Jul16 S	-13.13*	-16.59	Mar 16 H vs. Mar 17H	-6.20*	-7.05
May 16 S vs. May16 H	108.27*	91.05	May 16 C vs. May16 S	-68.67*	-42.77
May 16 S vs. Jul16 C	118.07*	88.13	May 16 C vs. May16 H	39.60*	52.47
May 16 S vs. Jul16 S	91.00*	66.44	Jul 16 S vs. Mar 17 C	-65.20*	-100.49
May 16 S vs. Jul16 H	119.67*	83.70	Jul 16 H vs. Dec16 S	-144.87*	-119.29
May 16 S vs. Dec16 C	65.00*	39.05	Jul 16 H vs. Dec16 H	-41.80*	-71.19
May 16 S vs. Dec16 S	-25.20*	-14.88	Jul 16 H vs. Mar 17 C	-93.87*	-165.28
May 16 S vs. Dec16 H	77.87*	60.00	Jul 16 H vs. Mar 17 S	-50.00*	-165.28
May 16 S vs. Mar 17 C	25.80*	15.91	Jul 16 H vs. Mar 17 H	-21.73*	-45.02
May 16 S vs. Mar 17 S	69.67*	45.73	Dec16 C vs. Dec16 S	-90.20*	-83.27
May 16 S vs. Mar 17 H	97.93*	61.94	Dec16 C vs. Dec16 H	12.87*	14.75
May 16 H vs. Jul16 C	9.80*	28.75	Dec16 C vs. Mar 17 C	-39.20*	-48.29
May 16 H vs. Jul16 S	-17.27*	-69.58	Dec16 C vs. Mar 17 S	4.67*	6.19
May 16 H vs. Jul16 H	11.40*	-69.58	Dec16 C vs. Mar 17 H	32.93*	64.39
May 16 H vs. Dec16 C	-43.27*	60.63	Dec16 C vs. Dec16 S	-90.20*	-83.27
May 16 H vs. Dec16 S	-133.47*	-115.23	Dec16 C vs. Dec16 H	12.87*	14.75
May 16 H vs. Dec16 H	-30.40*	-56.13	Dec16 C vs. Mar 17 C	-39.20*	-48.29
May 16 H vs. Mar 17 C	-82.47*	-115.14	Dec16 C vs. Mar 17 S	4.67*	6.19
May 16 H vs. Mar 17 S	-38.60*	-67.05	Dec16 C vs. Mar 17 H	32.93*	64.39
May 16 H vs. Mar 17 H	-10.33*	-15.50	Dec16 S vs. Dec16 H	103.07*	83.11
Jul 16 C vs. Jul16 S	-27.07*	-85.73	Dec16 S vs. Mar 17 C	51.00*	41.71
Jul 16 C vs. Jul16 H	1.60*	5.87	Dec16 S vs. Mar 17 S	94.87*	89.92
Jul 16 C vs. Dec16 C	-53.07*	-68.27	Dec16 S vs. Mar 17 H	123.13*	115.25
Jul 16 C vs. Dec16 S	-143.27*	-111.46	Dec16 H vs. Mar 17 C	-52.07*	-69.78
Jul 16 C vs. Dec16 H	-40.20*	-66.65	Dec16 H vs. Mar 17 S	-8.20*	-16.11
Jul 16 C vs. Mar 17 C	-92.27*	-138.70	Dec16 H vs. Mar 17 H	20.07*	29.24
Jul 16 C vs. Mar 17 S	-48.40*	-86.60	Mar17 C vs. Mar 17 S	43.87*	66.37
Jul 16 C vs. Mar 17 H	-20.13*	-30.14	Mar17 C vs. Mar 17 H	72.13*	97.17

Continued on next page.

Table 4.5 continued from previous page.

Pairwise	Mean Difference	t	Pairwise	Mean Difference	t
Jul 16 S vs. Jul16 H	28.67*	79.46	Mar17 H vs. Mar 17 S	28.27*	48.64
Jul 16 S vs. Dec16 C	-26.00*	-38.46			
Jul 16 S vs. Dec16 S	-116.20*	-79.16			
Jul 16 S vs. Dec16 H	-13.13*	-21.87			
Jul 16 S vs. Mar 17 S	-21.33*	-36.60			
Jul 16 S vs. Mar 17 H	6.93*	11.77			
Jul 16 H vs. Dec16 C	-54.67*	-79.49			

The mean difference is significant at the 0.003 level. * $p < 0.003$.

4.3.3.2 The relationship between *Arthrospira* abundance and phytoplankton biomass

A Spearman's rank-order correlation showed that there was a very strong positive association between Chl-a concentration (remote sensing method) as an indicator for phytoplankton biomass and *Arthrospira* abundance, $r_s = 0.9$, $p = 0.037$, $n = 5$ at Lake Bogoria over the period between Mar 2016 to Mar 2017 (Figure 4.11).

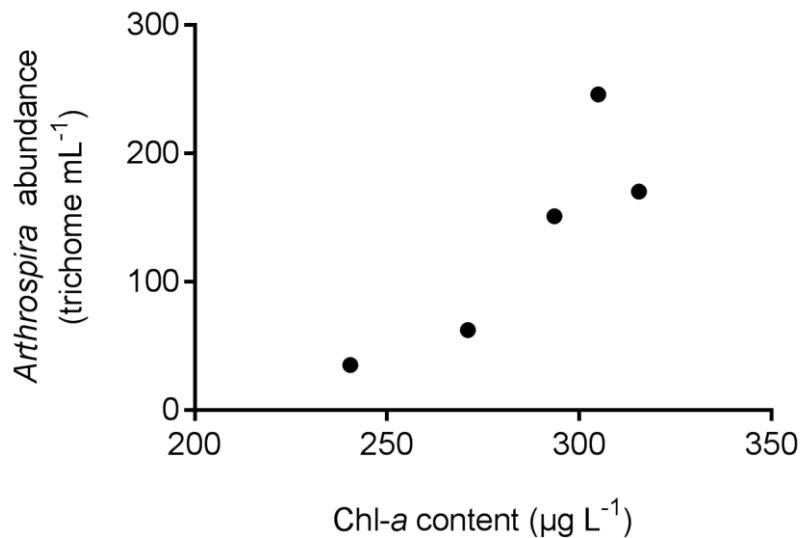


Figure 4.11: The relationship between phytoplankton biomass (Chl-a content) and *Arthrospira* abundance at Lake Bogoria.

Data represent the monthly means of Mar, May, Jul, Dec 2016 and Mar 2017, $n = 5$.

4.3.3.3 The relations between the abundance of three *Arthrospira* morphotypes and the properties of the lake

The abundance of three morphotypes C, S and H was not related to pH, $r_s = -0.046$, 0.028 and 0.100 ; 95 % BCa CI $([-0.378, 0.296]$, $[-0.312, 0.362]$ and $[-0.245, 0.424]$); $p = 0.79$, 0.87 and 0.56 , $n = 36$ respectively. The total P concentration was significantly positively correlated to the population of the three morphotypes, C, S and H, $r_s = 0.354$, 0.451 and 0.605 ; 95 % BCa CI $([0.019, 0.62]$, $[0.134, 0.684]$ and $[0.337, 0.783]$); $p = 0.034$, 0.006 and < 0.0001 ; $n = 36$. The abundance of C and H morphotypes was also significantly related to an increase in total N concentration, $r_s = 0.51$ and 0.534 ; 95 % BCa CI $([0.206, 0.722]$ and $[0.244, 0.741]$); $p = 0.002$ and 0.007 ; $n = 36$ respectively, with S-morphotype abundance had no relationship, $r_s = 0.153$; 95 % BCa CI $[-$

0.195, 0.466]; $p = 0.37$; $n = 36$. A Spearman's rank-order correlation also showed that the increase in salinity of Lake Bogoria was statistically associated with the increase in S and H morphotypes populations, $r_s = 0.426$ and 0.553 ; 95 % BCa CI ([0.104, 0.668] and [0.265, 0.751]); $p = 0.009$ and 0.005 ; $n = 36$ respectively, but not to the C-morphotype population, $r_s = 0.166$; 95 % BCa CI ([-0.182, 0.477]; $p = 0.33$; $n = 36$. The significant associations are shown in Figure 4.12.

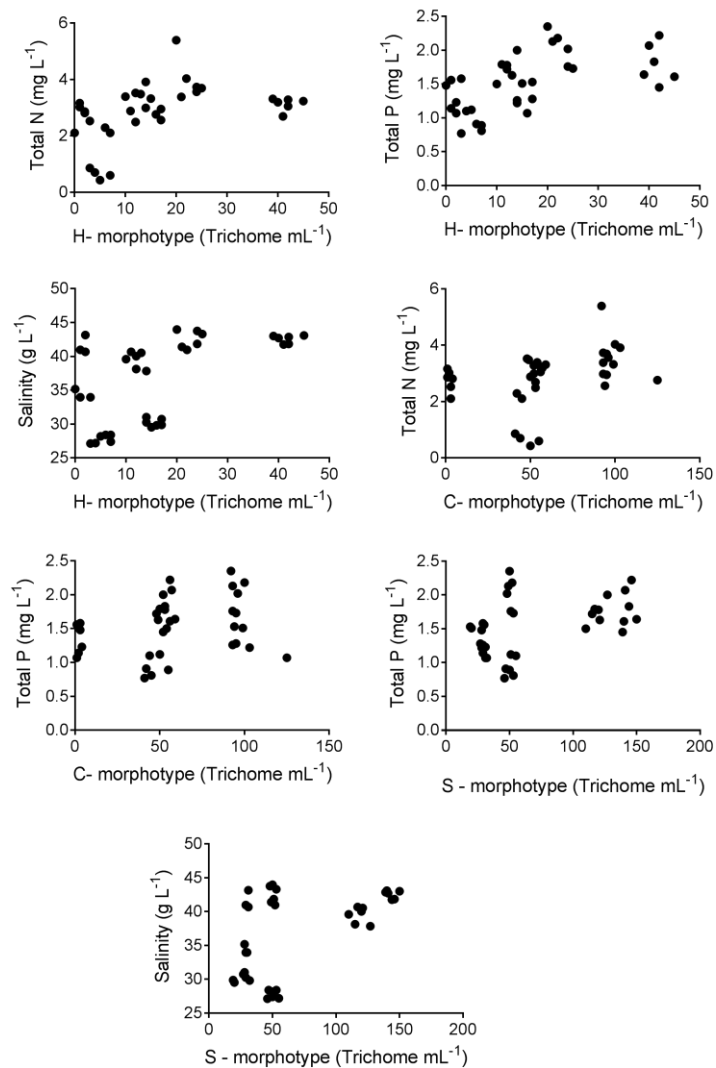


Figure 4.12: The significant relationships between the three *Arthrospira* morphotypes populations and Lake Bogoria characteristics during the period between August 2015 and Mar 2017, $n = 36$.

All these physico-chemical lake properties were not good predictors of *Arthrospira* abundance. This was because the regression model did not fit (ANOVA test was not significant, $p > 0.05$).

4.3.3.4 Comparison of trichome characters between three morphotypes

Three distinct morphotypes were characterized by the degree of coiling of trichomes (helicity), coils per trichome, diameter and pitch of helix, colour, and length of trichome (Table 4.6). The colour of the trichomes varied slightly from deep blue-green to light blue-green (Figure 4.5). All three morphotypes, however, differed in the degree of coiling, coils per trichome, and length of trichome, pitch, and diameter of the helix (Figure 4.13).

Table 4.6: Description of three *Arthrospira* morphotypes based on their morphological characteristics.

Morphological parameters	Morphotypes		
	C-morphotype	S-morphotype	H-morphotype
Degree of coiling (helicity)	Intermediate coil (wider helix than H-morphotype)	Loose helix (spiral)	Highly (tightly) coiled
Colour of trichome	light blue green	Blue-green	Deep blue green
Trichome end attenuation	Highly attenuated	Indistinctly attenuated	More attenuated than S-morphotype
Trichome length (μm)	134.49 \pm 17.53	782.66 \pm 137.60	188.46 \pm 33.79
Helix diameter in the middle (μm)	122.89 \pm 8.40	63.80 \pm 4.77	120.56 \pm 16.61
Helix pitch (μm)	36.19 \pm 5.76	45.27 \pm 8.04	0.912 \pm 0.63
Number of coils per trichome	3.98 \pm 0.66, <i>Mdn</i> =4	11.98 \pm 1.79, <i>Mdn</i> =12	13.98 \pm 2.55, <i>Mdn</i> =14

Means \pm SD of recorded values and medians (*Mdn*) of the coils per trichome parameter are shown, n= 40.

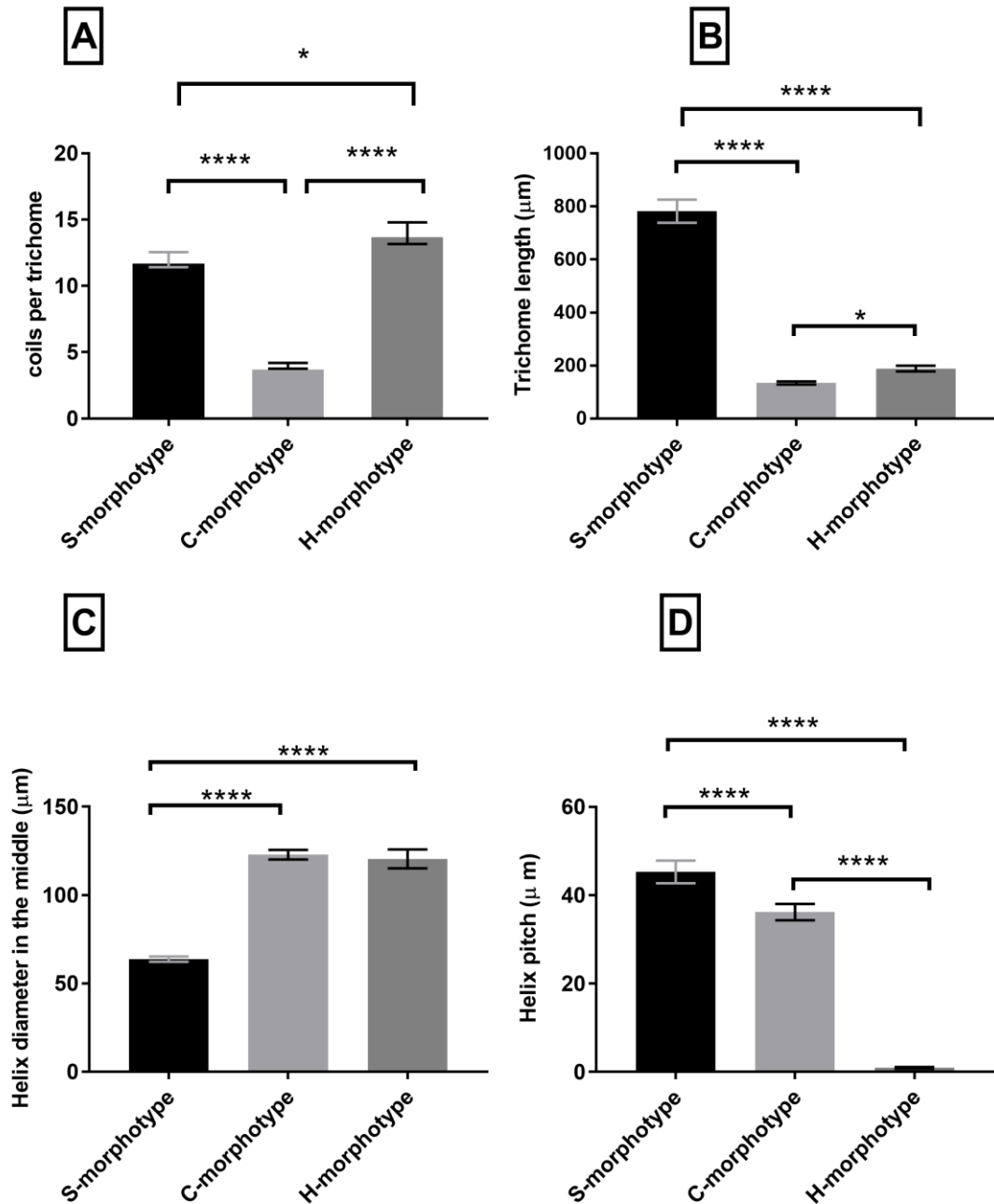


Figure 4.13: Comparison of mean and median (coils per trichome) values of morphological parameters of three morphotypes of *Arthrospira* spp. in Lake Bogoria.

A) coils per trichome, B) trichome length, C) helix diameter in the middle, D) helix pitch, errors bars represent 95%; n = 40, * $p < 0.05$, **** $p < 0.0001$.

All four helix dimensions (number of coils per trichome, trichome length, helix diameter and helix pitch) were significantly different between the different morphotypes (S, C and H), $\chi^2(2) = 87.01, p < 0.0001$ (Kruskal-Wallis); Welch(2, 63.06) = 458.18, $\eta^2 = 0.929, p < 0.0001$; Welch(2, 69.06) = 651.80, η^2

= 0.928, $p < 0.0001$; Welch(2, 66.72) = 2580.22, $\eta^2 = 0.966$, $p < 0.0001$, respectively.

The H-morphotype was so tightly coiled that the helix pitch was almost zero ($0.91 \pm 0.63 \mu\text{m}$) and significantly lower than that of the S ($45.27 \pm 8.04 \mu\text{m}$) and C morphotype ($36.12 \pm 5.76 \mu\text{m}$), $p < 0.0001$ (Figure 4.13d), and its coils per trichome (14 coils) was significantly higher than the S-morphotype (12 coils), $r = 0.29$, $p = 0.031$ and C-morphotype (4 coils), $r = -1.02$, $p < 0.0001$ (Figure 4.13a). It had a deep blue-green colour. The trichome length of this type was different from those of the other two variants (Figure 4.13 b); it ($188.46 \pm 33.80 \mu\text{m}$) was significantly lower than that of the S-morphotype ($782.66 \pm 137.60 \mu\text{m}$), $p < 0.0001$ and higher than that of the C-morphotype ($134.49 \pm 17.53 \mu\text{m}$), $p = 0.011$. As can be seen from the helix diameter (Figure 4.13c), this variant had a significantly higher helix diameter ($120.56 \pm 16.61 \mu\text{m}$) than the S-morphotype ($63.80 \pm 4.77 \mu\text{m}$), $p < 0.0001$; while the difference with the C-morphotype ($122.89 \pm 8.40 \mu\text{m}$) was not significant, $p = 0.364$.

The S-morphotype was loosely coiled (spiral) and its helix pitch was significantly higher than C and H morphotypes, $p = 0.0113$ and < 0.0001 respectively (Figure 4.13 d), and had an intermediate number of coils per trichome, which was significantly higher than that of the C-morphotype, $p < 0.0001$ and less than the H-morphotype, $p = 0.031$ (Figure 4.13a) and it had the longest trichome (Figure 4.13b). Its blue-green colour was less deep than that of the H-morphotype but darker than the C-morphotype. Its helix diameter was the lowest and it had a slight attenuation at the ends compared to the other morphotypes.

The C-morphotype was coiled intermediately between the two morphotypes. Its helix pitch was significantly closer than that of the S-morphotype, $p < 0.0001$ (Figure 4.13d). Its blue-green colour was lighter than the others. It had the shortest trichome length and its number of coils per trichome was the least among three morphotypes, $p < 0.0001$ (Figure 4.13a). The trichome had the largest diameter with regards to the helix in the middle, and was more attenuated at the ends than the S- morphotype (Figure 4.13c). It was

sometimes difficult to measure the length of this morphotype because it was lying on the surface of the slide.

4.3.4 The change in trichome helicity of *Arthrospira* spp.

A morphological change from a tight helix to a loose helix was observed after transferring the *Arthrospira* filaments from lake water to Zarouk's medium (for more than one month) (Figure 4.14B). After transferring them back to the lake water, these filaments gradually reverted to their original morphotype (Figure 4.14C). However, during the duration of the project, none of the morphotypes showed any tendency towards completely losing their helicity and changing to a straight morphotype.

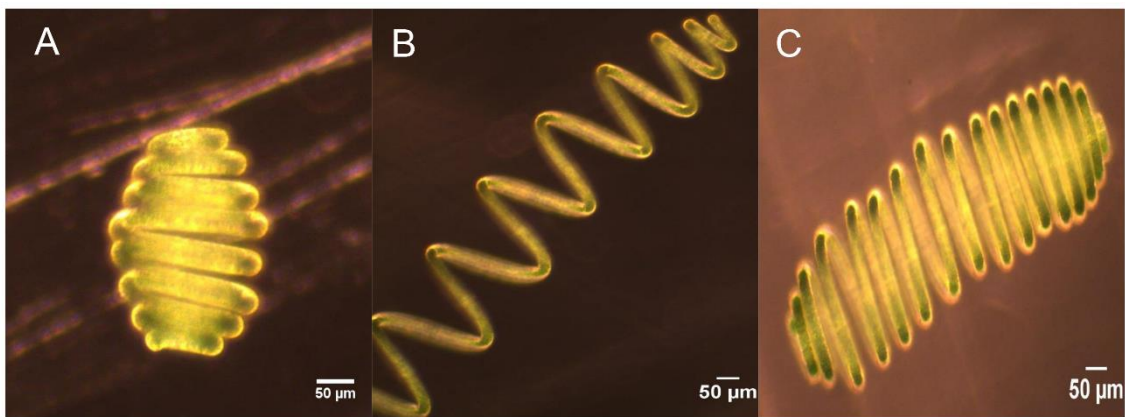


Figure 4.14: Morphological changes of *Arthrospira* of Lake Bogoria.

(A) Shows a tight helical trichome in Lake Bogoria water, (B) represents the change from a tight helix to a loose helix after transferring the filaments from the water sample (Lake Bogoria) to the Zarrouk's medium. (C) Represents the reverse morphotype from a loose helix to a tight helix after transferring the filaments back to the water sample (Lake Bogoria). Note, the increase in the length of trichome after being transferred from lake water to the medium. Bars marker = 50 µm.

Increasing pH led to a tightening of the helix in morphotypes C and H (Figure 4.15 A, B and C, D). They tended to change their morphology from loose to tight helices after the transfer of their trichomes from Zarrouk's medium (pH ~ 9.0) to the same medium with a pH of 10.2 for more than 3 months. However, the S-morphotype remained stable throughout the experiment and retained its helicity in both conditions (Figure 4.15. E, F).

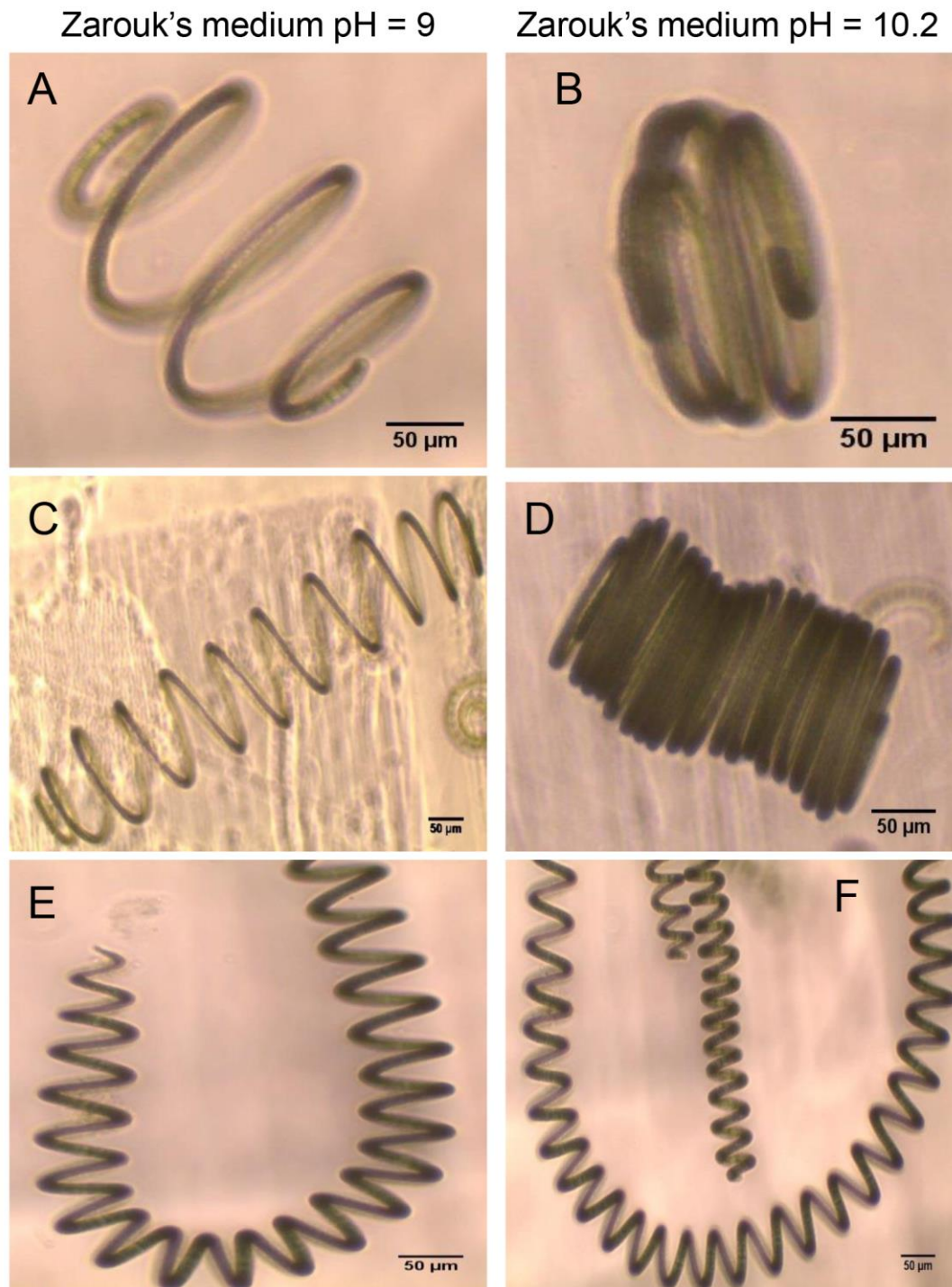


Figure 4.15: Light micrographs of morphological changes of three *Arthrospira* spp. morphotypes isolated from Lake Bogoria.

A and B represent the C-morphotype, where the loose trichome was altered to a tight morphotype after being transferred from pH 9.0 (A) to pH 10.2 (B). C and D represent the H-morphotype where the loose trichome was altered to a tight morphotype after being transferred from pH 9.0 (C) to pH 10.2 (D). E and F represent the S-morphotype where there was no effect of pH treatment on trichome helicity.

4.3.5 Motility of *Arthrospira* spp.

Only the S-morphotype expressed gliding behaviour (Figure 4.16). For more than five days of monitoring, S-morphotype trichomes migrated away from the inoculation point in the centre of the agar plate, until some of them reached the edge of the plate. In contrast, the other two morphotypes (H and C) did not express any mobility for the duration (Figure 4.17 and 4.18). Therefore, there is a correlation between the degree of mobility and the helical trichome morphology of *Arthrospira* spp..

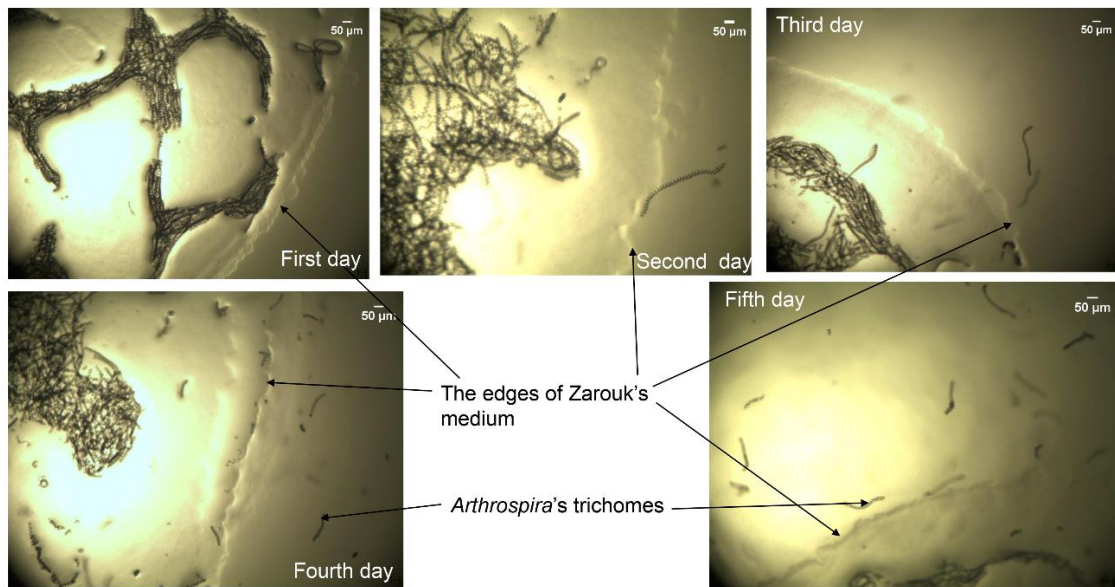


Figure 4.16: Micro images of *Arthrospira* S-morphotype plated on low strength agar (0.6%) of Zarrouk's medium showing the gliding motility of its filaments.

The edge of the drop of the medium on the first day, and how the filaments migrated away from the inoculation point day after day. Bars indicate 50 µm.

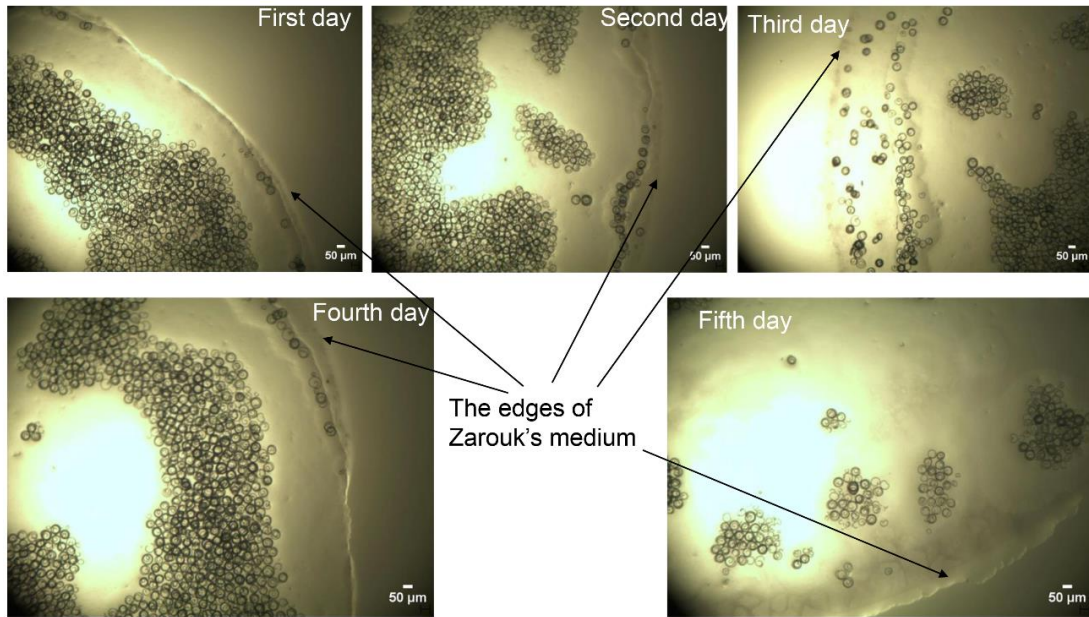


Figure 4.17: Micro images of *Arthrospira* C-morphotype plated on low strength agar (0.6%) of Zarrouk's medium showing no gliding motility of its filaments.

The edge of the drop of the medium on the first day, and how the filaments remained in place and did not move during the entire study duration. Bars indicate 50 µm.

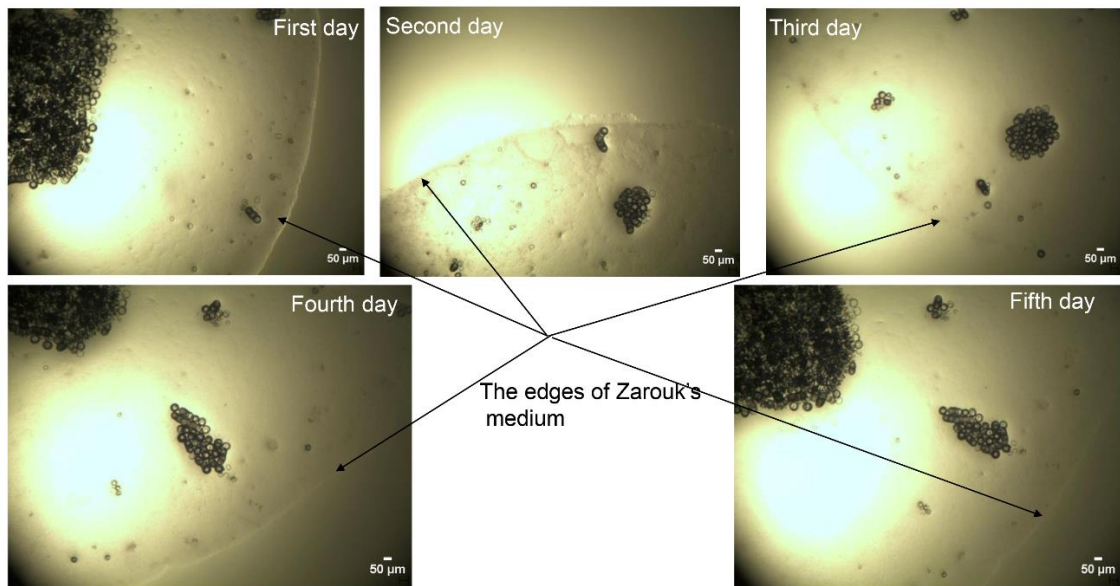


Figure 4.18: Micro images of *Arthrospira* H-morphotype plated on low strength agar (0.6%) of Zarrouk's medium showing no gliding motility of its filaments.

The edge of the drop of the medium on the first day, and how the filaments remained in place and did not move during the entire study duration. Bars indicate 50 µm.

4.3.6 Ultrastructure of *Arthrospira* spp.

The internal structure of *Arthrospira* was identical to that of other prokaryotes, with no organelles surrounded by membranes. A thin sheath surrounds the filament, while the surface of the trichomes is covered with deep ribs, and the trichome is divided into cells via cross-walls, bound together by plasmodesmata (Figure 4.19).

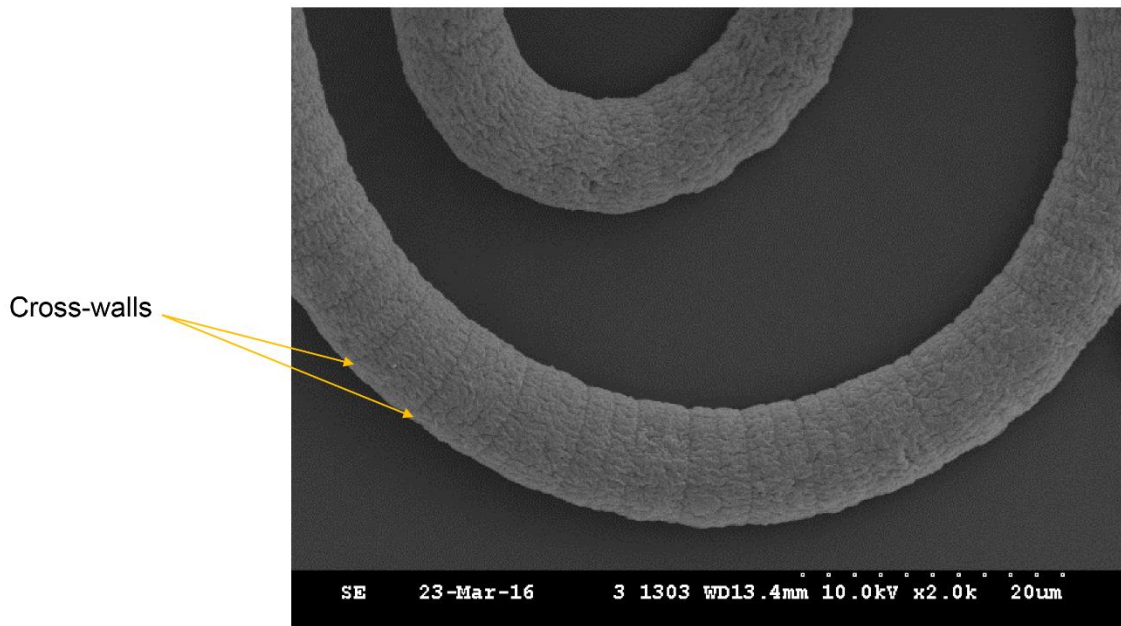


Figure 4.19: Scanning electron image of *Arthrospira* spp. from Lake Bogoria with a part of trichome in continual spiral coil.

The transverse cross-walls that divide the filament into the cells and apparent thin sheath that coats the surface of the trichome. Scale bar indicates 20 μm .

The cell wall consists of four layers (LI, LII, LIII and LIV), with regularly distributed “blebs” emerging from junctional pores which are distributed in the peptidoglycan layer on the surface of the cell, there are believed to be responsible for the secretion of the mucilage sheath (Figure 4.20 and 4.21).

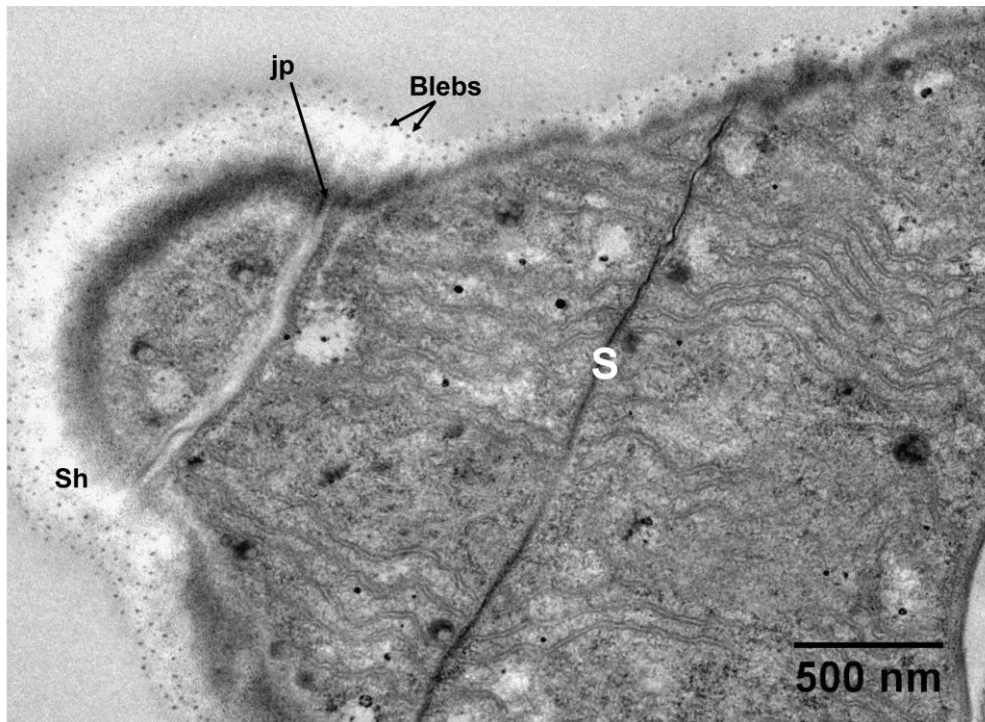


Figure 4.20: Electron micrograph of a longitudinal section of *Arthrospira* spp. from Lake Bogoria.

The image reveals a thin slime sheath (sh), with one row of junctional pores (jp) that envelop the cross-walls (s) with a regular distribution of blebs. Bar represents 500 nm.

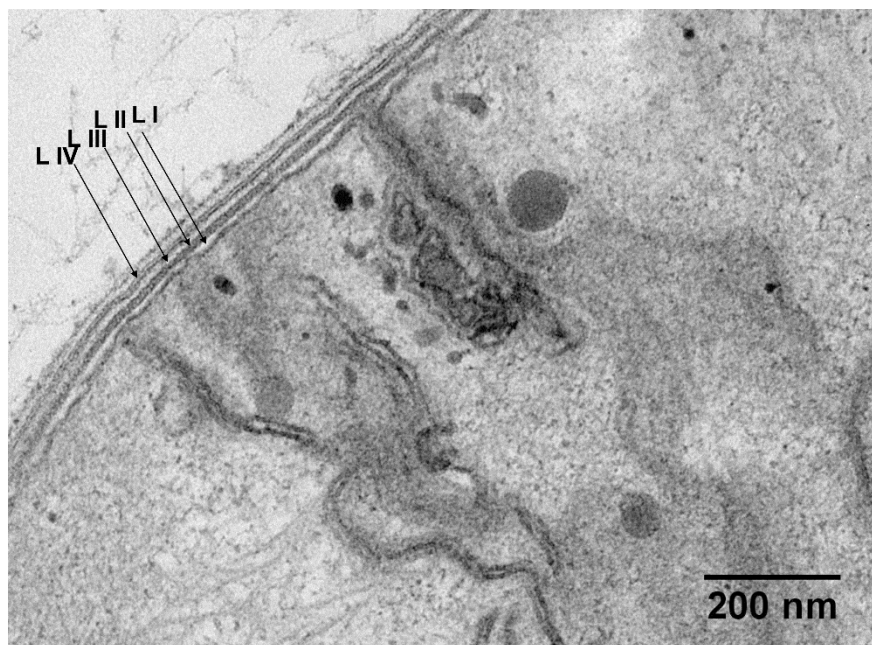


Figure 4.21: Electron micrograph of an *Arthrospira's* section, showing four layers of the cell wall (LI, LII, LIII and LIV).

Bar represents 200 nm.

There is a cell membrane under the cell wall, which encapsulates the cytoplasm. The richness of the *Arthrospira* cytoplasm is due to the inclusions which are highly organised within the cytoplasm (Figure 4.22 A). The circumferential region of the cell is filled with the storage bodies of cyanophycin with diameters larger than 500 nm in most cases (Figure 4.22 B), small lipid droplets, and gas vacuoles, whereas no hexagonal shapes of polyglucan granules were detected.

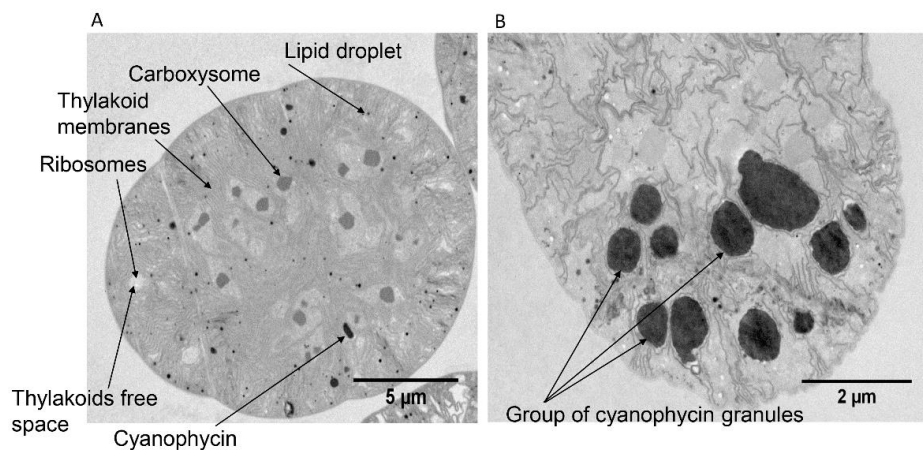


Figure 4.22: Electron micrographs of *Arthrospira* cellular architecture in cross-sections.

A) A high structure organisation of the cytoplasm showing periphery and central regions. B) Shows reserve granules of cyanophycin. Bars represent 5 and 2 µm respectively.

The gas vacuoles are composed of highly packed hexagonal gas vesicle structures. These were hollow cylinders with a diameter of about 78 nm (Figure 4.23).

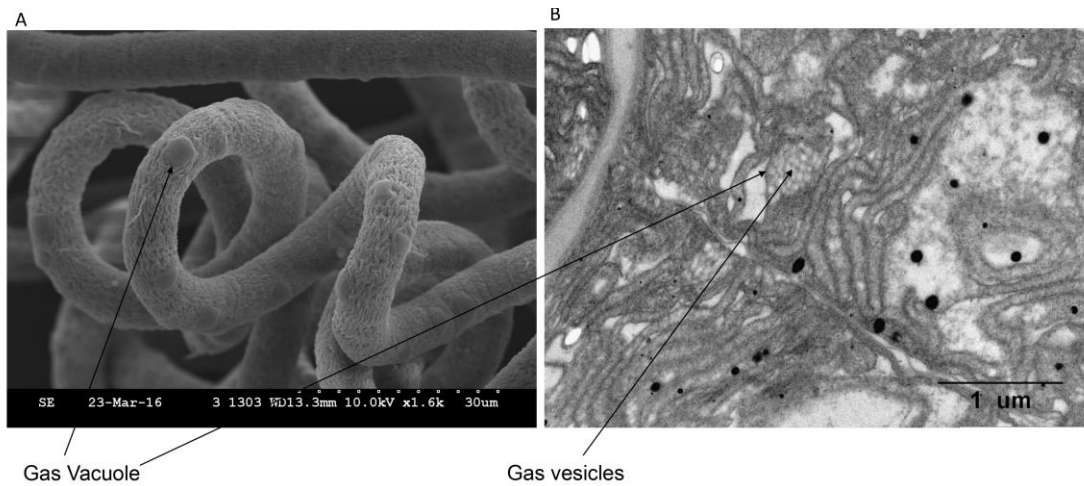


Figure 4.23: Ultrastructure of *Arthrospira* from Lake Bogoria showing gas vacuoles.

A) SEM image shows the gas vacuole along the cell walls. B) TEM image shows the hollow cylinders of gas vesicles. Scale bars represent 30 and 1 μm respectively.

The thylakoid membranes were present between peripheral and central regions of the cytoplasm (Figure 4.24 A). Attached to the thylakoid membranes are the light-harvesting antennae (phycobilisomes), which ranged between 18- 25 nm in size (Figure 4.24 B). They were found only within Jul 2016 sample (see chapter 6, section 6.3.2). Within the middle of the thylakoid membranes were the thylakoid-free areas rich with ribosomes and DNA strands.

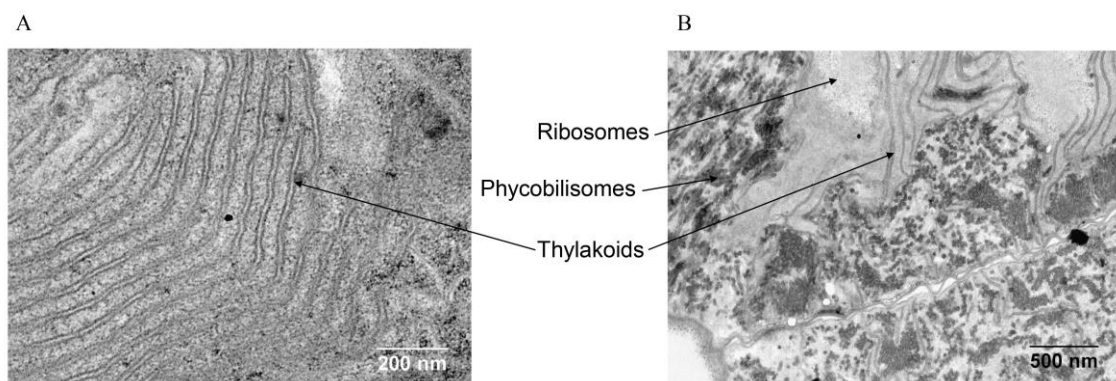


Figure 4.24: Electron micrographs of *Arthrospira* sections showing the photosynthetic lamellae (thylakoids).

A) Closed discs of thylakoids appear as two parallel lines with no phycobilisomes attached to them. B) Phycobilisomes attached to the surface of the photosynthetic lamellae. Bars represent 200 and 500 nm respectively.

Those membranes were organised differently among the three morphotypes. They were arranged in a circular manner in the S-morphotype (Figure 4.25) while they were arranged in a straight orientation in C and H morphotypes (Figure 4.26).

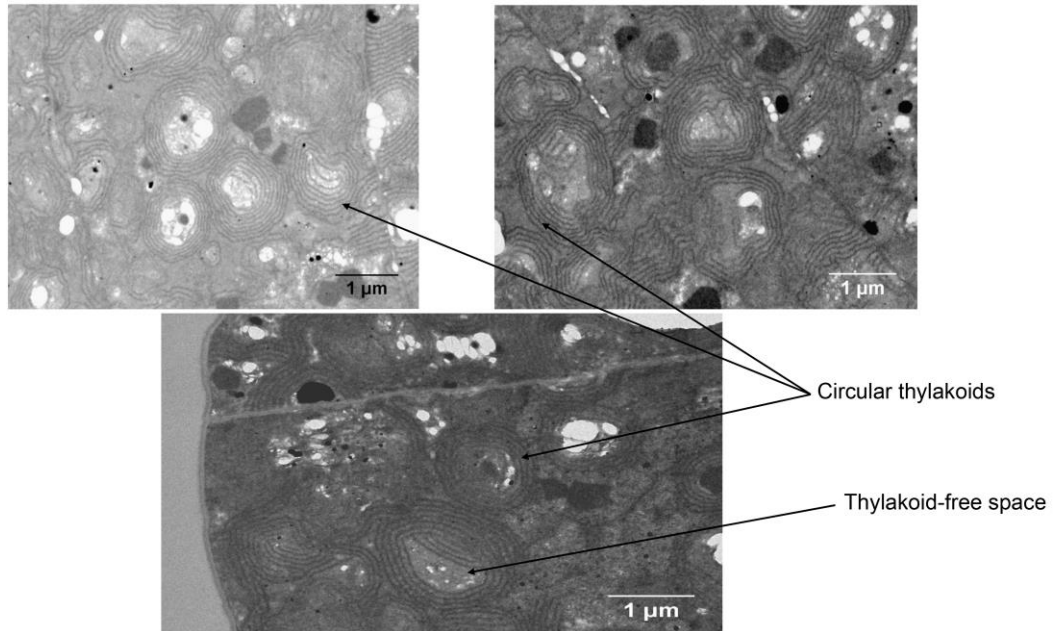


Figure 4.25: Electron micrographs of *Arthrospira* sections showing the circular arrangement of thylakoids in the S-morphotype.

In the middle of the circle of the thylakoids, there is a thylakoid-free space. Bars represent 1µm.

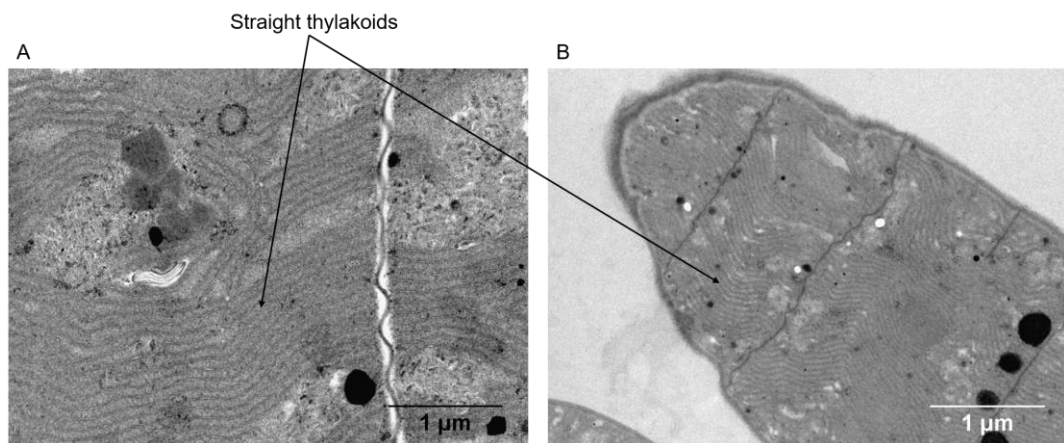


Figure 4.26: Electron micrographs of the cross and longitudinal sections of *Arthrospira* from Lake Bogoria showing the thylakoid membranes arrangement in C and H morphotypes (A and B respectively).

They are arranged in straight parallel lines for both morphotypes, and there are no phycobilisomes attached to photosynthetic lamella. Bars represent 1µm.

The central cytoplasmic region contains distinctive polygonal cytoplasmic structures called carboxysomes with a diameter larger than 500 nm in older cells, and cylindrical bodies with a diameter of about 300 nm (Figure 4.27).

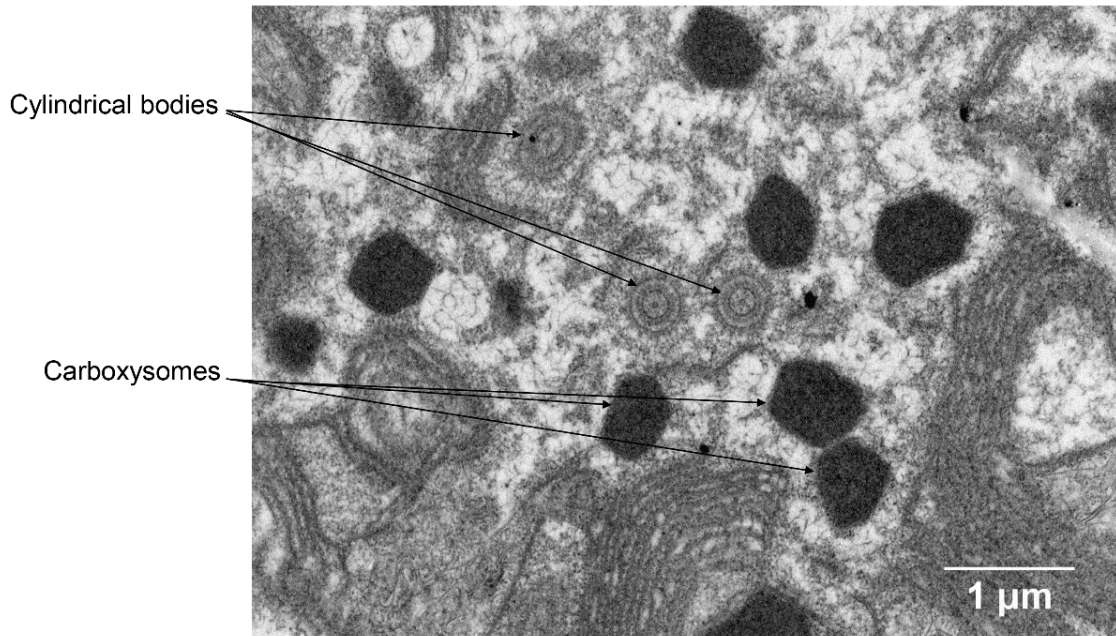


Figure 4.27: Electron micrograph of an *Arthrospira* section showing polyhedral bodies (carboxysomes) with a polygonal profile and cylindrical bodies.

The carboxysomes were thickly stained. Bar represents 1 μm.

Other inclusions were detected, such as unit membrane-like structures (mesosomes) (Figure 4.28) and unknown structures that have not, until now, been observed in *Arthrospira* cytoplasm (Figure 4.29).

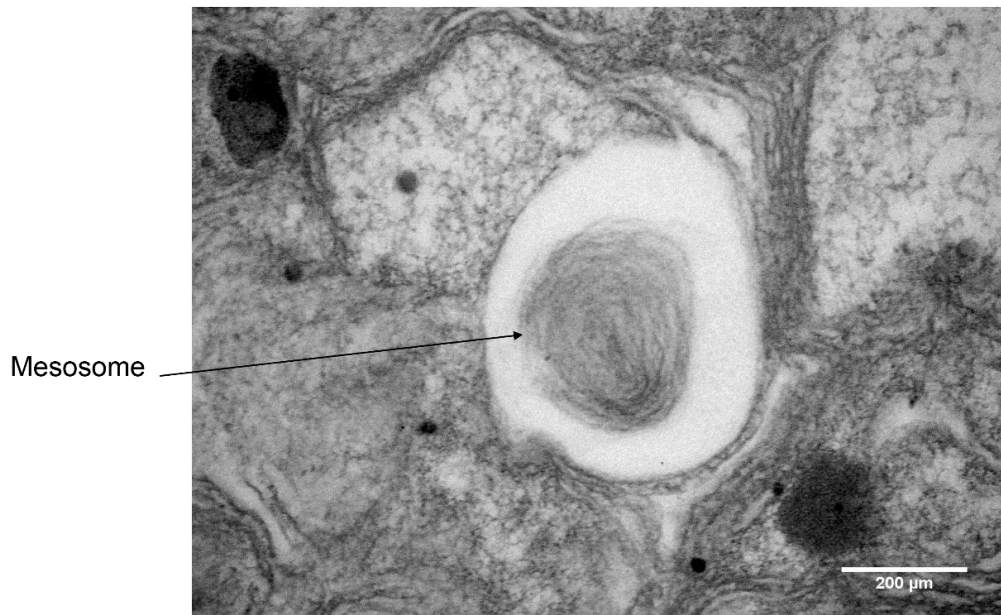


Figure 4.28: Ultrastructure of *Arthrospira* from Lake Bogoria showing a mesosome.

Scale bar indicates 200 nm.

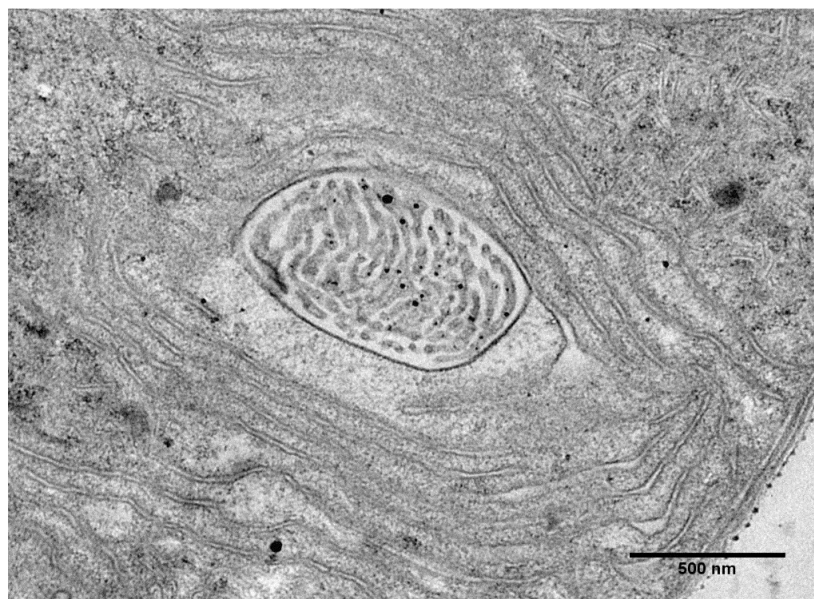


Figure 4.29: Ultrastructure of *Arthrospira* showing a new, unknown structure.

Scale bar = 500 nm.

4.3.7 Absence of gas vacuoles and sinking velocity of *Arthrospira* spp.

Arthrospira is a filamentous, free-floating cyanobacterium; this is due to the presence of gas vacuoles (aerotopes). After culturing *Arthrospira* in the laboratory for approximately 2 years, these filaments began behaving differently. When cultured for a period with Zarrouk's medium, the filaments

distribution changed throughout the medium column. The filaments for two morphotypes - C and H - showed an increase in sinking velocity until they settled down at the bottom of the flasks or well plates (Figure 4.30), whereas the trichomes of the S-morphotype were still floating on the surface of the medium. In addition, TEM analysis revealed that after culturing *Arthrospira* in the laboratory for more than 2 years, those inclusions were not present within the sections of morphotypes H and C, whereas there were inclusions which seemed to be gas vacuoles in the S-morphotype (Figure 4.31).

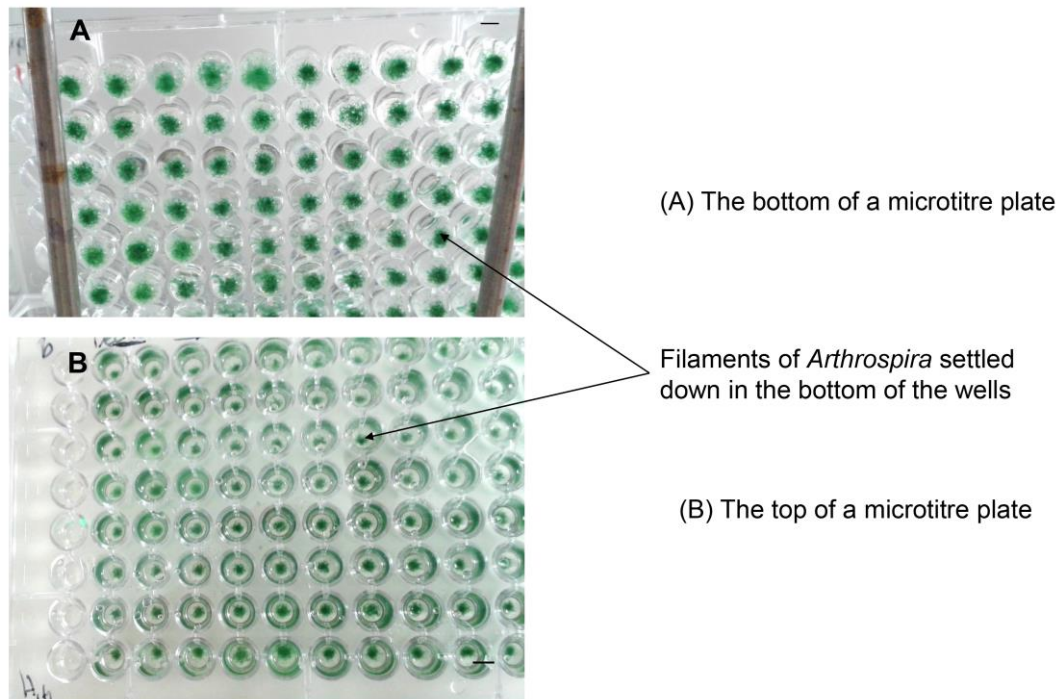


Figure 4.30: Macrographs of cyanobacterium *Arthrospira* cultures (H-morphotype) illustrating the different behaviour after sub culturing them in Zarrouk's medium.

Images were taken of the bottom and top of the microtiter plates (A and B).

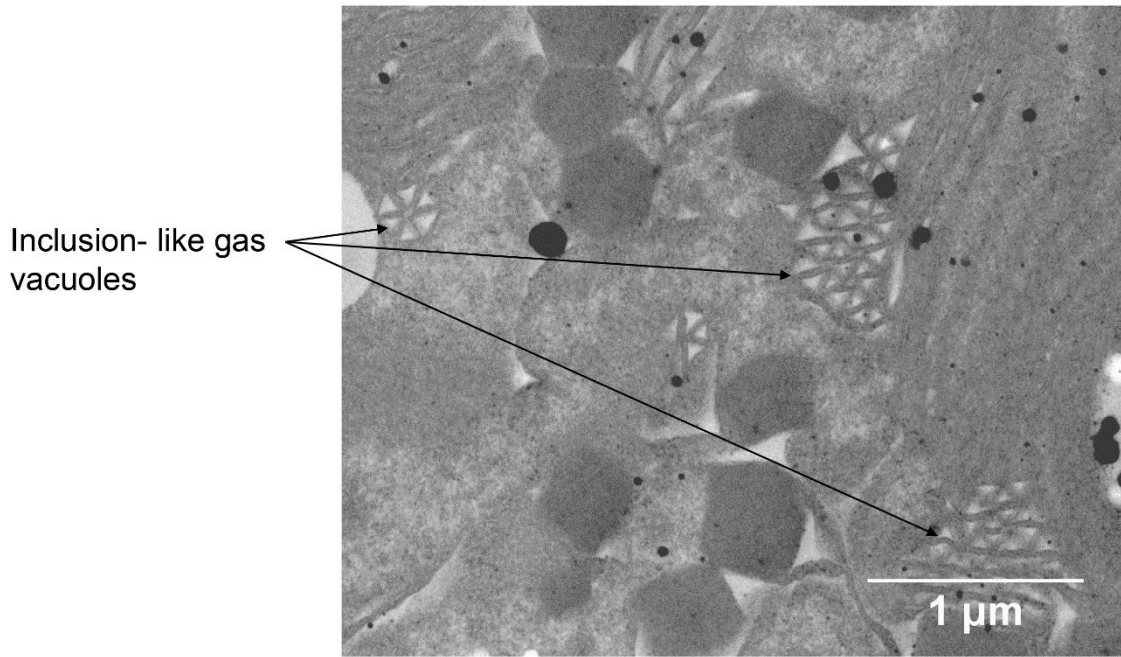


Figure 4.31: Macrographs of cyanobacterium *Arthrospira* cultures (S-morphotype) illustrating the presence of inclusions that look like gas vacuoles.

Scale bar indicates 1 μm.

4.4 Discussion

This chapter highlights the morphological variability among cyanoprokaryotic *Arthrospira* spp. from Lake Bogoria, and how environmental stresses can influence this variability. Three *Arthrospira* phenotypes: S, C and H were observed and isolated from the lake. However, all attempts made to purify and isolate the three morphotypes of *Arthrospira* free from contaminated bacteria have failed. The presence of the mucilage sheath that encapsulates the *Arthrospira* filaments is the most likely explanation for this contamination. The evidence for this is that after the filaments were sonicated and examined under the light microscope, the number of the heterotrophic bacteria present increased compared to those not sonicated. This implying that the bacteria were immersed in this slime sheath and may have a symbiotic relationship with the *Arthrospira*. Any physical or chemical treatment methods would affect the *Arthrospira* cells more than any other bacteria that may be present. It can be concluded that the axenic culture of *Arthrospira* is a very difficult task, and may not be possible to do so due to the complexities involved.

All attempts made to preserve the *Arthrospira* in the long-term were unsuccessful. The underlying cause behind the lack of viability post-preservation is unknown, but this could be due to the toxicity of cryoprotectants or that this resulted in a low temperature which led to a dramatic increase in the osmotic pressure of the cells. This, in turn resulted in cell lysis of *Arthrospira* (Figure 4.8) (Muhling, 2000). Therefore, it seems that there is no applicable or guaranteed procedure for maintaining the viability of the *Arthrospira* cells for long-term storage, either by cryopreservation or storage at low temperature and low light or dark.

The morphological parameters of *Arthrospira*'s trichome, such as trichome helicity and colour were distinctive parameters to differentiate between morphotypes. Three morphotypes have been previously reported from Lake Bogoria and Lake Nakuru as small, large-tight and large-loose (Kaggwa *et al.*, 2013a). Besides these three however, Hindák (1985) had described a fourth variant; the M-morphotype. The author classified *Arthrospira*'s variants of Lake Bogoria into two species, *A. fusiformis* and *A. maxima*. *A. fusiformis* have helical-tight trichomes, while *A. maxima* have helical-loose trichomes, which are described in my study as H and S morphotypes respectively. Sometimes, it was difficult to distinguish between the H and C morphotypes, and this was especially evident when the H-morphotype was immature. There are two options to overcome this difficulty of differentiating between H and C morphotypes, The first would be to classify them as a new morphotype and this most likely happened with Hindák (1985), as he classified a fourth form, M-morphotype. The second option would be to classify them as the C-morphotype, without focusing on all morphological parameters accurately. I feel, to avoid any misuse of trichome description, it is advisable to use three characters (C, H and S) to describe the *Arthrospira* morphotypes rather than using small, large-tight and large-loose terms.

All of the three filament phenotypes examined in this study were fusiform, with varying degrees of attenuation between the different phenotypes (Desikachary and Bai, 1996). The trichome length of the *Arthrospira* spp. in Lake Bogoria ranged from 134.5 to 782.7 μm , which is within the appropriate range of the

Lesser Flamingo beaks' filter (40–800 μm) (Jenkin, 1957). This is why *Arthrospira* forms the main diet of the lesser flamingos in these lake environments.

The dominant variant present was the S-morphotype, making up 47.67% of the entire *Arthrospira*'s population, followed by the C-morphotype (40.65%), and the least abundant H-morphotype (11.69%). The dominance of the S-morphotype has also been reported by Kaggwa *et al.* (2013a), who showed that it was dominant 44.01% and C-morphotype was 20.65%, at the same lake over the period July 2008 to October 2009. This was contrary to the observations made at the other soda lakes in the East African Rift Valley, however; for instance, at Lake Chitu, Ethiopia, between February 2012 to January 2013, Ogato and Kifle (2014) reported that the dominant variant was the H-morphotype (50%) followed by the S-morphotype (40%) and finally the C-morphotype (10%). A possible explanation for this difference might be that the properties of the lake affected the population of each morphotype. Earlier studies had revealed that the S-morphotype filaments predominate in low light conditions, whereas H-morphotype filaments predominate in bright light conditions (Jeeji Bai and Seshadri, 1980, Robinson, 2015). The sample collection of the current study was conducted between 10 am and 3 pm, when the S-morphotype dominated throughout. Therefore, I hypothesise that the S-morphotype is the original morphotype in the lake and is the fittest morphotype. The others, H and C are ecomorphotypes of the S-morphotype, they have evolved from the S-morphotype throughout history, and their abundance is subject to environmental conditions such as light.

The population of each three morphotypes (60.87 (C-morphotype), 71.38 (S-morphotype) and 17.50 (H-morphotype) trichome mL^{-1}) was less than previously reported for the same lake (Kaggwa *et al.*, 2013a). With the severe collapse found in Jul 2016 for the three morphotypes, where the H-morphotype counts were almost zero trichome mL^{-1} . The most likely cause for this, is the increase in the lake's water level/surface area, suggesting that the huge influxes of fresh water that the lake received since the beginning of the current decade carried a large amount of sediment. This resulted in restricted light penetration

into the lake's waters, which in turn led to a reduction in the population of the photosynthetic organisms present.

The C-morphotype was characterised here by short trichomes and no gliding motion on solidified medium. This intermediate shape has not been well reported compared to the other two morphotypes, but all three *Arthrospira* morphotypes have been recorded in freshwater in India, and soda lakes in Kenya (Ballot *et al.*, 2004a). The presence of *A. platensis* in tropical soda lakes as a planktonic form of *Arthrospira* is still a source of debate (Tomaselli, 1997). I suggest, based on literature findings, that plankton forming blooms on the surface of tropical lakes are *A. maxima* and *A. fusiformis* (planktonic forms of *Arthrospira* in tropical and subtropical saline lakes), whereas *A. platensis* and *A. jenneri* are benthic forms of *Arthrospira* in freshwater ecosystems (Komárek and Anagnostidis, 2005).

Most of the studies conducted on morphological changes in cyanobacteria revealed that helical filaments can alter to straight filaments, but the reverse has not been observed (Hickel, 1982, Jeeji Bai, 1985). However, in the present study, where a loose trichome reversed to a tight trichome, no morphological change to the completely straight trichome was observed. This is possible because the change to the straight morphology is a long process (years). Researchers have found that the change from the helical to the spiral shape is a relatively slow process, whereas the reverse process is rapid. The transition processes in the lab depend on agar's water content and is possibly related to the hydration or dehydration of the oligopeptides in the peptidoglycan layer, leading to alterations in the solidity of the cells (Van Eykelenburg *et al.*, 1980).

The coiled shape has been considered as a characteristic of *Arthrospira*'s filament and constant form, but it is possible that there may be natural variation in the degree of trichome helicity between the strains of the same species, as well as within the same strain (Tomaselli, 1997). The spontaneous alteration of *Arthrospira* filaments in shape from helical to straight is well reported. Previous work of Li *et al.* (2001) showed that after two months of isolation of *A. maxima* and *A. fusiformis* separately, both species were found in both cultures. The authors' morphological description was of the trichome helicity of *A. maxima* as

a loose trichome and *A. fusiformis* as a tight trichome, that I described them as S-morphotype and H-morphotype respectively, I reached to the same conclusion, that there is uncertainty as to whether they represent two different species. The next chapter examines this conclusion through genetic analyses.

Filaments of *A. platensis* retained their helical shape only in liquid culture (Ciferri, 1983). When transferred onto solid media, their shapes changed to true spirals (Van Eykelenburg and Fuchs, 1980). However, in my study, for a week of transferring the three *Arthrospira* morphotypes onto semi-solidified medium, none of the morphotypes changed to the straight filament configuration. The filaments began to dry, consequently, the experiment was terminated. I conclude that the change in the trichome helicity can be observed only in liquid cultures.

Differences in the helix parameters can also be induced with environmental stress (Ciferri, 1983) and are expressed as “ecomorphotypes” (Oduor and Kotut, 2016). The only environmental parameter that was tested to see the effect on trichome helicity in this study was pH. The results showed no change in S-morphotype trichome helicity for both tested conditions (pH 9.0 and 10.2), whilst the trichome helicity of the other two morphotypes changed according to the pH treatment. This result could add further support to the idea that the S-morphotype is a well-adapted morphotype that dominates EASLs. The same result was found when the temperature of the culture was used as an environmental stressor. Van Eykelenburg (1979) documented that there is a correlation between the helicity of *Arthrospira* trichomes and the temperature of the culture. He observed a decrease in the pitch and diameter of the helix, with an increase in a culture's temperature.

The mucilage sheath that is emitted from the pores in the second layer (L-II) of the cell wall (Figure 4.21) has been suggested to have a role in the gliding motion of these cyanobacterial species (Halfen and Castenholz, 1971). This does not always appear to be the case, because in this study, the slim sheath (Figure 4.20) was observed to be enveloping the trichomes of three morphotypes. The only morphotype expressing the gliding motion however, was the loose morphotype (S-morphotype), while the others (C and H) were not

motile. This supports earlier general agreement of there is a negative relationship between trichome helicity and the gliding behaviour of *Arthrospira* species (Mühling *et al.*, 2003). Authors classified *A. platensis* and *A. jenneri* as non-motile species and *A. maxima* and *A. fusiformis* as motile species of *Arthrospira*; based on that the first possible conclusion is that the S-morphotype belongs to either *A. maxima* or *A. fusiformis*, and the other two types (C and H) belong to *A. platensis* or *A. jenneri*. The second conclusion, which is more likely is that this sheath has no active role in the motion of this cyanobacterium. Therefore, other factors are considered responsible and the main factor to be considered is the pilus (see chapter 5, section 5.3.5).

The use of an algorithm to calculate the Chl-*a* concentration from satellite data for such water bodies has been criticized (Robinson, 2015). The criticism stems from the fact that the values obtained may not represent the whole biomass. This is because the satellite would not register the *Arthrospira* biomass sedimented in the deeper layers of the lake but would only focus on the surface phytoplankton. However, the results of the present study added further support to use the algorithm method, by proving that measuring the chlorophyll concentration using the satellite images and Tebb's satellite data strongly correlated with the *Arthrospira* abundance ($r_s = 0.9$). *Arthrospira* is the dominant producer in Lake Bogoria over a long continuous timescale, (Tebbs, 2014) longer than any previous records. It can thus be said that this algorithm is valid to analyse the time series of Landsat images for Chl-*a* concentration in such aquatic systems. The correlation further supports the idea of Tebbs (2014), who showed that an algorithm for the remote sensing of Chl-*a* can be used to monitor changes in phytoplankton biomass in these saline-alkaline aquatic bodies. Moreover, another important thing overlooked by Robinson (2015) and worth mentioning, is that Lake Bogoria is chemically stratified therefore the upper 5 metres of the lake never mixes with the lower waters. Therefore, only the dead *Arthrospira* filaments (that may not have nutritional value to lesser flamingos) and diatoms (less favourite diet by lesser flamingos) fall to the deeper layers of the lake.

No correlation was found between the lake's pH and the *Arthrospira* count for three morphotypes, $r_s = -0.046$ (C), 0.028 (S) and 0.100(H); $p = 0.79$ (C), 0.87

(S) and 0.56 (H). Other lake properties showed a moderate to strong positive correlation with *Arthrospira* abundance. However, none of the lake's properties could be used to predict *Arthrospira* abundance in Lake Bogoria (ANOVA test, $p > 0.05$). One can conclude that Lake Bogoria is not nutrient limited, and abiotic factors are far from responsible for causing bloom disruption events in EASLs, and biotic factors such as viral infections, are more likely to be the cause of these collapses.

A change in the behaviour of the *Arthrospira* trichomes after they were cultured in the laboratory for more than two years was observed. The trichomes of the C and H morphotypes started to sink to the bottom of the flasks, while the trichomes of the S-morphotype were somewhat still floating on the culture's surface. Within nature, gas vacuoles are responsible for floating the phytoplankton, consequently affecting their distribution through the water column, this is dependent on the daily and seasonal changes in light intensity. The presence of these intracellular components within the *Arthrospira*'s cytoplasmic region, suggests that they are either *A. maxima* or *A. fusiformis* (Mühling *et al.*, 2006). The ultrastructure comparison of the three morphotypes showed the presence of intracellular components in the raw *Arthrospira* sections from the lake, and their absence in the C and H morphotypes after the relative long-term culturing in the laboratory. This could explain the sinking of these trichomes. All raw samples that were examined immediately after their arrival to the laboratory contained a mixture of the three morphotypes, so it was difficult to determine whether the three morphotypes contained the gas vacuoles. However, I suggest that all three morphotypes contained the gas vacuoles because all of them were floating on the surface of the Bogoria's water.

The speed of sinking is greatly affected by the trichome morphology. There are three explanations for reducing sinking velocity (Sili *et al.*, 2012). The first possibility is that this may reduce the surface area of its bodies, which reduces the risk of being a target for grazers. The second possibility is that it may reduce their specific gravity by increasing the density of the gas vacuoles, or by reducing the production of certain substances, such as carbohydrates. The final

possibility is that it may increase its form resistance (Φ). It has been observed that the dimensions of this last factor are related to the sinking velocity, and it is decreased in helical forms and increased in straight forms (Padisák *et al.*, 2003). Therefore, coiled shapes can sink more quickly than straight shapes. The S-morphotype (less coiled than others) was most often floating on the surface of the medium, whereas the other two, C and H were quick to sink. This explanation reflects the work of Booker and Walsby (1979), who also found that the coiled trichomes of *Anabaena flosaquae* sank remarkably faster than the straight filaments.

As explained in chapter 3, Lake Bogoria is a meromictic lake, meaning that it is a stratified lake with two layers that do not fully mix (Renaut and Tiercelin, 1994). Harper *et al.* (2003) showed that oxygen concentration sharply decreases after one meter of depth and that Bogoria's waters became anaerobic at five meters deep and above in Feb 2000. This result was confirmed by Robinson (2015), who found that the oxygen concentration was 0 mg L⁻¹ at 5 meters, at all three of the Bogoria's basins in 2013. Based on these results, it is possible to explain the occurrence of *Arthrospira* spp. on the surface of this water body, by suggesting that the lake is aerobically and chemically stratified. Therefore, the *Arthrospira* filaments are floating on the surface of the lake to obtain light, nutrients, and to escape from the anaerobic conditions in the deeper layers of the lake.

The ultrastructure shifting of *Arthrospira* was observed where polyglucan granules were not detected whilst another storage body (cyanophycin) was present. Previous studies have suggested that culture conditions play a vital role in the disappearance of these two storage bodies. For example, cyanophycin granules were abundant at temperatures between 17.0 and 20.0 °C. Above this temperature, hexagonal rods about 25 nm wide and 400 nm long replaced these inclusions, called polyglucan granules. They were not present after cultivating *Arthrospira* in the dark (Fuhs, 1973). It is likely that the metabolism changes from nitrogen storage to carbohydrate storage (Van Eykelenburg, 1979). In the same context, Giesy (1964) found that the concentration of polyglucan granules decreased with increased light intensity.

Consequently, the most likely hypothesis is that the stratified feature of the lake and the floating nature of the *Arthrospira* have contributed to increasing the severity of the meteorological impact on the internal structure of this cyanobacterium.

The arrangement of the thylakoid membranes within the cytoplasm was an interesting observation made during this study. Although the uniform structure of these inclusions has been previously described (Busson, 1970), the cause of this difference is still unclear and has not been well investigated, thus it is difficult to interpret this result. It is possible therefore that their straight arrangement in the C and H-morphotypes, and circular arrangement in S-morphotype raises my hypothesis, where I again suggest that C and H-morphotypes are just ecomorphotypes of S-morphotypes, and the slight ultrastructure differences occurred during their evolutionary history.

Trypsin or pronase-treated cells are known to lose their phycobilisomes from the photosynthetic lamellae (Lecina *et al.*, 2017). In the current study, neither pronase nor trypsin was used, despite this, phycobilisomes were not found in every sample. This could be because of the sensitivity of these granules to the chemical treatments performed during the sample preparation. Another possible reason for this could be the decrease in nutrient concentration, particularly in nitrogen concentration. The large inflow of freshwater that Bogoria experienced diluted the nutrient concentrations (see chapter 3, section 3.3.1.3). This conclusion was built based on the findings of Ciferri (1983). Authors reported that there is an association between nitrogen concentration in the media, and phycocyanin content in the *Arthrospira*.

As shown in Figure 4.24, with the exception of the July 2016 sample, the Bogoria samples did not contain light harvested antenna as represented by phycobilisomes. The lack or absence of these important attached inclusions to the thylakoid membranes is likely to have increased the photoinhibition impact. This effect can increase in severity with increased penetration of UV-B radiation into Lake Bogoria's water body. Unlike marine phytoplankton, *Arthrospira* spp. do not require high concentrations of sodium to grow (Sili *et al.*, 2012). It has been demonstrated that photoinhibition caused by a rapid entry of sodium may

be due to the separation of phycobilisomes from the thylakoid membranes (Blumwald *et al.* (1984) cited in Sili *et al.* (2012)). Moreover, the salt stress could prevent the transfer of electrons at the donor and acceptor sites of the PSII (Lu and Vonshak, 2002). This situation results in damage to the phycobilisomes and a partial disconnection of these inclusions from PSII. This, in turn, led to a change in the distribution of excitation energy from PSII in favour of Photosystem I (PSI). The effect of salt stress would be more severe if accompanied by a high level of light exposure (Zeng and Vonshak, 1998). Summarizing the role of sodium in PSII photoinhibition in *Arthrospira*, Schlesinger *et al.* (1996) suggested that at a high pH, 150-250 mM of sodium is required for the optimal growth of *A. platensis*. It can thus be suggested that a time series analysis of sodium concentrations is required to help understand the reason behind the disappearance of the phycobilisomes.

According to the above, the collapse of the *Arthrospira* spp. population of Lake Bogoria can be explained by the detachment of the vital cyanobacterial inclusions (phycobilisomes) from the thylakoid membranes. This can be attributed to either the increase or decrease in sodium concentrations that can lead to pigment bleaching. It is more likely that a large amount of water received by the lake over the past few years has contributed to a significant reduction in the concentrations of its various salts (Chapter 3 & Figure 2.3). This, in turn, has a negative impact on the *Arthrospira* spp. population that is currently being observed.

The aforementioned discussion is built on the basis that these nanoparticles are *Arthrospira* inclusions (phycobilisomes). However, during the current study period, these nanoparticles within the *Arthrospira* cytoplasm were detected only in the July 2016 sample, which was accompanied by the largest *Arthrospira* population collapse (bloom breakdown event). In addition, the thylakoids were severely damaged. The assumption could be made however that they should be healthy if these nanoparticles were phycobilisomes. Another interesting point is that since these nanoparticles indicate the health status of these cyanobacteria, they are supposed to appear at the time of the *Arthrospira* bloom, however, the opposite has occurred. This observation may support the

hypothesis that these nanoparticles may not be phycobilisomes, but a biological agent such as cyanophages, that infect *Arthrospira* in such an extreme environment (see Chapter 6).

4.5 Conclusion and future work

It is now clear that the species nomenclature of *Arthrospira* spp. based on phenotypic features is more complicated than previously thought because members of this cyanobacterium genus have a high degree of trichome plasticity. However, these ecomorphotypes are an expression of environmental stress rather than permanent characteristics. The most obvious finding to emerge from the morphological comparison between three morphotypes which can be an answer to some of the questions that this chapter is about is that two morphotypes, C and H are morphologically and physiologically the same, although some slight differences such as the length and colour of the trichome. The S-morphotype which was found to be dominant throughout the study period is morphologically and physiologically different from the others, but the ultrastructure of the three morphotypes was very similar. Therefore, a further genetic study was conducted to answer the question as to whether the other two *Arthrospira* variants, C and H are just ecomorphotypes of the dominant S-morphotype variant? (Chapter 5).

The severe collapse in the population of its three morphotypes was observed during Jul 2016. Environmental conditions could play a vital role in the variation in morphological features of *Arthrospira*, but not in its abundance, which is likely to be a defence mechanism rather than a taxonomic characteristic. Further research should be undertaken to investigate the effects of other environmental factors on the morphology and physiology of *Arthrospira* outdoors.

Chapter 5 Comparative genomic analysis of *Arthrospira* of Lake Bogoria

5.1 Introduction

The taxonomy of *Arthrospira* at the species level is complex and challenging. Twelve species have been listed to date, *A. fusiformis*, *Arthrospira geitleri*, *Arthrospira gomontiana*, *Arthrospira indica*, *A. jenneri*, *Arthrospira khannae*, *Arthrospira massartii*, *A. maxima*, *Arthrospira miniata*, *A. platensis*, *Arthrospira neapolitana*, and *Arthrospira tenuis*; they have been described as different species, even though it is difficult to distinguish between them (Komárek and Lund, 1990, Tomaselli, 1997). This genus of cyanobacteria is well known for its high morphological variability that has been observed both in nature and in laboratory cultures. The use of the degree of trichome helicity as a taxonomic tool to distinguish between *Arthrospira* species has been heavily criticized (Li *et al.*, 2001), as some species are morphologically similar but their trichome arrangement changes according to the surrounding conditions rather than being a stable feature of a species (Chapter 4). For example, Tomaselli (1997) demonstrated that the appearance of straight filaments within spiral cultures is a common phenomenon and, indeed, a frequent occurrence. Four years later Li *et al.* (2001) showed that two *Arthrospira* morphotypes isolated from Lake Chitu, Ethiopia, in July 1999, one with a tight helix and described morphologically as *A. fusiformis*, and another with a loose helix and described as *A. maxima*, were both mixed in isolated cultures. Thus, a more effective approach of separating *Arthrospira* species must be determined.

The taxonomic investigation of genus and species in cyanobacteria has more recently changed from the use of classic morphological characteristics to the use of genetic features (Oren, 2004). This is because genotypic analysis has been found to be more informative than its counterpart (Jungblut *et al.*, 2005), although the polyphasic avenue is used to classify cyanobacteria (Palinska and Marquardt, 2008). The most commonly used molecular approach is a phylogenetic analysis of the sequence of the PCR products of marker genes. In the case of *Arthrospira*, three marker genes are widely used, a small subunit of ribosomal RNA (16S rRNA) (Ludwig and Schleifer, 1994), the internally

transcribed spacer region between 16S and 23S genes (ITS) (Baurain *et al.*, 2002) and the intergenic spacer of the phycocyanin operon between *cpcB* and *cpcA* subunit (PC-IGS) (Dadheech *et al.*, 2010). The phylogenetic analysis of ITS sequences of 21 strains of *Arthrospira* belonging to four different morphological *Arthrospira* species (*A. platensis*, *A. maxima*, *A. fusiformis*, *A. indica*) was used to establish their genotypes by (Baurain *et al.*, 2002). Ballot *et al.* (2004a) then conducted an independent molecular analysis of the above three markers in order to study genetic diversity of three cyanobacteria genera (*Arthrospira*, *Spirulina* and *Phormidium*) from two different locations (Kenyan soda lakes and the freshwater lakes of India). My study followed this latter approach to identify the species of *Arthrospira* spp. found in Lake Bogoria, parallel to those available in the database. It also investigated whether the three phenotypes found (called S, C and H) were of one species or more than one.

Whole-genome sequencing has become a useful tool with which to study the genetic features of organisms. The first use of this approach in cyanobacteria was in 1996, where the complete genome of the unicellular cyanobacterium of *Synechocystis* sp. PCC 6803 was achieved. Since then, more than 40 cyanobacterial species have been sequenced, most of which are unicellular cyanobacteria, both nitrogen-fixing and non-fixing (Masuda *et al.*, 2010). To date, the filamentous cyanobacteria have received less attention in terms of sequencing, in part because of the difficulty in obtaining pure cultures of them.

Genetic analysis of *Arthrospira* spp. has recently become the focus of several researchers, due to its useful properties in the fields of biotechnology and environmental technology. Since the end of the last decade, whole genome sequencing has been conducted for seven *Arthrospira* spp. from different environments as follows: *A. maxima* CS-328, *A. platensis* NITE-39, *A. platensis* PCC 8005, *A. platensis* Paraca, *A. platensis* C1, and *A. platensis* YZ and *Arthrospira* sp. TJDS091.

The genetic approach to classification may or may not be consistent with the traditional methods of classification, which are based on morphological and physiological characteristics. To have a holistic understanding of the strains used in this study, genetic, morphological and physiological approaches were

carried out. In the previous chapter, morphological and physiological tools were described that were used to determine whether the three *Arthrospira* morphotypes might belong to different species. In this chapter, the genetic approach is described that allowed me to arrive at a precise classification and to confirm or negate traditional classifications. My intention in this chapter was thus to identify the *Arthrospira* species that prevail in Lake Bogoria.

Genomic sequencing techniques have evolved rapidly, and several platforms have launched to gain the best result in terms of sequence quality. Most prominently is the Illumina sequencing platform (iSeq, MiniSeq, MiSeq, NextSeq, HiSeq, HiSeq X and NovaSeq series), the Ion Torrent, and Pacific Biosciences (PacBio) (Quail *et al.*, 2012). Whilst the Second-Generation Sequencing (SGS) applications have provided several features through Sanger sequencing, its shortcomings, which include short reads, make them particularly inappropriate for certain applications such as genomic assembly and methylation investigation (Rhoads and Au, 2015). The Single-Molecule Real-Time (SMRT) sequencing, as released by PacBio, provides an alternative path through which to avoid many of these flaws. PacBio is considered a Third-Generation Sequencing (TGS) techniques. It is distinguished from previous generations of genomic sequencing techniques (First-Generation Sequencing (FGS) and SGS applications) in the following ways. (1) during the sequencing process, there is no need to pause between reading steps; (2) higher output; (3) less time consuming; (4) longer reads ; (5) higher accuracy in detecting genetic variability; (6) smaller amount of raw material (genomic material) required and (7) lower cost (Schadt *et al.*, 2010).

In this study, to avoid the problems of short reads, the PacBio platform was selected as a tool to sequence the two *Arthrospira* morphotypes (S and H). The C-morphotype has not been sequenced because it is morphologically and physiologically similar to the H-morphotype (Chapter 4). This is its first use for the genome sequencing of *Arthrospira*.

My aim was achieved with the following objectives:

- 1- To amplify the marker genes for this cyanobacterium, using all three morphotypes and then conduct phylogenetic analysis on the base of

nucleotide sequences in order to identify the most closely related species from the database.

- 2- To perform whole genome sequencing for subsequent use, as well as a tool for identifying the *Arthrospira* species.
- 3- To conduct comparative genome analysis to study the differences between the two most visually different morphotypes (S and H) and other *Arthrospira* species that are available in the National Centre for Biotechnology Information (NCBI) database.

Guiding questions for the chapter

- 1- Are *Arthrospira* morphotypes of Lake Bogoria genetically different?
- 2- What are the species of *Arthrospira* from Lake Bogoria?

5.2 Material and methods

5.2.1 DNA extraction of *Arthrospira* of Lake Bogoria

The DNA genome extraction of this genus of cyanobacteria is a challenging task for several reasons. Firstly, it is well known that the DNA content of *Arthrospira* is relatively low compared with other bacteria, ~ 0.8% of the dry weight (Ciferri, 1983); therefore, a large quantity of culture is needed to yield sufficient quantities of DNA. Secondly, a slime sheath consisting of polysaccharides, which precipitate as white fibres during the alcohol precipitation step, covers its filaments; consequently, they interfere with the genome, which can lead to a decrease in genome quality. Thirdly, the axenic cultures of this cyanobacterium were unfortunately not achieved during the current study; therefore, contamination with other heterotrophic bacteria might affect the genome sequencing.

DNA was extracted from three morphotypes of *Arthrospira* (S, C and H) using the combination of two protocols (Singh *et al.*, 2011, William *et al.*, 2012), with certain optimisations made but overall following the sequencing company's recommendations. Briefly, three 250mL flasks of an exponential phase of each *Arthrospira* morphotype were washed with the growth medium several times

using a 71µm sterile sieve, and then immediately examined for contamination using a light microscope. This step was repeated for each morphotype until any bacterial contamination had been minimised. Afterwards, the pelleted filaments were transferred into 2mL nuclease-free Eppendorf tubes to which 400µL of lysis buffer (Urea 4M; Tris-HCl 0.2M, pH 7.4; NaCl 20mM and EDTA 0.2M)(Appendix 8.1) and 50µL of lysozyme (100 mg mL⁻¹) (Sigma Life Science, UK) (Appendix 8.1) was immediately added, and were incubated at 37°C for 30 min to lyse the cells. To digest the proteins, 50µL Proteinase K with an initial concentration of 20 mg mL⁻¹ (Appendix 8.1) (Fisher Scientific, Germany) were added. The treated cultures were then incubated for 15 min at 55°C and gently mixed every 5 min. Afterwards, 1mL of prewarmed (55°C) DNA extraction buffer (CTAB 3%; NaCl 1.4M; EDTA 20mM; Tris-HCl 0.1M, pH 8.0; Sarkosyl 1% and Mercaptoethanol 1%) (Appendix 8.1) was added and the tubes were incubated at 55°C for an additional 15 min to eliminate polysaccharides. The solution was homogenised by gentle inversion of the tubes every 5 min. Afterwards, the mixtures were divided into two parts, and to each portion, two volumes of chloroform: isoamyl alcohol (24:1 v/v) were added. After this, the mixtures were inverted manually until a white emulsion arose. Following this step, centrifugation at 13,000 g (Eppendorf centrifuge 5418, Germany) for 10 min was used to separate the DNA from the protein/cell wall debris, and then 500µL of the upper aqueous layer was carefully transferred to a sterile Eppendorf tube and a mix of 0.5mL of phenol: chloroform: isoamyl alcohol (25:24:1) was added and mixed well. The tubes were then centrifuged at 13.000 g for 10 min. After that, the upper layer was again carefully transferred to a fresh Eppendorf tube. Further purification was achieved by adding a further 0.5mL of a chloroform: isoamyl alcohol (24:1) solution that was well mixed and then centrifuged as above. After this step, a new upper aqueous layer that contained the pure, dissolved DNA was transferred to a 2mL sterile Eppendorf centrifuge tube. To precipitate the DNA, 2 volumes of ice-cold 100% ethanol, and 0.1 volumes of 3M sodium acetate (pH 5.2) were added. These mixtures were incubated at -20°C overnight; thereafter, DNA pellets were recovered by centrifugation at 13,000 g for 10 min, and washed twice with 70% ice-cold ethanol (500µL) to remove any remaining salt superfluity. Subsequently, the pellets were left to dry in the hood and then suspended in 40µL of 1mM Tris-Cl at pH 8.0 (Appendix

8.1). The DNA quality and quantity were analysed using a NanoDrop ND-1000 spectrophotometer and Qubit (Thermo Fisher Scientific, UK), respectively. Gel electrophoresis was conducted with a TAE buffer to confirm the integrity of the genomes before being immediately stored at two different cooling conditions (-20°C for PCR or 4°C for sequencing). The extracted DNAs for three morphotypes were run on a 0.5 % agarose gel along with GeneRuler High Range DNA Ladder (Thermo Scientific, UK) at 35 V for 17h.

5.2.2 PCR amplification and sequencing

5.2.2.1 PCR amplification

The DNA genomes extracted from the three *Arthrospira* morphotypes were used as targets to amplify the marker genes of this cyanobacterium using a SensoQuest LabCycler (SensoQuest GmbH, Germany). The primers of 16S3'F and 23S5'R were used to amplify the internally transcribed spacer (ITS) between the 16S rRNA and 23rRNA genes. The primers *cpc_arF* and *cpc_arR* were used to amplify the phycocyanin locus, namely the intergenic spacer (PC-IGS), including fractions of the beta (*cpcB*) subunit, IGS and alpha (*cpcA*) subunit (Li *et al.*, 2001, Baurain *et al.*, 2002, Ballot *et al.*, 2004a). The cyanobacterial specific primers of 27 F and 809 R were used to amplify the 16S rRNA gene (Rout *et al.*, 2015).

The final volume of each PCR reaction mixture was made up to 20µL. It contained 0.1µL *BioTaq* DNA polymerase (5 UµL⁻¹) (Bioline, UK), 0.6µL deoxynucleotide triphosphate (dNTPs) (10mM) (Appendix 8.1) (Bioline, UK), 2µL PCR reaction buffer (10x) (Bioline, UK), 1µL of each primer (10pmolL⁻¹) (IDT®, USA), 0.6 µL of MgCl₂ (50 mM) and 1µL genomic DNA, except for the negative control where UPW was used instead. *Arthrospira* from the laboratory collection was used as a positive control. To avoid any pipetting error, the master mixtures were made up as n+1. The primer sequences are listed in Table 5.1. The thermal cycling conditions applied to effect the amplifications were as follows: 95°C for 5 min, 30 cycles of 95°C for 30 s, 55°C for 1 min, 72°C for 1 min, with a final extension of 10 min at 72°C. 5µL of the PCR fragments were mixed with 1µL of 6x gel loading dye (New England Biolabs(NEB), UK) and then separated on 1% gel agarose at 100 V along with

GeneRuler™ 1 kb DNA Ladder (Biolabs, UK) for 1h. The gel was analysed using the Genesnap software in the UV Transilluminator (Syngene, UK). PCR products with the expected product sizes were purified with an Isolate II PCR and Gel kit (Bioline, UK), and sequenced by GATC Biotech using the same primers.

Table 5.1: Details of primers used in the present study.

Primer	Orientation	Sequence	Reference
Long 23S5'R 16S3'F	Reverse	5'-TCT GTG TGC CTA GGT ATC CAC CGT T-3'	(Baurain <i>et al.</i> , 2002)
	Forward	5'-TGY GGC TGG ATC ACC TCC TT-3'	(Baurain <i>et al.</i> , 2002)
27 F	Forward	5'- AGAGTTTGATCCTGGCTCAG-3'	(Rout <i>et al.</i> , 2015)
809 R	Reverse	5'- GCTTCGGCACGGCTCGGGTCGATA-3'	(Rout <i>et al.</i> , 2015)
cpc_arF	Forward	5'- TCGAAGATCGTTGCTTGAACG-3'	(Ballot <i>et al.</i> , 2004a)
cpc_arR	Reverse	5'- TTAGGTCCCTGCATTTGGGTG-3'	(Ballot <i>et al.</i> , 2004a)

5.2.2.2 Phylogenetic analysis

The [Geneious](http://www.geneious.com) 8.1 software (www.geneious.com, (Kearse *et al.*, 2012)) was used to analyse the sequences of three amplified genes for the three *Arthrospira* morphotypes. The 16S rRNA gene, ITS region and PC-IGS locus sequences obtained from GATC biotech were trimmed to remove the sequences that had low-quality scores (less than 20). The consensus sequence for each morphotype's amplified loci was generated by aligning the forward and reverse sequences of each gene together. The consensus sequences for all morphotypes were used for all subsequent phylogenetic analysis. A Basic Local Alignment Search Tool (BLAST) search was carried out to match them to the most closely related sequence from the GenBank, [National Center for Biotechnology Information](http://www.ncbi.nlm.nih.gov) (NCBI) (www.ncbi.nlm.nih.gov).

All *Arthrospira* fragments for the three target genes available in the NCBI database were collected, with only the unique ones being kept for further analyses. Before phylogenetic trees were built, the best substitution model was chosen for each set of the unique sequences that belong to the same amplified gene and consensus sequences of three morphotypes using the MEGA software, which were JC+G, K2 and GTR+G for 16S rRNA, PC-IGS locus and

ITS, respectively. Afterwards, unique sequences of the ITS region, 16S rRNA gene, PC-IGS locus, together with those analysed in the present study, were aligned using ClustalW multiple alignment in the Geneious software. Therefore, 53 (ITS), 41 (PC-IGS locus) and 28 (16S ribosomal DNA) sequences were considered for alignment and comparison. Subsequently, phylogenetic trees were constructed for each marker gene using the MrBayes method and *Lyngbya majuscula* CCAP 1446/4, *Lyngbya* sp. CCAP 7419 and *Lyngbya* sp. Ind63 cyanobacteria were used as the out-groups for ITS, PC-IGS locus and 16S rRNA, respectively.

5.2.3 Whole DNA sequencing and analysis

5.2.3.1 Whole genome sequencing

Good quality of DNA from two morphotypes (S and H; the C-morphotype was eliminated because it is first very morphologically and physiologically similar to the H-morphotype, second due to the high cost of the PacBio sequencing) were sent for sequencing at the Centre for Genomic Research in Liverpool.

Before the genomes were sequenced, the DNA genome of two samples was first purified with 1x cleaned AMPure beads (Agencourt), after which the quantity and quality were assessed using NanoDrop and Qubit assay. In addition, the Fragment Analyser (AAT), using a high sensitivity genomic DNA kit, was used to determine the average size of the DNA and the extent of degradation. This procedure was also used in the steps indicated below to determine average fragment size of the DNA. DNA samples were sheared with a covaris g-tube at 5200 rpm to approx. 10 kb and purified with AMPure beads. Thereafter, DNA was treated with Exonuclease VII at 37°C for 15 minutes. The ends of the DNA were repaired as recommended by PacBio. Samples were incubated for 20 minutes at 37°C with the DNA damage repair mix supplied in the SMRTbell library kit (PacBio). This was followed by a 5-minute incubation at 25°C with an end repair mix. DNA was cleaned using 0.5x AMPure and 70% ethanol washes. Then, the DNA was ligated to an adapter at 25°C overnight. Ligation was terminated by incubation at 65°C for 10 minutes, followed by exonuclease treatment for 1 hour at 37°C. The SMRTbell libraries were purified with 0.5x AMPure beads. These were size selected with a 0.75% blue pippin

cassette in the range 7000-50000 kb. The quantity of libraries, and therefore the recovery, was determined by Qubit assay and the average fragment size determined using a fragment analyser. SMRTbell libraries were annealed to a sequencing primer at values predetermined by the Binding Calculator (PacBio) and a complex made with the DNA polymerase (P6/C4 chemistry). The complex was bound to Magbeads, which were then used to set up 1 SMRT cell per library on the PacBio RSII instrument.

5.2.3.2 Genome assembly and annotation

Raw sequencing reads from the PacBio RS II instrument were assembled into the contigs using *de novo* assembly approach. To achieve this, the Canu assembler (<https://github.com/marbl/canu> (Koren *et al.*, 2017)) was used. Afterwards, the assemblies were polished to remove any single base/short insertion and deletion (indels) errors in the contigs by iteratively realigning reads to the assemblies and recalling the consensus sequence until none genomic variations were found. After the assembled genomes were received from Centre for Genomic Research in Liverpool, and because the analyses that will carry out later require certain types of files as recommended by software's producers, two annotation tools were used to annotate the *Arthrospira* genomes. The 1st was Rapid Prokaryotic Genome Annotation of the Prokka tool (<https://github.com/tseemann/prokka> (Seemann, 2014)) while the 2nd was Rapid Annotation using Subsystem Technology (RAST) (<http://rast.nmpdr.org/> (Aziz *et al.*, 2008, Brettin *et al.*, 2015)). RAST toolkit (RASTtk) version was used, and Fasta format files were used as inputs for both software.

5.2.3.3 Comparative genome analysis

Data analysis was performed as follows:

- 1- Comparative genome analysis between two *Arthrospira* morphotypes, S and H was performed to understand their relationship by using RAST. This comparison was function- and sequence-based. Based on the comparison result and the number of contigs, one *Arthrospira* morphotype (the S-morphotype) was chosen to finish the assembly of *Arthrospira* genome from Lake Bogoria. There are two different approaches to close the gaps and order the contigs. The first is an

experimental approach by amplifying the regions between the contigs (via PCR); the second is a computational approach by using bioinformatics-based tools. Due to a lack of time, the second approach was performed in this study, by mapping the Bogoria genome to the reference genome as described by Cheevadhanarak *et al.* (2012). To achieve this, *Arthrospira platensis* C1 was employed as a reference (see 5.3.4.3 section). Two alignment tools were used to reorder the *Arthrospira* genome into one circular chromosome (RAST and Mauve). Thereafter, to verify the rearrangement is correct, the visualisation tool of Circos ((Krzywinski *et al.*, 2009), <http://circos.ca/documentation/>) was used. Finally, the Nano text editor of the Linux operating system was used to concatenate the four contigs into one scaffold. A circular genome of one chromosome of *Arthrospira* from Lake Bogoria was constructed using Artemis tool, version 16.0.11 (Carver *et al.*, 2012).

- 2- Phylogenetic analysis was conducted using the six partial or complete genomes of the *Arthrospira* strains available in the NCBI database (*A. platensis* NIES 39, *A. platensis* str Paraca UASWS, *A. platensis* YZ, *A. platensis* C1, *A. maxima* CS-328 and *Arthrospira* sp. PCC 8005) together with those of the current study, and two species from the order Oscillatoriales – *Lyngbya* sp. PCC 8106 and *Gloeobacter violaceus* PCC 7421. Of 31 conserved genes in 578 complete bacterial genomes, 27 were concatenated to construct the species tree as described by Xu *et al.* (2016). The genes were as follows: *dnaG*, *frr*, *nusA*, *pgk*, *pyrG*, *rplA*, *rplB*, *rplC*, *rplD*, *rplE*, *rplF*, *rplK*, *rplL*, *rplM*, *rplN*, *rplP*, *rplS*, *rpoB*, *rpsB*, *rpsC*, *rpsE*, *rpsI*, *rpsK*, *rpsM*, *rpsS*, *smpB*, and *tsf*. The Artemis software (Carver *et al.*, 2012) was used to grab the amino acid sequences of these genes from two Bogoria isolates. Some genes were not present in all the species considered; therefore, *Gloeobacter violaceus* PCC 7421 was used as an outgroup to root the tree. A MyBayes phylogenetic tree was built with a WAG + G + F substitution model.
- 3- The whole genome analysis was conducted by pan-genome calculation. Two pipelines were used, the Pan Genome Pipeline of Roary (Page *et al.*, 2015) and the large-scale blast score ratio (LS-BSR) pipeline (Sahl *et al.*, 2014).

- a- **Roary pipeline:** The input files for Roary were GFF3 files constituting seven available genomes of *Arthrospira* in the NCBI database (*A. platensis* NIES 39, *A. platensis* str Paraca UASWS, *A. platensis* YZ, *A. platensis* C1, *A. maxima* CS-328, *Arthrospira* sp. PCC 8005 and *Arthrospira* sp.TJSD091) and two Bogoria isolates that were produced by the Prokka tool. The Roary script was used to run the software. The outputs were visualized using the roary_plots.py tool. This tool is used in combination with a Newick tree file and gene_presence_absence .cvs output file. Phylogeny was created using the fasttree tool (Price *et al.*, 2010), which used the core_gene_alignment.aln file from the Roary output as input to create the Newick tree file that was visualised using the Molecular Evolutionary Genetics Analysis (MEGA) tool (Kumar *et al.*, 2016).
- b- **LS-BSR pipeline:** Fasta files of seven available genomes of *Arthrospira* in the database (*A. platensis* NIES 39, *A. platensis* str Paraca UASWS, *A. platensis* YZ, *A. platensis* C1, *A. maxima* CS-328, *Arthrospira* sp. PCC 8005 and *Arthrospira* sp.TJSD091) and two *Arthrospira* Bogoria isolates were used as inputs. The pan-genome analysis was run on these isolates. Once the pangenome calculation was completed, the core genome was extracted using the LS-BSR script, extract_core_genome.py. This extract concatenates and aligns all regions that are common to all isolates. These core genome sequences were used to generate a phylogeny using the Randomized Axelerated Maximum Likelihood (RAxML) program (Stamatakis, 2014).
- 4- Multiple genome comparisons were also conducted by studying the recombination events. To achieve this, orthologous and xenologous regions of seven available genomes of *Arthrospira* in the NCBI database and two *Arthrospira* Bogoria isolates were aligned using the Mauve software (<http://darlinglab.org/mauve/user-guide/introduction.html>, (Darling *et al.*, 2007)). The software was designed to align closely related genomes with moderate to high levels of genome rearrangement and performs better when used in the alignment of a small number of closely related genomes, so the software options were left as default parameters

except for the seed size and locally collinear block (LCB) weight. These were set to 16 and 2955 respectively, to eliminate spurious rearrangements. Thereafter, a neighbour-joining tree was constructed using the aligned genomes of Mauve.

5.2.3.4 Gliding motility genes

Only the S-morphotype has the ability to glide on the semi-solid agar plate while the other two morphotypes (H and C) cannot (as noted in Chapter 4). Therefore, the presence of Type IV pil (T4P) genes involved in the twitching and gliding motility in bacteria was verified in two morphotypes (H and S) using the Artemis software. The amino acid sequences of these genes were aligned using the Multiple Sequence Comparison by Log- Expectation (MUSCLE) tool.

5.2.4 Overview

Figure 5.1 summarises the action plan for this chapter.

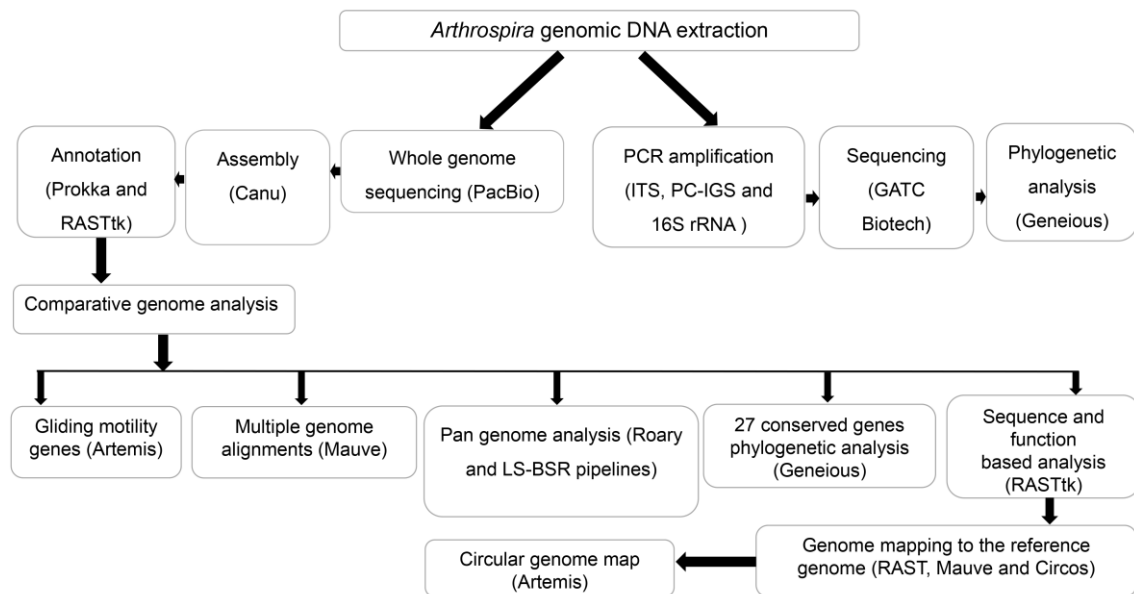


Figure 5.1: Schematic diagram of *Arthrospira* genome analysis pathway.

5.3 Results

5.3.1 PCR amplification

The use of the combinations of three set of primers, 16S3'F & 23S5'R, *cpc arF* & *cpc arR* and 27 F & 809 R was successful in amplifying the ITS region between 16S rRNA and 23S rRNA genes, the phycocyanin locus (PC-IGS) and

16S rRNA gene, respectively. The size of the resulting PCR products was, as expected, approximately 500, 500 and 780 bp respectively (Figure 5.2).

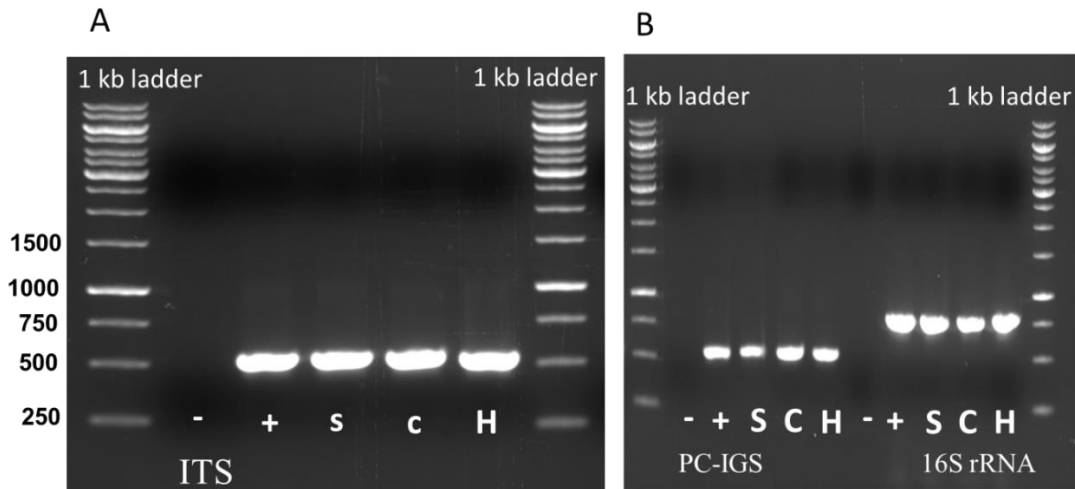


Figure 5.2: Gel Electrophoresis on 1% agarose gel of the PCR products of three *Arthrospira* marker genes for three *Arthrospira* morphotypes (S, C and H) from Lake Bogoria.

A) ITS region of 16S-23S rRNA gene. B) PC-IGS locus and 16S rRNA gene, respectively. From left to right, ladder, negative control, positive control, S-morphotype, C-morphotype, H-morphotype and ladder.

5.3.2 Marker genes sequences and Phylogenetic analyses

There was a high sequence identity in the ITS regions of the three morphotypes (99.80-100%) (Table 5.2 and Figure 5.2). The sequence alignment of the PC-IGS locus showed that those three sequence fragments for the three morphotypes were identical, with 100% identity (Table 5.3 and Figure 5.3). The alignment of the 16S rRNA gene also revealed a high sequence identity between the morphotypes, where H-morphotype was identical to C-morphotype by 100 %, and S-morphotype showed 99.87% identity with C-morphotype (Table 5.4 and Figure 5.4). Multiple sequence alignment of 16S rRNA, ITS and PC-IGS consensus sequences of three *Arthrospira* morphotypes (S, C and H) are shown in Appendix 8.2, Figure 8.1,8.2 and 8.3 respectively.

Table 5.2: Nucleotide identity of the consensus sequences of the ITS region of three *Arthrospira* morphotypes from Lake Bogoria.

Morphotype	S	C	H
S		100%	99.80%
C	100%		99.81%
H	99.80%	99.81%	

Table 5.3: Nucleotide identity of the consensus sequences of PC-IGS locus of the three *Arthrospira* morphotypes from Lake Bogoria.

Morphotype	S	C	H
S		100%	100%
C	100%		
H	100%	100%	

Table 5.4: Nucleotide identity of the consensus sequences of 16S rRNA gene of the three *Arthrospira* morphotypes from Lake Bogoria.

Morphotype	S	C	H
S		99.87%	99.87%
C	99.87%		100%
H	99.87%	100%	

The Nucleotide Basic Local Alignment Search Tool (blastn) revealed that *A. platensis* was the most homologous species to all three *Arthrospira* morphotypes from Lake Bogoria using ITS and 16S rRNA marker genes, with identity percentages of between 99.7% and 100% (Tables 5.5 and 5.7). Whereas *Arthrospira* sp. 'Nigrita M1' was the most closely related species to all three *Arthrospira* morphotypes from Lake Bogoria using the PC-IGS locus, at 100% identity (Table 5.6).

Table 5.5: Nucleotide identity of ITS region of the three *Arthrospira* morphotypes from Lake Bogoria to the close relative species present in GenBank.

Morphotype	Closest species in Gene Bank	% of identity	Accession no: Gene Bank
S	<i>A. platensis</i> GMPA7	100%	KX279415.1
C	<i>A. platensis</i> GMPC1	99.7 %	KX279418.1
H	<i>A. platensis</i> GMPC1	100 %	KX279418.1

Table 5.6: Nucleotide identity of PC-IGS locus of the three *Arthrospira* morphotypes from Lake Bogoria to the close relative species present in GenBank.

Morphotype	Closest species in Gene Bank	% of identity	Accession no: Gene Bank
S	<i>Arthrospira</i> sp. 'Nigrita M1'	100%	KU588154.1
C	<i>Arthrospira</i> sp. 'Nigrita M1'	100%	KU588154.1
H	<i>Arthrospira</i> sp. 'Nigrita M1'	100%	KU588154.1

Table 5.7: Nucleotide identity of 16S rRNA of the three *Arthrospira* morphotypes from Lake Bogoria to the close relative species present in GenBank.

Morphotype	Closest species in Gene Bank	% of identity	Accession no: Gene Bank
S	<i>A. platensis</i> IPPAS B-256	99.7%	KX262886
C	<i>A. platensis</i> IPPAS B-256	99.9%	KX262886
H	<i>A. platensis</i> IPPAS B-256	99.9%	KX262886

A phylogenetic tree of the ITS region sequences of the three *Arthrospira* morphotypes and other unique sequences available to the same gene in the NCBI database is depicted in figure 5.3. The tree shows a large cluster of the three *Arthrospira* morphotypes (C, H and S) with 39 different *Arthrospira* strains. The entire cluster was supported by a posterior probability value of 1. The relationship of three Bogoria morphotypes remains unsolved.

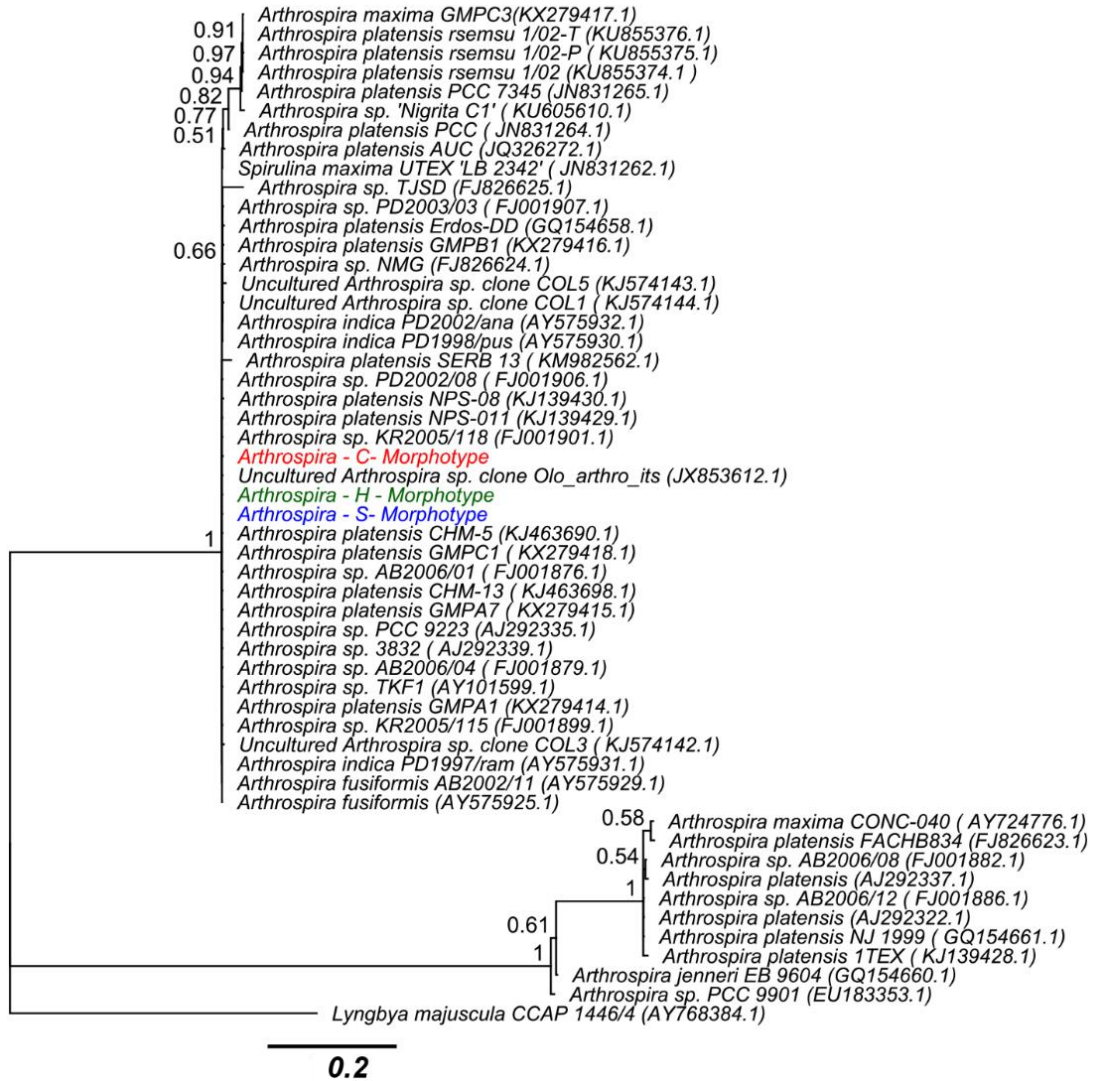


Figure 5.3: Molecular Phylogenetic analysis of *Arthrospira* strains made based on the alignment of ITS region sequences of 53 *Arthrospira* strains, as inferred with the Geneious software.

The tree was calculated using MrBayes' algorithm with the (GTR+G) substitution model. The *Arthrospira* morphotypes (H, C and S) examined in this study are shown in green, red and blue, respectively. The accession numbers are given in brackets. The scale bar represents the number of estimated changes per position for a unit of branch length.

Figure 5.4 depicts a phylogenetic tree of the phycocyanin locus (PC-IGS) sequences of the three *Arthrospira* morphotypes and other unique sequences available to the same gene in the NCBI database. The tree shows that the three *Arthrospira* morphotypes were localized in a single cluster with 20 other *Arthrospira* strains from the NCBI database belonging to five different *Arthrospira* species (*A. platensis*, *A. fusiformis*, *A. maxima*, *Arthrospira* sp. and

A. indica). The whole cluster was supported by a posterior probability value of 0.91.

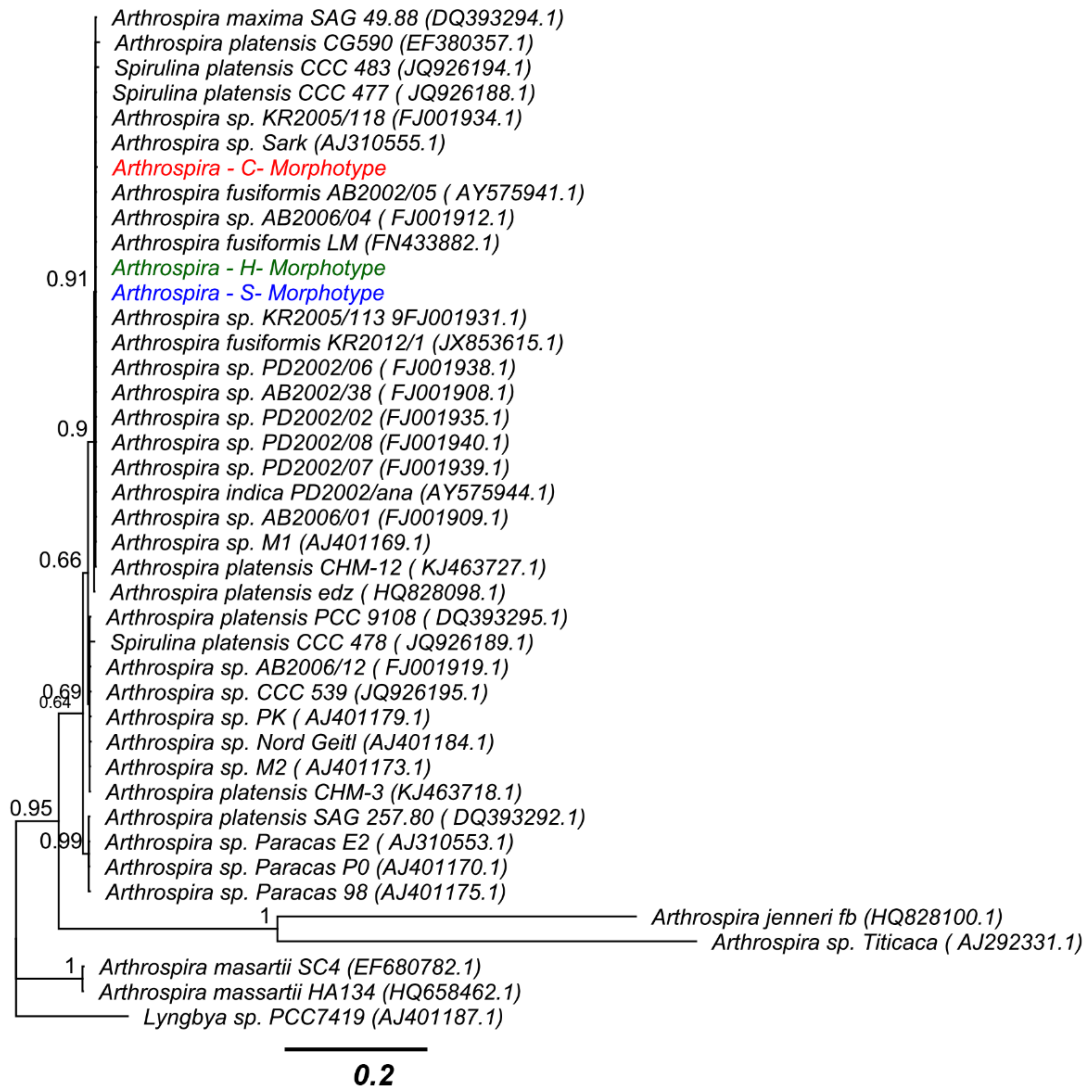


Figure 5.4: Molecular Phylogenetic analysis of *Arthrospira* strains made on the basis of the alignment of the phycocyanin locus (PC-IGS) sequences of 41 *Arthrospira* strains, as inferred with the Geneious software.

The tree was calculated using the MrBayes' algorithm with the (K2) substitution model. The *Arthrospira* morphotypes (H, C and S) examined in this study are shown in green, red and blue, respectively. The accession numbers are given in brackets. The scale bar represents the number of estimated changes per position for a unit of branch length.

A phylogenetic tree for the 16S rRNA gene is presented in figure 5.5. According to this tree, three *Arthrospira* morphotypes (S, Hand C) were sub-clustered together in one clade supported by a posterior probability value of 0.66.

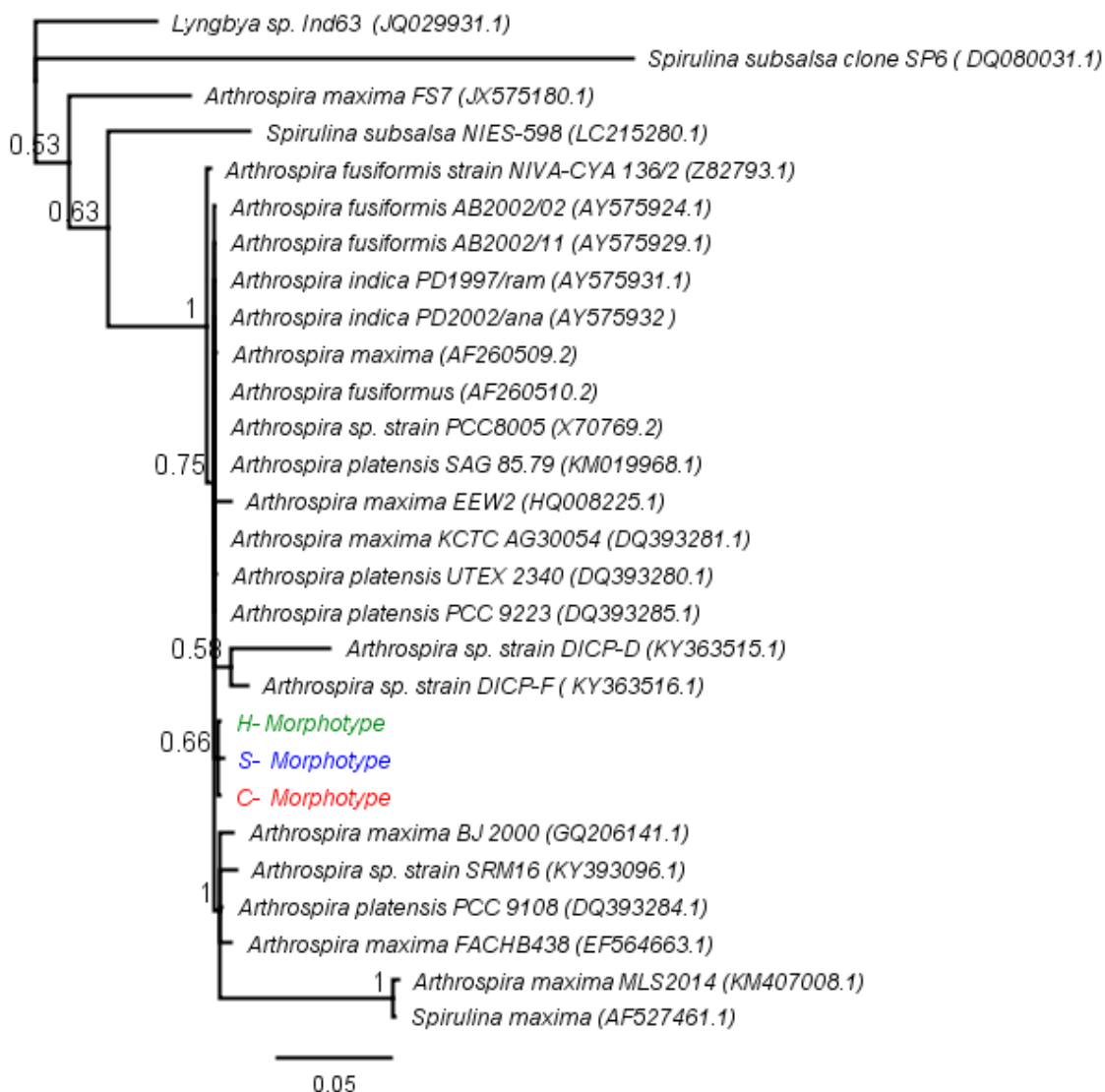


Figure 5.5: Phylogenetic tree of *Arthrospira* strains based on the alignment of 16S rRNA gene sequences of 28 *Arthrospira* strains as inferred by the Geneious software.

The tree was calculated using MrBayes' algorithm with the (JC+G) substitution model. The *Arthrospira* morphotypes (H, C and S) examined in this study are shown in green, red and blue, respectively. The accession numbers are given in brackets. The scale bar represents the number of estimated changes per position for a unit of branch length.

5.3.3 Whole genome sequencing, assembly and annotation

The whole-genome sequencing of two *Arthrospira* morphotypes, S and H, performed using a PacBio RSII instrument, produced 163,486 reads with an average length of 2236 bases for the H-morphotype and 163,481 reads with average length of 3396 bases for the S-morphotype. The reads from the sequencer assembled using Canu tool are shown in Table 5.8. The average

contig features are shown in Table 5.9. Because of the frequent repetition of sequence regions, neither assembler was able to produce a single, circular chromosome for both genomes. Therefore, the best assembly produced with Canu was chosen for further genomic analysis. This tool produced 4 contigs for the S-morphotype with a genome length of 6,458,720 bases and 14 contigs for the H-morphotype with a 6,576,727-base genome length.

Table 5.8: Canu assembly results of two *Arthrospira* morphotypes from Lake Bogoria.

Feature	H-morphotype	S-morphotype
Number of contigs	14	4
Total length (base)	6,576,727	6,458,720
N-bases	0	0
Non-N seqs	6576727	6458720
N50	1090469	4574491
L50	3	1
5 Longest	1306998,1243200,1090469,961794,715868,521475	4574491,1860788,15302,8139
5 Shortest	94225,75479,44180,17250,3989,1254	4574491,1860788,15302,8139
GC content %	44.951	44.788

Table 5.9: The average of contig properties for two *Arthrospira* morphotypes from Lake Bogoria.

Morphotype	Average contig Length	Average contig consensus concordance	Average contig bases called	Average contig coverage (x)
S	722307.1	0.99963	0.99960	87.048
H	412066.2	0.999382	0.999141	65.660

No plasmid DNA sequences were found in either morphotype. Both assembled genomes were annotated using the Prokka tool as *Arthrospira maxima*; further annotation details are shown in Table 5.10.

Table 5.10: Annotation details of two *Arthrospira* morphotypes from Lake Bogoria.

Annotation feature	H-morphotype	S-morphotype
Number of contigs	14	4
Genome size	6,578,493 Mb	6,459,664 Mb
tRNA	48	46
tmRNA	1	1
rRNA	6	6
protein-coding sequences (pro-CDSs)	6111	5792
Number of genes	6166	5845
Number of repeated region	15	8

5.3.4 Phylogenetic and comparative genomics analyses of *Arthrospira* from Lake Bogoria

5.3.4.1 General genomic features of two *Arthrospira* morphotypes (H and S)

The genome size of both morphotypes (H and S), 6.58 and 6.46 Mb respectively, were larger than previously registered sequences of *Arthrospira* genomes in the NCBI, *Arthrospira* sp. PCC 8005 (6.23 Mb), *Arthrospira* sp. TJSD091 (5.98 Mb), *A. maxima* CS-328 (6.0 Mb), and *A. platensis* C1 (6.09 M). However, both were a little smaller than the previously sequenced *A. platensis* YZ (6.79 Mb) and *A. platensis* str. Paraca (6.5 Mb) compared with *Arthrospira* Bogoria S (6.46 Mb). Both genomes were predicted to encode 6,166 and 5,792 total genes, respectively. Of these, 6,111 and 5,845 were annotated as protein-coding genes, respectively. Moreover, both genomes sequences were also predicted to contain 6 rRNA genes each and 48 and 46 tRNA genes, respectively. The number of rRNA gene clusters in both genomes was similar to that found in all other *Arthrospira* compared genomes., except for *Arthrospira* sp. TJSD091 (5) and *A. maxima* CS-328 (5), whereas the number of tRNA genes was higher than that of all strains (*Arthrospira* sp. PCC 8005 (42), *Arthrospira* sp. TJSD091 (37), *A. maxima* CS-328 (36), *A. platensis* NIES-39 (40), *A. platensis* YZ (39), *A. platensis* str. Paraca (40), and *A. platensis* C1 (39)). Other comparisons of genome properties (number of repeat sequences and GC percentage) are reported in Table 5.11.

Table 5.11: Genome feature comparison among *Arthrospira* species.

Genome property	Number of repeat sequence	GC content %
<i>Arthrospira</i> sp. PCC 8005	7	44.8
<i>Arthrospira</i> sp. TJSD091	13	44.9
<i>A. maxima</i> CS-328	12	44.7
<i>A. platensis</i> NIES-39	8	44.3
<i>A. platensis</i> YZ	7	44.2
<i>A. platensis</i> str. Paraca	14	44.3
<i>A. platensis</i> C1	7	44.8
<i>Arthrospira</i> Bogoria H	15	44.8
<i>Arthrospira</i> Bogoria S	8	44.7

The current study isolates from Lake Bogoria, *Arthrospira* Bogoria H and *Arthrospira* Bogoria S.

The amino acid identity of 27 conserved genes found in 578 complete bacterial genomes shows that the two *Arthrospira* Bogoria morphotypes (H and S) are similar to each other, with a sequence identity of 99.52%. The most similar species to the Bogoria isolates was *A. maxima* CS-328 with 99.38% and 99.42% sequence identity, respectively. In contrast, *A. platensis* was the least similar with a sequence identity of only 94%. The only *A. platensis* that was similar to the Bogoria isolates was *A. platensis* C1, at 99.37 % and 99.35% identity respectively (Table 5.12).

Table 5.12: Calculated amino acid sequences identity (%) of 27 conserved genes between nine *Arthrospira* strains.

Genomes	<i>Arthrospira</i> sp. PCC 8005	<i>Arthrospira</i> Bogoria H	<i>Arthrospira</i> Bogoria S	<i>A. maxima</i> CS-328	<i>A. platensis</i> C1	<i>A. platensis</i> NIES-39	<i>A. platensis</i> str <i>Paraca</i> UASWS	<i>A. platensis</i> YZ	<i>Arthrospira</i> sp. TJSD091
<i>Arthrospira</i> sp. PCC 8005	100	99.14	99.20	99.19	99.13	94.24	94.47	94.54	99.17
<i>Arthrospira</i> Bogoria H	99.14	100	99.52	99.38	99.37	94.05	94.30	94.39	99.40
<i>Arthrospira</i> Bogoria S	99.2	99.52	100	99.42	99.35	94.28	94.47	94.56	99.43
<i>A. maxima</i> CS-328	99.19	99.38	99.42	100	99.32	94.17	94.40	94.44	99.33
<i>A. platensis</i> C1	99.13	99.37	99.35	99.32	100	94.09	94.28	94.40	99.37
<i>A. platensis</i> NIES-39	94.24	94.05	94.28	94.17	94.09	100	99.68	99.41	94.31
<i>A. platensis</i> str. <i>Paraca</i> UASWS	94.47	94.30	94.47	94.40	94.28	99.68	100	99.49	94.51
<i>A. platensis</i> YZ	94.54	94.39	94.56	94.44	94.40	99.41	99.49	100	94.59
<i>Arthrospira</i> sp. TJSD091	99.14	99.40	99.43	99.33	99.37	94.31	94.51	94.59	100

The identity comparison includes seven strains from the NCBI database and the two isolates of the current study from Lake Bogoria, *Arthrospira* Bogoria H and *Arthrospira* Bogoria S.

The sequence- and function-based comparison tools of RAST provided further evidence for the close relationship between two Bogoria morphotypes, S and H. Figure 5.6 shows the protein sequence comparison. The vast majority of protein sequence identities were between 99.5 and 100 %. Moreover, of the 5539 total functional genes that compose a variant of a subsystem, 5355 were found in both genomes, whereas 75 and 109 functional genes were unique to S and H-morphotypes respectively (Figure 5.7 and 5.8).

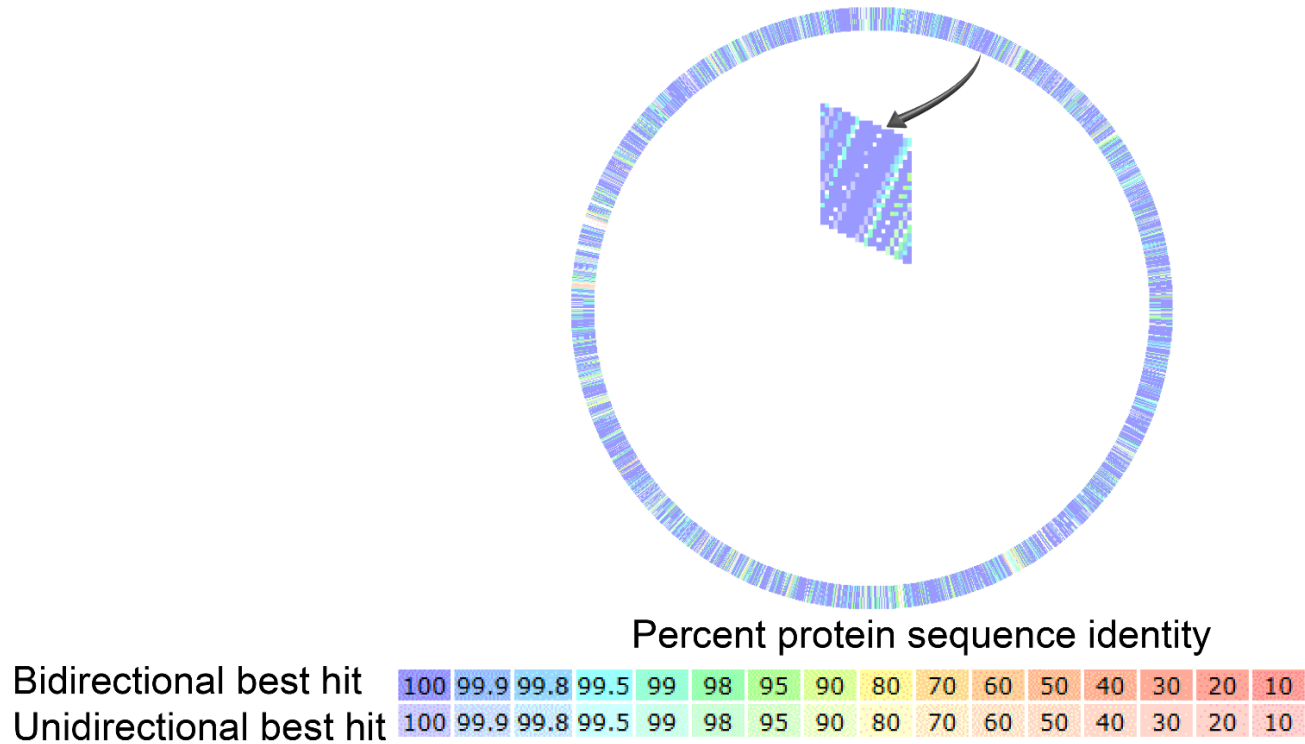


Figure 5.6: Circle plot showing the whole-genome schematic comparison of two *Arthrospira* morphotype S and H genomes.

The sequence-based comparison tool of RAST coloured each gene based on protein identity, and each gene is marked as being unique, a unidirectional best hit or a bidirectional best hit in comparison to another genome using BLASTP. The inner circle refers to S-morphotype and the external circle indicates H- morphotype. Note, the zoomed region ranges from the blue colour, which represents the highest protein sequence identity to the red colour, which represents the lowest.

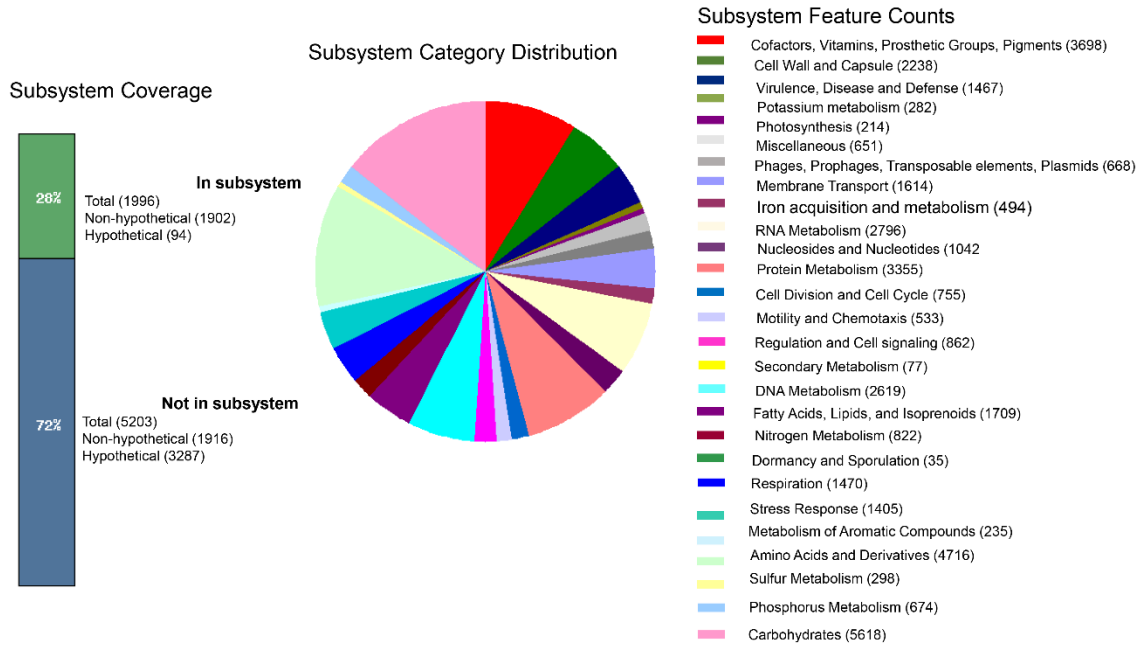


Figure 5.7: Subsystem statistics diagram of S-morphotype.

Subsystem is a cluster of summary functional roles. Exact genes in certain organisms connected to these functional roles to populate the subsystems. These subsystems comprise assertions of function for more than 500,000 protein-encoding genes in more than 500 bacterial and archaeal genomes (related to more than 6200 functional roles) (Aziz *et al.*, 2008).

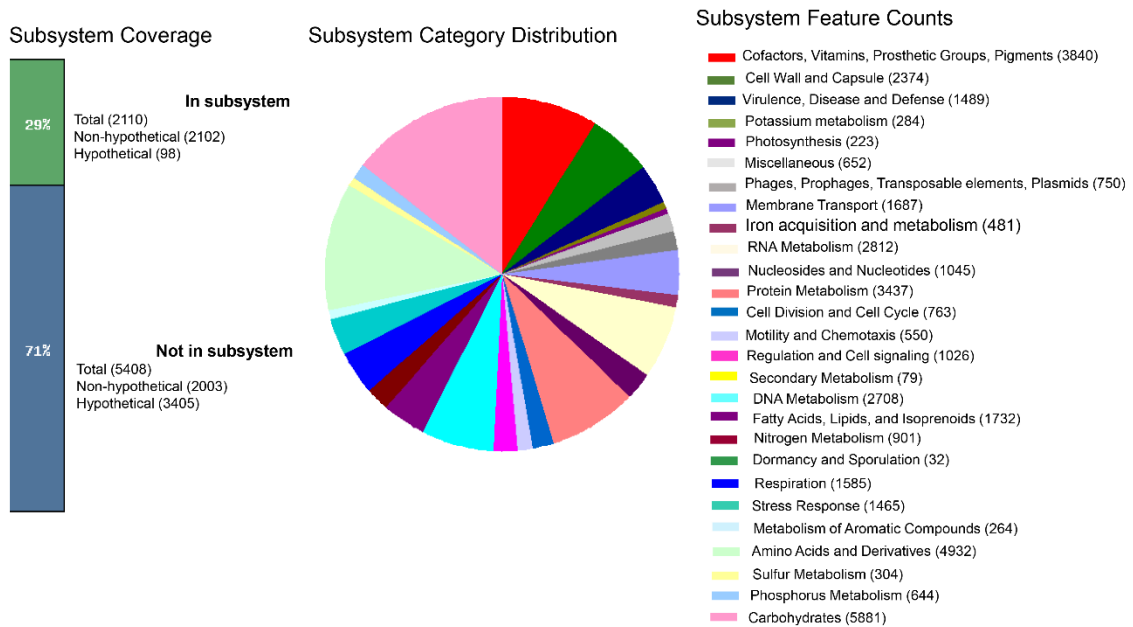


Figure 5.8: Subsystem statistics diagram of H-morphotype.

5.3.4.2 Phylogenetic analysis of whole genome of *Arthrospira*

The phylogenetic tree of 27 conserved genes in six *Arthrospira* from the NCBI database, the current study isolates, and two Oscillatoriales species showed that *Arthrospira* strains were clustered into two clades, A and B (Figure 5.9). Both current study isolates (H and S) were clustered together in one clade with another three *Arthrospira* strains, supported by a posterior probability value of 1. The unexpected result was that *A. platensis* C1 was clustered with clade B and not with the other *A. platensis* strains in clade A. Subclade C showed that the S-morphotype of the Bogoria isolate was phylogenetically more closely related to *A. maxima* CS-328 than the H-morphotype, as supported by a posterior probability value of 1 (Figure 5.9).

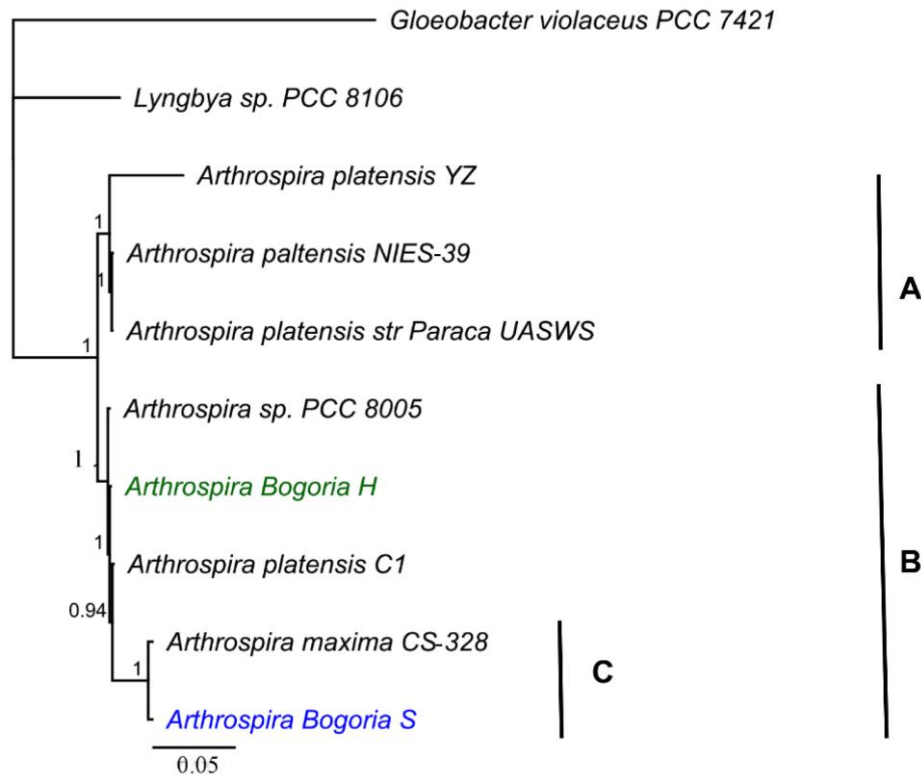


Figure 5.9: *Arthrospira* tree of eight strains, six of which are available in the NCBI database and the two Bogoria isolates (H and S) concatenated 27 conserved genes.

Bogoria isolates are coloured green and blue, respectively. The tree was constructed using the Bayesian method implemented in the Geneious software. Phylogenetic clades are grouped into two major clades, A and B, with the subclade C. The scale bar represents the number of estimated changes per position for a unit of branch length.

Figure 5.10 shows the phylogeny of aligning the core genes of nine *Arthrospira* strains using Roary. The topology of the tree was similar to the one above, where the strains were clustered into two clades (A and B). The two Bogoria isolates, *Arthrospira* sp. PCC 8005, *Arthrospira* sp. TJSD09, *A. maxima* CS-328 and *A. platensis* C1 were clustered together in a tight cluster (A) as supported by a bootstrap value of 100%. The unexpected relationship here is that *A. maxima* CS-328 was phylogenetically closer to *A. platensis* C1 than the two Bogoria isolates, H and S (Figure 5.10).

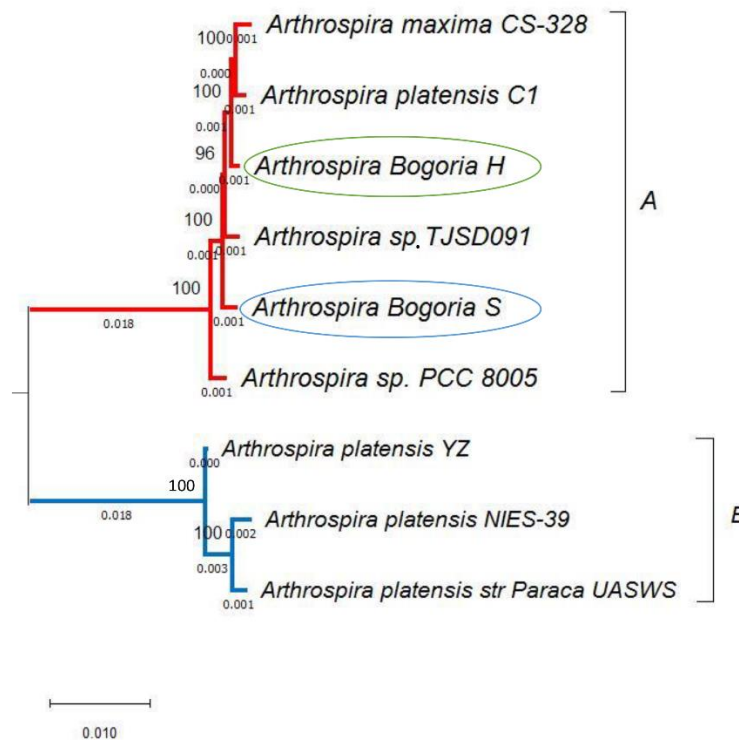


Figure 5.10: A rooted phylogenetic tree based on the aligned sequences of the core genes of nine *Arthrospira* strains that were produced by the Roary tool.

The two clades, A and B. The Bogoria isolates (H and S morphotypes) are labelled with green and blue ovals, respectively. The scale bar represents the number of estimated changes per position for a unit of branch length.

Another phylogeny generated using the aligned sequences of the core genes among nine *Arthrospira* strains, and produced with LS-BSR, showed that all these nine *Arthrospira* strains were again clustered into two main clades, A and B (Figure 5.11). The interesting and different thing to note in this tree from the one that was built with Roary is that the two Lake Bogoria isolates are clustered in one small clade and both have the same phylogenetic relationship with A.

maxima CS 328 (Figure 5.11). The relationship of *A. platensis* C1 confirmed the above phylogenies topology. It was not clustered with *A. platensis* clade.

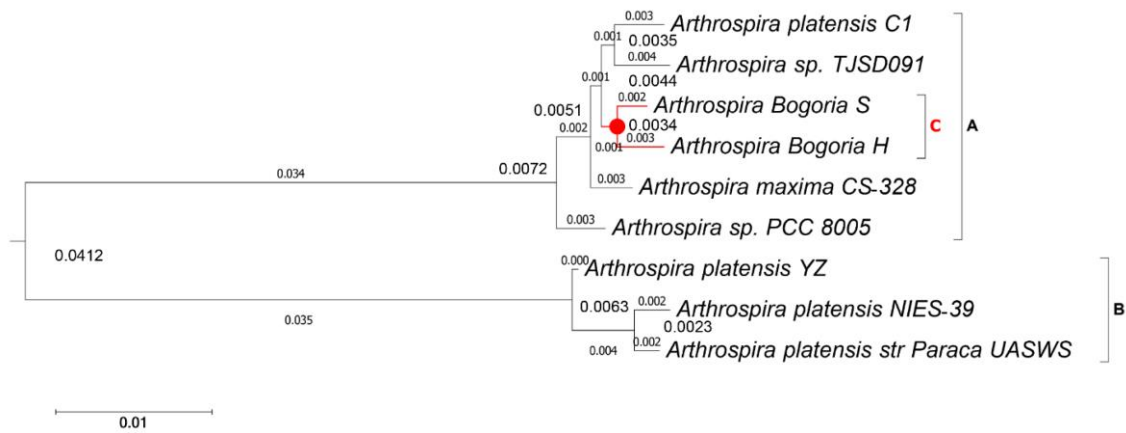


Figure 5.11: RAxML Rooted phylogenetic tree based on the aligned sequences of the core genes of the nine *Arthrospira* strains produced by the LS-BSR tool.

The two clades A and B. The Bogoria isolates (H and S morphotypes) were clustered in subcluster (c), as labelled in red. The scale bar represents the number of estimated changes per position for a unit of branch length.

Finally, the phylogeny constructed based on the alignment of orthologous and xenologous sequence regions, produced by the Mauve tool, showing the approximate topology of the above tree (built based on the alignment of the core genes). The two Bogoria isolates are clustered together into a small subclade (Figure 5.12). The only difference here is that *A. maxima* CS-328 and *Arthrospira sp. TJSD091*'s topologies are reversed. This is the fourth tool that has confirmed the misclassification of *A. platensis* C1.

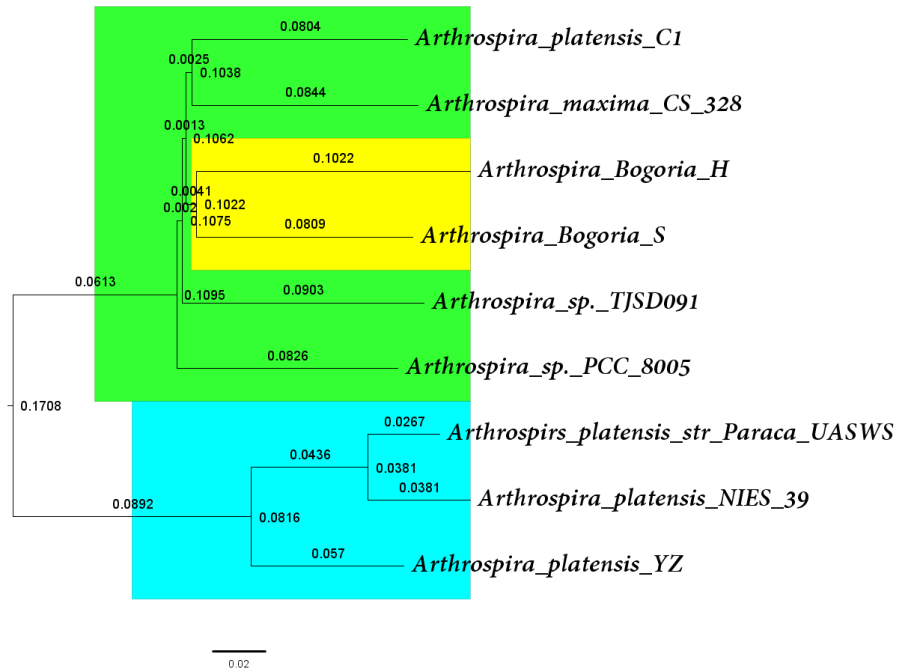


Figure 5.12: Neighbour-joining phylogeny based on the alignment of the orthologous and xenologous sequences regions of nine *Arthrospira* strains, as generated by the Mauve tool.

The two large clades coloured in sky blue and green, and the subclade of the Bogoria isolates coloured in yellow. The scale bar represents the number of estimated changes per position for a unit of branch length.

5.3.4.3 Comparative genome analysis

The Roary pan genome analysis tool of nine *Arthrospira* genomes (Figure. 5.13) shows the frequency of all genes in the nine *Arthrospira* genomes. The first column of the x-axis represents the genes in only one genome. These genes are related to only one strain, accounting for about 3,500 genes of the total 13,194 that were counted. This constitutes 26.5% of the total pan-genome. At the opposite end of the chart are the genes that have been counted in all nine genomes. These genes are the core genes, which constituted 2,019 of the total 13,194 genes. This represents 15.3% of the pan-genome.

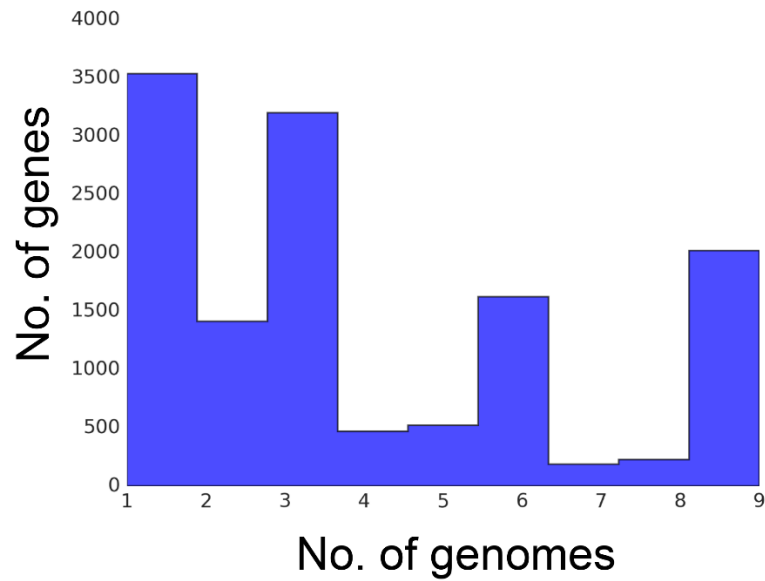


Figure 5.13: Frequency chart showing the frequency of genes for the *Arthrospira* genomes analysed.

The first column represents the genes that are present in the only one genome; the second column represents the genes that are present in two genomes, and so on.

Three genomes in the matrix (Figure. 5.14) appear to be only involved in certain basic genes, which belong to *A. platensis* species.

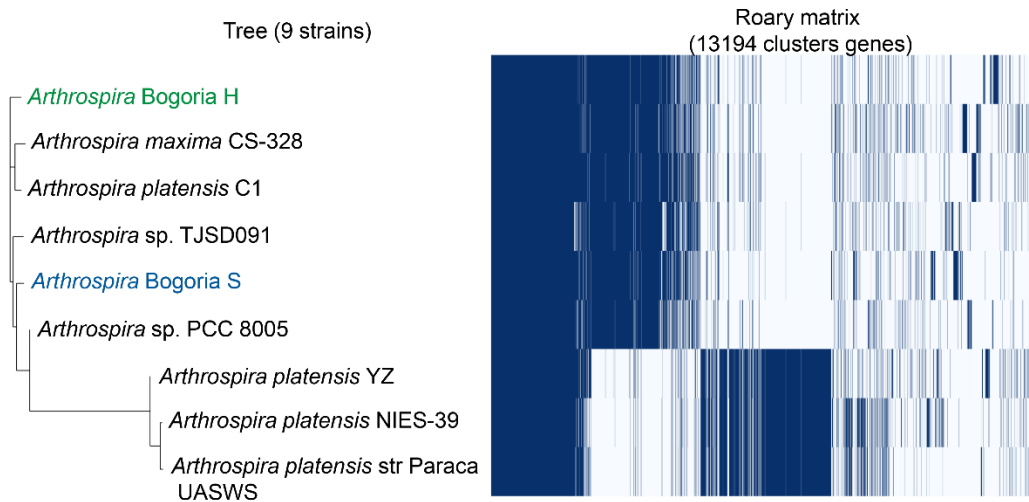


Figure 5.14: A heat map generated by Roary plots showing the tree compared to a matrix in the presence and absence of core and accessory genes.

The blue colour indicates that the gene is present, *Arthrospira* morphotypes (H and S) represented in green and blue colours respectively.

According to pan genome analysis, there are four categories of genes that make up the pan-genome; these are core genes (99-100% of the genes that are common to all genomes), softcore genes (the genes that are shared between

95-99% of all genomes), shell genes (the genes that are shared between 15-95% of all genomes) and cloud genes (the genes that are shared between 0-15% of all genomes). Based on Roary, the pan-genome of nine *Arthrospira* strains is as follows: 7,739 genes are shell genes with a percentage of 58.6% of the pan-genome, 3,536 genes are cloud genes with a percentage of 26.8% of the pan-genome, 2,019 genes are core genes with a percentage of 15.3% of the pan-genome, and there are no softcore genes (Figure 5.15).

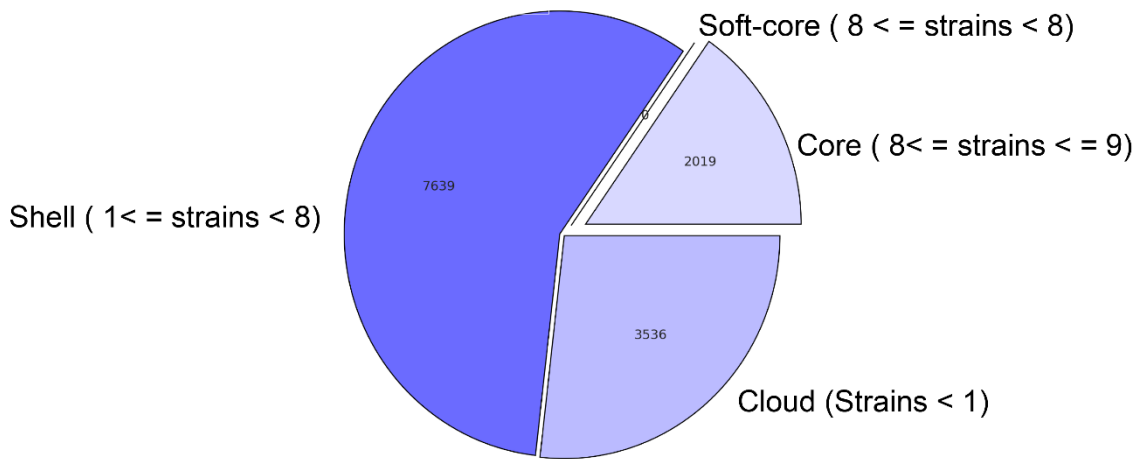


Figure 5.15: Pie chart showing the distribution of different categories of genes and the number of isolates they are present.

The scale of the *Arthrospira* pan-genome has grown, while the size of core genome (conserved genes) has decreased with the addition of new genomes (Figure 5.16 A). Moreover, as the number of genomes increased, the number of both new and unique genes also has decreased (Figure 5.16 B). More details are shown in Appendix 8.2, Figure 8.4 – 8.6.

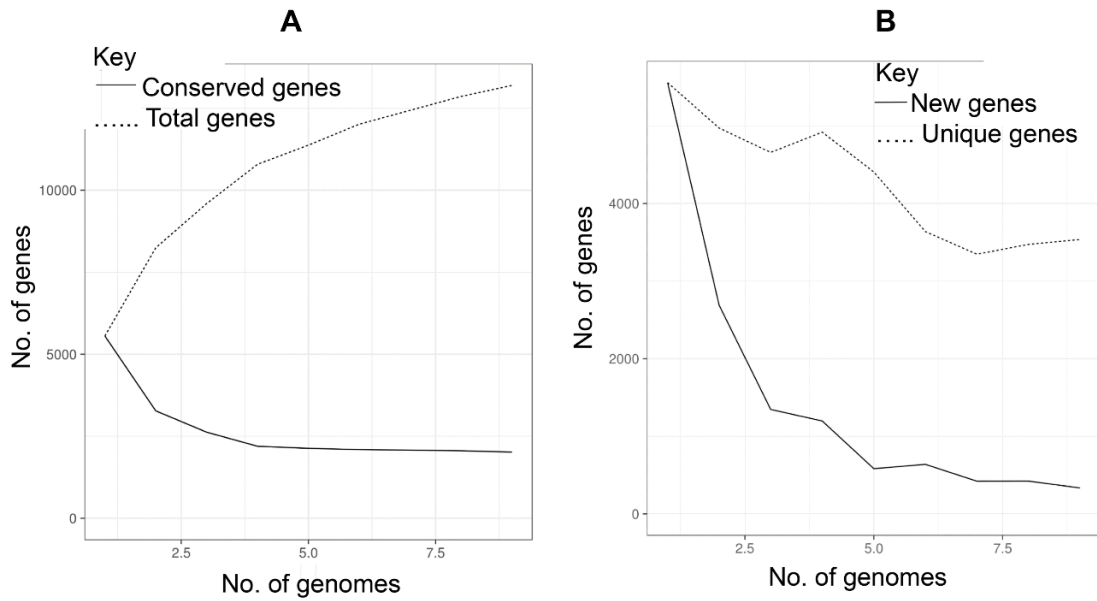


Figure 5.16: Pan-genome plots, showing how the pan genome changes with the addition of a new genome (arranged in random order).

A) Conserved genes and total genes. B) New genes and unique genes.

The alignment of the two Bogoria *Arthrospira* genomes using the Mauve aligner showed a high level of rearrangement events (Figure 5.17). When alignment included all nine *Arthrospira* genomes, the level of rearrangement was extremely complicated (Figure 5.18).

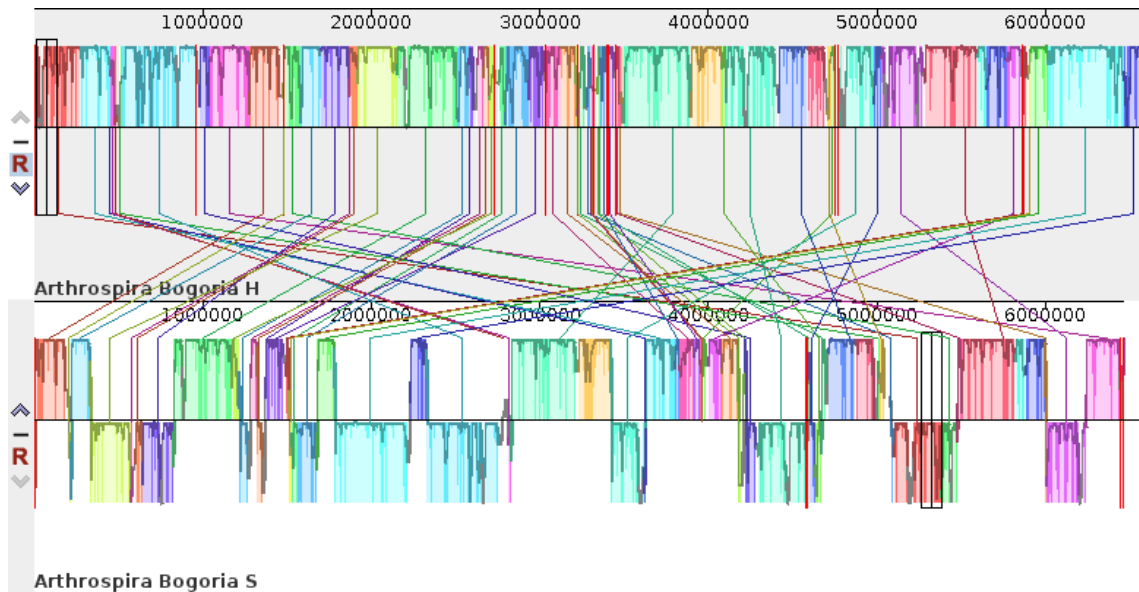


Figure 5.17: Progressive Mauve alignment shows an alignment of the two Bogoria *Arthrospira* morphotypes (H and S).

The figure shows the inverse regions between the two genomes, which is evident in the forms of blocks that appear below the central line of the *Arthrospira* Bogoria S genome. Lines to similarly coloured blocks in the second genome connect coloured blocks in the first genome. These lines indicate which regions in each genome are homologous. The crossing, locally collinear block (LCB) connecting lines give an initial impression of the complex rearrangement landscape between these two related genomes. Notice the crossing “X” pattern of lines. The boundaries of coloured blocks usually indicate the breakpoints of genome rearrangement, unless a sequence has been gained or lost in the breakpoint region.

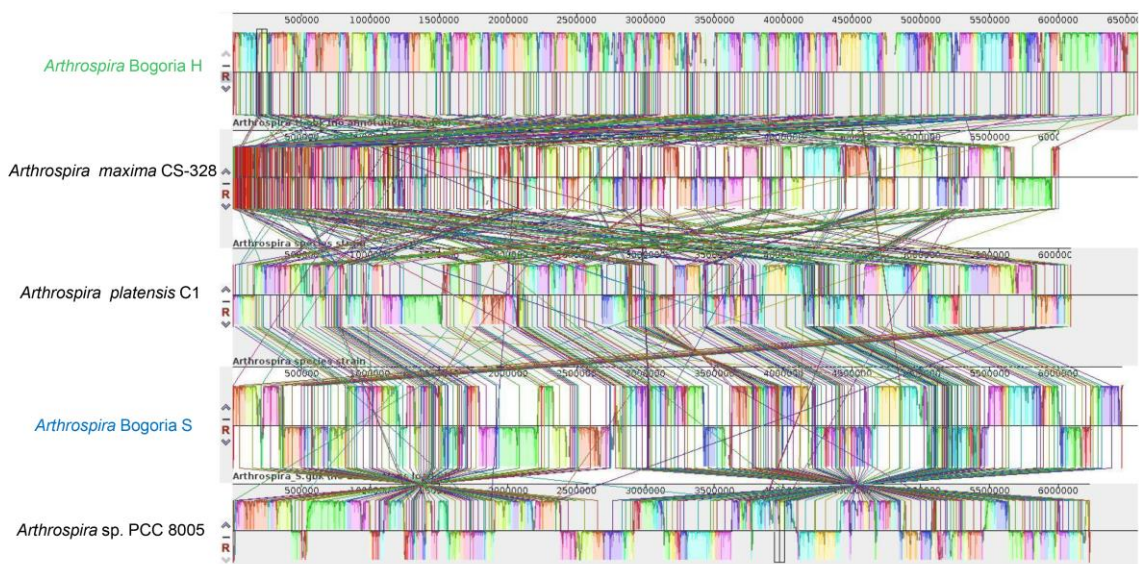


Figure 5.18: A Mauve alignment of five *Arthrospira* strains including Bogoria morphotypes.

The figure shows the complicated rearrangement events among these genomes. H and S of Lake Bogoria green and blue respectively.

In addition, according to the RAST result, the first most closely related species to both morphotypes (S and H) was *Arthrospira* sp. PCC 8005 with a score of 536 and 537 respectively. The second closest relative was *A. maxima* CS-328 with the score of 472 and 471 respectively. The *Arthrospira* sp. PCC 8005 genome is complete (one scaffold) while *A. maxima* CS-328 is not (129 contigs). Amongst seven *Arthrospira* genomes in the NCBI database, only two genomes are complete – *Arthrospira* sp. PCC 8005 and *Arthrospira platensis* C1. There was high identity of the 27 conserved genes between those two complete *Arthrospira* genomes and S and H *Arthrospira* morphotypes of the lake – 99.20 and 99.35 % for S-morphotype and 99.14 and 99.37 % for H-morphotype respectively (Table 5.13), so both genomes were used as a reference to finish the genome assembly by the computational approach. The S-morphotype was chosen as the representative of the *Arthrospira* genus in Lake Bogoria. This was first because of the significant identity between two *Arthrospira* morphotypes (99.52 %). Second their blast result against the reference genomes, where most of the matched regions between the S-morphotype and the reference were ordered (Figure 5.19 B and D), therefore, its genome (4 contigs) was finished into one circular chromosome by mapping it to the reference genome. The H-morphotype's matched regions were less suitable and random (Figure 5.19 A and C).

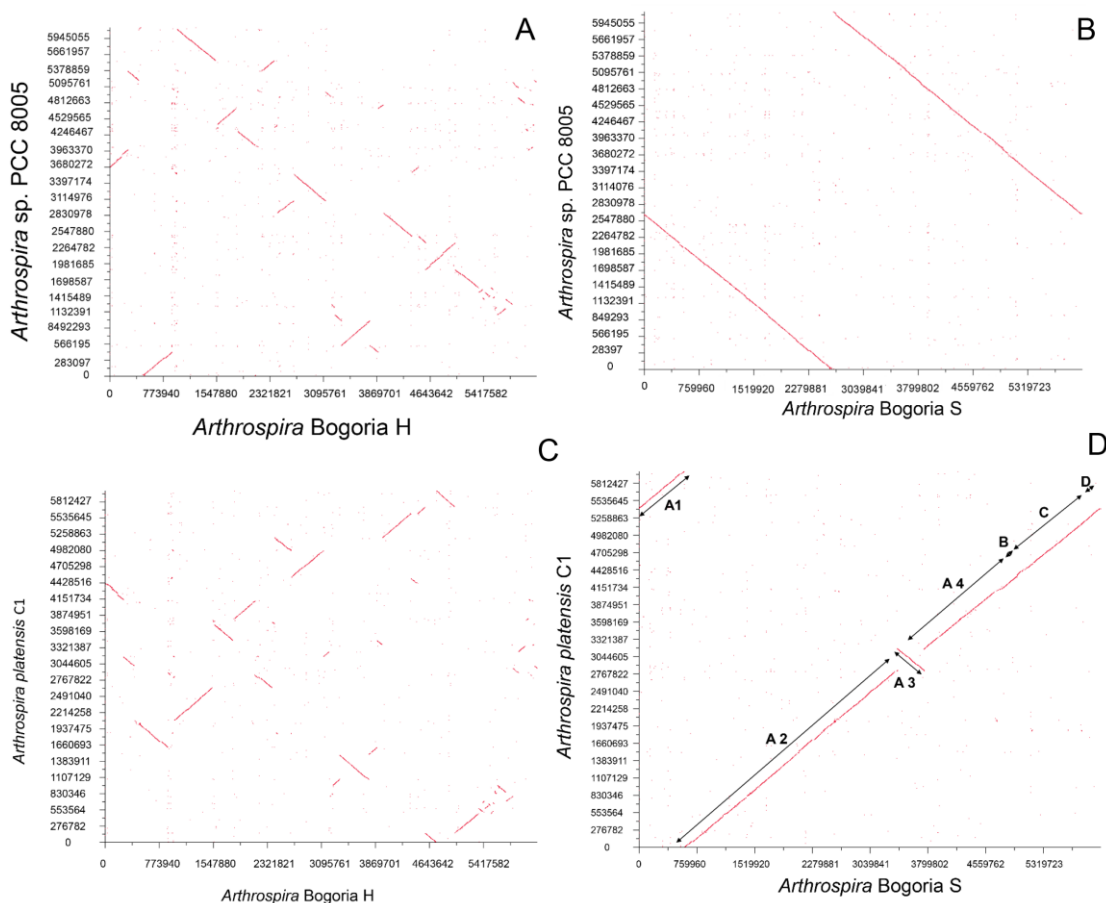


Figure 5.19: Blast dot plots of two *Arthrospira* morphotypes (H and S) with more identical complete genomes in the NCBI database using RAST tool.

(A and B) *Arthrospira* sp. PCC 8005 vs H and S *Arthrospira* morphotypes, (C and D) *Arthrospira platensis* C1 vs H and S *Arthrospira* morphotypes respectively. A1-A4 are the sequence pieces of contig 1, B contig 2, C contig 3 and D contig 4. Aligned fragments are represented as dots or lines. The X and Y-axis show the genome size of the targeted aligned genomes.

The Mauve tool reordered the *Arthrospira* Bogoria contigs into one circular chromosome, using the reference genome as a guide (Figure 5.20 A and B). The alignment results between *Arthrospira* sp. PCC 8005 as a first reference and the query genome (*Arthrospira* Bogoria S) showed that many of the matched regions were in the opposite direction (Figure 5.20 A). When *Arthrospira platensis* C1 was used as a second reference, however, two LCBs (Labelled 3 and 4) at the beginning of the Bogoria isolate genome were aligned to the end of the reference (Figure 5.20 B). Consequently, the *Arthrospira platensis* C1 genome was used to rearrange the contigs. The Nano text editor of the Linux based operating system was used to determine the length of

sequences of these two LCBs. Their positions were incorrect compared to the reference genome, so they were cut and pasted to the end of the genome (the end of the contig 4). The alignment to the reference genome was repeated to verify the usefulness of the reorder. Figure 5.20 C and 5.21 show how the matched regions between the reference genome and *Arthrospira* genome from the lake were in the same direction. The new contig order is shown in Table 5.13.

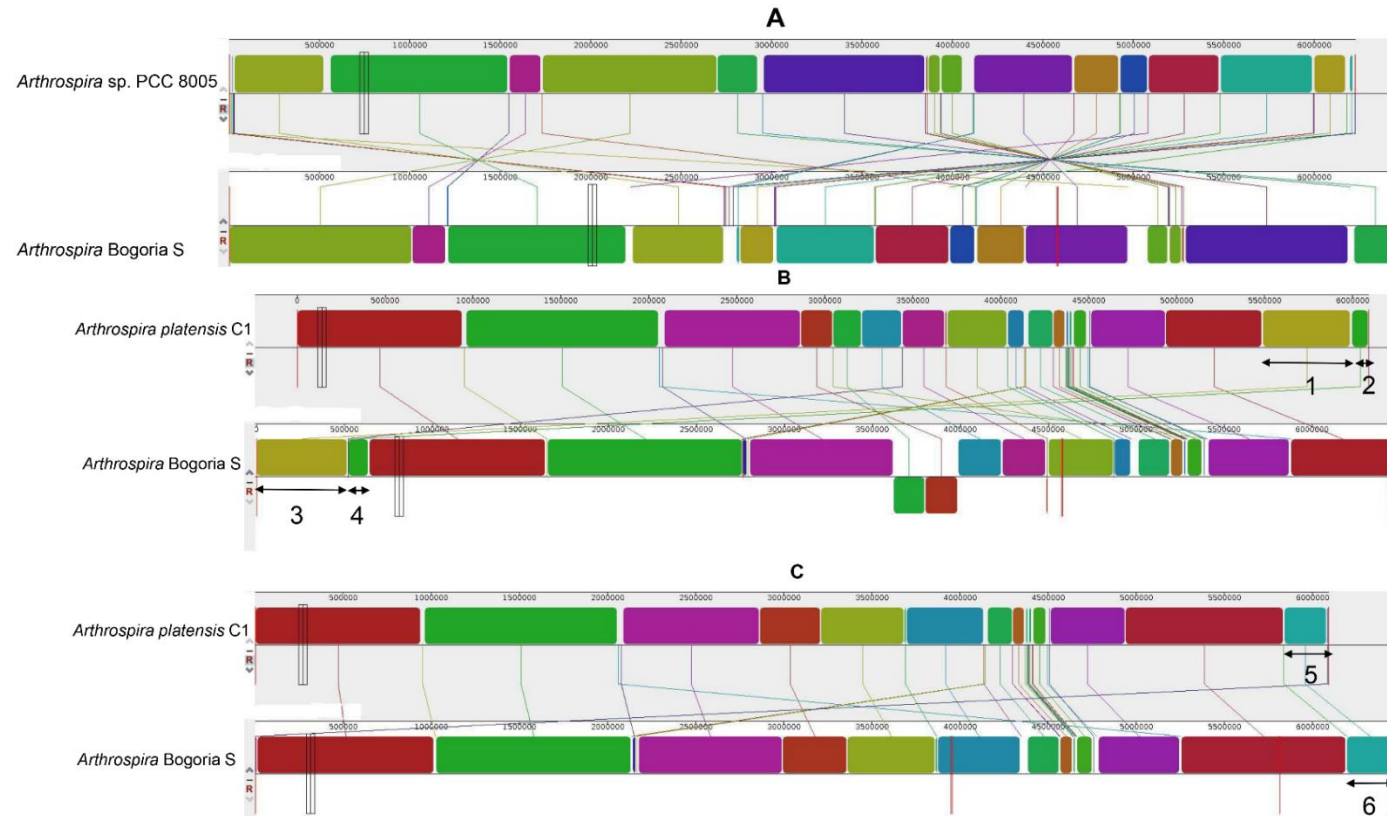


Figure 5.20: Genome alignment of the representative *Arthrospira* (S-morphotype) of Lake Bogoria with the reference genomes using Mauve tool.

(A) *Arthrospira* Bogoria isolate vs *Arthrospira* sp. PCC8005, (B) and (C) vs *Arthrospira platensis* C1 before and after reordering the contigs respectively. Two LCBs, 3 and 4 of the lake isolates aligned to the same LCBs of the reference genome but at the end, 1 and 2. Thereafter. They were cut and repasted to the end of the genome. (C) realignment showing the correct position of the genome piece after rearrangement of the contigs 5 and 6.

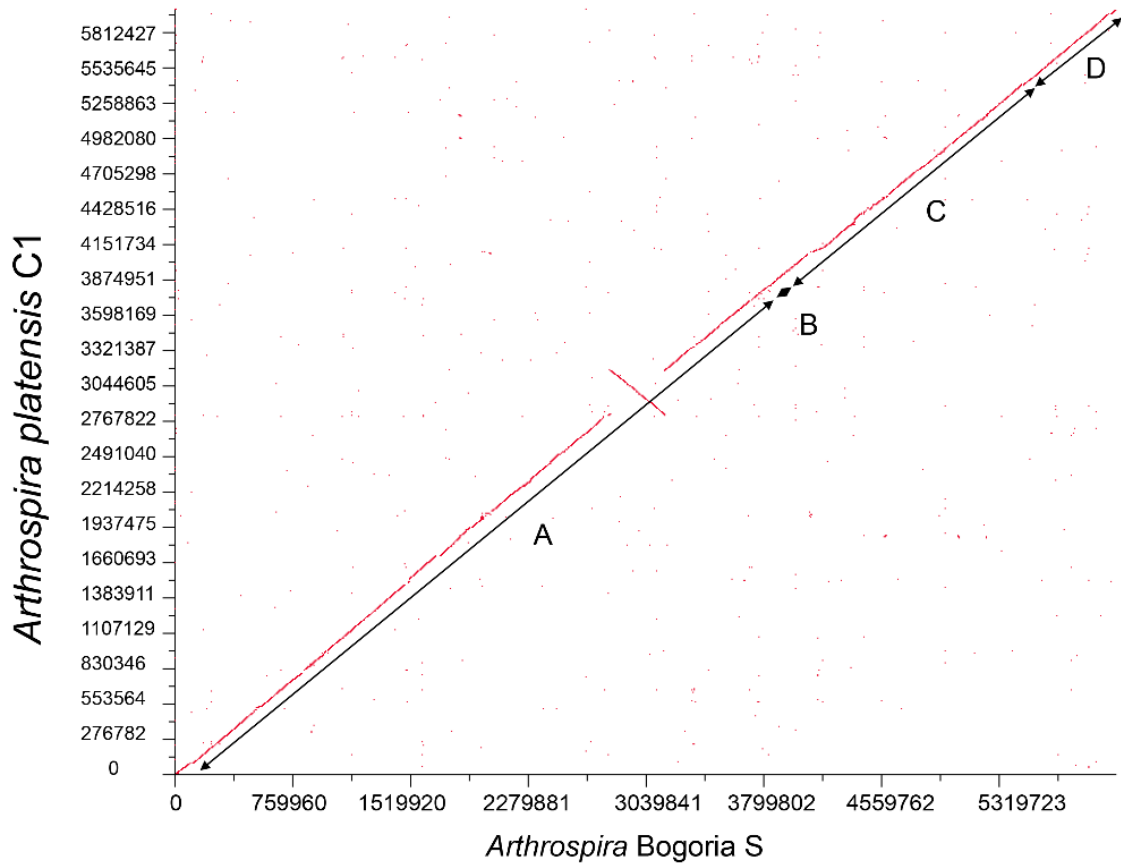


Figure 5.21: Blast dot plot of *Arthrospira* from Lake Bogoria (*Arthrospira Bogoria S*) against *Arthrospira platensis C1* after reordering the contigs.

The red dots represent the aligned fragments and the continuous dots in the shape of a red line represent the overall trend of the fragments. A) Contig 1, B) contig 2, C) contig 3 and D) contig 4. Four contigs of the Bogoria isolate were reordered in the same direction as a reference genome. The inverse region in the middle aligned in the opposite direction, but within the same contig (1). The length of contig 1 and 4 has changed.

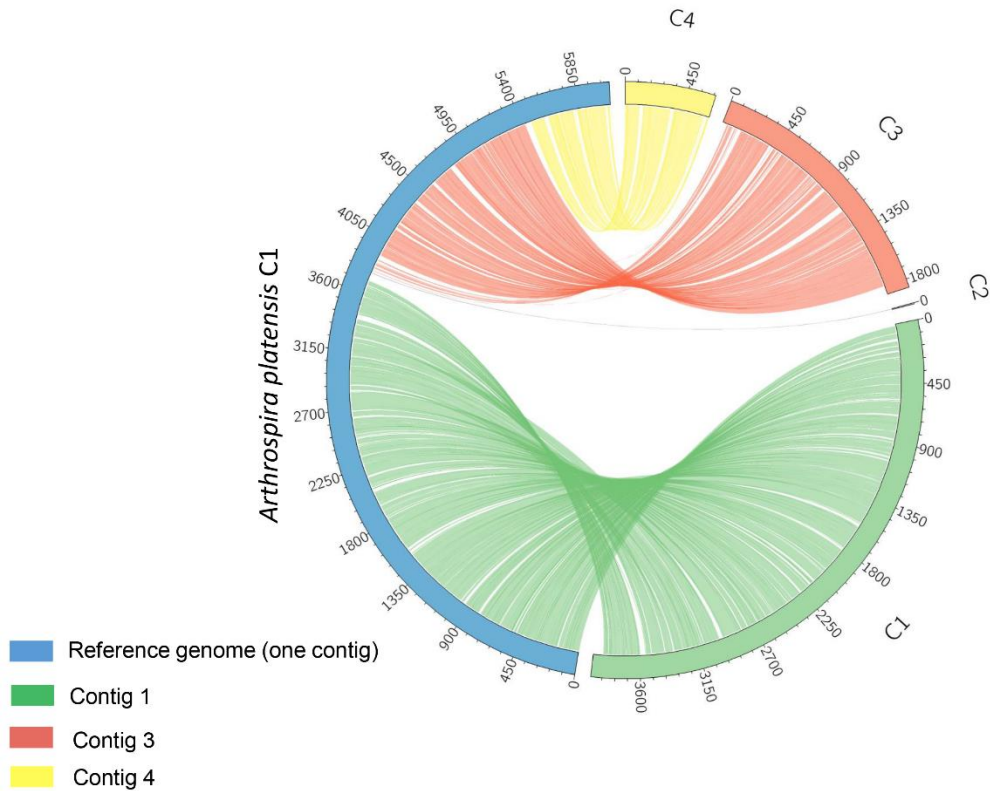


Figure 5.22: Genome comparison of *Arthrospira* Bogoria S and the reference genome of *Arthrospira platensis* C1.

A Circos map depicting the blastn alignment results. Each coloured segment indicates contig with the numbers on the external ring representing genome size in kb. The *Arthrospira* Bogoria S genome consists of 4 contigs, coloured green (1), pink (3), yellow (4) and contig 2 was a short sequence (8136 bp) therefore it had no colour. The reference genome (*Arthrospira platensis* C1), one contig coloured with blue.

Table 5.13: The contig number, start and end position of each contig before and after rearrangement the contigs.

The first contig order	Start (nucleotide number)	End (nucleotide number)	The new contig order	Start (nucleotide number)	End (nucleotide number)
1	1	4,575,283	1	1	3,94,7290
2	4,575,284	4,583,420	2	3,947,291	3,955,427
3	4,583,421	6,444,331	3	3955428	5,816,338
4	6,444,332	6,459,664	4	5,816,339	6,459,664

The order of the contig was as before, but the start and end have changed.

Finally, the four contigs were concatenated into one scaffold. The circular genome is shown in the figure 5.23 and the name of *Arthrospira* spp. Bogoria is proposed to present the *Arthrospira maxima* var. *Bogoriensis*. The circular genome is shown in the figure 5.23.

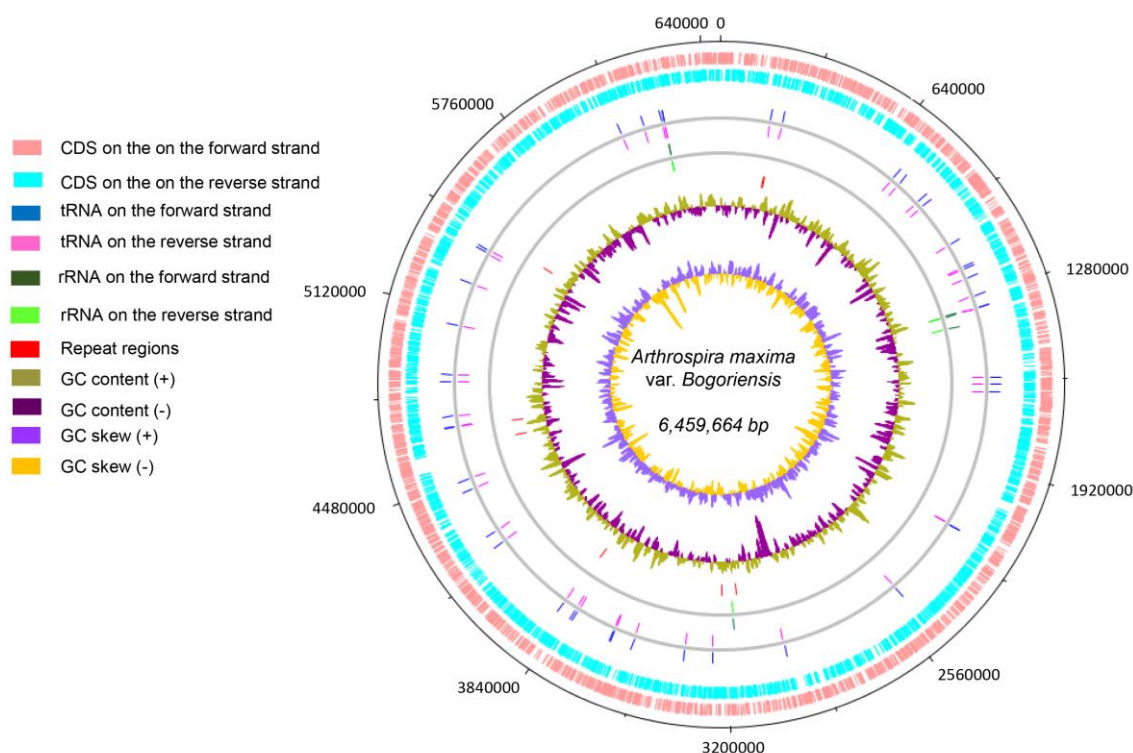


Figure 5.23: Graphical circular map of *Arthrospira maxima* var. *Bogoriensis* genome.

The rings represent from the outside to centre. Outermost circle (1), DNA base location (bp); circle 2, protein-coding regions orientated on the positive strand (clockwise); circle 3, protein-coding regions orientated on the negative strand (anticlockwise); circle 4 shows the position of tRNA genes; circle 5 marks the location of rRNA genes; ring 6 indicates G+C content plotted using a 10-kb window. Regions with GC content below the average are shown in magenta and those with content above the average are shown in olive. The inner circle (7) demonstrates GC skew ($[G+C]/[G-C]$) plotted using a 10-kb window (light purple represents values above average and yellow represents values below average). The genome plot was drawn using DNAPlotter tool, release 1.11 from Artemis 16.0, Sanger (<https://www.sanger.ac.uk/science/tools/artemis>).

5.3.5 Gliding motility genes

Genes function in gliding and twitching motilities, which are type IV pilus (T4P) genes were detected in the genomes of two *Arthrospira* morphotypes (H and S). Both genomes harbour four type IV pil genes; *pilT-1*, *pilT-2*, *pilT-3* and *pilQ*. The MUSCLE alignment result showed that the four genes were identical in the two morphotypes (98.3.-100%). Their amino acid alignments shown in Appendix 8.2, Figures 8.7-8.10. Those genes considered as a part of the natural competence that facilitates the DNA uptake by bacteria (see chapter 7).

5.4 Discussion

Historically, the taxonomy of *Arthrospira* has been a controversial issue for taxonomists, although sequencing of the ITS region has become the most predominant method by which to differentiate species and strains of cyanobacteria (Boyer *et al.*, 2001). In this study, it was not possible to distinguish between the three *Arthrospira* morphotypes, as they had 99.8-100% sequence identity confirmed by blastn tool, where they were most closely related to *A. platensis*.

The phycocyanin locus results were somewhat similar to those of the ITS region, in that all three morphotype sequences were identical but closely related to *Arthrospira* sp. 'Nigrita M1'. The results for the 16S rRNA gene were also in agreement with those seen in previous studies conducted on *Arthrospira* strains using this gene. Li *et al.* (2001), for example, showed that two *Arthrospira* phenotypes from Lake Chitu, Ethiopia, had a similarity of 100% using the 16S rRNA gene. They concluded that the 16S rRNA gene is a highly conserved gene; therefore, it is not a suitable tool by which to resolve close relationships and interspecies variability. This could be because of the high similarity between the *Arthrospira* species. Ballot *et al.* (2004a) found that *Arthrospira* strains from different geographical regions (India and Kenya) were morphologically distinct but were phylogenetically in the same clusters using the 16S rRNA gene and PC-IGS locus, supporting the idea that different morphotypes could genetically be the same species. Rout *et al.* (2015) showed that three *Arthrospira* strains from different locations in Mexico were morphologically different but genetically similar using the ITS region, at an 87% similarity. Baurain *et al.* (2002) also demonstrated that the ITS region is a highly conserved region. Nelissen *et al.* (1994) stated that the ITS gene may be better than 16S rRNA for resolving relationships at the species level, but in this study all three common genes were not able to identify the relevant *Arthrospira* species.

My results raise two possibilities. Firstly, the strong relationships may be explained by these morphotypes belonging to the same species, even though their morphologies are different. Secondly, the investigated genes that were

used are conserved and are unable to distinguish *Arthrospira* at the species level. The findings of the current study support the previous work of Dadheech *et al.* (2010) in this, who confirmed that the dependence on morphological features as taxonomic tools to identify cyanobacteria might lead to incorrect identification at the species level. Moreover, the members of the *Arthrospira* genus are able to change their morphology from coiled to straight and vice versa (Mühling *et al.*, 2003). A previously unpublished study by Clough (2015) suggested that the dominant *Arthrospira* species in Lake Bogoria is *A. maxima*, whereas earlier morphological studies of *Arthrospira* in the soda lakes of the East African Rift Valley had concluded that *A. fusiformis* (Voronichin) is the filamentous cyanobacterium that forms almost all cyanobacterial blooms (Vareschi, 1978, Kaggwa *et al.*, 2013a).

This is the first whole genome sequence that has been conducted for environmental samples of *Arthrospira* that inhabit such extreme environments. Phylogenetic analyses based on the alignment of different regions of *Arthrospira* genomes such as core genes, the 27 conserved genes, and homologous region revealed that the two *Arthrospira* morphotypes of Lake Bogoria are closely related to each other. They are most likely *A. maxima* or a new *Arthrospira* species, but definitely not *A. platensis*, as both morphotypes were only distantly related to this species. One unanticipated finding was that the previously identified *Arthrospira* strain of *A. platensis* C1 from NCBI was only distantly related to other *A. platensis* strains, and clustered with Bogoria isolates, to *A. maxima* as well as to two other unknown species of *Arthrospira*. The results of this study support evidence from previous phylogenetic analyses; for example, Cheevadhanarak *et al.* (2012) found that *A. platensis* C1 was more closely related to *Arthrospira* sp. PCC 8005 and *A. maxima* than to *A. platensis*. Four years later, further phylogenetic support for this finding was reported by Xu *et al.* (2016), who showed that this strain has a more distant relationship to *A. platensis* than *Arthrospira* sp. PCC 8005. It thus seems that the strain should be reconsidered by the original authors.

The lack of plasmid DNA sequences in the *Arthrospira* genome of Lake Bogoria was confirmed by all previous whole-genome analyses of *Arthrospira* strains.

For example, Masuda *et al.* (2010) confirmed this with *A. platensis* NIES-39, whilst two years later, Cheevadhanarak *et al.* (2012) reported the absence of plasmid in *A. platensis* C1 (PCC9438). Another two years after this, Lefort *et al.* (2014) documented that there was no plasmid sequence in the *A. platensis* str. Paraca genome.

It is highly probable that during periods of evolution, genomes are subject to high levels of mutation such as rearrangement and lateral gene transfer. These mutations can result in significant differences in the order of genes and genetic content, even among closely related organisms (Darling *et al.*, 2007). Mauve tool performs well when a few closely related genomes are aligned and the level of nucleotide identity among all aligned genomes should be greater than 60% as a cause of the current *Arthrospira* genomes (> 94%). Therefore, *Arthrospira* strains were an ideal example for alignment with this tool. My results of this alignment showed a high number of rearrangement events that could give an indication as to how this genus underwent genetic recombination during its evolutionary history. This could explain the variation in the morphology and physiology of *Arthrospira* morphotypes of Lake Bogoria.

The gliding motion of cyanobacteria is achieved with the help of mucilage secreted by the junctional pore complex (JPC) (Hoiczky, 1998). This slime sheath encapsulates the three *Arthrospira* morphotypes, but only the S-morphotype had the ability to glide on the semi-solid agar. I followed the molecular approach, in this study, therefore, to identify the genes affecting motility. Type IV pili genes are thought to be involved in twitching motility in *Nostoc punctiforme* (Duggan *et al.*, 2007) and twitching motility in unicellular *Synechocystis* (Yoshihara and Ikeuchi, 2004). Masuda *et al.* (2010) found that *A. platensis* NIES-39 has the ability to glide, and its genome holds type IV pilus-related genes, but exhibits no twitching motility. They suggested that type IV pili genes are also involved in gliding motility. I found four type IV pilus genes (*pilQ*, *pilT-1*, *pilT-2* and *pilT-3*) in both *Arthrospira* morphotypes genomes, although the H-morphotype is not motile. Cheevadhanarak *et al.* (2012), found that *A. platensis* C1 harboured all the genes involved in type IV pili, despite its lack of gliding motility. It is possible; therefore, that the expression of these genes could

be suppressed by an environmental factor during the evolutionary history of H-morphotype, or other factors may play a vital role in the motility mechanism.

Phylogenetic analyses were carried out on the three *Arthrospira* marker genes (16S rRNA, ITS and PC-IGS) of three morphotypes – S, H and C from Lake Bogoria. Additionally, comparative genome analysis of two *Arthrospira* genomes – namely the S and H morphotypes (C-morphotype analysis was eliminated as this C-morphotype was morphologically and physiologically similar to the H-morphotype) and the other available *Arthrospira* genomes in the NCBI database lead to the following conclusions:

- 1- All three morphotypes genetically belong to the same species.
- 2- Relying on the database is sometimes misleading, and the best evidence of that is the classification *A. platesis* C1 that should not be *platensis*.
- 3- The *Arthrospira* species of the lake is not *A. platensis*.
- 4- There are two possibilities:
 - a- It is more likely to be *A. maxima* (99.42% identity) (Figure 5.9). Therefore, all the unknown species that clustered together in one clade (see Figures 5.9-5.12) are simply *A. maxima*.
 - b- Or, the remaining 0.6% identity divergence is enough to support the previous morphological studies that identified the *Arthrospira* of Lake Bogoria as *A. fusiformis*.

In conclusion, I agree with Li *et al.* (2001) that *A. maxima* and *A. fusiformis* are the same species and that the *Arthrospira* found in Lake Bogoria should be referred to as *A. maxima*. I think, however, that the 0.6% divergence is enough to consider that the name of the *Arthrospira* of Lake Bogoria should be *Arthrospira maxima* var. *Bogoriensis*.

5.5 Conclusion and future work

It is clear that due to the high sequence identity percentage among the members of this genus, it is difficult to use marker genes as a classification tool to study phylogenetic relationships at the species level. Whole genome sequencing was able to achieve this by aligning interesting regions. Therefore, based on these regions, I can say that in all likelihood, the *Arthrospira* of Lake

Bogoria is *A. maxima* and the morphological view, which argues that the *Arthrospira* of Lake Bogoria belongs to *A. fusiformis*, is less likely. There is no whole genome of *A. fusiformis* in the GeneBank database to enable a final conclusion.

The structural and genetic factors that have been suggested as being responsible for the motility of *Arthrospira* spp. are present in the two morphotypes, but only the S-morphotype exhibits gliding motility. Thus, further gene expression studies are required to understand the mechanism of trichome motility. To date, no transformation system has been successfully completed for *Arthrospira*. Genome sequencing can help, therefore, to understand and determine the causative factors in the failure of the transformants. After the whole genome of *Arthrospira* from this extreme environment has become available, a further study with more focus on understanding the genetic features behind the survival of this cyanobacterium in the extreme aquatic system of the soda lakes is required.

Chapter 6 *Arthrospira* phage investigation

6.1 Introduction

The impact of phage-mediated primary producer decline on aquatic ecosystems is best understood by considering the concept of trophic cascades. These enable researchers to understand the consequences of removing a component of the food web. This removal of a specific component can have a strong, indirect effect, which can control the whole ecosystem through two possible mechanisms. Firstly, is the top-down effect, which occurs when the highest level of the consumer is removed, Second is a bottom-up effect, that occurs when the primary producer is removed (Eisenberg, 2010). Trophic cascades phenomenon has been observed in both terrestrial and aquatic ecosystems, though its effects on aquatic ecosystems are believed to be more severe, perhaps because the productivity of aquatic systems is higher than that of terrestrial systems (Cebrian, 1999). However, the severity of trophic cascades effects on aquatic systems could also be due to the fact that herbivores consume plankton in aquatic environments three times the rate at which plants are consumed in terrestrial environments (Cyr and Face, 1993). Top-down effects have been extensively discussed and studied, whereas bottom-up effects have received less attention (Shurin *et al.*, 2002).

The irregular movements of lesser flamingos in EASLs has been attributed to changes in food quantity and quality – this is associated monocultures of the cyanobacterium *A. fusiformis* (Tuite, 1979, Owino *et al.*, 2001, Krienitz and Kotut, 2010, Zaccara *et al.*, 2011). Changes in the lesser flamingo populations often occur when the populations of primary producers crash. Peduzzi *et al.* (2014) tested the hypothesis that cyanophages can cause phytoplankton crash; hence mediate the bottom-up cascade, in one of the Kenyan soda lakes, Lake Nakuru. Here they found that the food web was disrupted by a collapse of the population of *Arthrospira* spp., the primary producer. These authors suggested that viruses were responsible for the breakdown of the *Arthrospira* spp. population in this lake. In this chapter, I test the same hypothesis on another Kenyan soda lake, Lake Bogoria.

6.1.1 Aim and objectives

The goal of this chapter was to investigate the presence of viruses that may infect *Arthrospira* spp. in Lake Bogoria. Hence, the objectives of this chapter were to:

- 1- Use different methods and techniques to isolate potential *Arthrospira* viruses, and then establish the conditions that are needed to do so.
- 2- Characterise *Arthrospira* phages according to their genome, proteome and host range.
- 3- Quantify the probable magnitude of phytoplankton crash.

Guiding research questions:

- 1- How can cyanobacteria be infected by cyanophages?
- 2- To what extent are cyanophages responsible for the crash of the cyanobacterium *Arthrospira* population?

6.2 Material and methods

In this study, several methods were used to investigate *Arthrospira* phages in Lake Bogoria waters, as follows:

6.2.1 Cyanophage Isolation (well assay)

Liquid *Arthrospira* cultures were used as sources to potentially isolate viruses from the water samples. This was because of the difficulty in obtaining confluent lawns during plaque assays caused by the gliding motility of one morphotype of *Arthrospira* spp., and due to the clumping nature of its filaments (Deng and Hayes, 2008). Therefore, I modified the assay method of Millard (2009). Four mL of exponentially growing *Arthrospira* cultures at an OD₅₆₀ nm of 0.3 (Deshnium *et al.*, 2000) were added to each well of a 12 well plate (Greiner bio-one, UK). Thereafter, 500µL of a 0.2µm filtrated water sample (May 2015 – March 2017) was introduced into the wells, in triplicate, along with negative control cultures containing no water sample. These steps were performed for three *Arthrospira* morphotypes. The plates were incubated in the chamber as described in Chapter 2, section 2.3.2. Visual monitoring for any lytic activity was performed daily. When clearing of incubated cultures was observed, digital images were taken. Cultures were collected and centrifuged at 6000 rpm for 10

min to remove the debris and any remaining cells. Afterwards, the supernatant was transferred to a new Eppendorf tube. An aliquot of a virus-positive lysate was analysed with TEM as described in Chapter 4, section 4.2.7. This method was repeated several times (with some modifications) in order to improve the chance of obtaining a phage infection.

6.2.2 Screening the *Arthrospira* samples for cyanophage infection (TEM analysis)

TEM is an important tool for confirming the presence of phages and characterizing them according to their morphology. Six fresh unfiltered water samples from Lake Bogoria (Aug 2015, Mar 2016, May 2016, Dec 2016 and Mar 2017), the lysed filaments of the only presumed infection, and one sample from the *Arthrospira* laboratory collection, which served as a negative control, were subject to TEM analysis as described in Chapter 4, section 4.2.7. The technique was also used to investigate any protozoan (*Amoeba*) activity in the Begonia's waters.

6.2.3 NanoSight Technology assay

A nanoparticle tracking system called NanoSight (NanoSight LM 10, UK) was used to measure actual concentrations of virus-sized particles in liquid solution. The principle of this method is based entirely on tracking those nanoparticles undergoing Brownian motion in a liquid using laser illumination, directly captured by a camera. Subsequently, the nanoparticles can be identified and tracked individually. The Nanoparticle Tracking Analysis (NTA) software measures their concentrations in a given liquid according to the Stokes-Einstein equation (NanoSight, 2012):

$$Dt = \frac{K_B T}{6\pi\eta rh}$$

Where Dt is the particle diffusion coefficient, K_B is the Boltzmann constant, T is temperature, rh is the hydrodynamic radius and η is solvent viscosity.

Nanoparticle (VLPs) concentrations were measured using this technique on two occasions. The first was when all the samples collected from the lake were analysed to investigate for the presence of VLPs and determine their

concentrations. To do this, first, the chamber of the NanoSight instrument was cleaned of any remnants or debris such as dust by loading 1-2mL of filtered 70% ethanol via the inlet port, the remnants were received onto a tissue through the outlet port. This was followed by loading 1-2mL of filtered Milli-Q water (18.2 MΩcm) and collecting the flow through in the same manner. After the window was cleaned, 1mL of the 0.2µm filtered water sample was loaded into the chamber, cautiously not to introduce bubbles, as this could interrupt the laser. The temperature of each sample was recorded using the attached meter. Thereafter, the concentration of the VLPs was measured for 90 seconds by laser reflection. NTA 2.0 software was used to analyse the recorded data. NTA software settings are given in Appendix 8.2, Table 8.6. The laser chamber was cleaned as above between samples to ensure that there was no cross-contamination between samples. Each sample was repeated until the number of tracks was acceptable (~200 tracks).

The second occasion where the NanoSight used was to study the water sample of July 2016, as this was used as a target sample to investigate the presence of cyanophages that infect *Arthrospira* in Lake Bogoria. To do this, 20mL of an exponential phase of *Arthrospira* (S-morphotype) were incubated with 5mL of 0.2µm filtered water sample for 19 days. *Arthrospira* without a water sample was used as a negative control. To ensure the adequate number of tracks was achieved, five technical repeats were performed for every 10 biological repeats. The VLPs concentrations were measured every day for 19 days. To do this, an aliquot of 300 µL of each culture was taken daily, filtered through a 0.2 µm syringe filter, diluted (five times) using the growth medium and then measured. Zarrouk's medium was used as a blank. All the software settings and the procedure used were as described above.

6.2.4 Phycocyanin fluorescence intensity assay

The visual observation of the interaction between viruses and the *Arthrospira* host is difficult and time-consuming. Thus, an alternative technique was used to screen the water samples from the lake for lytic viral activity. This method relied on the periodic measurement of phycocyanin fluorescence of the cultures (Wilhelm and Poorvin, 2001, Wilhelm *et al.*, 2006). The theoretical basis of this

method is that the fluorescence of the infected cell will gradually decrease, but it will increase in the control sample.

To test this on the water from Lake Bogoria, 30 μ L of filtered water sample was introduced to 250 μ L of exponentially growing *Arthrospira* cultures in a microtiter plate (Greiner Bio-One, UK). This step was repeated with 12 technical replicates, control cultures that received no water sample were maintained for comparison, and Zarrouk's medium was used as a blank. Before each reading, the cultures were mixed using mini-pipettes and 10 μ L of fresh growth medium was added to each well. Fluorescence measurements were taken using a Varioskan Flash Microplate Reader (Thermo Fisher Scientific, UK) set at wavelengths of 630 and 660 nm for excitation and emission, respectively (Mohanty *et al.*, 1997). All water samples collected from the lake were screened for the presence of cyanophage activity. These measurements were repeated daily for 13 days. Between the measurements, the microplates were incubated under standard conditions as described in section 2.3.2. This method was conducted with two morphotypes, S and C, while the H morphotype was eliminated because of the clumping of the filaments, which led to a discrepancy in the reading between replicates.

6.2.5 Epifluorescence microscopy examination

As it is well-known that virus propagation is the main signal for virus infection, an enumeration-based method was used to investigate this aspect further. The target water sample, which is July 2016 (the water sample most expected to possess viruses as examined by TEM, see section 6.3.2) was incubated with an S- morphotype of *Arthrospira* (This was the only morphotype, in which cell lysis was observed when incubated with water samples from the lake, see section 6.3.1). This water sample was examined for the presence of cyanophages, as described by (Patel *et al.*, 2007).

Sample preparation

To prepare the culture for fluorescence microscopy, 4mL of an exponential phase of S-morphotype *Arthrospira* culture was incubated with 500 μ L of 0.2 μ m filtered water sample from July 2016 in triplicate. A cyanobacterium culture without any water sample added served as a negative control, and a

Clostridium difficile phage was used as a positive control. Aliquots of 300µL of each culture were taken and filtered through 0.2µm syringe filters on the first day. The cultures were then incubated in a cyanobacteria chamber for 19 days. Once the incubation was completed, 300µL aliquots of each culture were filtered through 0.2µm syringe filters. All four filtered samples (day 1, day 19, negative control, and just the water sample from the lake) were diluted by a factor of 1:10, except for a sample of water that was not incubated with the *Arthrospira* culture, which was diluted by 1:2. In order to verify that the procedure was working, two dilutions of the positive control were tested (10^{-3} , 10^{-4}). To achieve this, a spot test was conducted. The CDHS1 phage was propagated on the lawn of *C. difficile* strain CD105LC1 ribotype 027 as a host. Ten-fold dilutions of the CDHS1 phage were prepared to determine the phage concentration (PFU/mL). Thereafter, 550 µL of a *C. difficile* overnight culture in Fastidious Anaerobe Broth (FAB) was added to 8 mL of 0.4% brain heart infusion (BHI) agar mixed with salt in order to prepare the *C. difficile* lawn. Before pouring the bacterial culture onto the plate, the tube was mixed thoroughly by continuously inverting it for a minute. This was followed by the spotting of 10 µL drops of each dilution onto the set lawn of the bacterial culture. To avoid mixing the spots, the plates were left to dry then incubated anaerobically at 37°C overnight. After the incubation time was completed, the plates were removed from the anaerobic chamber and the PFU/mL was calculated based on the recorded plaques.

The results obtained from the NanoSight were compared with those of the epifluorescence microscope. To do this, 0.2µm of filtered water samples belonging to nine different collection time points (May 2015, Jun 2015, Jul 2015, May 2016, Jun 2016, Jul 2016, Dec 2016, Jan 2017 and Feb 2017) were diluted as above, and then tested with the epifluorescence microscope. First, all the equipment used was sterilised and cleaned by autoclaving and then rinsed with 0.02µm filtered autoclaved 18.2 MΩcm water, followed by 70% ethanol. Kimwipe tissues (Kimwipes® disposable wipers, Sigma-Aldrich, UK) were used to dry them. Then, 1mL of diluted sample was fixed with 4% formaldehyde solution (Appendix 8.1) for 30 min. During the fixation time, the filtration unit (Figure 6.1) was prepared, where 0.8µm of 25mm membrane filter (white track-

etched polycarbonate membrane filters, Whatman™ Nuclepore™, UK) was mounted on the filter holder and then wetted with a few drops of 0.02µm autoclaved UPW. A 0.02µm 25mm Anodisc AlO₃ filter (Anodiscs 25, Whatman, UK) was carefully placed on the top of this filter. Because Anodisc filters are fragile, each filter was checked before being used and any cracked filters were discarded. Both the funnel and filter holder were joined together using clamps (Figure 6.1). After the fixed sample was transferred into the funnel by the pipette, the pump was operated with a pressure up to ~20 kPa.

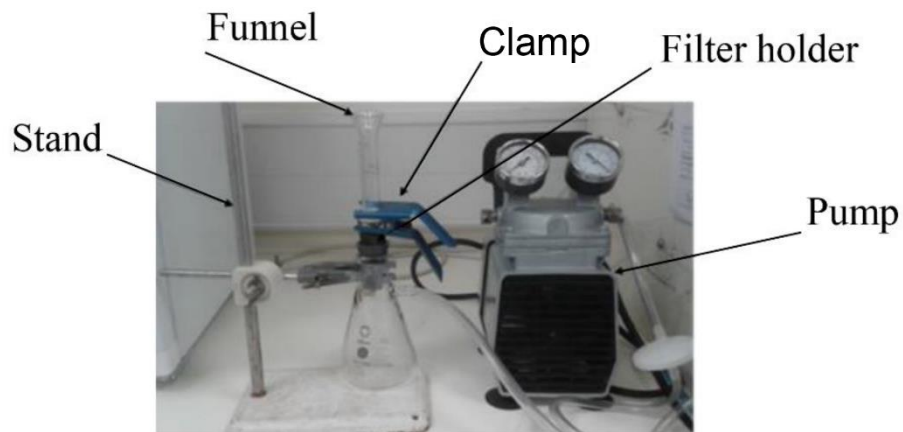


Figure 6.1: The filtration unit structure.

The Anodisc filter was then moved from the filter unit by removing the clamp and funnel and picking it up using forceps and placing it on a tissue inside a sterile Petri dish. The filter was placed in the Petri dish face up. After filtering all the samples, the filters were again placed separately on the tissues inside the sterile Petri dishes. They were left to dry inside a bench drawer in the dark, checked every three mins. Based on the TEM results obtained, the nanoparticles that were observed within the *Arthrospira*'s sections were largely similar to positive-sense single-stranded RNA (+) ssRNA viruses in terms of shape and size (icosahedral and 18-25 nm); it has been assumed that the viruses infecting *Arthrospira* spp. in Lake Bogoria could be a form of a RNA phage, so SYBR Green II was used to stain the samples. Whilst the filters were drying, 1:400 of SYBR Green II (for the samples) and SYBR Green I (for the positive control) (SYBR® Green II RNA gel stain, Life technology, USA) solutions and 0.1% (vol/vol) *p*-phenylenediamine anti-fade mounting medium (Alfa Aesar, USA) were prepared (Appendix 8.1). A 70 µL of the SYBER Green

II and I working solutions were separately dropped into the middles of the clean Petri dishes. The dried filters were placed onto the droplet of the dyes. The filters were incubated in the dark for 18 min at room temperature. After the staining time was complete, the filters were picked up with sterile forceps, the back of the filters were blotted with Kimwipe tissues and then dried as described above. Then, 20 μ L of anti-fade was mounted onto a clean glass slide, and the filter directly placed onto this. An additional 10 μ L of this anti-fade was then dropped onto the filter, after which it was covered with a 1.5 mm thick coverslip using sterile forceps. The slides were either immediately examined under a fluoresce microscope or stored at -20°C until examined.

Epifluorescence microscopy examination

Samples were viewed using a 100x fluorescence oil-immersion objective with a drop of immersion oil that was placed on the middle of the coverslip. Epifluorescence microscopy settings are listed in Appendix 8.2, Table 8.7.

Image Analysis

After the samples were processed via epifluorescence microscopy, 10 images were captured per replicate. An image processing package (Fiji software) was used to analyse the images. Images were calibrated and then ten 100 μ m² squares were randomly chosen per image and the number of VLPs was manually counted for each square. The average of these particles per image was calculated, and the average per replicate calculated from the 10 images. Subsequently, the number of particles per filter was calculated as follows:

$$\text{Filter area} = \pi r^2$$

Where r is an internal radius of the circle, which is 8mm for an Anodisc filter, the number of the VLPs was then calculated for the whole filter by considering the number of these particles in a 100 μ m² square.

6.2.6 Protein profile of Lake Bogoria

Further phage investigation was conducted by profiling the lake protein content. Several methods were tested for best results. The only method that was successful was as below.

Sample preparation

880mL of the water sample that was collected in July 2016 was concentrated into 2mL using centrifugal filter units (Merck Millipore Ltd, Germany). 1.5mL of the concentrated water sample was further concentrated using the StrataClean Resin Protocol (Agilent Technologies, Australia). To do this, 100µL of StrataClean Resin was added to 1mL of UPW, mixed, and then centrifuged at 20,000 *g* for 3 min. To ensure the resin was thoroughly cleaned, this step was repeated three times and the supernatant discarded each time. The pelleted resin was then suspended in 100µL of UPW. Afterwards, 10µL of the suspension was added to 1.5mL of the concentrated water sample, and incubated at room temperature for 15 min. After the incubation was completed, the tube was centrifuged at 1,400 rpm for 3 min. The supernatant was discarded and the pellet was retained.

Polyacrylamide Gel Electrophoresis (SDS-PAGE)

20 µL of sodium dodecyl sulphate (SDS) loading dye (Appendix 8.1) was then added to the pellet and resuspended by pipetting. This was incubated at 95°C for 3 min, before being centrifuged at 13,000 rpm for 3 min, followed by loading the supernatant into a 10% polyacrylamide gel (Appendix 8.1), along with the protein ladder (Protein Marker, Broad Range (2-212 kDa), *BioLabs*, UK). The electrophoresis was carried out by running the gel at 200 V for 40 minutes. The gel was stained with EZ-Run Protein Gel Staining solution (*Fisher Scientific*, UK) on a rotator overnight. The following day, the gel was washed with distilled water several times and then visualised using a gel imager. The gel was sent to the Protein-Nucleic Acid Chemistry Laboratory (PNAACL) at the University of Leicester for sequencing via mass spectrometry.

The mass spectrometry outputs (MS/MS data) were searched against a non-redundant protein database, the Universal Protein Resource (UniPort) (The UniProt Consortium, 2017) using the Mascot Server (Perkins *et al.*, 1999). More searches were performed with the metagenomics data to look for matching regions using the same server, where the metagenome sequence data was converted into amino acid sequences, and the matching regions were identified.

6.2.7 Metagenomics work

Metagenomics is a genome-wide analyses, recently recognised as a powerful tool by which microbial communities in environmental samples can be investigated. In this study, I used it to investigate whether *Arthrospira* phages were present in Lake Bogoria.

Virus concentrations

The water samples were concentrated following the protocol of John *et al.* (2011). First, 200mL of each water sample was passed through a 0.22µm filter (Millex[®], Germany) to remove any large particles. The filtrates were then treated with 10µL of 10g L⁻¹ Fe (FeCl₃) stock solution (Appendix 8.1), and vigorously shaken for 1 min to precipitate the viruses. Afterwards, an extra 10µL of 10g L⁻¹ FeCl₃ was added, shaken several times, and then left to incubate in the dark at room temperature for 1 hour. Once the incubation was complete, the samples treated with FeCl₃ were filtered again using a 0.22µm 47mm PES filter (Express Plus[®] Membrane, Ireland) attached to a sterile filter apparatus with a pump. The apparatus was repeatedly sterilised before each sample was filtered. The filter papers with the virus fraction were then carefully transferred into sterile 50 mL centrifuge tubes using sterile forceps. Virus re-suspension was done by adding 500 µL of 0.1 M EDTA, 0.2 M MgCl₂ and 0.2 M Ascorbate Buffer (Appendix 8.1) to each tube, tubes were placed on the rotator and incubated in the dark at 4°C overnight. The following day, the re-suspended samples were collected into fresh 2 mL tubes using sterile pipettes. To ensure all the re-suspended precipitates were collected, tubes were centrifuged at 500 rpm for 4-5 min, and the suspensions were collected as before. Sometimes the precipitate was not re-suspended adequately, in which case additional suspension buffer was added, and incubated again for 2 hours and then collected as described above.

Virus DNA extraction

After the water samples had been concentrated, viral DNA genomes were extracted using Wizard Columns (Wizard[®] PCR Preps DNA Purification System, Promega, USA)(John *et al.*, 2014). To achieve this, 1mL of DNA purification resin was mixed with 0.5mL of each concentrated sample.

Afterwards, the minicolumns were attached to 5mL sterile syringes with their plungers removed, each mixture was added to the syringe by pipette, and then expelled using the plunger. To wash the resin, 2 mL of 80% isopropanol (Appendix 8.1) was added to each syringe and passed through using the plunger. This step was followed by placing the tubes in fresh 1.5 mL centrifuge tubes and centrifuging at 10,000 *g* for 2 min to remove any remaining liquid. The columns were then again placed in fresh 1.5mL tubes. After that, 100 μ L of prewarmed elution buffer (TE buffer) warmed to 80°C (Appendix 8.1) was added to each column, vortexed gently for 10 sec, and then left to incubate on the bench at room temperature for 1 min. Finally, to elute DNA, the columns were centrifuged at 10,000 *g* for 30 sec, after which the DNA was extracted from all samples. The DNA quantity and quality was assessed using the NanoDrop and Qubit instruments, respectively. TE buffer was used to zero the NanoDrop machine, and then stored at - 80°C to be sent for sequencing at the University of Warwick using Illumina MiSeq Next Generation Sequencing Platform.

Metagenomics sequencing and analysis

Four water samples that had an acceptable DNA concentration were sent for sequencing. The quality and quantity of their DNA are outlined in Table 6.1. After receiving the sequencing data as FASTQ files, each sample had a forward and reverse FASTQ file (F.FASTQ and R.FASTQ), the shotgun metagenomics analysis was used to identify the species composition of each metagenomics sample, using Metagenomics Phylogenetic Analysis (MetaPhlan2) software (Truong *et al.*, 2015). Shotgun analysis uses sequencing data produced randomly from total genomic DNA in the environmental samples, rather than targeting particular genes. The entire analysis was performed via the command line using Linux operating systems. The outputs of the MetaPhlan2 software were visualised as an interactive taxonomy plot using the Krona tool (Ondov *et al.*, 2011). To visualize and compare multiple metagenomes, a heatmap plot was created using the R programming language (Team, 2013).

Table 6.1: The quality and quantity of DNA for four water samples from Lake Bogoria.

Sample name	DNA ($\mu\text{g } \mu\text{L}^{-1}$)	260/280 ratio	260/230 ratio
Sept 2014	1.5	1.72	1.55
May 2015	2.5	1.78	1.61
Jul 2015	5.2	1.69	1.60
Sep 2015	3.7	1.82	1.58

6.2.8 Prophage detection

In general, two methods can be used to identify any prophage sequences integrated within bacterial genomes. The first is an experimental approach and the second computational and based on bioinformatics. The first approach involves stimulating the bacterial cell to release the virus particles after exposure to any conditions that lead to DNA damage, such as ultraviolet radiation, certain antibiotics such as mitomycin-C or other virus-inducing agents can also exert a pressure on the cell, resulting in the release of viral particles. However, this method cannot detect defective prophages; not all prophages can be induced under the same conditions and sometimes the conditions of prophage induction are unknown, or not yet defined (Casjens, 2003). The most important condition for using this approach is that the bacterial culture being induced should be an axenic culture, meaning that it is free of any other bacterial contamination. Unfortunately, this condition was not achieved for *Arthrospira* cultures from Lake Bogoria as explained in chapter 4. For this reason, this approach of inducing phages was firstly conducted and then eliminated, and the computational approach used instead. To do this, the PHAge Search Tool – Enhanced Release (PHASTER) (Arndt *et al.*, 2016) was used to detect prophage sequences in the two *Arthrospira* genomes, S and H morphotypes.

6.2.9 Genome protection (CRISPR identification)

CRISPRs that give resistance to phages are highly dispersed within the genomes of many bacteria, and the majority of archaea. The CRISPRs web server (Labrie *et al.*, 2010) was used to detect CRISPR arrays in two genomes of *Arthrospira* morphotypes of Lake Bogoria, the S and H morphotypes. Thereafter, sequences of these CRISPRs were blasted against the metagenome data derived from the lake samples to find regions of similarity. In

addition to the metagenomics data of Lake Bogoria for the current study (Table 6.1), another set of metagenomics data for the same lake that had been found by a University of Leicester student (Sophie Clough) in September 2014 (Clough, 2015) were analysed. She conducted metagenomics sequencing from the three Bogoria basins (north, south and central), from four different depths for each basin (0 cm, 25 cm, 50 cm, 75 cm, 100 cm and from the scum). To achieve this, a database was first created, thereafter; the Nucleotide Basic Local Alignment Search Tool (blastn) was used on the command line on a Linux open source software operating system. The matching regions were selected and then again 'blasted' against all non-redundant GenBank+EMBL+DDBJ+PDB sequences (nr). High identity sequences (blastn) were used to see whether there were any matches for any known cyanophage in the database.

6.2.10 Statistical analyses

For the statistical analysis of VLPs concentration, every two months were treated as data points (time point); therefore samples were classified into 11 time points ($n = 6$). All data were first tabulated in Microsoft Excel 2013 to determine whether there were any statistically significant differences between the distributions of related groups for each parameter. These data were then imported into the IMS SPSS Statistics version 24 software as a repeated-measures design. The data for all parameters were approximately normally distributed as assessed by the Shapiro-Wilk test or Kolmogorov-Smirnov^a tests ($p > 0.05$) (Appendix 8.2, Table 8.8) with no outliers, as assessed by the inspection of a boxplot. The Z-scores (Skewness/Std. Error and Kurtosis/Std. Error) for skewness and kurtosis were in the range of normally distributed data (± 2.58) for all variables (Appendix 8.2, Table 8.8); however, the small sample size has affected the histograms, Q-Q plots and Mauchly's test of sphericity. Thus, a nonparametric Friedman's ANOVA test was used and then followed by pairwise comparisons with a Bonferroni correction for multiple comparisons (Statistics, 2012). Data are presented as medians.

A Spearman's rank-order correlation was used to study the relationship between VLPs concentration and Lake Bogoria properties. To determine if there were significant differences in VLPs concentration between the S-

morphotype cultures that were incubated with the water sample of July 2016 for 19 days and the control culture, a rank-based nonparametric test of the Mann-Whitney U test was used using an adjusted alpha level (α) of 0.005, $n = 10$. The data were approximately normally distributed, as assessed by the Shapiro-Wilk and Kolmogorov-Smirnov^a tests, where the p -value was >0.05 for each level of comparison except for the control culture of 13 days, where p was 0.05 for the Shapiro-Wilk test and 0.017 for Kolmogorov-Smirnov^a test for the culture incubated for 15 days (Appendix 8.2, Table 8.9). However, the concentrations of both incubated and control cultures were slightly skewed, as assessed by a visual inspection of the appropriate histograms and normal Q-Q plots. There was the homogeneity of variances for VLPs concentrations for control and incubated cultures, as assessed by the Levene's test for equality of variances ($p > 0.05$) except for 3, 7 and 15 days where the data were heterogeneous ($p < 0.05$) (Appendix 8.2, Table 8.10).

The nonparametric Kruskal-Wallis H test was performed to determine whether there was a difference in VLPs counts using epifluorescence microscopy between groups that differed in their incubation time, $n = 3$. The VLPs counts for all levels of independent variables were not normally distributed, as assessed by a visual inspection of the appropriate histograms, P-P plots and Q-Q plots. The variance between the different variables was homogenous ($p > 0.05$) (Appendix 8.2, Table 8.11). There is a similarity in the distribution of VLPs counts for all levels of independent variables as tested by a visual inspection of a boxplot. Consequently, medians are used to express the values unless otherwise stated. A Spearman's rank-order correlation was used to assess the association between the VLPs counts using two methods: NanoSight and Epifluorescence microscopy.

The presence of the variability in phycocyanin fluorescence intensity between the incubated *Arthrospira* culture (S and C morphotypes) with a water sample from Lake Bogoria and the control (*Arthrospira* culture without water samples from the lake) were tested. The sample size was small ($n = 6$), so difficult to decide whether the data were normally distributed by visual inspection of the histogram and Q-Q plot; consequently, a nonparametric Mann-Whitney U test

was conducted using an adjusted alpha level (α) of 0.007. This test was performed for the 11-time points of water samples between May 2015 and Mar 2017. If the distributions of the pigment fluorescence for controls and incubated cultures were visually similar, the medians were presented. If they were not, mean ranks were used instead (<https://statistics.laerd.com/spss-tutorials/mann-whitney-u-test-using-spss-statistics.php>).

6.2.11 Overview

Figure 6.2 illustrates the overall work flow for this chapter.

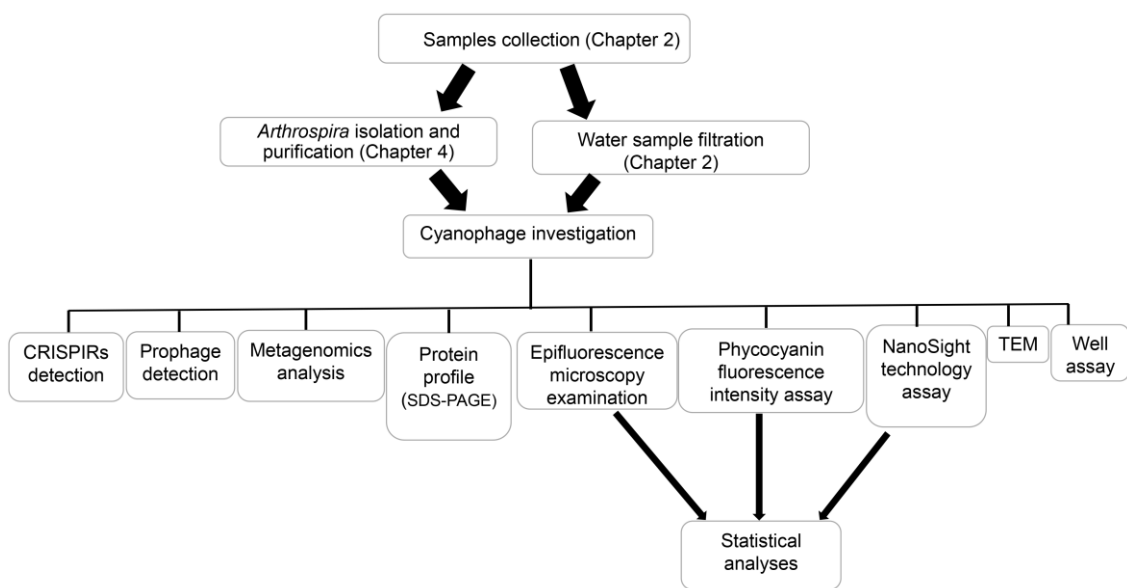


Figure 6.2: Schematic pathway for the *Arthrospira* phage investigation.

6.3 Results

6.3.1 Cyanophage isolation (well assay)

Cell lysis was observed with all-time points for the S-morphotype of *Arthrospira* cultures that were incubated with the water samples except with the Oct and Nov 2015 and Jan-Mar 2017 water samples (Figure 6.3). The *Arthrospira* filaments were observed to have been fragmented into small pieces compared with the control cultures (Figures 6.4 A and B).

The greatest cell lysis of the *Arthrospira* filaments incubated with water was May 2015, TEM results showed that the average number of phages in the sample was 5.3, whereas only one phage was detected in the control sample

(Figure 6.5 and Table 6.2). Almost all the observed phages had the same morphology, with an icosahedral head and a long non-contractile tail (Figure 6.5) which are close to siphoviruses. In some phages, it was found that the head was detached from the tail, which could be due to a technical issue of sample preparation. Very thin sections of the fragmented filaments examined under TEM (see section 6.3.2). Unfortunately, when the well assay was repeated, no cell lysis was detected with any of the incubated cultures for any sample May 2015 – Mar 2017. There were also no infection symptoms observed for the other two *Arthrospira* isolated morphotypes (C and H).

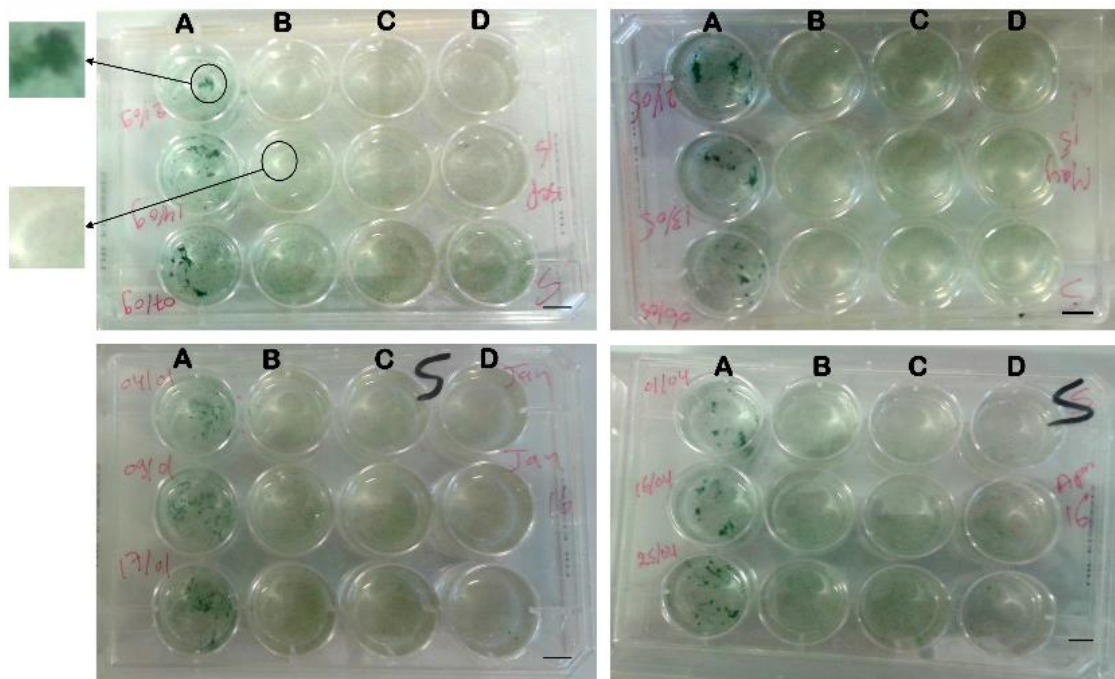


Figure 6.3: Lysis of S-morphotype filaments that were incubated with water samples from Lake Bogoria.

Macrographs showing the lines A; control culture where no water samples were added. Lines B, C and D are the incubated *Arthrospira* cultures with water samples from the lake. Note, the fragmentation of *Arthrospira* trichomes in the incubated cultures compared with the control. The scale bars represent 2 cm.

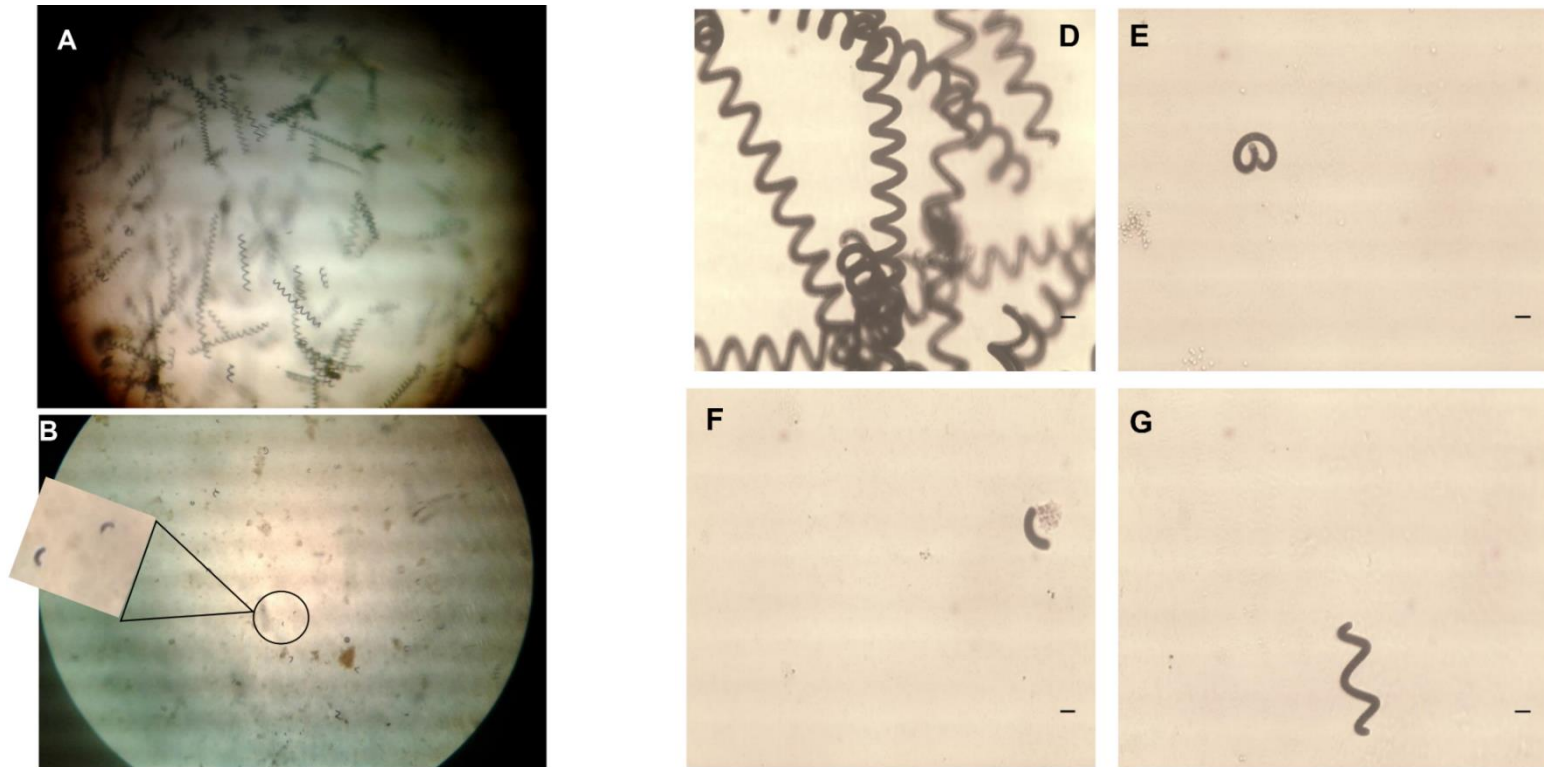


Figure 6.4: Lysis of S-morphotype filaments that were incubated with water samples from Lake Bogoria.

Micrographs showing (A and D) control culture where no water sample was added, the trichomes were long and healthy. (B, E, F and G) The incubated *Arthrospira* culture with the water sample from May 2015. Note the fragmentation of *Arthrospira* trichomes in the incubated cultures compared to the control, scale bars represent 50 μm .

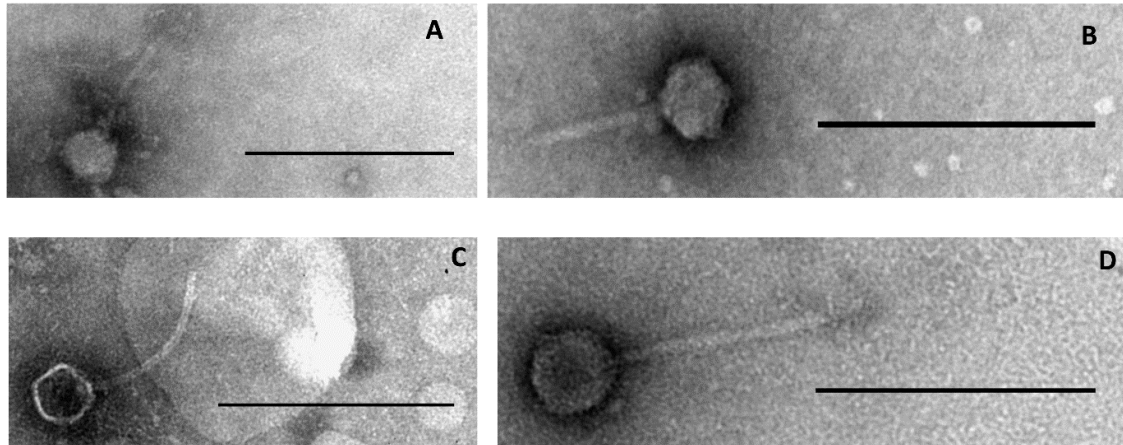


Figure 6.5: Electron micrographs of 0.2 μm filtered *Arthrospira* cultures showing the phage morphology.

(A) Control culture of S-morphotype where no water sample was added, (B, C and D) are triplicates of the incubated cultures with the water sample from May 2015. The scale bars represent 200 nm.

Table 6.2: Description of the phages based on their morphological parameters.

Culture	Average number of the phages ^a	Average diameter of the head (nm \pm SD)	Average length of the tail (nm \pm SD)	Characteristic of head and tail
Control culture	0.33 \pm (0.58)	58.9	115.2	Icosahedral head attached to long non-contractile tail
Incubated culture	5.3 \pm (4.1)	82.12 \pm (19.77)	182.91 \pm (74.28)	Icosahedral head attached to long non-contractile tail

a: Means and standard deviations (in parentheses) of recorded values are given, n = 3.

6.3.2 Screening the *Arthrospira* samples for cyanophage infection (TEM analysis)

No symptoms of phage infections were observed in the sections of *Arthrospira*'s samples investigated (Aug 2015, Mar 2016, May 2016, Dec 2016 and Mar 2017), and compared to lab strain no different structures observed (Figure 6.6 A-F).

There had been no visible signs of cyanophage infections in the sample of *Arthrospira* lysate (well assay (S-morphotype), previous section) (Figure 6.6 G) with the exception of July 2016. The TEM results from this sample (July 2016) showed a large number of icosahedral particles that seemed to be phages (Figure 6.7). The shape, size (18- 25 nm) and the pattern of distribution of these

particles were similar to phages. The two TEM results for the same sample were compared to the TEM result of the sample lacking these particles. Stacks of thylakoid membranes were damaged in the former sample but healthy in the sample lacking these particles (Figures 6.6 and 6.7).

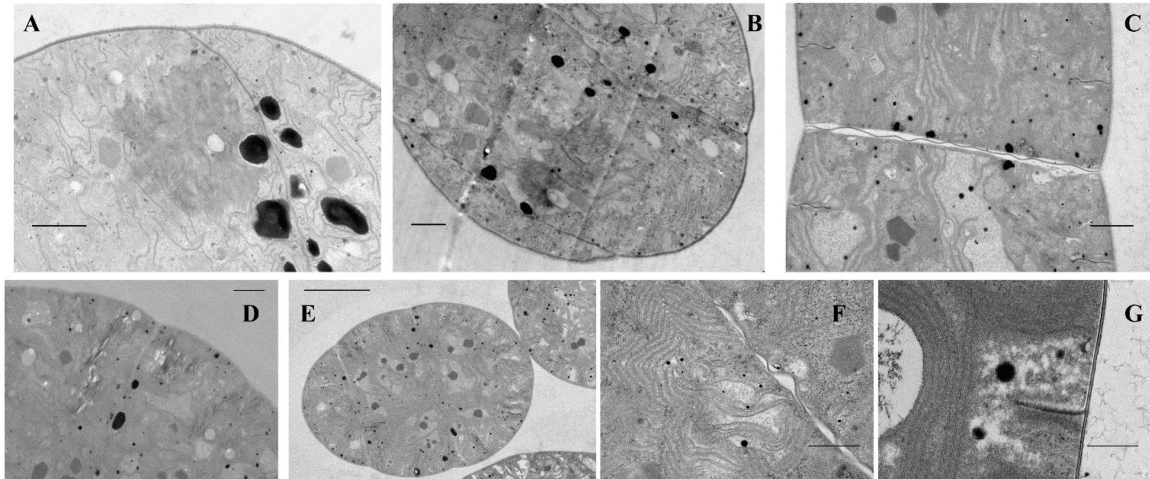


Figure 6.6: TEM images of the *Arthrospira* sections for the entire period of study.

A: Aug 2015, B: Mar 2016, C: May 2016, D: Dec 2016, E: Mar 2017, F: Negative control of *Arthrospira* laboratory collection and G: The fragmented filaments of S morphotype that were incubated with the water sample from May 2015. No viruses were detected within the cyanobacterium sections. Scale bars, A = 1 μm , B, C, D = 2 μm , E = 5 μm , F and G = 200 nm.

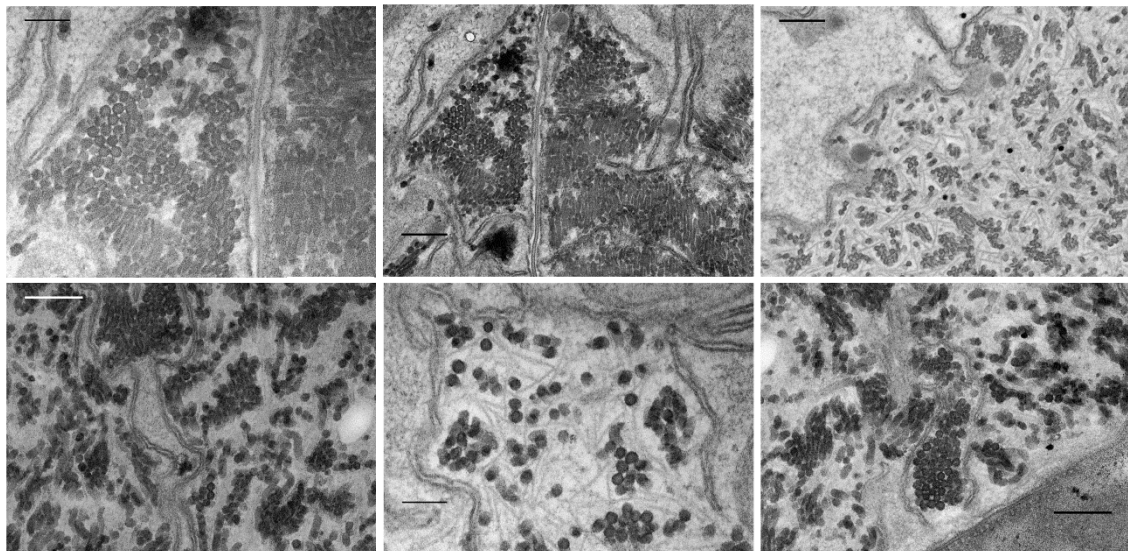


Figure 6.7: Electron micrographs of *Arthrospira* sections from Lake Bogoria (Jul 2016).

Visible icosahedral particles within cyanobacterium sections of the Jul 2016 sample. The scale bar represents 200 nm.

6.3.3 VLP concentrations using NanoSight

6.3.3.1 Variability in VLPs concentration of Lake Bogoria

There was a general tendency for the concentration of the VLPs to increase from $Mdn = 0.885 \times 10^8$ VLP mL^{-1} at the beginning of the study until they reached their highest value ($Mdn = 1.755 \times 10^8$ VLP mL^{-1}) in Jul – Aug 2016. After Oct 2016, the concentration of these particles decreased rapidly until it reached $Mdn = 0.842 \times 10^8$ VLP mL^{-1} at the end of the study (Figure 6.8). Descriptive analyses of the selected size (0 – 200 nm) of the VLP concentrations for the entire study period is shown in Table 6.3. The significant difference, $\chi^2(10) = 45.51$, $p < 0.0001$ in VLP concentrations across the 11 data points showed that among 55 pairwise comparisons, only seven were significantly different, (Table 6.4).

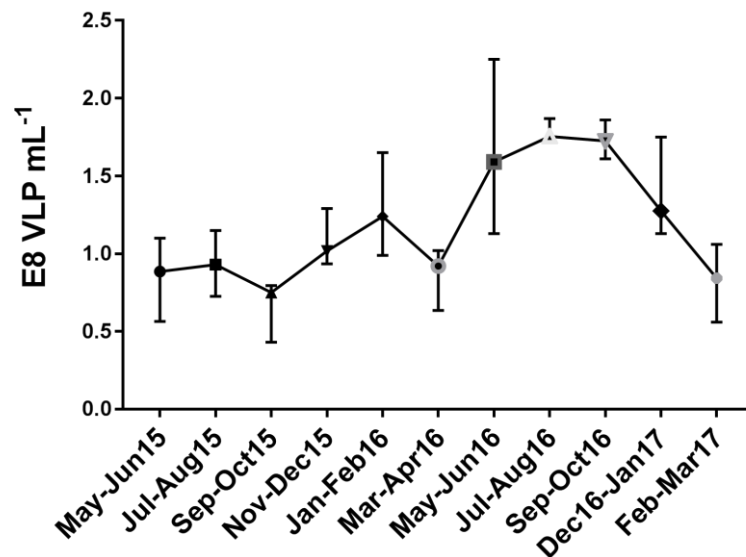


Figure 6.8: The variation in VLPs concentrations during the period May 2015- Mar 2017.

Error bars represent 95% CI; n = 6.

Table 6.3: Descriptive analysis results for VLPs concentrations for Lake Bogoria samples for the entire study period (May 2015-Mar 2017).

Property	Median	Min	Max	Mean \pm SD
VLPs concentrations (VLP $\times 10^8 mL^{-1}$)	1.10×10^8	0.430×10^8	2.250×10^8	$1.183 \times 10^8 \pm 0.449 \times 10^8$

n = 66.

Table 6.4: The significant results of the Bonferroni post hoc tests for pairwise comparisons in the VLPs concentration from Lake Bogoria (May 2015- Mar 2017).

Pairwise	Test statistic	Adjusted <i>P</i> value	Effect size (<i>r</i>)
Sep – Oct15 vs. May – Jun16	-6.583	0.032	0.64
Sep – Oct15 vs. Sep-Oct16	-7.500	0.005	0.64
Sep – Oct15 vs. Jul-Aug16	-8.167	0.001	0.64
Feb-Mar17 vs. Sep-Oct16	6.500	0.038	0.64
Feb-Mar17 vs. Jul-Aug16	7.167	0.010	0.64
Mar-Apr16 vs. Jul-Aug16	-6.667	0.027	0.64
May-Jun15 vs. Jul-Aug16	-6.417	0.044	0.64

Significance level (α) is 0.05.

6.3.3.2 *The relationship between the VLPs concentration and the limnological properties of Lake Bogoria*

A weak positive correlation was found between VLP concentrations and pH, total P parameters and salinity (Figure 6.9 A, B and C). Spearman's rank correlation coefficients were $r_s(64) = 0.259$, 95% BaCa CI [0.022, 0.454], $p = 0.035$; $r_s(64) = 0.343$, 95% BaCa CI [0.108, 0.561], $p = 0.005$; $r_s(64) = 0.383$, 95% BaCa CI [0.148, 0.599], $p = 0.002$, respectively. By contrast, their concentration was strongly negatively correlated with the Chl-*a* concentration of the lake, which was measured using the acetone extraction method (Figure 6.9 E), $r_s(64) = -0.629$, 95% BaCa CI [-0.779, -0.433], $p < 0.0001$.

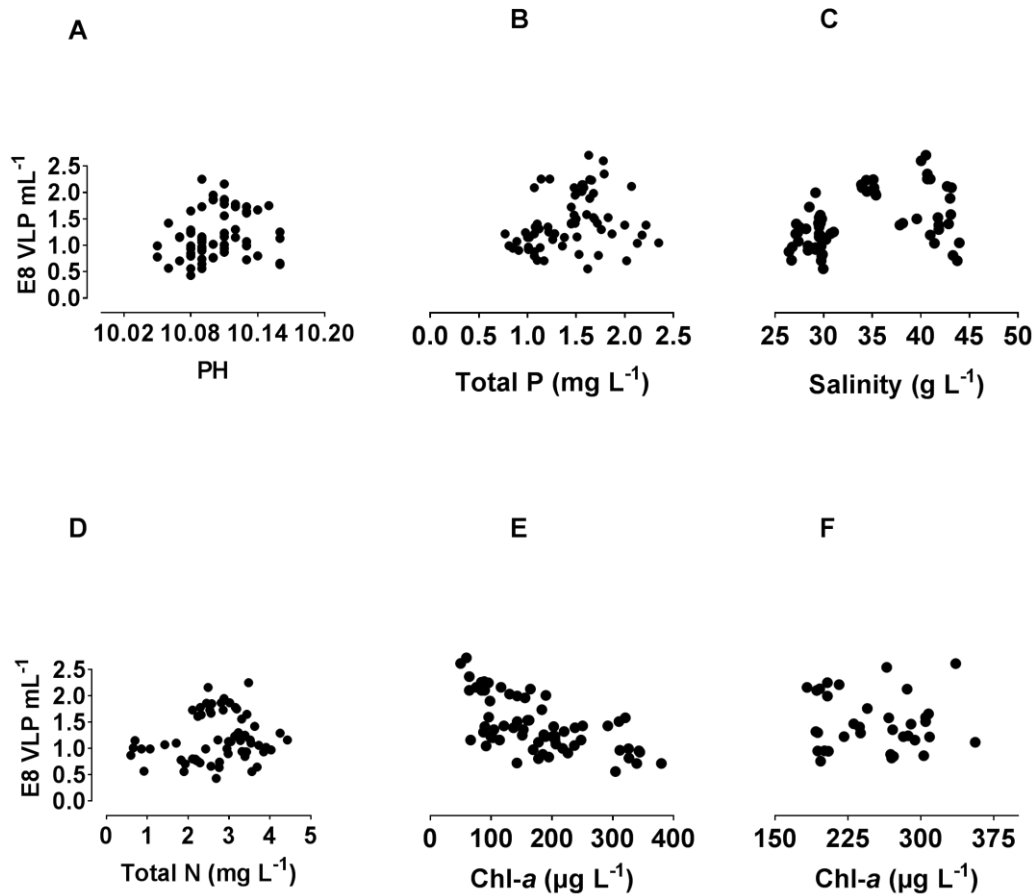


Figure 6.9: Scatterplots of the relationships between Lake Bogoria properties and VLPs concentration (E8 VLP mL⁻¹) over the period of the study.

A, B and C show a positive monotonic relationship between the VLP concentrations and pH, total P and salinity, respectively, whereas E represents a negative association between the VLPs concentration and Chl-a content, as measured using the acetone extraction method. For D and F, the relationship was not monotonic between the VLP concentrations and total N and Chl-a measured using remote sensing, respectively. F used $n = 35$, all other parameters $n = 66$.

6.3.3.3 The variability in VLP concentrations between control and incubated culture with water sample of Lake Bogoria

The sample of water (Jul 2016) showing VLPs in TEM, incubated with the S-morphotype of *Arthrospira*, showed the highest concentration ($Mdn = 11.65 \times 10^8$) at 5 days (Figure 6.10). There were significantly higher VLP concentrations in the incubated culture than control at days 5, 7, 11, 13, 15 and 19 (Figure 6.10). The highest difference was recorded at day 5 and 7. For both days, their concentration in the incubated culture (11.65×10^8 Day 5, 8.96×10^8 Day 7) were significantly higher than in the control culture (6.04×10^8 Day 5, 3.96

$\times 10^8$ Day 7), Mann-Whitney U test statistic (U) = 0.00, standardised test statistic (z) = -3.780, p (using an adjusted alpha level (α) of 0.005) < 0.0001, effect size (r) = -0.846. The significant differences for other days are shown in Table 6.5. No significant difference in the VLPs concentrations between the control and incubated culture was observed for days 1, 3, 9 and 17, $p > 0.005$ (Table 6.5).

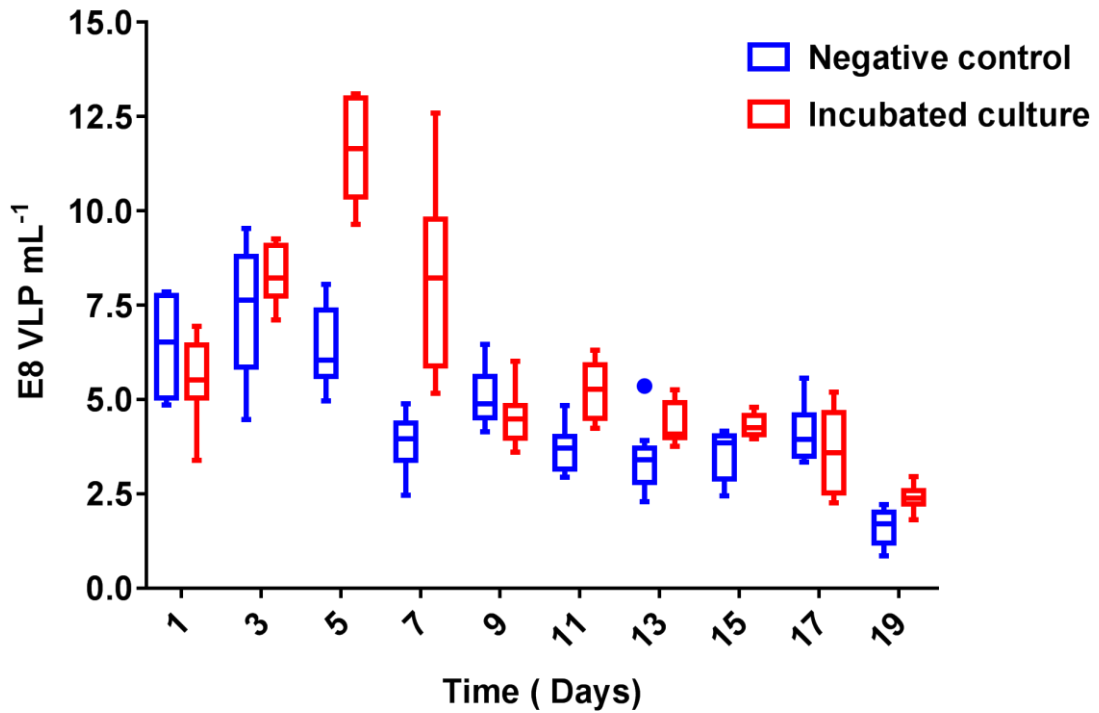


Figure 6.10: Box-plots of differences in VLPs concentrations of the incubated S-morphotype of the *Arthrospira* culture with and without water sample of Jul 2016 for 19 days.

The whiskers of the box plots were created using the Tukey method, and the median is illustrated by the horizontal line within the boxes, outliers are represented as dots outside the boxes, $n = 10$.

Table 6.5: Independent-Sample Man-Whitney U Test for the differences in VLPs concentration between the control and incubated *Arthrospira* culture.

Incubation day	U	z	p	r
11	3	-3.553	< 0.0001	-0.799
13	11	-2.948	0.002	-0.660
15	12	-2.875	0.003	-0.643
19	5.5	-3.366	< 0.0001	-0.753
1	64	1.058	0.315	0.237
3	32	-1.361	0.190	0.304
9	76	1.052	0.052	0.440
17	65	1.134	0.280	0.254

The significance level (α) is 0.005. The significant differences are in bold.

6.3.4 The variability in phycocyanin fluorescence

There was no clear gradual decrease pattern in phycocyanin fluorescence in incubated cultures with water samples compared to the control cultures for two morphotypes C and S throughout the 13 days of incubation. In the C-morphotype (Figures 6.11), phycocyanin fluorescence was significantly higher in the control cultures than the cultures incubated with the water samples of Jul-Aug15^{Day7}, Jul-Aug15^{Day9}, Jan-Feb16^{Day7}, Mar-Apr16^{Day7} and Feb-Mar17^{Day9}, $p < 0.007$ (test statistic and related details are shown in Table 6.6 A). However, the medians of the control cultures were significantly lower than those of the cultures incubated with the water samples of Jul-Aug 15^{Day3}, Nov-Dec15^{Day1}, Nov-Dec15^{Day3}, May-Jun16^{Day3}, Jul-Aug16^{Day3}, Dec16-Jan17^{Day3} and Feb-Mar17^{Day3}, $p < 0.007$ (Table 6.6 B). The non-significant results are shown in Appendix 8.2, Table 8.12.

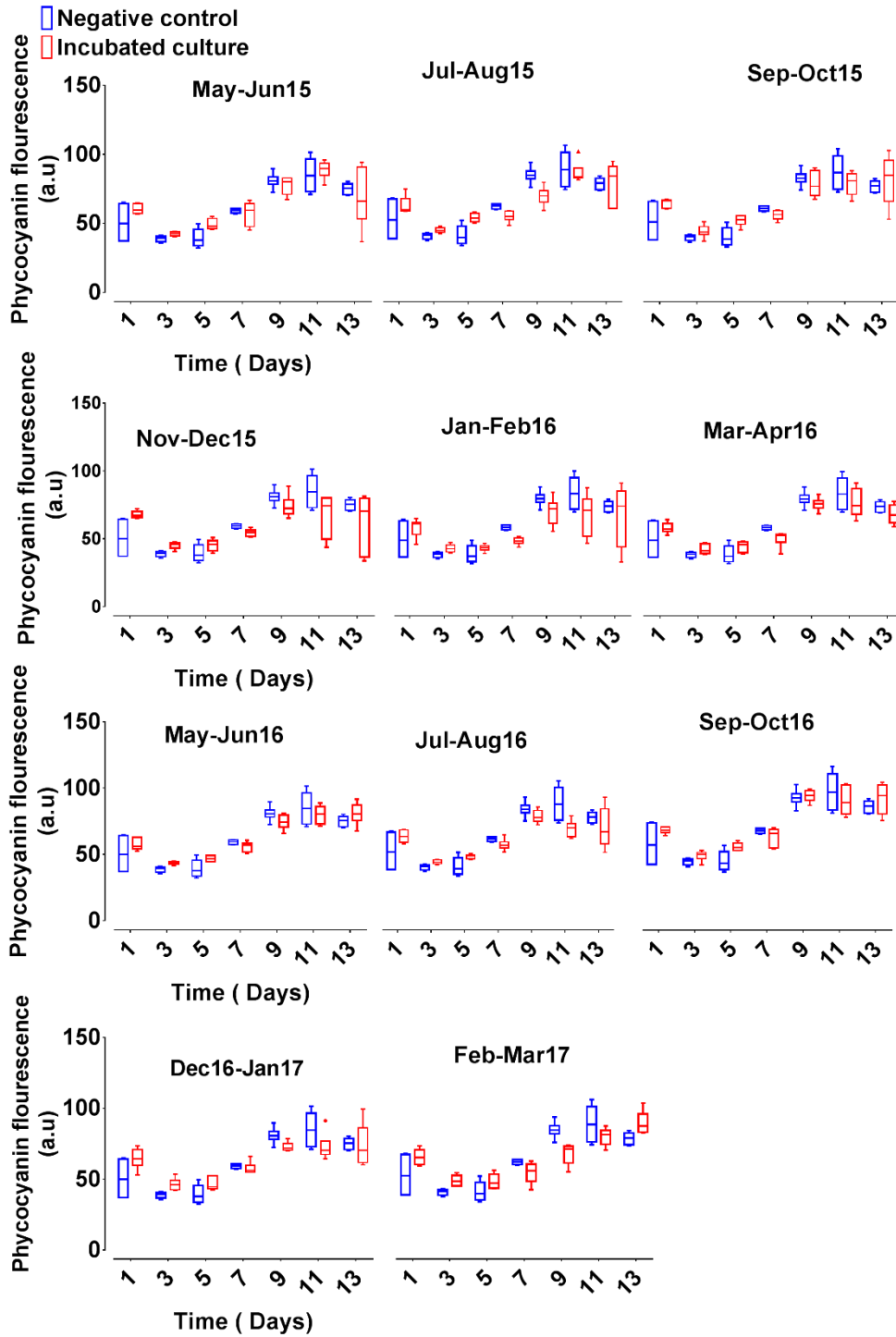


Figure 6.11: Comparisons of phycocyanin fluorescence intensity of cyanobacterium *Arthrospira* between the C-morphotype (incubated with water samples from Lake Bogoria (May 2015-Mar 2017) and the control culture (without water sample).

The pigment fluorescence was measured for 13 days. The whiskers of the box plots were created using the Tukey method, the median is illustrated by the horizontal line within the boxes, and outliers are represented as dots outside the boxes, n = 6.

Table 6.6: The median values and test statistic for the significant time points of phycocyanin fluorescence of the control and C-morphotype incubated cultures with water samples from the lake over the period of the study.

Time point	Incubation day	Median of the control culture (a. u)	Median of the incubated culture (a. u)	Test statistic	Sig. (p)	Effect size (r)
A						
Jul-Aug 15	7	59.46	52.33	0	0.002	-0.83
Jul-Aug 15	9	80.78	66.48	1	0.004	-0.79
Jan-Feb16	7	59.46	49.13	0	0.002	-0.83
Mar-Apr16	7	59.46	53.58	0	0.002	-0.83
Feb-Mar17	9	80.78	68.12	0	0.002	-0.83
B						
Jul-Aug 15	3	39.36	42.65	35	0.004	0.79
Nov-Dec15	1	49.86	67.20	36	0.002	0.83
Nov-Dec15	3	39.36	46.11	35	0.004	0.79
May-Jun16	3	39.36	43.83	36	0.002	0.83
Jul-Aug16	3	39.36	42.60	35	0.004	0.79
Dec16-Jan17	3	39.36	46.04	36	0.002	0.83
Feb-Mar17	3	39.36	46.21	36	0.002	0.83

The significant level (α) is 0.007. A is the median of control culture higher than incubated culture, B is the median of control culture lower than incubated culture.

The S-morphotype (Figure 6.12) showed 31 out of 77 pairwise comparisons significantly different from each other, with the median phycocyanin fluorescence for the control was significantly lower than the median value for the incubated cultures, $p < 0.007$ (Table 6.7). The non-significant results are shown in Appendix 8.2, Table 8.13. H-morphotype filament clumping did not allow the fluorescence to be measured properly.

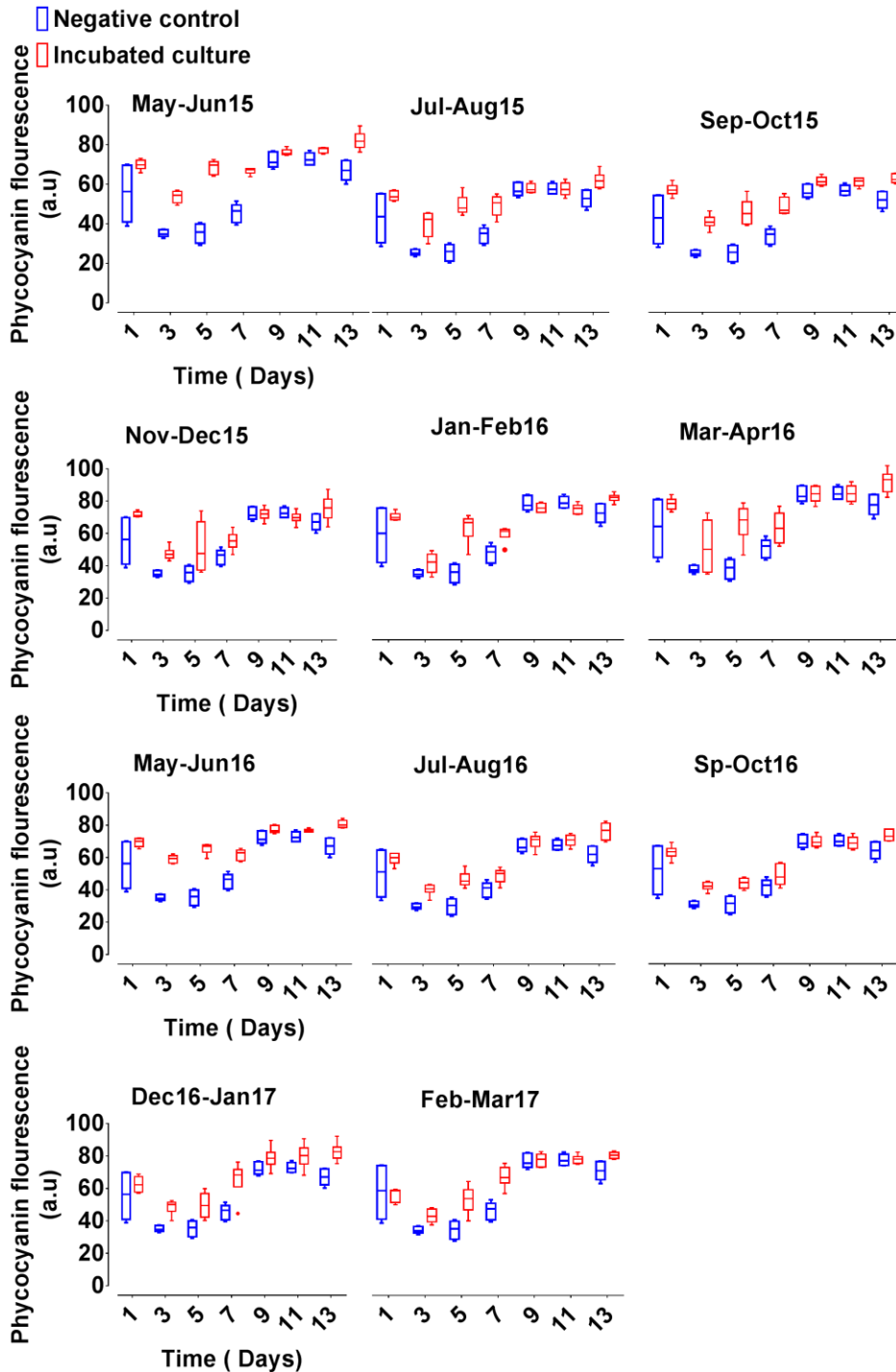


Figure 6.12: Comparisons of phycocyanin fluorescence intensity between the S-morphotype of cyanobacterium *Arthrospira* that was incubated with water samples from Lake Bogoria (May 2015-Mar 2017) and the control culture (*Arthrospira* without water sample).

The pigment fluorescence was measured for 13 days. The whiskers of the box plots were created using the Tukey method, the median is illustrated by the horizontal line within the boxes, and outliers are represented as dots outside the boxes, $n = 6$.

Table 6.7: The median values and test statistic for the significant time points of phycocyanin fluorescence of the control and S-morphotype incubated cultures with water samples from the lake over the period of the study.

Time point	Incubation day	Median of the control culture (a. u)	Median of the incubated culture (a. u)	Test statistic	Sig. (<i>p</i>)	Effect size (<i>r</i>)
May-Jun15	3	34.71	54.50	36	0.002	0.83
May-Jun15	5	35.84	69.79	36	0.002	0.83
May-Jun15	7	46.58	67.40	36	0.002	0.83
May-Jun 15	13	67.06	81.77	36	0.002	0.83
Jul-Aug15	3	34.71	54.83	36	0.002	0.83
Jul-Aug15	5	35.84	61.37	36	0.002	0.83
Jul-Aug15	5	46.58	64.56	36	0.002	0.83
Jul-Aug15	13	67.06	77.37	36	0.002	0.83
Sep-Oct15	3	34.71	53.74	36	0.002	0.83
Sep-Oct15	5	35.84	58.86	36	0.002	0.83
Sep-Oct15	7	46.58	60.84	36	0.002	0.83
Sep-Oct15	13	67.06	79.27	36	0.002	0.83
Nov-Dec15	1	56.31	70.98	36	0.002	0.83
Nov-Dec15	3	34.71	47.06	36	0.002	0.83
Jan-Feb16	5	35.84	62.07	36	0.002	0.83
Mar-Apr16	5	35.84	59.54	36	0.002	0.83
May-Jun16	3	34.71	59.42	36	0.002	0.83
May-Jun16	5	35.84	66.93	36	0.002	0.83
May-Jun16	7	46.58	63.00	36	0.002	0.83
May-Jun16	13	67.06	80.18	36	0.002	0.83
Jul-Aug16	3	34.71	46.03	36	0.002	0.83
Jul-Aug16	5	35.84	50.67	36	0.002	0.83
Jul-Aug16	13	67.06	81.82	36	0.002	0.83
Sep-Oct16	3	34.71	45.90	36	0.002	0.83
Sep-Oct16	5	35.84	48.04	36	0.002	0.83
Sep-Oct16	13	67.06	75.38	36	0.002	0.83
Dec16-Jan17	3	34.71	50.05	36	0.002	0.83
Dec16-Jan17	5	35.84	49.39	35	0.004	0.79
Dec16-Jan17	13	67.06	82.59	36	0.002	0.83
Feb-Mar17	3	34.71	42.46	36	0.002	0.83
Feb-Mar17	5	35.84	51.99	35	0.004	0.79
Feb-Mar17	7	46.58	63.36	36	0.002	0.83
Feb-Mar17	13	67.06	75.32	36	0.002	0.83

The significant level (α) is 0.007.

6.3.5 The variability in VLPs concentration using Epifluorescence microscopy

There was a difference in the VLP counts between different incubation times (Figure 6.13). Median VLPs concentration gradually increased from the negative control (1.1×10^7 VLP mL⁻¹), to 1.2×10^8 VLP mL⁻¹ on day one, to 2.9×10^8 VLP mL⁻¹ on day 19, to 3.9×10^8 VLP mL⁻¹ with only the water sample from the lake (Figure 6.14 A). The Kruskal-Wallis H test showed a significant difference in VLPs, $X^2(3) = 10.385$, $p = 0.016$. Pairwise comparisons with a Bonferroni correction to the p -value for multiple comparisons showed that this

significant difference was only recorded between the negative control and water sample of Jul 2016 ($p = 0.013$, $r = -1.2$). There were non-significant differences between VLP counts in both pairwise comparisons; control culture vs. 19 days of incubation and the first day of incubation vs. water only sample of Jul 2016 ($p = 0.249$). There were also no significant differences in their counts in both pairwise comparisons, the control culture vs. the first day of incubation, first day of incubation vs. 19 days of incubation and 19 days of incubation vs. water only sample of Jul 2016 ($p = 1.0$, $r = -0.416$).

More statistical analysis, conducted after the VPL counts in the negative control subtracted from the first and 19th day of incubation (Figure 6.14 B), showed median VLPs counts were statistically significantly different between groups, $X^2(2) = 7.200$, $p = 0.027$. Pairwise comparisons gave significant differences between the first day of incubation and the water only sample of Jul 2016 ($p = 0.022$, $r = -0.913$). However, there were no significant differences between VPL counts for 19 days compared to the first day of incubation ($p = 0.539$, $r = -0.548$).

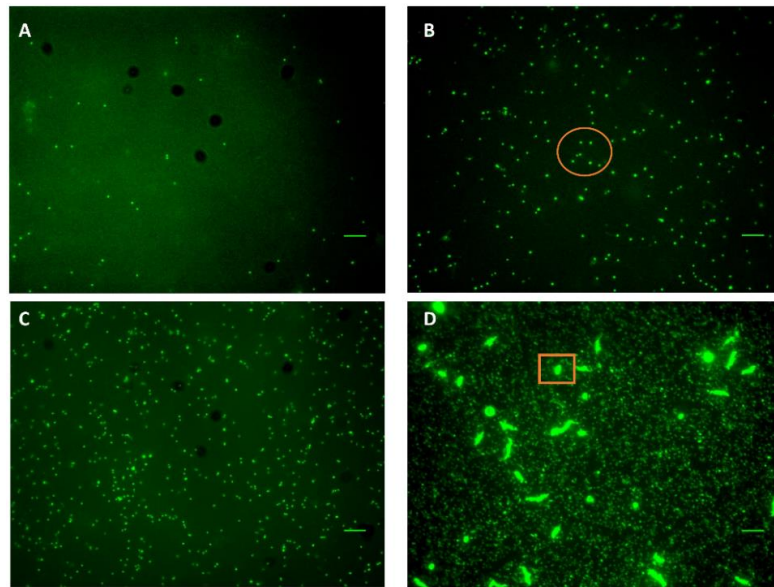


Figure 6.13: Epifluorescence microscopy images of S-morphotype of *Arthrospira* cultures.

The culture was filtered through a Whatman 0.02 mm Anodisc filter, stained with SYBR Green II. All the culture are incubated with the water sample from Lake Bogoria (Jul 2016). A: Negative control (*Arthrospira* culture without water sample), B: day first, C: day 19 of incubation and D: only Water sample. The rectangle represents a prokaryote; the ellipse represents VLPs. The scale bars indicate 10 μm .

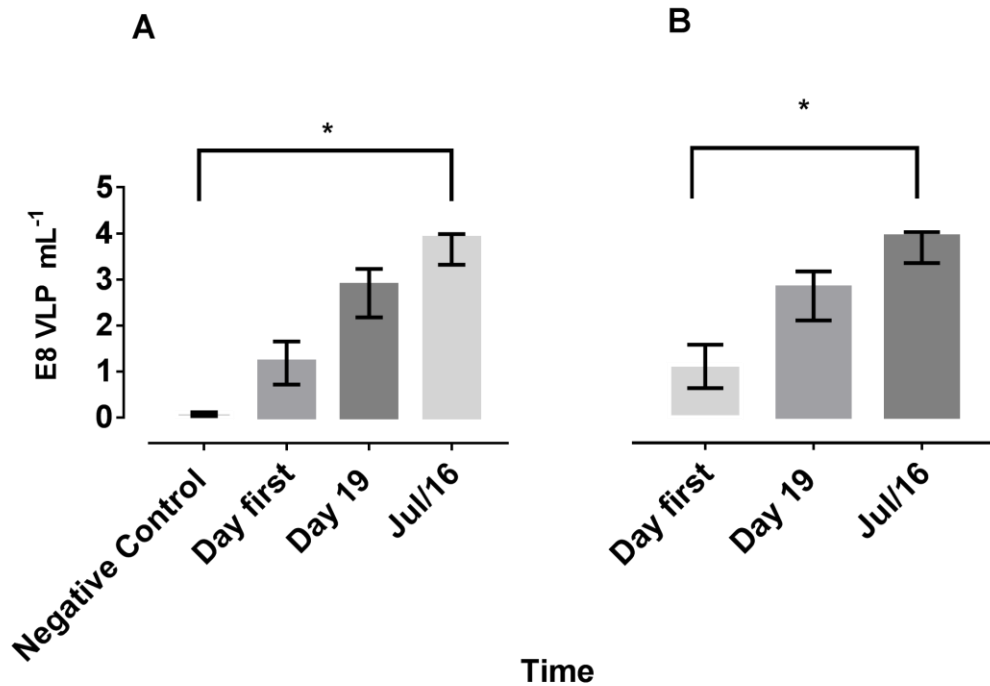


Figure 6.14: Comparison of median values of VLPs count between different S-morphotype *Arthrospira* cultures incubated with the Lake Bogoria water sample (Jul 2016).

(A) The comparison was with the negative control, (B) the comparison was with a negative control subtraction. Error bars represent 95% CI; * $p < 0.05$, $n = 3$.

Spearman's rank-order correlation to estimate the association between VLP counts using NanoSight and Epifluorescence microscopy revealed a monotonic relationship by visual inspection of a scatterplot. A strong positive association was found, $r_s = 0.728$ and $p = 0.026$ (Figure 6.15). Therefore, each method supported the other.

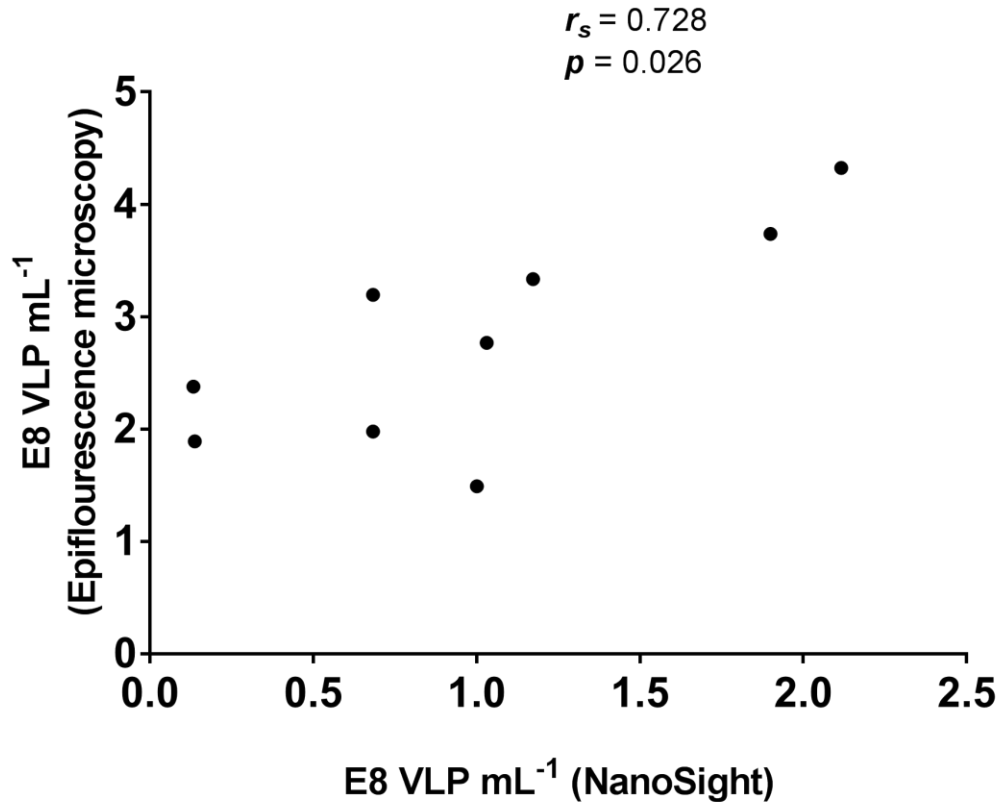


Figure 6.15: The correlation between the mean values of the E8 VLP mL⁻¹ by using two different techniques, NanoSight and Epifluorescence microscopy.

6.3.6 Protein profile of Lake Bogoria

The most predictable water sample from Jul 2016 that contained viruses (see section 6.3.2) analysed on SDS-PAGE showed four protein bands with sizes between 55 and 65 kDa on the gel (Figure 6.16). The sequenced data searched against known proteins in the Universal Protein Resource (UniPort) (The UniProt Consortium, 2017) database did not show a match. Moreover, MS/MS data searched against the metagenome data for four water samples achieved no hits.

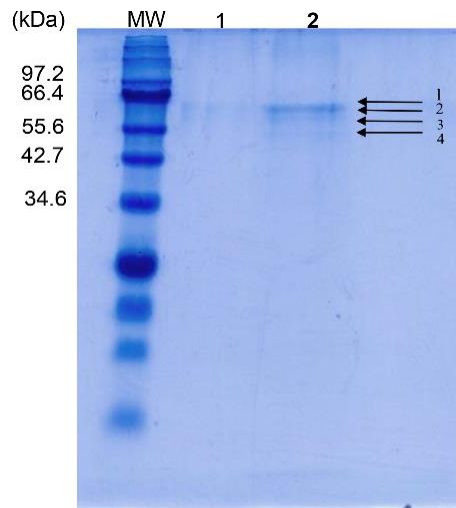


Figure 6.16: Protein profile of Lake Bogoria.

10% SDS PAGE gel stained with EZ-Run Protein Gel Staining solution shows the protein profile of Lake Bogoria. MW, protein molecular weight marker; Lane 1 a negative control; Lane 2 Lake Bogoria sample from Jul 2016, four protein bands were detected.

6.3.7 Metagenomics analysis

The results of the Illumina platform used to sequence the metagenome of four samples of the lake are shown in Table 6.8. Shotgun metagenomic analyses detected no phages with the MetaPhlan2 tool (Figures 6.17-6.20). No known cyanophages were detected. Two water samples, May 2015 and Sep 2015, contained eukaryotic viruses (Figures 6.18 and 6.20). The Sep 2014 water sample contained *Mycobacterium tuberculosis* (Figure 6.17). Two water samples (Sep 2014 and Jul 2015) contained 100% bacteria, whereas water samples from May and Sep 2015 contained 93.28% and 77.53% bacteria and 6.72% and 22.47 % viruses, respectively. The species comparison between the four water samples is displayed in Figure 6.21. For further details related to the species composition and the percentage of each species in total; Appendix 8.2, Tables 8.14 – 8.19.

Table 6.8: Illumina sequencing results for four metagenomics of Lake Bogoria water samples.

Sample name	Number of reads in R.fastq file	Number of reads in F.fastq file	DNA genome length(base)
Sep 2014	96297.8	96238.2	11494130
May 2015	417510	405951	153474149
Jul 2015	598191	575718	197518794
Sep 2015	463476	458781	169214683

The sequencing data is paired end and saved as F and R fastq files for each sample.

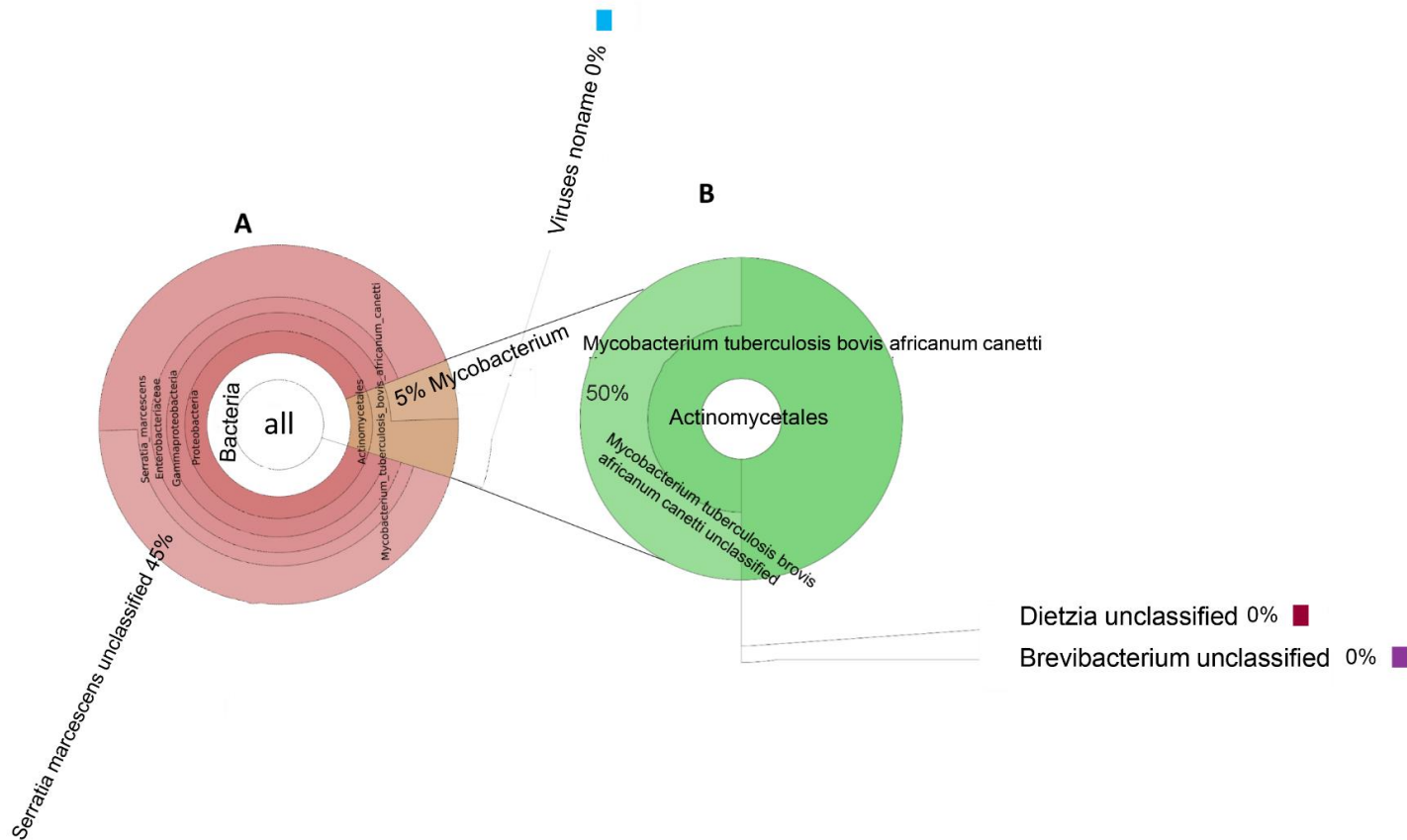


Figure 6.17: Taxonomic spectrum of metagenome reads for Sep 2014 water sample visualised with Krona.

The MetaPhlan2 result was imported into the Krona visualization tool. Circles represent taxonomic classifications. The inner circles represent higher taxonomic ranks, while more taxonomic detailed ranks (up to the species level) are presented in the outer circles. Less abundant taxa are listed outside the charts together with their relative abundances. The abundances of the taxonomic groups correspond to the percentage of spectra based on a total number of 200 spectra (A). Circle B represents Actinobacteriales order, which contributes 11% to the total.

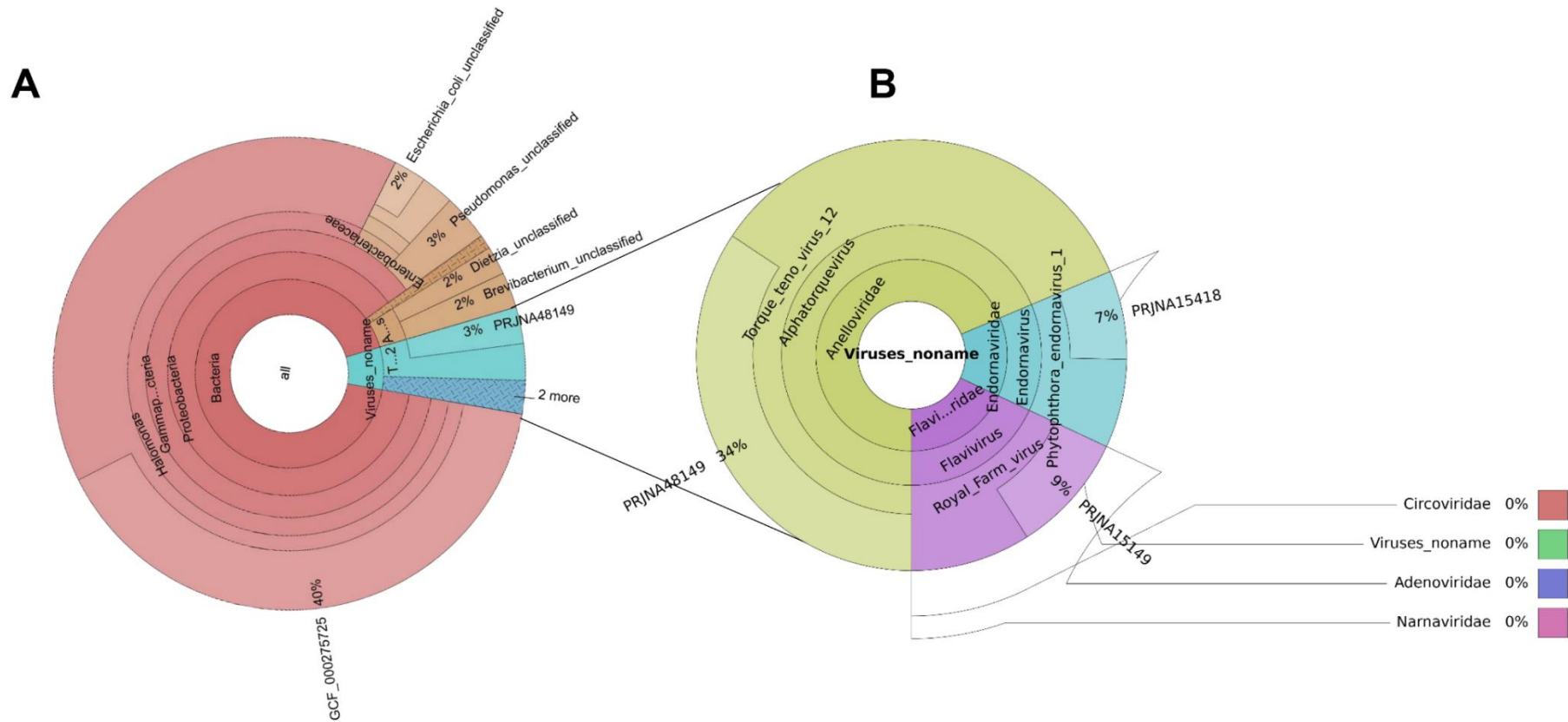


Figure 6.18: Krona Classification plot of metagenome data of May 2015 water sample.

The MetaPhlan2 result was imported into the Krona visualization tool. Circles represent taxonomic classifications. The inner circles represent higher taxonomic ranks, while more taxonomic detailed ranks (up to the species level) are presented in the outer circles. Less abundant taxa are listed outside the charts together with their relative abundances. The abundances of the taxonomic groups correspond to the percentage of spectra based on a total number of 184.2371 spectra (A). Circle B represents viruses' composition, which contributes 7% of the total.

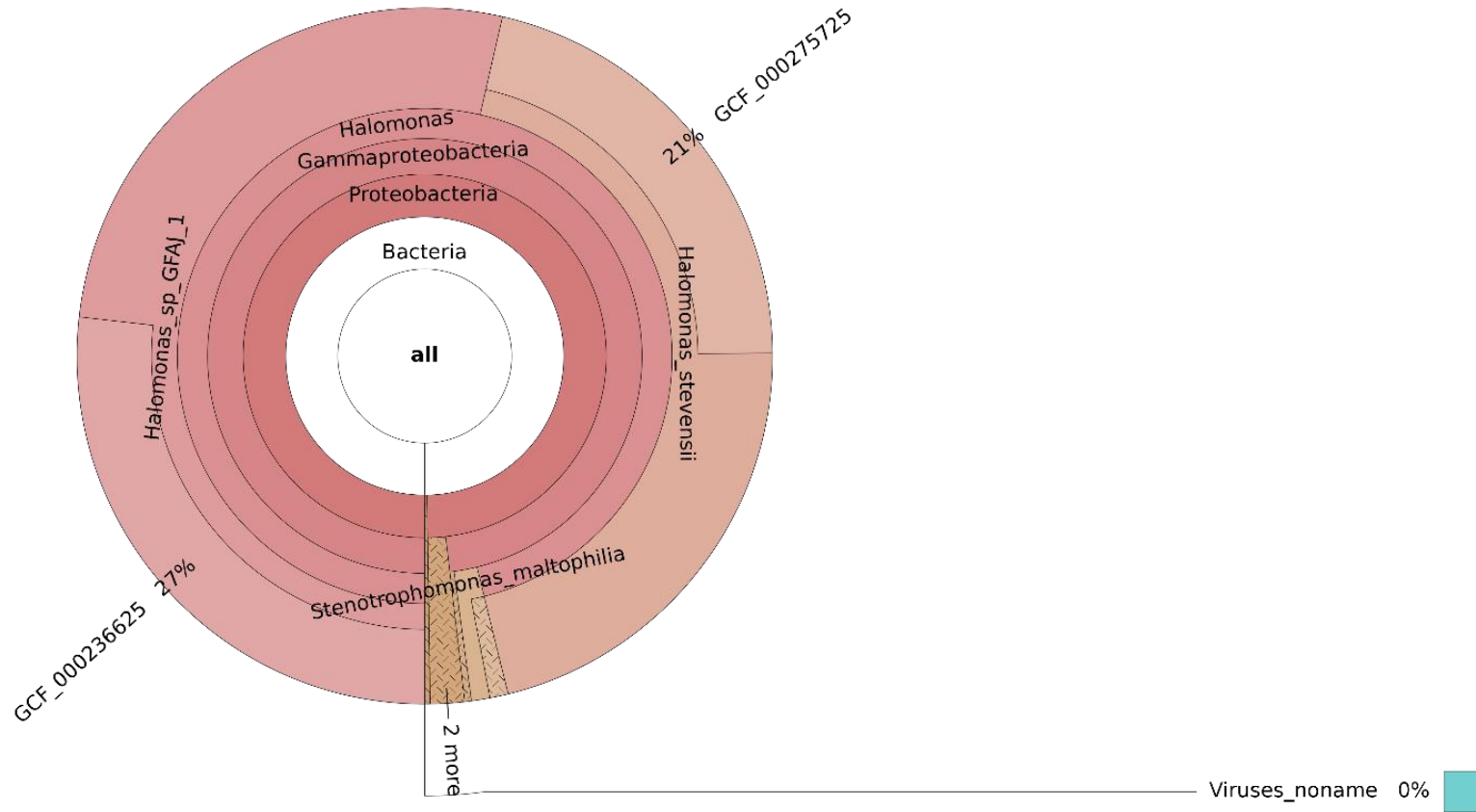


Figure 6.19: Krona Classification plot of metagenome data of Jul 2015 water sample.

The MetaPhlan2 result was imported into the Krona visualization tool. Circles represent taxonomic classifications. The inner circles represent higher taxonomic ranks, while more taxonomic detailed ranks (up to the species level) are presented in the outer circles. Less abundant taxa are listed outside the charts together with their relative abundances. The abundances of the taxonomic groups correspond to the percentage of spectra based on a total number of 197.15732 spectra.

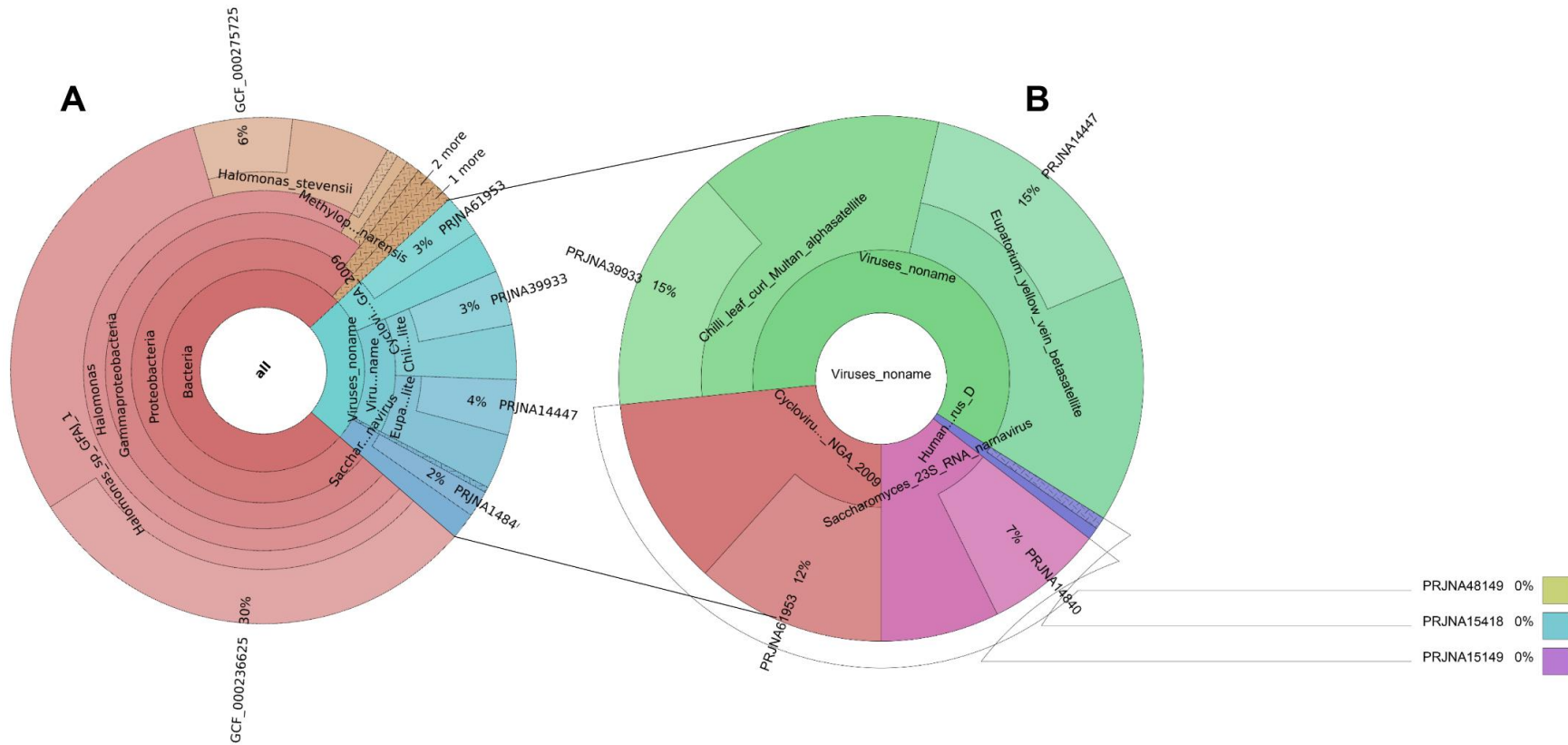


Figure 6.20: Taxonomic spectrum of metagenome reads for Sep 2015 water sample visualized with Krona.

The MetaPhlan2 result was imported into the Krona visualization tool. Circles represent taxonomic classifications. The inner circles represent higher taxonomic ranks, while more taxonomic detailed ranks (up to the species level) are presented in the outer circles. Less abundant taxa are listed outside the charts together with their relative abundances. The abundances of the taxonomic groups correspond to the percentage of spectra based on a total number of 193.64757 spectra (A). Circle B represents viruses 'composition, which contributes 23% to the total

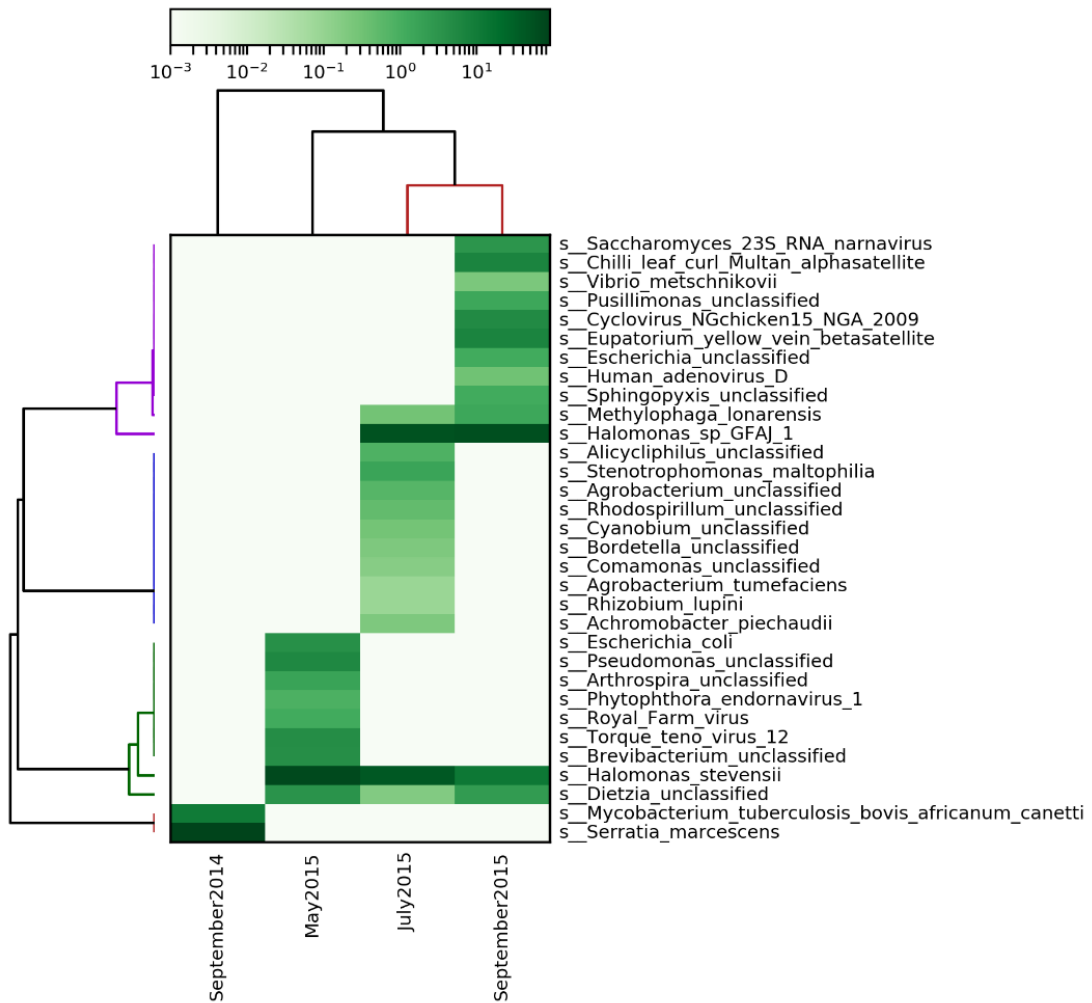


Figure 6.21: Heatmap comparison of the species abundance between four metagenomics samples.

The species assemblage is on the y-axis and the time collection on the x-axis. The relative abundance of each species is indicated by a green-coloured gradient; dark green (high abundance) and light green (low abundance), as indicated in the colour key at the top of the figure.

6.3.8 Prophage identification

The results of the PHASTER software revealed the presence of only three incomplete prophages within *Arthrospira* genomes from Lake Bogoria. One was integrated into the H-morphotype and two into the S-morphotype genome (Table 6.9).

The prophage of H-morphotype consisted of eight hypothetical proteins, one plate protein and two phage-like-proteins (Figure 6.22). The first incomplete

prophage within S-morphotype includes six hypothetical proteins, one plate protein, one coat protein, one phage-like particle and one tail shaft, while the second prophage contained nine hypothetical proteins, one plate protein and two phage-like proteins (Figure 6.23 and 6.24). More details are given in Appendix 8.2, Figure 8.11-8.13.

Table 6.9: Total prophages detected within two *Arthrospira* genomes of Lake Bogoria using the PHASTER tool.

<i>Arthrospira</i> morphotype	Region	Region Length	Completeness	Score	Total Protein	Region Position	Most Common Phage	GC%
H	1	9.8 kb	Incomplete	20	11	1162444-1172329	PHAGE_Salmon_SJ46_NC_031129(4)	42.45%
S	1	13.8kb	Incomplete	40	10	8010004-814810	PHAGE_Citrob_Margaery_NC_028755(5)	40.52%
S	2	9.5kb	Incomplete	20	12	225615-235129	PHAGE_Salmon_SJ46_NC_031129(4)	41.91%

One incomplete prophage region was identified within the H-morphotype and two incomplete prophages (score < 70) have been identified within the S-morphotype.

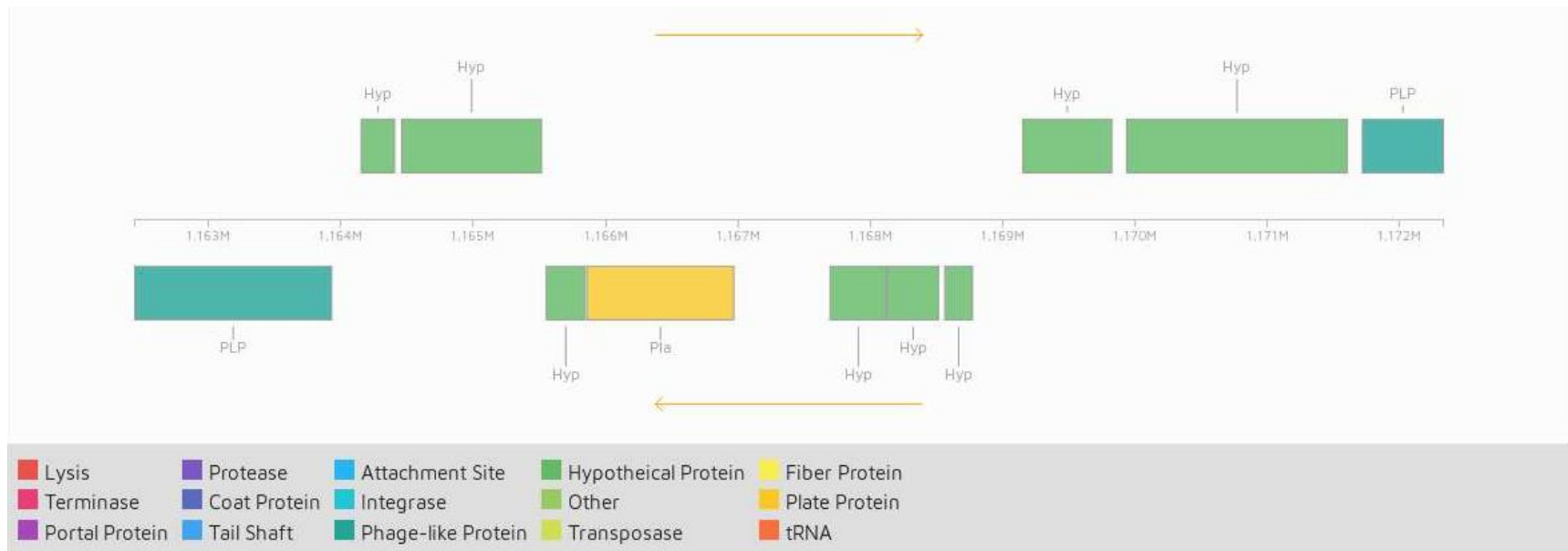


Figure 6.22: Linear genome view of the incomplete prophage integrated within H-morphotype genome of *Arthrospira* from Lake Bogoria.

The colours indicate the functions of the genes. Yellow arrows represent the forward and reverse.

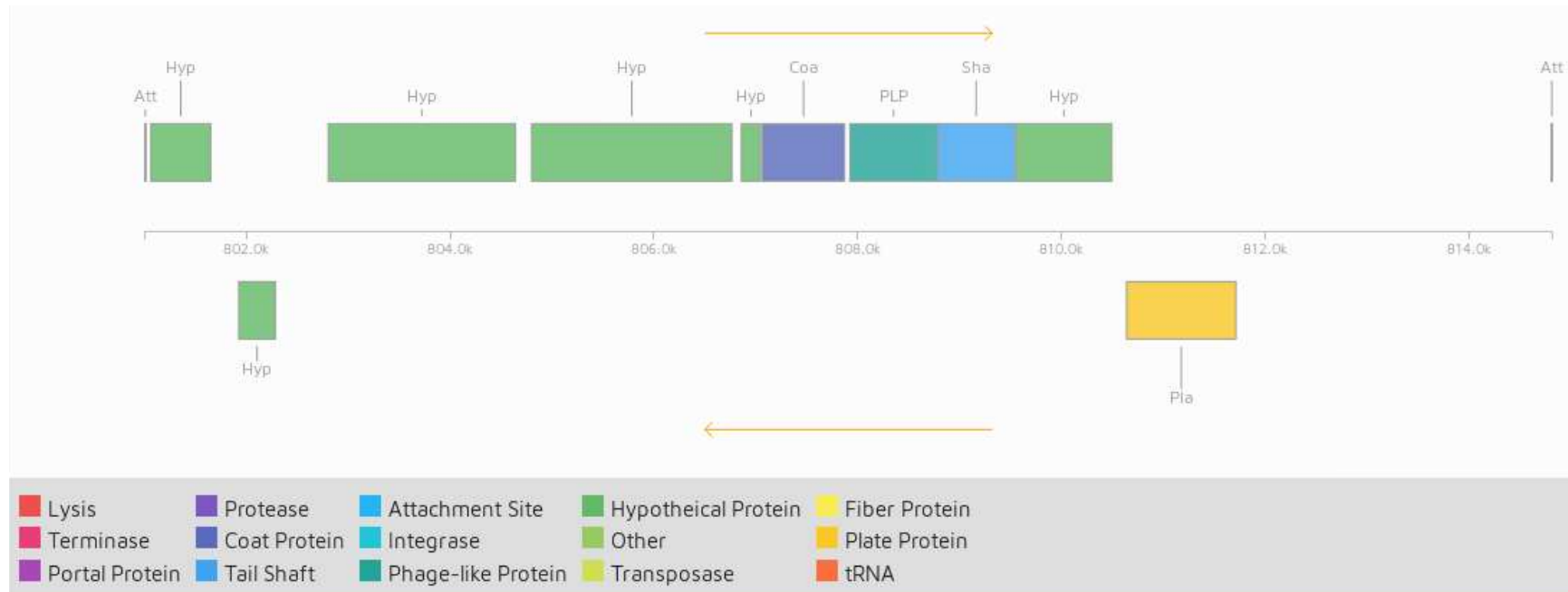


Figure 6.23: Linear genome view of the first incomplete prophage integrated within the S-morphotype genome of *Arthrospira* from Lake Bogoria.

The colours indicate the functions of the genes. Yellow arrows represent the forward and reverse. Att indicates attachment gene.

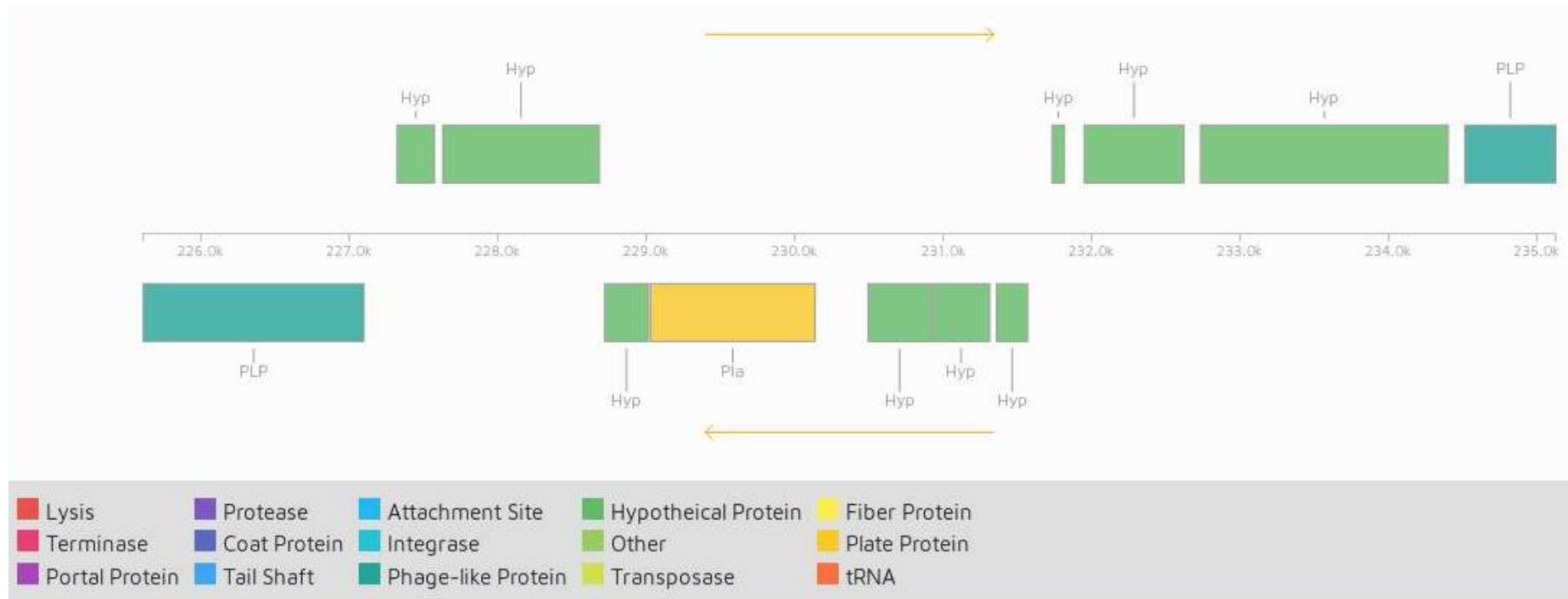


Figure 6.24: Linear genome view of the second incomplete prophage found in the S-morphotype genome of the *Arthrospira* from Lake Bogoria.

The colours indicate the functions of the genes. Yellow arrows represent the forward and reverse.

6.3.9 CRISPR identification

A total of 22 CRISPRs were identified in each, 5 confirmed and 17 questionable. Features such as, the start position, end position, length, direct repeat (DR) consensus, DR length and number of spacers of the confirmed CRISPR for both morphotypes are shown in tables 6.10 and 6.11, respectively. Their number in both morphotypes was identical to *A. platensis* C1, but fewer than in all other *Arthrospira* strains (Table 6.12). Unfortunately, the regions between CRISPRs and metagenomics data did not match any known phages in the database (Table 6.13). Moreover, there were no hits found between these CRISPRs and previous metagenomics data of Clough (2015).

Table 6.10: Details of identified CRISPRs in the H-morphotype of *Arthrospira* genome from Lake Bogoria.

CRISPR feature	First CRISPR	Second CRISPR	Third CRISPR	Fourth CRISPR	Fifth CRISPR
Start position	30309	434173	677159	682121	22145
End position	30562	436296	677496	683037	23915
Length (base)	253	2123	337	916	1770
DR consensus	ATTCACGCAAC CTGCACCGGG GC	GTTTCCGTCCCC TGACGGGGAATT GGTAGGGTTGGA C	CTTTAAACTTCTCTG AAAGTTAAACGTAT GGAAAC	CTTTAAACTTCTT TGAAAGTTAAAC GTATGGAAAC	GTCCAACCCTACCA ATTCCCCGTCAGGG GACGGAAAC
DR length	23	37	35	35	37
Number of spacers	4	26	4	12	22

Table 6.11: Details of identified CRISPRs in S-morphotype of the *Arthrospira* genome from Lake Bogoria.

CRISPR feature	First CRISPR	Second CRISPR	Third CRISPR	Fourth CRISPR	Fifth CRISPR
Start position	840061	845023	3781096	3854177	638654
End position	840398	845865	3782721	3856954	641541
Length (base)	337	842	1625	2777	2887
DR consensus	CTTTAAACTTCTCTGA AAGTTAAACGTATGG AAAC	CTTTAAACTTCT TTGAAAGTAAA CGTATGGAAAC	GTTTCCGTCCC CTGACGGGGAA TTGGTAGGGTT GGAC	GTCCAACCCTAC CAATTCCCCGTC AGGGGACGGAA AC	GTCCAACCCTAC CAATTCCCCGTC AGGGGACGGAA AC
DR length	35	35	37	37	37
Number of spacers	4	11	20	34	36

Table 6.12: Comparison of number of CRISPR arrays between *Arthrospira* strains.

Genome property	Number of CRISPR arrays
<i>Arthrospira</i> sp. PCC 8005	7
<i>Arthrospira</i> sp. TJSD091	8
<i>A. maxima</i> CS-328	9
<i>A. platensis</i> NIES-39	9
<i>A. platensis</i> YZ	6
<i>A. platensis</i> str. Paraca	6
<i>A. platensis</i> C1	5
<i>Arthrospira</i> Bogoria H	5
<i>Arthrospira</i> Bogoria S	5

Arthrospira isolates from Lake Bogoria, H and S morphotypes were coloured green and blue respectively.

Table 6.13: Features of matching regions between the CRSPIRs of the two *Arthrospira* morphotypes (H and S) and metagenomic data of four samples – Sep 2014, May 2015, Jul 2015 and Sep 2015.

CRISPR vs metagenome matching region	E value	Score (Bits)	Length (base)	Identity (%)	Description
CRISPR1 vs Sep14	6e-38	138	278	78	1- <i>Arthrospira</i> sp.TJSD092 2- <i>Arthrospira</i> sp. PCC 8005
(H-morphotype) CRISPR1 vs May15	/	/	/	/	/
(H-morphotype) CRISPR1 vs Jul15	/	/	/	/	/
(H-morphotype) CRISPR1 vs Sep15	/	/	/	/	/
(H-morphotype) CRISPR2 vs Sep14	/	/	/	/	/
(H-morphotype) CRISPR2 vs May15	8e-17	91.6	288	76	1- <i>Arthrospira</i> sp.TJSD092 2- <i>Arthrospira</i> sp. PCC 8005
(H-morphotype) CRISPR2 vs Jul15	/	/	/	/	/
(H-morphotype) CRISPR2 vs Sep15	/	/	/	/	/
(H-morphotype) CRISPR3 vs Sep14	6e-27	121	278	76	1- <i>Arthrospira</i> sp.TJSD092 2- <i>Arthrospira</i> sp. PCC 8005
(H-morphotype) CRISPR3 vs May15	/	/	/	/	/
(H-morphotype) CRISPR3 vs Jul15	/	/	/	/	/
(H-morphotype) CRISPR3 vs Sep15	/	/	/	/	/
(H-morphotype) CRISPR4 vs Sep14	/	/	/	/	/
(H-morphotype) CRISPR4 vs May15	/	/	/	/	/
(H-morphotype) CRISPR4 vs Jul15	/	/	/	/	/
(H-morphotype) CRISPR4 vs Sep15	/	/	/	/	/
(H-morphotype) CRISPR5 vs Sep14	2e-27	122	278	76	1- <i>Arthrospira</i> sp.TJSD092 2- <i>Arthrospira</i> sp.PCC 8005
(H-morphotype) CRISPR5 vs May15	4e-14	82.4	288	75	1- <i>Arthrospira</i> sp.TJSD092 2- <i>Arthrospira</i> sp.PCC 8005
(H-morphotype) CRISPR5 vs Jul15	/	/	/	/	/
(H-morphotype) CRISPR5 vs Sep15	/	/	/	/	/
(S-morphotype) CRISPR1 vs Sep14	/	/	/	/	/
(S-morphotype) CRISPR1 vs May15	/	/	/	/	/
(S-morphotype) CRISPR1 vs Jul15	/	/	/	/	/
(S-morphotype) CRISPR1 vs Sep15	/	/	/	/	/
(S-morphotype) CRISPR2 vs Sep14	/	/	/	/	/

Continued on next page.

Table 6.13 continued from previous page.

CRISPR vs metagenome matching region	E value	Score (Bits)	Length (base)	Identities (%)	Description
(S-morphotype) CRISPR2 vs May15	/	/	/	/	/
(S-morphotype) CRISPR2 vs Jul15	/	/	/	/	/
(S-morphotype) CRISPR2 vs Sep15	/	/	/	/	/
(S-morphotype) CRISPR3 vs Sep14	6e-27	121	278	76	1- <i>Arthrospira</i> sp.TJSD092 2- <i>Arthrospira</i> sp.PCC 8005
(S-morphotype) CRISPR3 vs May15	5e-13	78.7	288	78	1- <i>Arthrospira</i> sp.TJSD092 2- <i>Arthrospira</i> sp.PCC 8005
(S-morphotype) CRISPR3 vs Jul15					
(S-morphotype) CRISPR3 vs Sep15					
(S-morphotype) CRISPR4 vs Sep14	1e-25	117	278	75	1- <i>Arthrospira</i> sp.TJSD092 2- <i>Arthrospira</i> sp.PCC 8005
(S-morphotype) CRISPR4 vs May15	8e-18	95.3	288	82	1- <i>Arthrospira</i> sp.TJSD092 2- <i>Arthrospira</i> sp.PCC 8005
(S-morphotype) CRISPR4 vs Jul15	/	/	/	/	/
(S-morphotype) CRISPR4 vs Sep15	/	/	/	/	/
(S-morphotype) CRISPR5 vs Sep14	1e-30	134	278	77	1- <i>Arthrospira</i> sp.TJSD092 2- <i>Arthrospira</i> sp.PCC 8005
(S-morphotype) CRISPR5 vs May15	1e-16	91.6	288	80	1- <i>Arthrospira</i> sp.TJSD092
	5e-10	69.4			2- <i>Arthrospira</i> sp.PCC 8005
(S-morphotype) CRISPR5 vs Jul15	7e-10	69.4	426	89	/
(S-morphotype) CRISPR5 vs Sep15	/	/	/	/	/

/ = no matching.

6.3.10 Microzooplankton and *Arthrospira*

Protozoan cells (*Amoeba* sp.) were found in the sections of the filaments of the Dec 2016 sample (Figure 6.25). Surprisingly, *Arthrospira* was found within the *Amoeba* sp. cell (Figure 6.26).

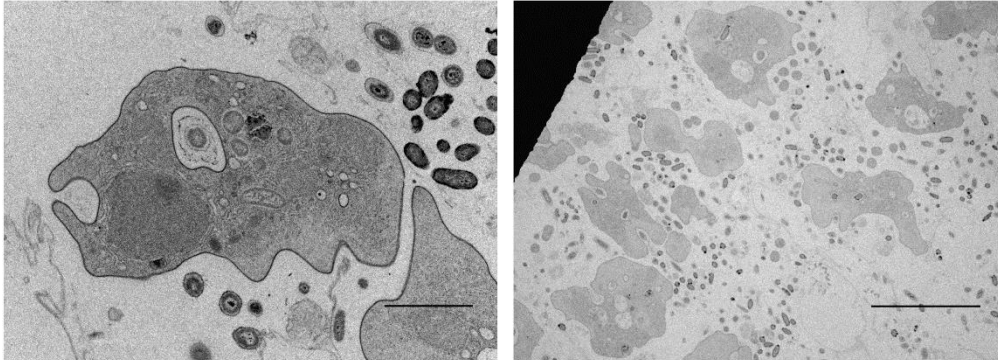


Figure 6.25: Electron micrographs of Lake Bogoria sample (Dec 2016).

Images are illustrating the presence of the amoeba cells. Bars represent 5 left and 10 μm right.

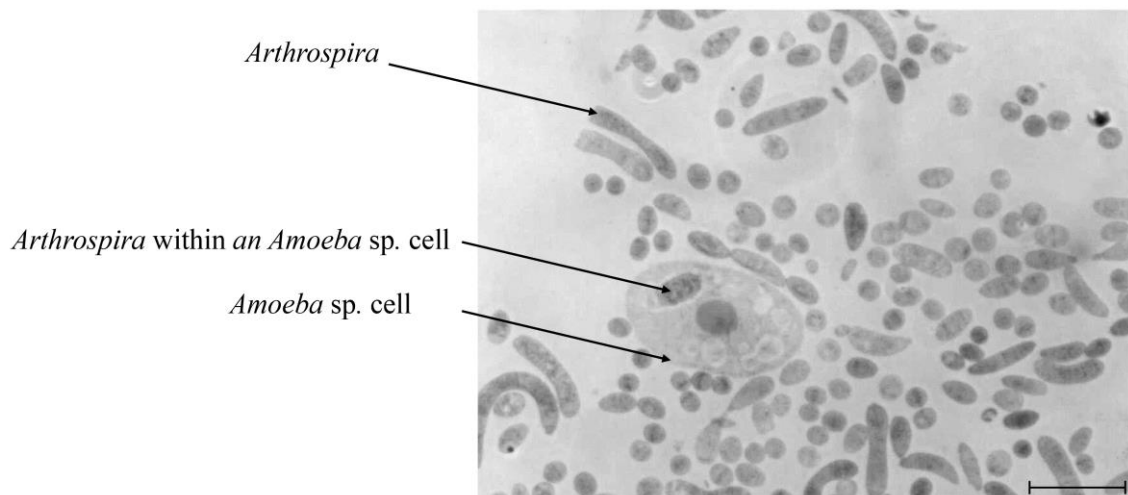


Figure 6.26: Micrograph of *Arthrospira* sections from Lake Bogoria (Dec 2016).

The image illustrating the presence of *Arthrospira* within the amoeba cell. The bar presents 50 μm .

6.4 Discussion

The aim of this chapter was to extend the earlier work of Peduzzi et al. (2014), by further investigating the hypothesis that cyanophage infections could be a controlling factor in the *Arthrospira* spp. population in EASLs. They tested this hypothesis at one of the Kenyan amplifier soda lakes, Lake Nakuru. The current study investigated the possibility of an occurrence of viral infections at another Kenyan soda lake, Lake Bogoria.

Cell lysis is a major cause of phytoplankton decline (Van Boekel *et al.*, 1992, Brussaard *et al.*, 1995). I observed cell lysis, as filament fragmentation occurred at an OD₅₆₀ nm of 0.3. These symptoms appeared within five days of incubation but only with the S-morphotype. The other two morphotypes (H and C) showed no signs of infection, even after a month of incubation. The symptom of host lysis, meaning the fragmentation of the cyanobacterium trichome into small, visible fragments, has been noted with other viral infections of other filamentous cyanobacteria. Pollard and Young (2010) showed that when *C. raciborskii* were incubated with natural VLPs from Australian freshwater lakes, the trichomes of the cells were cut into small, viable fragments. Moreover, Simis *et al.* (2007) found that changes in the optical signatures of cyanobacterium *Leptolyngbya boryana*, could be attributed to the fragmentation of the filaments as blooms broke down with cyanophage LPP-1 infection and lysis. This mechanism of filamentous host lysis by viral infection provides an insight that may help us to understand the process of cyanobacterium spread in aquatic systems.

The current study found further confirmation of the condition required for viral infection through the enumeration of VLPs using the NanoSight technique. The highest (and significantly different) numbers of these particles were after five days of incubation ($Mdn = 11.65 \times 10^8$). This suggests that this might be a chronic infection, where the new phages are liberated from the infected host cell without lysis of the host (Mann and Clokie, 2012). The results presented here are significant in at least two major respects; first, if the cell lysis of *Arthrospira* filaments occurred because of cyanophage infection, it is the first time where viral infection of *Arthrospira* from EASLs has been observed in the laboratory.

Second, a potential viral infection is thus more likely to occur during the first week of incubation at approximately an OD₅₆₀ of 0.3.

The enumeration of VLPs using the NanoSight tool was positively correlated with the enumeration carried out with epifluorescence microscopy ($r_s = 0.728$), confirming NanoSight as a useful instrument under different conditions. Moreover, this finding has important implications for developing the nanoparticle investigation tools and this would enhance their validity and credibility.

The relationship between the VLP count and limnological features of Lake Bogoria was investigated. There was an interesting negative correlation between VLPs count and the biological parameter of the lake, (Ch-a using acetone extraction), $r_s = -0.629$, $p < 0.001$. This result further supports the idea of phage infection.

Even though the TEM results showed a difference in virus numbers between the control and incubated cultures, these results must be interpreted with caution. Firstly, cyanobacterium cultures were not axenic, and secondly, there are several factors in addition to viruses that could lead to cyanobacterial cell lysis including bacteria (Shilo, 1967, Gumbo *et al.*, 2008), volatile organic compounds ((Ozaki *et al.*, 2008), fungi (Redhead and Wright, 1980), light (Miyake *et al.*, 2014) nutrients, and hydrologic conditions (Paerl, 2008). Therefore, any one of these mentioned factors could explain the single observed cell lysis.

Using flow cytometry, host-range and TEM, Jacquet *et al.* (2013) reported a cyanopodovirus that infected the *A. platensis* that inhabits pools in the south of France. However, the authors did not take into account the purity of the culture due to contaminants, which is the main condition in phage infection investigation protocols such as phage induction. The authors state that “*A. platensis* grew in outdoor and under glass pools inside” and contamination was not accounted for. Nevertheless, their results are somewhat in agreement with my findings; although phage induction was carried out with caution, results remained similar, where the number of viruses found using TEM did not differ between the control cultures, and all the induced cultures with different

Mitomycin C concentrations (data not shown). Kaggwa *et al.* (2013a) and Schagerl *et al.* (2015) reported that *Arthrospira* is susceptible to cyanophages in Lakes Bogoria and Nakuru, but are not able to control *Arthrospira* biomass. Their evidence was meagre; they referred to the use of electron microscopy in order to verify the viral infection but did not display any image to confirm that and their conclusion was only based on the count of infected cells as a viral infection.

No complete prophage sequences were identified in either of the *Arthrospira* genomes. This is a similar result to that of Lefort *et al.* (2014), who found no complete prophage within *A. platensis* str. Paraca. The most likely reason for these negative results is that the available database does not contain enough virus genomes at present.

During my study period, a decrease in the *Arthrospira* population was seen, leading to a collapse at Jul 2016. This crash was accompanied by strange particles visible within *Arthrospira* sections. At the same time, the concentration of nanoparticles increased considerably. Even though these particles were found only once in all samples, their shape indicates that they were most likely cyanophages, positive-sense single-stranded RNA virus ((+)ssRNA virus) through comparison with the virus taxonomy (van Regenmortel *et al.*, 2000). Their geometries, icosahedral and spherical and size (18-25 nm) resemble viruses belonging to the *Leviviridae* family that infect *Enterobacteria*, *Caulobacter*, *Pseudomonas*, and *Acinetobacter*. Peduzzi *et al.* (2014) detected similar particles within *Arthrospira* from Lake Nakuru under TEM (about 117 km south of Lake Bogoria (<http://alldistancebetween.com/in/distance-between/lake-nakuru-lake-bogoria-ec1706df239ec59ee7d340b32b76f358/>)). They counted the viruses using an epifluorescence microscope and found that the frequency of visibly infected cells between Jun and Sept 2009 was high. In general, these results are consistent with my results in terms of the time of the *Arthrospira* breakdown, thus suggesting that the particles found within the *Arthrospira* sections are phages and that there could be a seasonality in viral infection. However, before deciding the identity of these particles, we should once again

consider the anatomy and structure of *Arthrospira* from Lake Bogoria (Chapter 4) for the following reasons.

- 1- When these particles are anatomically compared to those found by Van Eykelenburg (1979) in terms of their distribution and size (18-25 nm), they could alternatively be internal structures, called phycobilisomes. They could appear and disappear according to the culture's nutritional condition (such as nitrogen concentration), salt stress (sodium concentration), photoinhibition (Blumwald *et al.* (1984) cited in Sili *et al.* (2012)), as well as the treatments to which the samples are subjected during preparation.
- 2- Peduzzi *et al.* (2014) considered these particles to be viral but did not refer to the ultrastructure composition of this cyanobacterium or compare their sizes. Viruses are the most dominant biological entities in aquatic systems (Suttle, 2007b), and whilst those counted by epifluorescence microscopy were considered to be *Arthrospira* viruses, they might have been heterotrophic.
- 3- Cell lysis that accompanies the viral infection is usually confirmed by the presence of VLPs inside the cell. For example, Van Hannen *et al.* (1999) reported that two freshwater cyanobacteria, *Limnothrix* spp. and *Prochlorothrix hollandica* from the shallow eutrophic lake, Loosdrecht (Netherlands) were almost completely lysed, with TEM images revealing VLPs within both cyanobacteria sections. This was accompanied by a significant increase in the number of viruses, which in turn led to the conclusion that the viral infection caused a breakdown of the filamentous cyanobacterial blooms. However, when the fragments of the S-morphotype (the only observed cell lysis) were analysed using TEM in my study, there were no symptoms of a viral infection within the sections.

Thus, these nanoparticles could thus be cyanophages infecting *Arthrospira* spp. based on their shape, distribution, damage to the thylakoids and the timing of their appearance, which coincided with the collapse of the *Arthrospira* population, despite the uncertainty over their identity, if my results are combined with the genetic findings.

Cyanophages are the most common component of the marine viral load (Rohwer *et al.*, 2009, Ghai *et al.*, 2010). In an aquatic ecosystem, both lysogenic and lytic phage life cycles are important. The abundance of the host is a crucial factor in phage infection (Weinbauer, 2004). The transition from the lysogenic to the lytic cycle requires certain inducing factors that depend on the environment of the host (Jiang and Paul, 1996). In the case of Lake Bogoria, the salinity level increased at the same time as the *Arthrospira* collapse in the middle of 2016; this could be the cause of phage induction. We did not collect data on UV exposure, but it might have played an important role during the calm period when the *Arthrospira* filaments flourish on the surface of the lake.

My epifluorescence microscopy revealed that there was an increase in the number of VLPs in the S-morphotype of *Arthrospira* cultures after incubation with Bogoria water samples for 19 days. Surprisingly, this difference was not statistically significant between the 1st and 19th day of incubation as had been expected. The first possible explanation for this might be because of the small sample size and the second is likely that the presence and increase in the VLPs could indicate a chronic infection. This latter explanation is also supported by the results of the phycocyanin intensity assay, as the symptoms of a lytic infection were not clearly shown as a severe reduction in the phycocyanin intensity in incubated cultures with water samples from the lake compared to the control.

Like other *Arthrospira* spp. genomes, the *Arthrospira* genome of Lake Bogoria contains several repetitive sequence regions that account for 9% of its genome (Cheevadhanarak *et al.*, 2012). These are considered as one of the most important factors for the failure of transformation in *Arthrospira* spp. (ibid). Genome comparisons between cyanobacteria demonstrated that these regions play an active role in the defence mechanisms of the members of this phylum against foreign DNA uptake. Five CRISPR arrays were detected in each *Arthrospira* genomes (H and S), but the matching regions of these genetic defence mechanisms, with the metagenome data of the lake samples did not match any known virus sequence in the database. The same results obtained from protein profile of the lake where the MS/MS data did not match any known protein in the database. The database is still limited, and does not contain an

extensive number of genomes and proteins. These negative results, therefore, need to be interpreted with caution. It does not mean that Lake Bogoria water is free from *Arthrospira* DNA viruses. This lack of available data, which combined by the scarcity of conducted research on viruses that may affect *Arthrospira* in general and in these particularly harsh environments, added more complexity and difficulty in reaching concrete and decisive results and showed the fact that they are just really hard to work with.

The analysis of phage diversity and his interaction with his host have developed rapidly after the molecular approaches have launched. Indeed, one of the most important of these approaches, which is metagenomics analysis, supports the idea of that phage infections enhance and maintain the diversity of their hosts (Rodriguez-Valera et al., 2009). Although the metagenomics data did not detect any cyanophages, the Sept 2014 water sample was found to contain the *M. tuberculosis* bacterium. This organism has been reported to be a causative agent of avian mycobacteriosis in lesser flamingos at Lakes Nakuru and Bogoria (Kaliner and Cooper, 1973, Cooper et al., 1975, Sileo et al., 1979, Kock et al., 1999). This confirms the continued presence of this opportunistic bacterium in water, thus enabling it to infect populations of *P. minor* when they become susceptible through stressors (Harper et al., 2016).

Natural enemies of unicellular cyanobacteria include both phages and protozoa (Mann and Clokie, 2012). For example, amoebic grazing has been shown to have an active role in controlling *Synechococcus* populations (Dillon and Parry, 2009). In addition, this grazer has an effect on the genetic structure of the cyanobacterium *Microcystis* (Van Wichelen et al., 2010). For filamentous species, this situation is still unclear and in this instance is likely to be more complex (Mann and Clokie, 2012). I have observed *Arthrospira* fragments inside *Amoeba* sp. for the 1st time in the alkaline soda lakes of Kenya. The first detection of the amoeba in Lake Bogoria was achieved by Walsh (2015) who genetically identified *Tetramitus ameobae* and an unknown free-living amoeba. The grazing role of this protozoan has been confirmed in other aquatic systems; for instance, Rogerson and Hauer (2002) showed that cyanobacterial and algal filaments were actively grazed by the amoebae in the Salton Sea in California.

Viruses are estimated to remove between 84% and 97% of potential cyanobacterial production, while microzooplankton are estimated to have the ability to remove between 90% and 99% of the potential unicellular cyanobacterial blooms (Tijdens *et al.*, 2008b). Therefore, it is possible to hypothesise that the appearance of this protozoan is likely to occur seasonally.

6.5 Conclusion and future work

This chapter tested the hypothesis that cyanophages responsible for *Arthrospira* die-off events in Lake Bogoria. My results suggest that, although there were VLPs inside the *Arthrospira* trichomes of Lake Bogoria, it was difficult to show that virus infection caused *Arthrospira* population crashes without isolating any phages and confirming their genetic identity. The increase of VLPs in the extracellular space without cell lysis may have increased the likelihood of a chronic infection. There is abundant room for further progress in investigating and determining the roles of viruses in trophic interactions and cascades in this raw and extreme environment.

Chapter 7 Overall discussion and recommendations

This research project has been the first attempt to thoroughly examine the role of cyanophages in regulating the *Arthrospira* spp. biomass in EASLs, and the first comprehensive investigation into the role of cyanophages in Lake Bogoria. The overall philosophy of my research was to address this knowledge gap by taking a holistic approach. This involved analysis of samples collected on a weekly basis for 23 months (May 2015 to Mar 2017) from Lake Bogoria, Kenya. The key limnological characteristics of the lake and their relationship with the *Arthrospira* biomass (Ch-*a* content), were measured and the identity of the *Arthrospira* species that inhabit Lake Bogoria analysed. I searched for evidence of viral infections of *Arthrospira* in this harsh environment and linked these to the lake's characteristics to establish the ideal conditions required for the occurrence of the potential cyanophage infection. Finally, I suggest opportunities for future work.

7.1 Key findings of the limnological features of Lake Bogoria and their relationship with the *Arthrospira* population

Arthrospira is the primary producer of Lake Bogoria; it has been suggested that it is present as a monoculture (Robinson, 2015). I used the Ch-*a* content as an indicator of the biomass of phytoplankton and thus the state of the lake. This study considered the variance of five key limnological properties of the lake, namely conductivity, pH, nutrients concentration (total N, and total P), salinity as well as Ch-*a* content. The Ch-*a* content was measured using a direct method (acetone extraction) and an indirect method (remote sensing) using a Chl-*a* retrieval algorithm. The latter had been successfully demonstrated by Tebbs *et al.* (2013) to monitor the primary producers of Lake Bogoria. Dr. Tebbs has kindly provided Ch-*a* content data obtained using her method for the period between 1999 and 2017.

Conductivity and salinity, both gradually increased, with average lake conductivity rising from 40.9 - 65.30 mS cm⁻¹. This remains quite low conductivity, compared to 5-15 years ago, when Harper *et al.* (2003) and

McCall (2010), observed 72 and 77 mS cm⁻¹ respectively, at lower lake levels. This change has occurred after the lake has received large amounts of rainfall since early 2010, leading to dilution. Conductivity decline had no effect on the pH level. This emphasises the fact that the lake water is well buffered against changes to other parameters (Harper *et al.*, 2003, Schagerl *et al.*, 2015).

The Ch-*a* concentration generally showed a significant decrease. The Ch-*a* of measured samples decreased from 334.6 µg L⁻¹ in Sept-Oct 2015 to less than 200 µg L⁻¹ at the end of the study. That estimated by remote sensing showed a gradual decrease of Ch-*a* over the last five years. The Chl-*a* content data using the first method was heterogeneous, even at identical collection time points; differences in phytoplankton content on the replicates filter papers had a significant effect on the results. The most likely explanation is that the *Arthrospira* migrates to the surface of the water, and therefore its horizontal distribution on surface and sub-surface is not homogenous. In the future, alternative and further developed methods could be used; for instance, continuous fluorometers, which have the advantage of being able to measure ^aCDOM and Chl-*a*, without the need for samples be collected.

The direct influx of freshwater from heavy rainfall 2010-15 had clear effects on the total N and total P concentrations. The two concentrations 1.49 mg L⁻¹ (total P) and 2.87 mg L⁻¹ (total N) were lower than previous records (Ballot *et al.*, 2004b). Nutrient input during heavy precipitation events has had no effect on the nutrient concentrations at the surface layers of the lake. This result can be explained by the stratification, as *Arthrospira* is a planktonic cyanobacterium, and therefore consumes surface nutrients. Consequently, the water dilution combined with the lack of mixing could have led to reduced nutrient concentrations.

Total N only had a slight linear relationship with Ch-*a*, explaining 14 % of the variance in Chl-*a*. Tebbs (2014) also was suggested very weak, only direct rainfall and lake height explaining 20% of the variance with Ch-*a*. These strengthen theories that bloom breakdowns in such extreme aquatic systems, are very likely to be due to biological agents (such as viruses) rather than environmental factors.

7.2 Phenotypic and genetic analyses of morphotypes.

The S-morphotype was the dominant morphotype, accounting for 47.67% of the entire *Arthrospira* population in the lake. This S-morphotype was able to withstand changes in environmental conditions such as pH. It can thus be suggested that the S-morphotype is the 'original' *Arthrospira* morphotype, and which has dominated the lake for an extended time. The other two morphotypes, C and H, are eco-morphotypes that have appeared because the *Arthrospira* has adapted to changes in the environmental conditions of the lake, as the lake undergoes changes to its properties, such as water levels, which may affect the morphology of the primary producers.

There was a good positive correlation found between remotely-sensed Chl-*a* and measured *Arthrospira* abundance over a one year period between Mar 2016 to Mar 2017, confirming that *Arthrospira* must be the main contributor to chlorophyll all over the lake.

There was no relationship between the lake's pH and the *Arthrospira* count for the C, S and H morphotypes, but a positive correlation between the total P and the abundance of all three *Arthrospira* morphotypes. Abundances of the C and H morphotypes were also significantly related to total N. A positive association were also found between the lake's salinity and abundance of the S and H morphotypes, however, none of the lake's properties could be used to predict *Arthrospira* abundance in Lake Bogoria. One can hypothesise that Lake Bogoria is not nutrient limited, and thus abiotic factors are far from responsible for bloom disruption events in the EASLs.

Members of the *Arthrospira* genus have the ability to change their morphology according to surrounding environmental and nutritional conditions, such as ultraviolet radiation (Wu *et al.*, 2005, Helbling *et al.*, 2006), salinity (Kebede, 1997), temperature (Gao *et al.*, 2008, Vonshak and Novoplansky, 2008) and pH (Current study). I found that the H and C morphotypes are behaviourally similar, neither motile and both change their morphology according to surrounding environmental conditions. The third morphotype (S-morphotype) is motile and stable *Arthrospira*. Four types of IV pilus genes (*pilQ*, *pilT-1*, *pilT-2* and *pilT-3*) were found in both S and H *Arthrospira* genomes. It is possible; therefore, that

these genes could have been suppressed by an environmental factor during the evolutionary history of the H-morphotype, or other factors may play a vital role in influencing the motility mechanism. Therefore, further research should be undertaken to investigate this mechanism.

The *Arthrospira* trichomes behaved differently after they were cultured in the laboratory for more than two years. The trichomes of the C and H morphotypes started to sink to the bottom of the flasks. The ultrastructure comparison between the three incubated morphotypes and the raw samples from the lake showed that gas vacuoles were present within the sections of the raw samples. Whereas they were absent within the C and H morphotypes, whilst they appeared to be present within the S-morphotype. A possible explanation is that, as Lake Bogoria is a stratified lake (Robinson, 2015), an aerobic organism such as *Arthrospira* will try to escape from the non-aerobic conditions in the deeper layers to the surface where light is available. In the laboratory setting, with the daily mixing of samples, light is available throughout the entire medium column, so there is no need to migrate towards the surface layers. This suggests that the *Arthrospira* in Bogoria are well-adapted cyanobacterial species. Once again, changes to the environmental factors would seem unlikely to cause bloom collapse.

The anatomical structure of the *Arthrospira* from Lake Bogoria was identical to the literature description of the *Arthrospira* anatomy except for a strange inclusion (see Figure 4.29). It was difficult to identify this inclusion, it appeared to be surrounded by a membrane, even though it should be impossible for a prokaryotic organism to have membrane organelle. Comparisons between the ultrastructure of the three morphotypes showed no differences. Accordingly, it was clear that any dependence on morphological features as a taxonomical tool to distinguish between different *Arthrospira* species would add even more complexity to the *Arthrospira* spp. nomenclature.

Phylogenetic analyses revealed that one of the *Arthrospira* strains in the NCBI database had been incorrectly classified, this being *A. platensis* C1. It would be better to revise its taxonomy to a different species other than *platensis*. Two Bogoria morphotypes were closely related to *A. maxima*-CS-328, whilst there

were two other unknown strains (*Arthrospira* sp. PCC 8005 and *Arthrospira* sp. TJSD091) and the incorrectly identified strain of *A. platensis* C1. It can thus be suggested that the *Arthrospira* species of Lake Bogoria are, firstly, more likely to be *A. maxima*. A second suggestion is that they are a species of *Arthrospira* that have not yet been recorded in the database as a whole genome (possibly *A. fusiformis*). Even though this question arose after answering several questions about the identity of the *Arthrospira* from Lake Bogoria, it also gave rise to other several questions that need further investigation to provide a satisfactory answer.

As detailed in chapter 4, the S-morphotype is the dominant morphotype within the lake, as was the fact that it also had the best genomic sequence assembly (four contigs). Therefore, it has been selected to represent the *Arthrospira* of Lake Bogoria. Rearrangement of its contigs by mapping them to the reference genome was successful. The genome was assembled into a chromosome of 6,459664 Mb, with the assigned name *Arthrospira maxima* var. *Bogoriensis*.

7.3 The role of cyanophage infection in the breakdown of *Arthrospira* spp. in Lake Bogoria.

As mentioned in Chapter 6, section 6.4, the evidence of Peduzzi *et al.* (2014) is limited; it is difficult to assert that the nanoparticles that they identified are viruses infecting *Arthrospira* unless they are supported by isolation and the identification of their genetic identity. My study used several techniques to investigate this potential viral infection.

The symptoms of phage infection were observed within 5 days of incubation, due to the appearance of filaments after fragmentation of the *Arthrospira* S-morphotype, very likely to be caused by viral infection. The fragmentation of the cyanobacterium trichome into small, visible fragments was an indicator of host cell lysis. These symptoms of viral infections have also been observed with other filamentous cyanobacteria. Pollard and Young (2010) showed that after incubating *C. raciborskii* cultures with virus-like particles (VLPs) from Lake Samsonvale (southeast Queensland, Australia), the host population reduced by 86% in only 5 days, whilst the number of VLPs increased gradually. Filament fragmentation was observed as cells were lysed.

The viral infection symptoms were observed only once during the study period, and with only one morphotype (S-morphotype), however, these results do suggest that viral infections may play a role in the spread of filamentous cyanobacteria in aquatic systems.

Further evidence that a potential phage infection could occur within five days of incubation comes from the counts of VLPs using the NanoSight instrument. Although during the period of study, the proposed viruses were not isolated; these results are nevertheless important in two respects. Firstly, if these VLPs are cyanophages that infect *Arthrospira*, this study would be the first to stipulate the ideal conditions that would be needed for this infection to occur. Secondly, the number of these VLPs increased without the occurrence of typical lytic infection symptoms, which represent lysis of the infected cells. This, in turn, would increase the likelihood that this infection is a chronic infection. The results of the phycocyanin intensity assay further support the idea of a chronic infection. The phycocyanin fluorescence of the incubated cultures with water samples from the lake did not show the same decrease as the phycocyanin fluorescence of the control, however, as would be expected to occur with a typical lytic infection.

Nanoparticles resembling phages were detected in the July 2016 sample sections. This detection was associated with the highest increase in the VLP count, during the Jul-Aug 2016 time point ($Mdn = 1.755 \times 10^8$ VLP mL⁻¹). The VLPs detected within the *Arthrospira* sections (consistent with Peduzzi *et al.* (2014)). However, confirming their identity as viruses, particularly as positive-sense ssRNA phages was difficult, and still needs considerable further investigation. This is because there is a possibility that these observations may just be the internal structures of the *Arthrospira*, called phycobilisomes (Van Eykelenburg, 1979). If these particles are viruses infecting *Arthrospira*, this study would be the first to provide any direct evidence of a cyanophage attack in an *Arthrospira*-dominated natural system. Again, this aspect needs a further in-depth study to fully understand the potential phage-host relationship.

During my study period, the relationship between the VLP count and limnological features showed an interesting negative correlation between the

VLP count, and Ch-a concentration measured using the acetone extraction method, with a weak positive correlation between VLP concentrations and pH, total P and salinity parameters. These results confirm that since the salinity of the lake had no effect on the Ch-a concentration, its effect on its phages would be slight or non-existent.

The difference in VLP counts between the control and incubated cultures with the Jul 2016 water sample was not statistically significant ($p > 0.05$), as determined using an epifluorescence microscope. This is because the small size appears to affect the results. Therefore, this work could be extended in the future by applying more data points to obtain results that are more precise. The two different methods that were used to count VLPs, the NanoSight technique and epifluorescence microscopy were positively correlated. This result provides strong support for the use of NanoSight technology as a tool for quantifying the size and concentration of viruses.

Cyanophage metagenomic results showed no hit with any in the NCBI database, as found for the mass spectrometry data (MS/MS). However, *M. tuberculosis* was detected in the sample of Sep 2014, which has been suggested to one of the factors causing lesser flamingo mortality events (Kaliner and Cooper, 1973, Cooper *et al.*, 1975, Sileo *et al.*, 1979, Kock *et al.*, 1999, Oaks *et al.*, 2006). The most likely reason for this result is that the database does not contain enough virus genomes at present.

The four genes that encode for T4P pilin proteins detected in the genomes of S and H morphotypes are involved in a natural competence of bacteria, by assisting the bacteria cell to take up the foreign DNA (Chen and Dubnau 2004). Hence, it is possible that the presence of these genes in the *Arthrospira* genomes of Lake Bogoria could increase the chance of the phage infection.

It is possible that the nanoparticles observed in *Arthrospira* sections along with the detection of nanoparticles from the July 2016 sample, were associated with the collapse of *Arthrospira* population. The presence of phycobilisomes provides an insight into the health status of the cyanobacteria, so the lack of

phycobilisomes indicates the loss of the phycocyanin pigment, which leads to the occurrence of phycocyanin bleaching. These nanoparticles are thus more likely to be a biological agent such as cyanophages that infect the *Arthrospira* spp. that inhabit EASLs, such as Lake Bogoria.

The greatest probability is that the cyanophages may be RNA viruses ((+) ssRNA virus), based on their size. A natural progression of this work would thus be to perform RNA sequencing, as this would provide definitive evidence as to whether these particles are phages that infect *Arthrospira*, or just natural inclusions of phycobilisomes. The comparison of the gene expression of these inclusions between the Jul 2016 sample and one that does not contain these phycobilisomes should be conducted, to establish the conditions that led to their disappearance.

The presence of *Arthrospira* fragments inside *Amoeba* sp. that were observed in the Dec 2016 sample shows the food chain between them. Rogerson and Hauer (2002) showed that there was a correlation between the distribution of the amoebae and *A. fusiformis* abundance in Lake Bogoria. The question that arises now is whether this protozoan plays an active, and vital role in controlling the *Arthrospira* spp. blooms in these lakes. This then raises the question; what are the conditions that help them to do so? All these questions and others need further research and scrutiny to provide any convincing scientific conclusions.

7.4 A summary of the evidence for cyanophage-caused collapse of blooms.

I have shown above that there is a minimal effect of environmental factors upon bloom dynamics, as *Arthrospira* are well-adapted cyanobacteria. I have also found limited evidence for grazing impact. I do, however, have evidence that the *Arthrospira* population, in July 2016, crashed through cyanophage infection. The evidence is as follows:-

- 1- This breakdown was associated with the spread of VLPs within the *Arthrospira*'s cells and the damage of thylakoids.
- 2- The increase of those nanoparticles was negatively correlated with Chl-a concentration throughout the study.

- 3- The highest increase in VLPs occurred during the first week of incubation with the most dominant morphotype (S-morphotype).

However, during the current study period, these potential viruses have not been isolated; therefore, their identity as viruses that infect *Arthrospira* spp. has not yet been confirmed. Overall, this study strengthens the idea that cyanophages could contribute dramatically to the *Arthrospira* population decline. Further in-depth investigations into the roles of viruses in trophic interactions and cascades in such aquatic systems is therefore needed.

7.5 A summary of this project's contribution to overall understanding of EASLs

The overall project story is shown in figure 7.1, in the context of studies upon our understanding of the alkaline-soda lake ecosystem of East Africa.

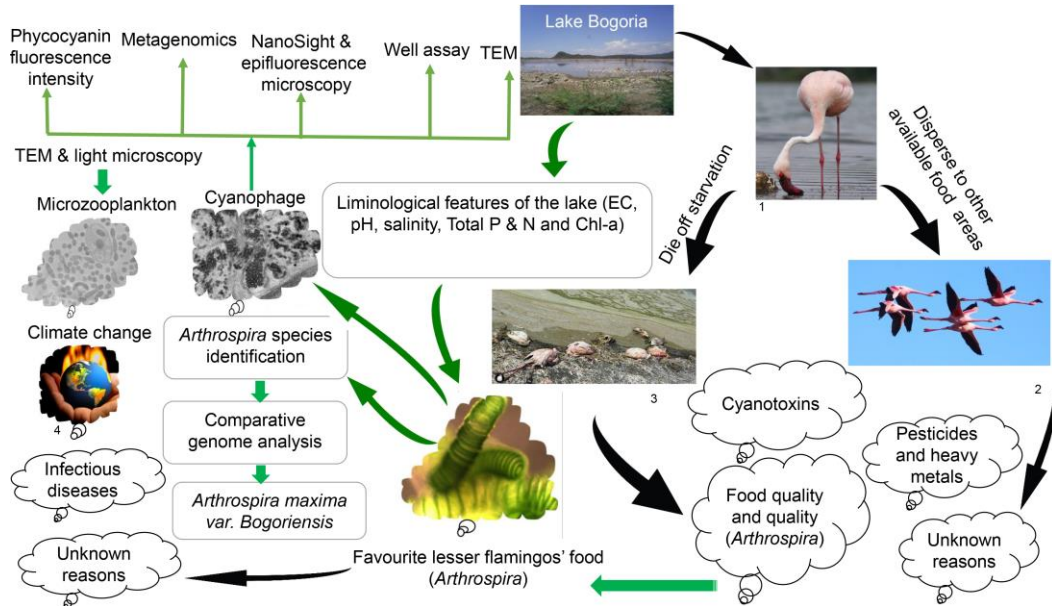


Figure 7.1: Schematic diagram of my research contribution to the overall lesser flamingo lakes ecosystem in East Africa.

Green arrows represent what have done during the current study. Images 1, 2, 3 and 4 taken from:

- 1- (Robinson, 2015), 2-<https://blog.nationalgeographic.org/2013/10/26/message-from-a-50-year-old-flamingo/>, 3- (Krienitz *et al.*, 2016b) and
- 4-<https://carolkobyradio.com/2016/10/24/market-based-approach-addressing-climate-change/>

7.6 Recommendations for Future Work

Each chapter contains future proposals based on the results obtained for that chapter. These suggestions are as follows:

- 1- Since the study site is a special environment and its characteristics distinguish it from other aquatic systems, as well as through my own experience, researchers should be personally present at the study site. This is because any changes that occur can then be closely observed and recorded as they happen. Therefore, with the next visit to this lake,

the mistakes made herein can be avoided, and how to deal with such circumstances can be developed.

- 2- Another important point would be to plan well before starting the sample collection. This can be achieved as follows:
 - a- The sample size should be large enough to be able to generalize any results obtained.
 - b- The sampling should cover the whole lake area (three basins), including different depths.
 - c- *Arthrospira* spp. trichomes are very fragile and can easily fragment under the influence of any physical pressures, even, for instance, grains of sand. Therefore, cyanobacterium filaments must be first carefully separated using sieves, as shown in chapter 4, and then preserved if required.
 - d- Samples should be sent out as soon as possible, or if not, some initial processing conducted at the study site itself, such as virus concentrations and measuring the physical properties of the lake.
 - e- As noted in chapter 3, the salinity of such water can be measured by either of two methods: the indirect method using Williams's equation, or the more direct by summing the total concentration of all cations and anions responsible for salinity (Na^+ , K^+ , Mg^{2+} , Ca^{2+} , Cl^- , HCO_3^- , CO_3^{2-} , and NO_2^-). This study used an indirect method due to the long storage time. However, it would be better and more accurate to use the direct method.

Chapter 8 Appendices

8.1 Appendix 1: Medium, Buffers and Solutions

8.1.1 Zarrouk's medium

1- Composition of salts

All chemical compositions of Zarrouk's medium were dissolved in one liter of water and then autoclaved as described in section 2.3.1.

NaHCO ₃	18.00 g
K ₂ HPO ₄	0.5g
NaNO ₃	2.5g
K ₂ SO ₄	1g
NaCl.....	1g
MgSO ₄ .7H ₂ O.....	0.2g
CaCl ₂ .6H ₂ O.....	0.06g
FeSO ₄ .7H ₂ O.....	0.01g
EDTA-Na ₂	0.08g

2- Trace elements solution

H ₃ BO ₃	2.86g
MnCl ₂	1.8g
ZnSO ₄ .7H ₂ O.....	0.22g
(NH ₄) ₆ Mo ₇ O ₂₄	0.018g
CuSO ₄ .5H ₂ O.....	0.08g
NiSO ₄ .7H ₂ O.....	0.049g

3- 0.6 % low strength cyanobacterial agar in 100 volume

Cyanobacteria agar.....0.6 g

Zarouk's medium.....100 mL

Autoclave, store at 55 °C.

4- Enriched cyanobacterial agar in 100 ml volume

Glucose.....1 g

Yeast extract.....0.3 g

Peptone.....0.5 g

Zarouk's medium.....to make up to 100 mL

Autoclave, store at 55 °C.

5- 3 % agar

Cyanobacterial agar.....3 g

Zarouk's medium.....to make up to 100 mL

Autoclave, store at 55 °C.

8.1.2 Solutions

1- 90% aqueous acetone solution

Acetone900 mL

Distilled water.....to make up to 1 L

2- Ultra-pure water (UPW)

Add a specific amount of Nano pure water in Duran bottle and then autoclave.

3- 0.1 N HCl

37.5% concentrated HCl8.1774 mL

Distilled water.....to make up to 1 L

Sterile by 0.2µm syringe filter.

4- Digestion reagent solution

Potassium sulfate (K ₂ SO ₄).....	134 g
Concentrated sulfuric acid (H ₂ SO ₄).....	134 mL
Copper (II) sulfate pentahydrate.....	11.4 g
Deionised water.....	to make up to 1 L

5- Phosphorus reagents

1- Colour reagent (10g/L ammonium molybdate, 0.3 g/L Sb-K-tartrate)

Stock ammonium molybdate solution	25 mL
Stock antimony potassium tartrate solution.....	10 mL
Deionised water.....	to make up to 100 mL
Stock ammonium molybdate reagent solution, 4% w/v	
Ammonium molybdate tetrahydrate.....	4 g
Deionised water.....	to make up to 100 mL
Stored at 4 °C, discard if its colour change to blue	
Stock antimony potassium tartrate solution, 3 g/L	
Antimony potassium tartrate.....	0.3 g
Deionised water.....	100 mL
Stored in a dark bottle at 4 °C.	

2- Ascorbic acid, 60 g/L

Ascorbic acid.....	6 g
Deionised water.....	to male 100 mL
Stored for 1 week at 4 °C, it should discard if the solution change to yellow.	

3- Working acid (with o-phosphate spike)

Sulfuric acid solution, 5 N.....	45 mL
Ortho-Phosphate spike.....	15 µL of 10000 ppm P
Deionised water.....	55 mL

6- Phosphorus standardStandard solution 10 mg P L⁻¹Stock standard solution (1000mgP L⁻¹).....10mL

Deionised water.....to make 100 mL

Stock standard solution (1000mg P L⁻¹)4.393g potassium dihydrogen orthophosphate (KH₂PO₄)

Deionised water.....to make up to 1 L

7- Nitrogen reagents**1- Buffer solution**

Stock buffer.....20 mL

Sodium potassium tartrate 10 % w/v50 mL

Sodium hydroxide 20% w/v.....15.5mL

Deionised water.....to make 100 mL

Sodium potassium tartrate, 10% w/v (pH7-8)

Sodium potassium tartrate tetrahydrate.....20 g

Sodium hydroxide.....~ 1 pellet

Sulfuric acid, 5 normal..... pH adjustment

Deionised water.....to make up to 200 mL

Stock buffer

Sodium phosphate. Dibasic heptahydrate.....13.4 g

Sodium hydroxide..... 2 g

Deionised water.....to make up to 100 mL

Sore at room temperature.

Sodium hydroxide, 20% w/v

Sodium hydroxide.....20 g

Deionised water.....100 mL

2- Sodium hypochlorite, (1.3% active chlorine, 1.25% NaCl (w/v))

Sodium hypochlorite (bleach), 6%.....20 mL

Deionised water.....make up to 100 mL

3- Salicylate/nitroferri-cn

Sodium salicylate, 150 g/L.....40 mL

Sodium nitroferricyanide, 30 g/L0.25 mL

Sodium salicylate, 150 g/L

Sodium salicylate.....15 g

Deionised water.....to make up to 100 mL

Discard if it becomes dark

Sodium nitroferricyanide, 30 g/L

Sodium nitroferricyanide dihydrate.....3 g

Deionised water.....to make up to 100 mL

Discard if it becomes blue-green.

8- Nitrogen standard solution

Ammonia-N stock standard solution (1000 mg N/L)

Ammonium chloride, anhydrous.....3.819 g

Sulfuric acid, 5 normalup to 3 mL

Deionised water.....to make up to 1 L

Store at 4 °C.

Sulfuric acid, 5 normal concentrated.....70 mL

Deionised water.....to make up to 500 mL

9- 5 M HCl in 100 ml volume

37% HCl.....41.05 mL

Autoclaved UPWto make up to 100mL

Sterile by 0.2µm syringe filter.

10- 5 M NaOH in 100 ml volume

NaOH pellets20 g

Autoclaved UPW.....to make up to 100 mL

Dissolve, Sterile by 0.2µm syringe filter.

11-Urea 60 mg/ L

Stock urea.....2.4 mL

Add to 25 mL of cyanobacterium culture

Stock Urea solution (100µg mL) in 3 ml volume

Urea.....300 µg

Autoclaved UPW3 mL

Dissolve, sterile by 0.2µm syringe filter.

12-100 mg/L Ammonium bicarbonate

Stock Ammonium bicarbonate solution......4 mL

Add to 25 mL of cyanobacterium culture

Stock Ammonium bicarbonate solution (100 $\mu\text{g mL}^{-1}$) in 5 ml volume
 Ammonium bicarbonate.....500 μg
 Autoclaved UPW5 mL
 Dissolve, sterile by 0.2 μm syringe filter.

13-Cycloheximide (20 $\mu\text{g mL}^{-1}$)

Stock cycloheximide2.5 mL
 Add to 25 ml of cyanobacterium culture
 Stock cycloheximide (200 $\mu\text{g mL}^{-1}$) in 5 ml volume
 cycloheximide.....1 mg
 DMSO.....5 mL
 Dissolve, sterile by 0.2 μm syringe filter.

14-ampicillin 61.6 $\mu\text{g/ml}$

Stock ampicillin.....1.54 mL
 Add to 25 ml of cyanobacterium culture
 Stock ampicillin solution (1000 $\mu\text{g mL}^{-1}$) in 2 ml volume
 Ampicillin.....2 mg
 Autoclaved UPW.....2 mL
 Dissolve, sterile by 0.2 μm syringe filter.

15-penicillin G 85.8 $\mu\text{g/ml}$

Stock penicillin G.....2.145 mL
 Add to 25 ml of cyanobacterium culture
 Stock penicillin G (1000 $\mu\text{g mL}^{-1}$) in 3 ml volume
 Penicillin G.....3 mg
 Autoclaved UPW.....3 mL
 Dissolve, sterile by 0.2 μm syringe filter.

16-Cefoxitin (76.6 $\mu\text{g/ml}$)

Stock cefoxitin.....1.915 g
 Add to 25 ml of cyanobacterium culture
 Stock cefoxitin solution (1000 $\mu\text{g mL}^{-1}$) in 3 ml volume
 Cefoxitin.....3 mg
 Autoclaved UPW.....3 mL
 Dissolve, sterile by 0.2 μm syringe filter.

17-Meropenem (38.9 $\mu\text{g/ml}$)

Stock meropenem solution.....0.9725 mL

Add to 25 ml of cyanobacterium culture

Stock meropenem solution (1000 µg mL⁻¹) in 3 ml volume

Meropenem.....3 mg

Autoclaved UPW.....3 mL

Dissolve, sterile by 0.2µm syringe filter.

18-Glycerol 50% in 20 ml volume

Glycerol 99+%10 mL

Zarouk's medium.....10 mL

Sterile by 0.2µm syringe filter.

19-DMSO 5, 10 and 30% in 10 ml volume

DMSO0.5, 1 and 3 mL

Zarouk's medium9.5, 9 and 7 mL

To get the required concentration each amount of DMSO was added to the corresponding amount of Zarouk's medium, sterile by 0.2µm syringe filter.

20-Methanol 10% in 10 ml volume

Methanol.....1mL

Zarouk's medium.....9 mL

Sterile by 0.2µm syringe filter.

21-Glutaraldehyde 2.5% in 25 ml volume

Glutaraldehyde 25%.....2.5 mL

Zarouk's medium.....to make up to 25 mL

Close the tube, store at 4 °C.

22- Modified 'Spurr'Formulation- Hard Mixture in 20 ml volume

ERL 4221.....8.2 g

ERL 736.....1.9 g

NSA.....11.8 g

DMAE.....0.2g

Firstly, mix the ERL, ERL and NSA for 5 minutes and then add DMAE, mix for additional 5 minutes.

23- 1 % uranyl acetate

Uranyl acetate 0.1 g

dH₂O.....to mke up to 10 mL

Dissolve Uranyl acetate in the dH₂O in the hood, and then filter it through 0.2µm syringe filter, aliquot into Eppendorf tubes and wrap with aluminium foil store at room temperature in the dark.

24-1% Osmium tetroxide/1.5 %potassium ferricyanide

Potassium ferricyanide.....0.03 g

Osmium tetroxide 2 %.....1 mL

Zarouk's medium.....1 mL

25- Ethanol 10, 30, 50, 70 and 90 % in 100 ml volume

Ethanol 99.5%.....10, 30, 50, 70 and 90 mL

Deionized water90, 70, 50, and 10 mL

Each required ethanol concentration was as mixture of each corresponding components.

26- CTAB 3%; NaCl 1.4 M; EDTA 20 mM; Tris-HCl 0.1 M, pH 8.0;

Sarkosyl 1% and Mercaptoethanol 1% in 100 ml volume.

CTAB.....3g

NaCl.....8.18g

EDTA.....0.74 g

Tris-HCl1.576 g

Sarkosyl1 mL

Mercaptoethanol1mL

Dissolve EDTA in 70 mL of UPW at pH 8 and then add the rest except Mercaptoethanol top up to 99 ml, autoclave, let to cool then add mercaptoethanol, store at room temperature.

27- Lysozyme 100 mg/ml

Lysozyme powder.....100mg

Autoclaved UPW.....1 mL

28-Proteinase K 20 mg/ml

Proteinase K powder.....20 mg

Autoclaved UPW.....1 mL

29-10 mM dNTPs in 1 mL volume

100 mM dATP.....10 µL

100 mM dCTP.....	10 µL
100 mM dTTP.....	10 µL
100 mM dGTP.....	10 µL
Autoclaved UPW.....	60 µL
Store at – 20 °C.	

30- 10 % (w/v) of p-phenylenediamine in 1 ml volume

p-phenylenediamine.....	0.1 g
0.02 µm autoclaved UPW.....	1 mL
Store at – 20 °C, discard if its colour becomes brownish.	

31- 50 % glycerol/ 50% PBS(1:1) in 20 mL volume

Glycerol.....	10 mL
PBS	10 mL
Autoclave, Aliquot and then Store at -20 °C.	

32- 0.1 % (v/v) p-phenylenediamine anti-fade mounting medium

10 % p-phenylenediamine.....	3 µL
50 % glycerol/ 50% PBS (1:1).....	300 µL

33- 1:400 SYBR Green I and II solution in 1 ml volume

Stock SYBR Green I or II.....	2.5 µL
0.02 µl autoclaved UPW.....	997.5 µL

34-10 g/L Fe Stock Solution

FeCl ₂ ·6H ₂ O (FW = 270.3)	4.83g
dH ₂ O.....	to make 100mL

35- 0.1 M EDTA-0.2M MgCl₂-0.2M Ascorbate Buffer

Tris-base (FW = 121.14).....	1.51g
Na ₂ -EDTA dehydrate (FW = 372.24)	3.72g
MgCl ₂ hexahydrate (GW = 203.3)	4.07g
Ascorbic Acid (FW = 176.12).....	3.52g
5N NaOH.....	4.0mL
MiliQ H ₂ O.....	to make 100 mL

Dissolve 1.51 g Tris-base in 80 mL MiliQ H₂O (pH will change to be ~ 8.0). After that, add 3.72g of Na₂-EDTA dehydrate into the solution.

After dissolving the EDTA, add 4.07 g of MgCl₂ hexahydrate ((pH will change to be ~ 4.5) and the solution become cloudy, which means the EDTA is returned to be unsolved. To dissolve the EDTA again, add 3 mL of NaOH which will increase the pH to ~ 8.3. Before adding the last 1 mL of NaOH, dissolve 3.52g of ascorbic acid. Finally, pH should be 6.0-6.5; therefore, some adjustment with NaOH or HCl may be needed, top up the volume to 100 mL with MiliQ water and then store the buffer in dark. If any changing in the colour has notice it, you have to discarded and prepare the new one.

35- 5 x SDS Loading Dye (8.5) in 10 ml volume

1 M Tris pH 6.8.....	2.5 mL
Glycerol 100%.....	4.0 mL
Beta- Mercaptoethanol	2.0 mL
Bromophenol blue.....	.005 g
SDS.....	1 g
UPW.....	to make 10 mL

36- 4% formaldehyde solution

Paraformaldehyde powder.....	40 g
1X PBS.....	to make 1L

Heat 800 mL of 1X PBS at 60 °C on a stir plate, then add 40 g of Paraformaldehyde powder. To dissolve the powder into the solution, add 1 N NaOH dropwise from a pipette until the solution clears. Let the solution to be cool. Afterwards, adjust the volume to 1 L with 1X PBS, and then recheck the pH to be 6.9, store at 4 °C up to a month.

37- 80% isopropanol

Isopropanol.....	80 mL
Autoclaved MiliQ H ₂ O	to make 100 mL

8.1.3 Buffers**1- lysis buffer (Urea 4 M; Tris-HCl 0.2 M, pH 7.4; NaCl 20 mM and EDTA 0.2 M) in 100 ml volume**

Urea.....	24.024 g
Tris-HCl	3.152 g
NaCl.....	0.11688g
EDTA (disodium ethylenediaminetetraacetic acid)	7.4 g
UPW.....	to make to 100 mL

Dissolve EDTA in 70 ml of UPW at pH 8 and then add Tris-HCl adjusted the pH to 7.4 then add the rest, top up top 100 ml with UPW, autoclave, store at room temperature.

2- 0.5 M EDTA, pH 8.0 in 500 ml

EDTA.....	93.05 g
UPW.....	350 mL

To dissolve it, adjust pH to 8.0, add UPW to make up to 500 mL, autoclave and then store at room temperature.

3- 1 M Tris-HCl in 100 ml volume

Trise base.....	12.11 g
UPW.....	70 mL
Adjust pH to 8.0	
UPW.....	up to 100 mL

Autoclave and then store at room temperature.

4- 1 M Tris-HCl in 100 ml volume

Trise base.....	12.11 g
UPW.....	70 mL
Adjust pH to 6.8	
UPW.....	up to 100 mL

Autoclave and then store at room temperature.

5- 1 x TE buffer (10 mM Tris-Cl, 1 mM EDTA)pH 8.0 in 100 mL

1 M Tris-Cl pH 8.0	1 mL
0.5M EDTA pH 8.0	0.2 mL
UPW.....	to make up to 100 mL

6- 10 mM Tris-Cl pH 8.0 in 100 volume

Tris-Cl.....	0.157 g
Add 70 ml UPW, adjust pH to 8.0	
UPW.....	to make up to 100 mL
Autoclave, store at room temperature.	

7- 50 x TAE buffer (2M Tris-acetic acid and 0.05 EDTA)

Tris Base.....	242 g
UPW.....	600 mL
Dissolve and then add 57.1 mL Glacial Acetic Acid along with 100 mL of 0.5 M EDTA , top up to 100 mL with 1000 UPW, store at room temperature.	

8- 1 x TAE buffer in 1 L volume

50 x TAE buffer.....	20 mL
UPW.....	980 mL

9- SDS PAGE resolving gel (10%)

30 % Acrylamide/bis- acrylamide.....	3.3 mL
1.5M Tris-HCl, pH 8.8.....	2.5 mL
10 % SDS	100 µL
10 % APS.....	50 µL
TEMED.....	10 µL
DH2O.....	4.7 mL

10-SDS PAGE stacking gel (5%)

30 % Acrylamide/bis- acrylamide.....	83.3 µL
0.5 M Tris-HCl, pH 6.8.....	1.25 mL
10 % SDS	50µL
10 % APS.....	25 µL

TEMED.....	5 µL
dH ₂ O.....	2.8 mL

11-10 % SDS in 100 ml volume

SDS.....	10 g
UPW.....	to make up to 100 mL

12-0.5 M Tris-HCl, pH 6.8 in 200 ml volume

1 M Tris-HCl, pH 6.8.....	100 mL
UPW.....	100 mL

13-1x SDS-PAGE Running buffer

Glycine.....	28.8 g
Tris base	6.04 g
SDS.....	2 g
UPW.....	1.8 L

Dissolve, add SDS, top up to 2 L store at room temperature.

14-1.5 M Tris-HCl, pH 8.8 in 100 ml volume

Tris-HCl.....	23.64 g
UPW.....	to make 100 mL

Dissolve Tris-HCl into 80 mL water and adjust pH 8.8, top up to 100 mL and then autoclave, store at room temperature.

15-PBS buffer in 1 L volume

NaCl.....	8 g
KCl.....	0.2 g
Na ₂ HPO ₄	1.44 g
KH ₂ PO ₄	0.24g

Dissolve in 800 mL of UPW adjust pH to 7.4 with 5M HCl

Autoclaved UPW.....to make up to 1 L

Autoclave, store at room temperature.

8.2 Appendix 2: Supplementary Data

8.2.1: Data from Chapter 3: Limnological features of Lake Bogoria (May 2015-March 2017).

Table 8.1: Normality test result of lake characteristics (EC, pH, total N, total P, salinity and chl-a content using acetone extraction method and remote sensing method.

Property	Time (months)	Kolmogovo-Smirnov ^a	Shapiro-Wilk	Z-score (Skewness)	Z-score (kurtosis)
		Sig. (p)	Sig. (p)		
EC (mS cm ⁻¹)	May-Jun 15	0.200*	0.642	-0.191	-1.028
	Jul- Aug 15	0.200*	0.082	-0.033	-1.688
	Sep- Oct 15	0.165	0.187	0.115	-1.475
	Nov- Dec 15	0.200*	0.062	0.815	-1.120
	Jan- Feb 16	0.107	0.193	-1.73	1.173
	Mar- Apr16	0.200*	0.654	0.549	-0.801
	May- Jun16	0.200*	0.247	-0.69	-1.045
	Jul- Aug16	0.200*	0.134	0.164	-1.510
	Sep- Oct16	0.200*	0.421	-0.433	-0.929
	Dec16- Jan17	0.152	0.073	-0.930	-1.067
Feb- Mar17	0.200*	0.294	-0.095	-1.469	
pH	May-Jun 15	0.200*	0.755	0.546	-0.724
	Jul- Aug 15	0.200*	0.271	-0.700	-1.026
	Sep- Oct 15	0.200*	0.167	0	-1.077
	Nov- Dec 15	0.117	0.091	-1.014	-0.172
	Jan- Feb 16	0.031	0.212	-0.994	-0.373
	Mar- Apr16	0.200*	0.315	0.310	-1.190
	May- Jun16	0.094	0.035	-0.540	-1.373
	Jul- Aug16	0.200*	0.804	-0.495	-0.493
	Sep- Oct16	0.200*	0.456	0	-1.077
	Dec16- Jan17	0.194	0.121	-0.014	-1.578
Feb- Mar17	0.056	0.004	0	-1.914	
Total N (mg L ⁻¹)	May-Jun 15	0.200*	0.294	-0.218	-1.391
	Jul- Aug 15	0.200*	0.232	0.541	-1.229
	Sep- Oct 15	0.159	0.349	0.443	-0.678
	Nov- Dec 15	0.200*	0.298	0.641	-1.067
	Jan- Feb 16	0.200*	0.818	-0.541	-0.454
	Mar- Apr16	0.200*	0.512	1.320	0.689
	May- Jun16	0.200*	0.357	-0.780	-0.525
	Jul- Aug16	0.200*	0.598	-1.186	0.403
	Sep- Oct16	0.200*	0.427	0.233	-1.237
	Dec16- Jan17	0.200*	0.933	-0.761	0.419
Feb- Mar17	0.200*	0.526	0.852	0.091	
Chl-a content (ug L ⁻¹)	May-Jun 15	0.200*	0.446	0.333	-1.157
	Jul- Aug 15	0.200*	0.424	0.241	-1.210
	Sep- Oct 15	0.200*	0.656	0.899	0.230
	Nov- Dec 15	0.200*	0.261	0.102	-1.494
	Jan- Feb 16	0.200*	0.737	-0.379	-0.813

Continued on next page

Table 8.1: continued from previous page.

Time (months)	Kolmogovo-	Shapiro-	Z-score (Skewness)	Z-score (kurtosis)	
	Smirnov ^a	Wilk			
	Sig. (<i>p</i>)	Sig. (<i>p</i>)			
Mar- Apr16	0.200*	0.198	0.089	-1.287	
May- Jun16	0.101	0.086	0.214	-1.565	
Jul- Aug16	0.200*	0.072	-1.603	0.537	
Sep- Oct16	0.200*	0.860	-0.196	-0.835	
Dec16- Jan17	0.159	0.139	0.302	-1.495	
Feb- Mar17	0.131	.077	0.361	-1.499	
Salinity(g L ⁻¹)	May-Jun 15	0.200*	0.642	-0.189	-1.029
	Jul- Aug 15	0.200*	0.082	-0.033	-1.689
	Sep- Oct 15	0.165	0.188	0.116	-1.474
	Nov- Dec 15	0.200*	0.384	0.473	-1.017
	Jan- Feb 16	0.107	0.194	-1.73	1.170
	Mar- Apr16	0.200*	0.653	0.551	-0.800
	May- Jun16	0.200*	0.248	-0.700	-1.046
	Jul- Aug16	0.200*	0.134	0.1680	-1.505
	Sep- Oct16	0.200*	0.421	-0.431	-0.931
	Dec16- Jan17	0.153	0.074	-0.929	-1.068
	Feb- Mar17	0.200*	0.294	-0.092	-1.470
Nanoparticles (VLPmL ⁻¹)	May-Jun 15	0.200*	0.632	-0.378	-0.916
	Jul- Aug 15	0.200*	.858	0.073	-0.917
	Sep- Oct 15	0.034	0.068	-1.45	0.004
	Nov- Dec 15	0.105	0.132	0.817	-0.625
	Jan- Feb 16	0.200*	0.852	0.742	0.337
	Mar- Apr16	0.200*	0.121	-0.853	-1.056
	May- Jun16	0.140	0.074	0.137	-1.695
	Jul- Aug16	0.129	0.025	0.801	-1.200
	Sep- Oct16	0.200*	0.272	0.130	-1.431
	Dec16- Jan17	0.200*	0.274	1.118	-0.316
	Feb- Mar17	0.200*	0.755	-0.298	-0.674
Total P (mg L ⁻¹)	May-Jun 15	0.097	0.357	-0.900	-0.493
	Jul- Aug 15	0.200*	0.339	0.541	-1.009
	Sep- Oct 15	0.200*	.915	0.711	0.1476
	Nov- Dec 15	0.200*	0.217	-0.365	-1.316
	Jan- Feb 16	0.200*	0.424	0.760	-0.43
	Mar- Apr16	0.200*	0.474	0.115	-0.554
	May- Jun16	0.200*	0.921	0.325	0.519
	Jul- Aug16	0.200*	0.230	-0.146	-1.481
	Sep- Oct16	0.200*	0.539	-0.716	-0.442
	Dec16- Jan17	0.200*	0.730	0.487	-0.758
	Feb- Mar17	0.200*	0.579	-0.183	-0.826

*. This is a lower bound of the true significance, a. Lilliefors Significance Correction.

The significant level (α) is 0.05.

Table 8.2: Normality test of Chl-a content using remote sensing.

	Kolmogovo-Smirnov ^a	Shapiro-Wilk	Z-score (Skewness)	Z-score (kurtosis)
Time	Sig. (p)	Sig. (p)		
May-Jul 15	0.167	.0351	-0.79518	-0.829
Aug-Oct 15	0.200*	0.829	0.486309	-0.6335
Nov15-Jan 16	0.200*	0.742	0.366922	-0.4055
Feb-Apr 16	.0200*	0.971	0.411829	0.202
May-Jul 16	0.200*	0.835	0.329682	-0.81
Aug-Oct 16	0.200*	0.420	-0.81818	-0.0665
Dec 16-Feb 17	0.200*	0.279	-0.6035	-1.2845

*This is a lower bound of the true significance, Lilliefors Significance Correction. The significant level (α) is 0.05.

Table 8.3: Model Summary of linear regression.

Model	R	R Square	Adjusted R Square	Std. Error of the Estimate	Durbin-Watson
1	0.426 ^a	0.181	0.140	39.7937	2.141

a. Predictors: (Constant), Total Nitrogen concentration, b. Dependent Variable: Chl-a content.

Table 8.4: ANOVA Summary of linear regression.

ANOVA ^a						
Model		Sum of Squares	df	Mean Square	F	Sig.(p)
1	Regression	7006.078	1	7006.078	4.424	0.048
	Residual	31670.820	20	1583.541		
	Total	38676.898	21			

The significant level (α) is 0.05.

8. 2.2: Data from Chapter 4: *Arthrospira* Morphology and physiology**Table 8.5: Normality test of two-way ANOVA of *Arthrospira* spp. abundance during the period of study.**

Variable	Kolmogorov-Smirnov ^a (<i>p</i>)	Shapiro-Wilk (<i>p</i>)
Aug15 C-morphotype	0.200	0.132
Aug15 S-morphotype	0.200	0.142
Aug15 H-morphotype	0.200	0.264
Mar16 C-morphotype	0.193	0.067
Mar16 S-morphotype	0.200	0.222
Mar16 H-morphotype	0.200	0.615
May16 C-morphotype	0.200	0.322
May16 S-morphotype	0.200	0.261
May16 H-morphotype	0.200	0.210
Jul16 C-morphotype	0.200	0.175
Jul16 S-morphotype	0.200	0.183
Jul16 H-morphotype	0.114	0.071
Dec16 C-morphotype	0.200	0.404
Dec16 S-morphotype	0.200	0.367
Dec16 H-morphotype	0.200	0.365
Mar17 C-morphotype	0.200	0.171
Mar17 S-morphotype	0.200	0.500
Mar17 H-morphotype	0.200	0.458

The significant level (α) is 0.05.

Chapter 8. Appendices

	1	10	20	30	40	50	60
C- Morphotype	-----ACGCTGGCGGTCTGCTTAACACATGCAAGTCGAACGGGCTCTTCG						
H- Morphotype	-----ACGCTGGCGGTCTGCTTAACACATGCAAGTCGAACGGGCTCTTCG						
S- Morphotype	CCTGGCTCAGGATGAATGCTGGCGGTCTGCTTAACACATGCAAGTCGAACGGGCTCTTCG						
C- Morphotype	GAGCTAGTGGCGGACGGGTGAGTAACACGTGAGAATCTGGCTCCCGTCCGGGACAAACAG						
H- Morphotype	GAGCTAGTGGCGGACGGGTGAGTAACACGTGAGAATCTGGCTCCCGTCCGGGACAAACAG						
S- Morphotype	GAGCTAGTGGCGGACGGGTGAGTAACACGTGAGAATCTGGCTCCCGTCCGGGACAAACAG						
C- Morphotype	AGGGAAACTTCTGCTAATCCCGGATGAGCCGAAAGTAAAAGATTTATCGCCGGGAGATG						
H- Morphotype	AGGGAAACTTCTGCTAATCCCGGATGAGCCGAAAGTAAAAGATTTATCGCCGGGAGATG						
S- Morphotype	AGGGAAACTTCTGCTAATCCCGGATGAGCCGAAAGTAAAAGATTTATCGCCGGGAGATG						
C- Morphotype	AGCTCGCTCTGATTAGCTAGTTGGTGAGGTAAGGCTCACCAAGGCGACGATCAGTAGC						
H- Morphotype	AGCTCGCTCTGATTAGCTAGTTGGTGAGGTAAGGCTCACCAAGGCGACGATCAGTAGC						
S- Morphotype	AGCTCGCTCTGATTAGCTAGTTGGTGAGGTAAGGCTCACCAAGGCGACGATCAGTAGC						
C- Morphotype	TGGTCTGAGAGGATGATCAGCCACACTGGGACTGAGACACGGCCAGACTCCTACGGGAG						
H- Morphotype	TGGTCTGAGAGGATGATCAGCCACACTGGGACTGAGACACGGCCAGACTCCTACGGGAG						
S- Morphotype	TGGTCTGAGAGGATGATCAGCCACACTGGGACTGAGACACGGCCAGACTCCTACGGGAG						
C- Morphotype	GCAGCAGTGGGAATTTTCGCAATGGGCGCAAGCCTGACGGAGCAAGACCGCTGGGGG						
H- Morphotype	GCAGCAGTGGGAATTTTCGCAATGGGCGCAAGCCTGACGGAGCAAGACCGCTGGGGG						
S- Morphotype	GCAGCAGTGGGAATTTTCGCAATGGGCGCAAGCCTGACGGAGCAAGACCGCTGGGGG						
C- Morphotype	AGGAAGGCTCTTGGGTTGTAACCCCTTTTCTCAAGGAAGAACACAATGACGGTACTTGA						
H- Morphotype	AGGAAGGCTCTTGGGTTGTAACCCCTTTTCTCAAGGAAGAACACAATGACGGTACTTGA						
S- Morphotype	AGGAAGGCTCTTGGGTTGTAACCCCTTTTCTCAAGGAAGAACACAATGACGGTACTTGA						
C- Morphotype	GGAATAAGCCTCGGCTAACTCCGTGCCAGCAGCCGCGTAATACGGAGGAGGCAAGCGTT						
H- Morphotype	GGAATAAGCCTCGGCTAACTCCGTGCCAGCAGCCGCGTAATACGGAGGAGGCAAGCGTT						
S- Morphotype	GGAATAAGCCTCGGCTAACTCCGTGCCAGCAGCCGCGTAATACGGAGGAGGCAAGCGTT						
C- Morphotype	ATCCGGAATGATTGGGCGTAAAGCGTCCGTAGTGGCTGTTCAAGTCTGCTGTCAAAGAC						
H- Morphotype	ATCCGGAATGATTGGGCGTAAAGCGTCCGTAGTGGCTGTTCAAGTCTGCTGTCAAAGAC						
S- Morphotype	ATCCGGAATGATTGGGCGTAAAGCGTCCGTAGTGGCTGTTCAAGTCTGCTGTCAAAGAC						
C- Morphotype	AGTGGCTTAACTACTGAAAGGCAGTGGAACTGAACAGCTAGAGTACGGTAGGGGCAGAG						
H- Morphotype	AGTGGCTTAACTACTGAAAGGCAGTGGAACTGAACAGCTAGAGTACGGTAGGGGCAGAG						
S- Morphotype	AGTGGCTTAACTACTGAAAGGCAGTGGAACTGAACAGCTAGAGTACGGTAGGGGCAGAG						
C- Morphotype	GGAATCCCGGTGTAGCGGTGAAATGCGTAGATATCGGGAAGAACACCGGTGGCGAAAGC						
H- Morphotype	GGAATCCCGGTGTAGCGGTGAAATGCGTAGATATCGGGAAGAACACCGGTGGCGAAAGC						
S- Morphotype	GGAATCCCGGTGTAGCGGTGAAATGCGTAGATATCGGGAAGAACACCGGTGGCGAAAGC						
C- Morphotype	GCTCTGCTGGGCCGTAAGTACACTGAGGGACGAAAGCTAGGGAGCGAATGGGATTAGA						
H- Morphotype	GCTCTGCTGGGCCGTAAGTACACTGAGGGACGAAAGCTAGGGAGCGAATGGGATTAGA						
S- Morphotype	GCTCTGCTGGGCCGTAAGTACACTGAGGGACGAAAGCTAGGGAGCGAATGGGATTAGA						
C- Morphotype	TACCCAGTAGTCCCTAGCCGTAACGATGGAACTAGGTGTAGCCTGTATCGACCCGAG-						
H- Morphotype	TACCCAGTAGTCCCTAGCCGTAACGATGGAACTAGGTGTAGCCTGTATCGACCCGAGC						
S- Morphotype	TACCCAGTAGTCCCTAGCCGTAACGATGGAACTAGGTGTAGCCTGTATCGACCCGAGC						
C- Morphotype	-						
H- Morphotype	C						
S- Morphotype	C						

Figure 8.1: Multiple sequence alignment of 16S rRNA consensus sequences of three *Arthrospira* morphotypes (S, C and H) from Lake Bogoria, using Geneious software.

Chapter 8. Appendices

	1	10	20	30	40	50	60
H - Morphotype	--CCTTTT TAGGGAGACCTACTTCAGGACATCGTGCGATGATAATAATAGCCGAGTCTTG						
C - Morphotype	CTCCTTTT TAGGGAGACCTACTTCAGGACATCGTGCGATGATAATAATAGCCGAGTCTTG						
S - Morphotype	CTCCTTTT TAGGGAGACCTACTTCAGGACATCGTGCGATGATAATAATAGCCGAGTCTTG						
H - Morphotype	AGGTCATCCTTAGGTCGGATGGGGCGGTCAGAGAGCTTTCAAACCTTAGGGTTCGTGTTA						
C - Morphotype	AGGTCATCCTTAGGTCGGATGGGGCGGTCAGAGAGCTTTCAAACCTTAGGGTTCGTGTTA						
S - Morphotype	AGGTCATCCTTAGGTCGGATGGGGCGGTCAGAGAGCTTTCAAACCTTAGGGTTCGTGTTA						
H - Morphotype	TGGGCTATTAGCTCAGGTGGTTAGAGCGCACCCCTGATAAGGGTGAGGTCCCTGGTTCAA						
C - Morphotype	TGGGCTATTAGCTCAGGTGGTTAGAGCGCACCCCTGATAAGGGTGAGGTCCCTGGTTCAA						
S - Morphotype	TGGGCTATTAGCTCAGGTGGTTAGAGCGCACCCCTGATAAGGGTGAGGTCCCTGGTTCAA						
H - Morphotype	GTCCAGGATGGCCACATCCACCCCAAACCTGGGGGTATAGCTCAGTTGGTAGAGCGCTGC						
C - Morphotype	GTCCAGGATGGCCACATCCACCCCAAACCTGGGGGTATAGCTCAGTTGGTAGAGCGCTGC						
S - Morphotype	GTCCAGGATGGCCACATCCACCCCAAACCTGGGGGTATAGCTCAGTTGGTAGAGCGCTGC						
H - Morphotype	CTTTGCACGGCAGAAGTCAGCGGTTTCGAGTCCGCTTACCTCCACTCTCCTAGAATTAGGT						
C - Morphotype	CTTTGCACGGCAGAAGTCAGCGGTTTCGAGTCCGCTTACCTCCACTCTCCTAGAATTAGGT						
S - Morphotype	CTTTGCACGGCAGAAGTCAGCGGTTTCGAGTCCGCTTACCTCCACTCTCCTAGAATTAGGT						
H - Morphotype	GCTAGTTGGGGTGAGGTAGTCTTGAATTGAGAAATTGAGAGTTGGTGACTGTACAGCTCC						
C - Morphotype	GCTAGTTGGGGTGAGGTAGTCTTGAATTGAGAAATTGAGAGTTGGTGACTGTACAGCTCC						
S - Morphotype	GCTAGTTGGGGTGAGGTAGTCTTGAATTGAGAAATTGAGAGTTGGTGACTGTACAGCTCC						
H - Morphotype	TAAGTCTGTAGATGTTAATCTAGGACT TAGCTGGACATAAGTTCCAGTCAGAACCTT						
C - Morphotype	TAAGTCTGTAGATGTTAATCTAGGACTTAGATAGCTGGACATAAGTTCCAGTCAGAACCTT						
S - Morphotype	TAAGTCTGTAGATGTTAATCTAGGACTTAGATAGCTGGACATAAGTTCCAGTCAGAACCTT						
H - Morphotype	GAAAACCTGCATAGAGAAAAGCATAATGGTGTAGGAAAACGTCGTCAGAACAAATCCAATG						
C - Morphotype	GAAAACCTGCATAGAGAAAAGCATAATGGTGTAGGAAAACGTCGTCAGAACAAATCCAATG						
S - Morphotype	GAAAACCTGCATAGAGAAAAGCATAATGGTGTAGGAAAACGTCGTCAGAACAAATCCAATG						
H - Morphotype	TAGGTCAAGCTACAAAGGGCTAACGGTGGAT-----						
C - Morphotype	TAGGTCAAGCTACAAAGGGCTAACGGTGGATACCTAGGCACACAAA						
S - Morphotype	TAGGTCAAGCTACAAAGGGCTAACGGTGGATACCT-----						

Figure 8.2: Multiple sequence alignment of ITS consensus sequences of three *Arthrospira* morphotypes (S, C and H) from Lake Bogoria, using Geneious software.

Chapter 8. Appendices

	1	10	20	30	40	50	60
H - Morphotype	--TGAACGGTTTGCGTGAAACTTACCTGGCTTTGGGAACTCCCGGTTCCCTCCGTTGCTGT						
C - Morphotype	-TTGAACGGTTTGCGTGAAACTTACCTGGCTTTGGGAACTCCCGGTTCCCTCCGTTGCTGT						
S - Morphotype	CTTGAACGGTTTGCGTGAAACTTACCTGGCTTTGGGAACTCCCGGTTCCCTCCGTTGCTGT						
H - Morphotype	CGGTGTTGGCAAAATGAAAGAAGCTGCTCTGGCGATCGTTAACGATCCCGCAGGTATCAC						
C - Morphotype	CGGTGTTGGCAAAATGAAAGAAGCTGCTCTGGCGATCGTTAACGATCCCGCAGGTATCAC						
S - Morphotype	CGGTGTTGGCAAAATGAAAGAAGCTGCTCTGGCGATCGTTAACGATCCCGCAGGTATCAC						
H - Morphotype	TCCTGGCGATTGTAGCGCTTTGGCTTCAGAAATCGCTAGTTACTTTGATCGTGCATGTGC						
C - Morphotype	TCCTGGCGATTGTAGCGCTTTGGCTTCAGAAATCGCTAGTTACTTTGATCGTGCATGTGC						
S - Morphotype	TCCTGGCGATTGTAGCGCTTTGGCTTCAGAAATCGCTAGTTACTTTGATCGTGCATGTGC						
H - Morphotype	TGCAGTTTCCTAATCAAGCAGATCCATAGCATATAACAATTGAAACAGTTTAGCTGAAGT						
C - Morphotype	TGCAGTTTCCTAATCAAGCAGATCCATAGCATATAACAATTGAAACAGTTTAGCTGAAGT						
S - Morphotype	TGCAGTTTCCTAATCAAGCAGATCCATAGCATATAACAATTGAAACAGTTTAGCTGAAGT						
H - Morphotype	CTAAGTGACTGGACTTCTGTTTGTACCTAATTTTTTGTAACCAATCGGGAGATAACTC						
C - Morphotype	CTAAGTGACTGGACTTCTGTTTGTACCTAATTTTTTGTAACCAATCGGGAGATAACTC						
S - Morphotype	CTAAGTGACTGGACTTCTGTTTGTACCTAATTTTTTGTAACCAATCGGGAGATAACTC						
H - Morphotype	GAGAATGAAAACCCCTAACCGAAGCAGTTTCTATCGCTGATTCCCAAGGTCGTTTCCT						
C - Morphotype	GAGAATGAAAACCCCTAACCGAAGCAGTTTCTATCGCTGATTCCCAAGGTCGTTTCCT						
S - Morphotype	GAGAATGAAAACCCCTAACCGAAGCAGTTTCTATCGCTGATTCCCAAGGTCGTTTCCT						
H - Morphotype	AAGCAGCACCGAAATCCAAGTGGCTTTTGGCCGTTTTCGTCAAGCCAAAGCTGGTCTGGA						
C - Morphotype	AAGCAGCACCGAAATCCAAGTGGCTTTTGGCCGTTTTCGTCAAGCCAAAGCTGGTCTGGA						
S - Morphotype	AAGCAGCACCGAAATCCAAGTGGCTTTTGGCCGTTTTCGTCAAGCCAAAGCTGGTCTGGA						
H - Morphotype	AGCTGCTAAAGCTTTGACCTCTAAAGCTGATAGTCTGATCAGTGGTGTGCCAAGCAGT						
C - Morphotype	AGCTGCTAAAGCTTTGACCTCTAAAGCTGATAGTCTGATCAGTGGTGTGCCAAGCAGT						
S - Morphotype	AGCTGCTAAAGCTTTGACCTCTAAAGCTGATAGTCTGATCAGTGGTGTGCCAAGCAGT						
H - Morphotype	GTACAACAAGTTCCCCTACACCACCCAA-----						
C - Morphotype	GTACAACAAGTTCCCCTACACCACCCAAATGCAGGGGACCTAA						
S - Morphotype	GTACAACAAGTTCCCCTACACCACCCAAA-----						

Figure 8.3: Multiple sequence alignment of PC-IGS locus consensus sequences of three *Arthrospira* morphotypes (S, C and H) from Lake Bogoria, using Geneious software.

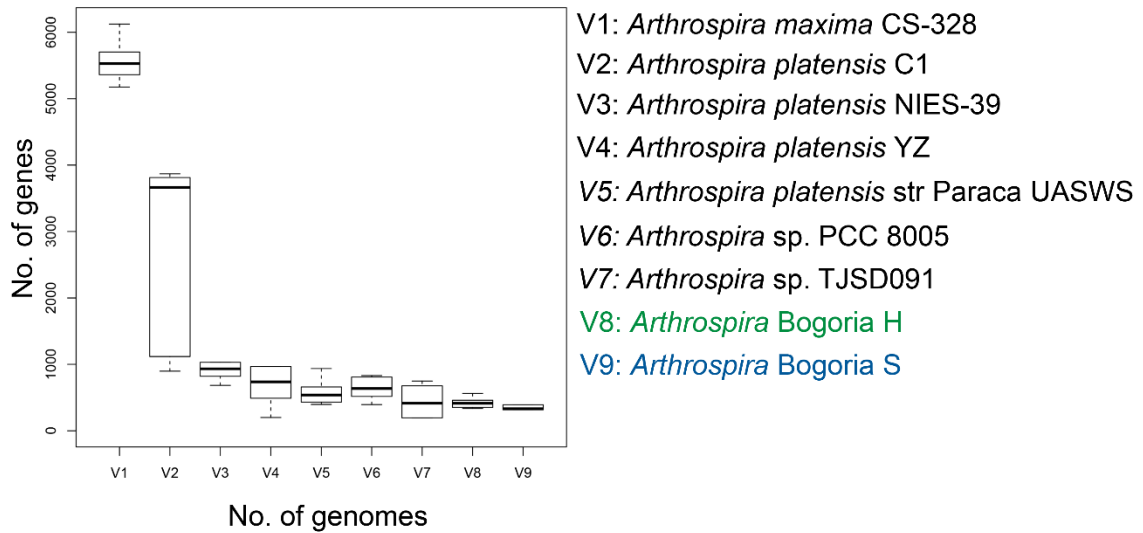


Figure 8.4: Box plot of the number of new genes of nine *Arthrospira* genomes produced pan genome pipeline of Roary.

Note the decrease of new genes with the addition of new genome. *Arthrospira* Bogoria morphotypes, H and S are coloured with green and blue colours respectively.

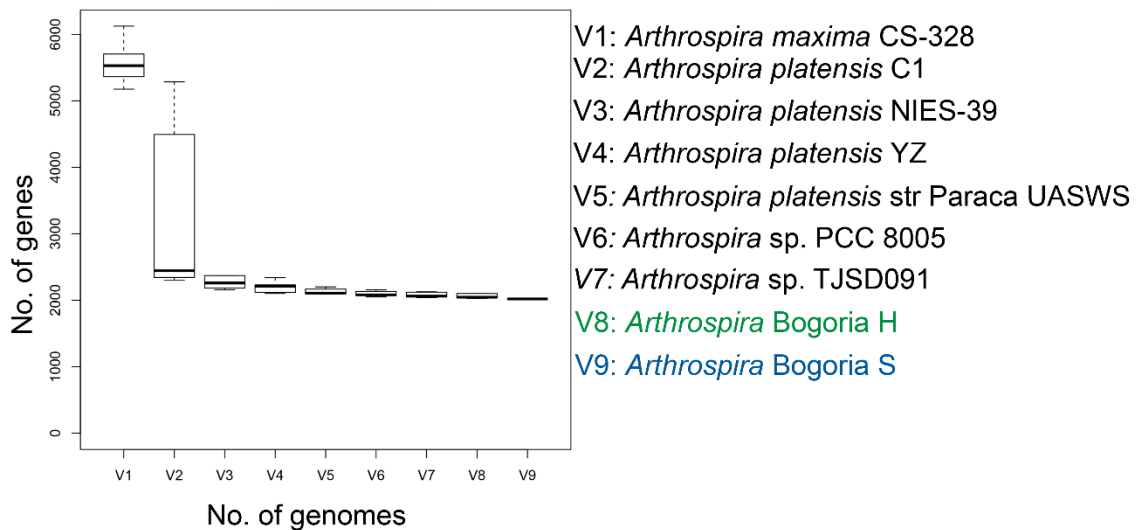


Figure 8.5: Box plot of the number of conserved genes of nine *Arthrospira* genomes produced pan genome pipeline of Roary.

Note the decrease of conserved genes with the addition of new genome. *Arthrospira* Bogoria morphotypes, H and S are coloured with green and blue colours respectively.

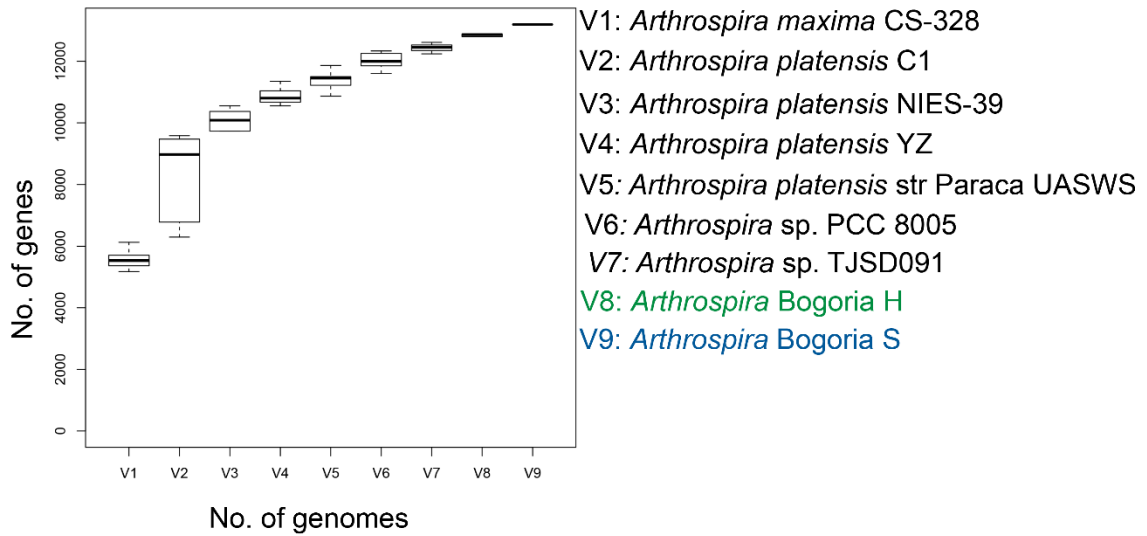


Figure 8.6: Box plot of the number of nine genomes produced pan genome pipeline of Roary.

Note the increase of pan genome with the addition of new genome. *Arthrospira* Bogoria morphotypes, H and S are coloured with green and blue colours respectively.

Chapter 8. Appendices

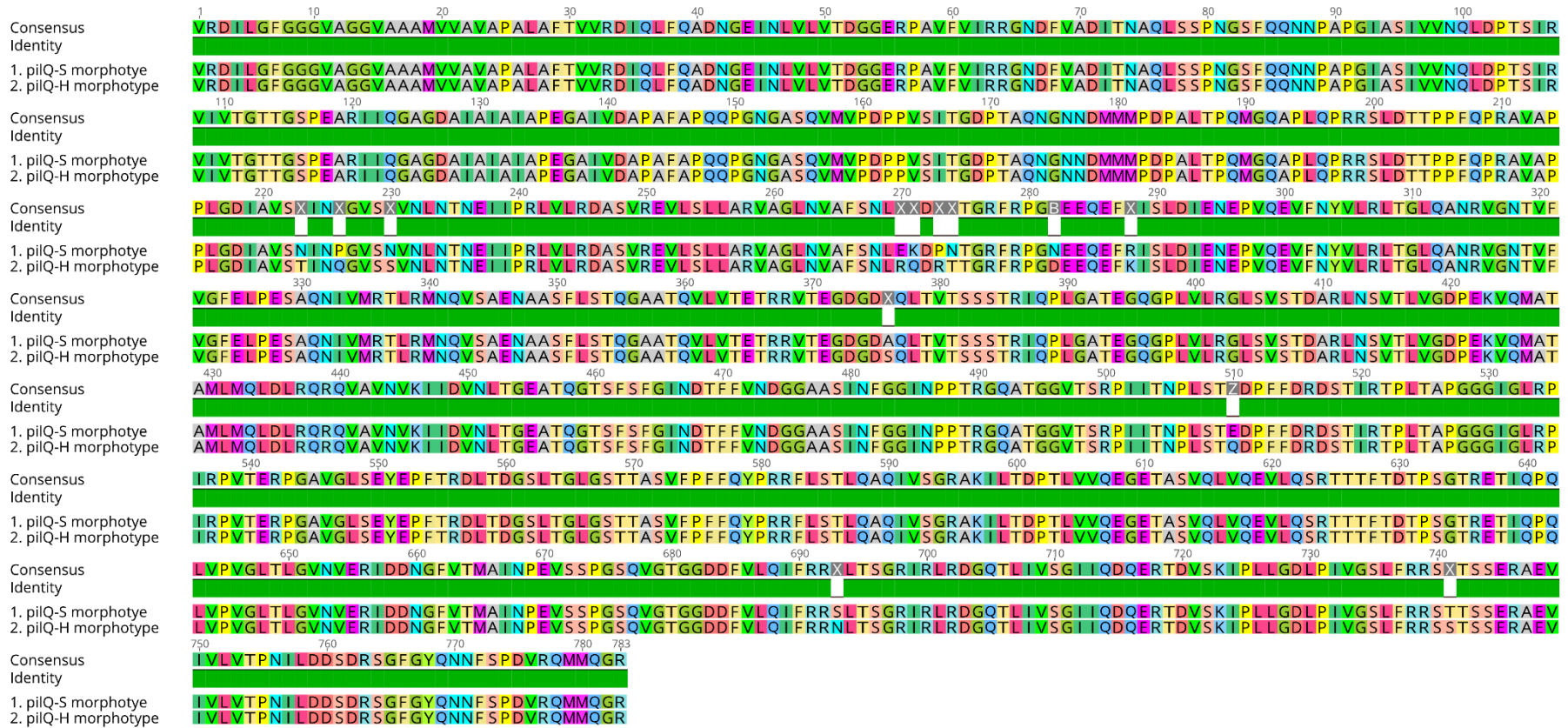


Figure 8.7: Pairwise amino acid sequences alignment of pilQ consensus sequences of two *Arthrospira* morphotypes (H and S) from Lake Bogoria using Muscle tool.

Chapter 8. Appendices



Figure 8.8: Pairwise amino acid alignment of pilT-1 consensus sequences of two *Arthrospira* morphotypes (H and S) from Lake Bogoria using Muscle tool.

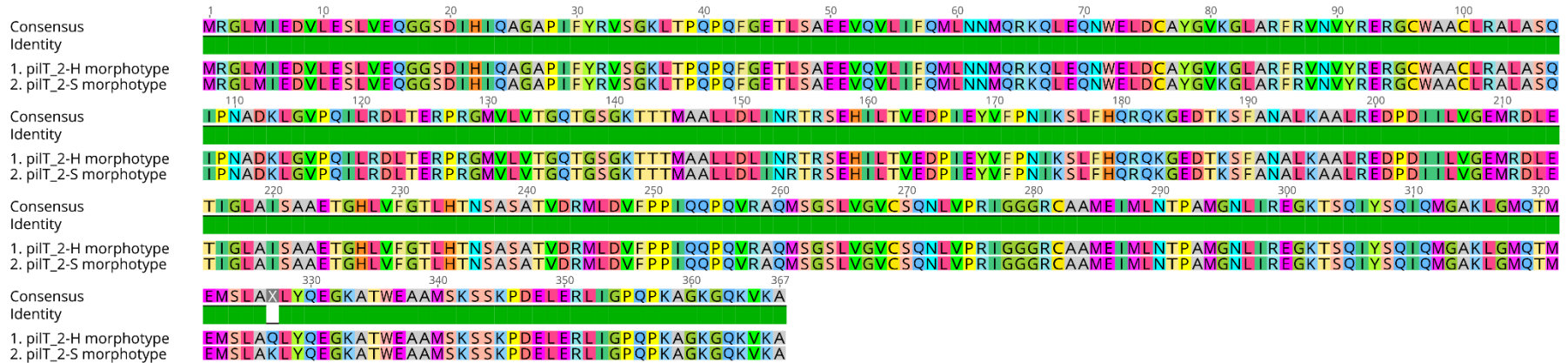


Figure 8.9: Pairwise amino acid sequences alignment of pilT-2 consensus sequences of two *Arthrospira* morphotypes (H and S) from Lake Bogoria using Muscle tool.

Chapter 8. Appendices



Figure 8.10: Pairwise amino acid sequences alignment of pilT-3 consensus sequences of two *Arthrospira* morphotypes (H and S) from Lake Bogoria using Muscle tool.

8.2.4: Data from Chapter 6: *Arthrospira* phage investigation**Table 8.6: NanoSight NTA 2.0 software settings.**

Screen Gain	10
Detection Threshold	4
Min Expected Particle Size	30 nm
Calibration	
Temperature	(recorded by connected temperature meter)
Viscosity	Water viscosity (0.95)
Camera Control	
Camera Level	15
reproducibility	High
Polydispersity	Med
Capture Duration	90 second

Table 8.7: Epifluorescence microscopy settings.

Setting	Value
Software	Volocity 6:3.0
Camera	Hamamatsu C10600-10B (ORCA-R2)
Exposure	444 ms
Binning	X1
Auto Contrast	79
Offset	0
Light Mode	Low Light
Scan Speed	High Quality
Depth	12 Bits Per Channel
Rotation	0
Flip	None
Dummy Fluo Shutter	Closed
Dummy TL Shutter	Closed
Dummy x Axis	0
Dummy y Axis	0
Dummy z Axis	Position: 0.000 μm Top: 10.000 μm Thickness: 20.000 μm
Dummy Objective Turret	Objective 1 Magnification: 4x Numerical Aperture: 0.13
Dummy Filter Turret 1	Filter 1
Dummy Filter Turret 2	Filter 1
Dummy Laser Changer	All Off
Dummy Bleaching Device	0
Dummy TTL Out	0
Dummy TTL in	0

Table 8.8: Normality test of VLPs concentration using NanoSight technique for the entire period of study (May2015-March2017).

Time point	Kolmogovo-Smirnov ^a (Sig. (p))	Shapiro-Wilk	Z-score (Skewness)	Z-score (kurtosis)
May-Jun 15	0.200	0.937	- 0.378	- 0.916
Jul- Aug 15	0.200	0.965	0.073	- 0.917
Sep- Oct 15	0.034	0.807	- 1.45	0.004
Nov- Dec 15	0.105	0.841	0.817	- 0.65
Jan- Feb 16	0.200	0.964	0.742	0.337
Mar- Apr16	0.200	0.836	- 0.852	- 1.056
May- Jun16	0.140	0.811	0.137	- 1.695
Jul- Aug16	0.129	0.759	0.801	-1.200
Sep- Oct16	0.200	0.881	0.130	- 1.431
Dec16- Jan17	0.200	0.881	1.118	- 1.316
Feb- Mar17	0.200	0.95	- 0.298	- 0.673

The significant level (α) is 0.05.

Table 8.9: Normality test results of VLPs concentration in control culture and incubated culture with water sample of Jul-2016 for 19 days.

Sample	Kolmogovo-Smirnov ^a (Sig)	Shapiro-Wilk (Sig. (p))	Z-score (Skewness)	Z-score (kurtosis)
Negative control day 1	0.200	0.09	0.054	-1.37
Negative control day 3	0.200	0.609	-0.752	-1.287
Negative control day 5	0.200	0.249	0.758	-0.5322
Negative control day 7	0.200	0.755	-0.1.108	0.371
Negative control day 9	0.059	0.319	1.301	1.229
Negative control day 11	0.200	0.715	0.985	0.438
Negative control day 13	0.200	0.274	1.808	2.074
Negative control day 15	0.075	0.050	-1.211	-0.718
Negative control day 17	0.200	0.323	1.285	-0.013
Negative control day 19	0.200	0.964	-0.489	0.833
Incubated culture day 1	0.200	0.531	-1.79	-0.839
Incubated culture day 3	0.200	0.309	-0.444	-0.869
Incubated culture day 5	0.200	0.206	-0.322	-1.154
Incubated culture day 7	0.200	0.728	0.706	-0.183
Incubated culture day 9	0.200	0.349	1.608	1.561
Incubated culture day 11	0.200	0.468	0.140	-0.750
Incubated culture day 13	0.017	0.099	0.977	-0.869
Incubated culture day 15	0.055	0.162	0.468	-1.233
Incubated culture day 17	0.200	0.415	0.314	-0.013
Incubated culture day 19	0.200	0.750	-0.166	0.833

The significant level (α) is 0.05.

Table 8.10: Levene's Test for Equality of Variance results for VLPs concentration in the control and incubated cultures with water sample of Jul-2016 for 19 days.

Time (Day)	F	Sig. (p)
Day 1	0.980	0.335
Day 3	6.198	0.03
Day5	1.380	0.225
Day7	6.807	0.018
Day 9	0.202	0.658
Day 11	0.582	0.455
Day 13	0.377	0.547
Day 15	8.827	0.008
Day 17	2.813	0.111
Day 19	2.550	0.128

The significant level (α) is 0.05.

Table 8.11: The homogeneity of variance test result of the VLPs concentration between different treatments.

	Levene statistic	df1	df2	Sig. (p)
With the negative control	2.028	3	8	0.189
With negative control subtraction	0.210	2	6	0.186

The significant level (α) is 0.05.

Table 8.12: Non-significant results of Mann-Whitney U test for phycocyanin fluorescence intensity assay(C-morphotype).

Time point	Incubation day	Test statistic	Sig. (p)	Effect size (r)
May-Jun 15	1	22	0.589	0.15
May-Jun 15	3	34	0.009	0.74
May-Jun 15	5	32	0.026	0.65
May-Jun 15	7	20	0.818	0.09
May-Jun 15	9	16	0.818	-0.09
May-Jun 15	11	21	0.699	0.13
May-Jun 15	13	13	0.485	-0.23
Jul-Aug 15	1	22	0.589	0.18
Jul-Aug 15	5	34	0.009	0.74
Jul-Aug 15	11	16	0.818	-0.09
Jul-Aug 15	13	23	0.485	0.22
Sep-Oct15	1	29	0.093	0.29
Sep-Oct15	3	31	0.041	0.58
Sep-Oct15	5	34	0.009	0.74
Sep-Oct15	7	4	0.026	-0.56
Sep-Oct15	9	11	0.310	-0.32
Sep-Oct15	11	12	0.394	-0.28
Sep-Oct15	13	24	0.394	0.28
Nov-Dec15	5	28	0.132	0.46
Nov-Dec15	7	2	0.009	-0.74
Nov-Dec15	9	7	0.093	-0.51
Nov-Dec15	11	6	0.065	-0.56
Nov-Dec15	13	13	0.485	0.485
Jan-Feb16	1	24	0.394	0.28
Jan-Feb16	3	34	0.009	0.74
Jan-Feb16	5	27	0.180	0.42

Continued on next page.

Table 8.12: continued from previous page.

Table 8.12: continued from previous page.	Incubation day	Test statistic	Sig. (<i>p</i>)	Effect size (<i>r</i>)
Jan-Feb16	7	0	0.002	-0.83
Time point	9	8	0.132	-0.46
Jan-Feb16	11	8	0.132	-0.46
Jan-Feb16	13	19	1	0.05
Jan-Feb16	1	21	0.699	0.14
Mar-Apr16	3	31	0.041	0.60
Mar-Apr16	5	27	0.180	0.42
Mar-Apr16	9	9	0.180	-0.42
Mar-Apr16	11	11	0.310	-0.32
Mar-Apr16	13	10	0.24	-0.37
Mar-Apr16	1	20	0.818	0.09
May-Jun16	5	30	0.065	0.65
May-Jun16	7	6	0.065	-0.65
May-Jun16	9	6	0.065	-0.065
May-Jun16	11	14	0.589	-0.19
May-Jun16	13	28	0.132	0.46
May-Jun16	1	25	0.301	0.09
Jul-Aug16	5	30	0.065	0.66
Jul-Aug16	7	6	0.065	-0.065
Jul-Aug16	9	9	0.180	-0.035
Jul-Aug16	11	2	0.009	-0.59
Jul-Aug16	13	11	0.310	0.26
Jul-Aug16	1	18	1.00	0
Sep-Oct16	3	31	0.041	0.60
Sep-Oct16	5	12	0.394	0.394
Sep-Oct16	7	23	0.485	0.23
Sep-Oct16	9	23	0.485	0.23
Sep-Oct16	11	13	0.485	-0.23
Sep-Oct16	13	26	0.24	0.37
Sep-Oct16	1	28	0.132	0.46
Dec16-Jan17	5	29	0.093	0.51
Dec16-Jan17	7	7	0.093	-0.51
Dec16-Jan17	9	2	0.009	-0.74
Dec16-Jan17	11	6	0.065	-0.56
Dec16-Jan17	13	14	0.589	-0.19
Dec16-Jan17	1	26	0.24	0.37
Feb-Mar17	5	29	0.093	0.51
Feb-Mar17	7	5	0.041	-0.60
Feb-Mar17	11	10	0.240	-0.37
Feb-Mar17	13	34	0.009	0.74
Feb-Mar17				

The variability in phycocyanin fluorescence intensity between the control culture of C-morphotype of *Arthrospira* and incubated culture of the same morphotype that incubated with water sample from Lake Bogoria over the period of (May15- Mar17). The pigment fluorescence was measured day after day for 13 days. The significant level (α) was adjusted to 0.007.

Table 8.13: Non-significant results of Mann-Whitney U test for phycocyanin fluorescence intensity assay (S- morphotype).

Time point	Incubation day	Test statistic	Sig. (p)	Effect size (r)
May-Jun 15	1	29	0.093	0.51
May-Jun 15	9	28	0.132	0.46
May-Jun 15	11	33	0.015	0.69
May-Jun 15	13	36	0.002	0.83
Jul-Aug 15	1	24	0.394	0.28
Jul-Aug 15	9	22	0.589	0.19
Jul-Aug 15	11	18	1.00	0
Sep-Oct15	1	33	0.015	0.69
Sep-Oct15	9	32	0.026	0.65
Sep-Oct15	11	33	.012	0.69
Nov-Dec15	5	30	0.065	0.56
Nov-Dec15	7	33	0.015	0.69
Nov-Dec15	9	20	0.181	0.09
Nov-Dec15	11	7	0.093	-0.51
Nov-Dec15	13	30	0.065	0.56
Jan-Feb16	1	18	1.00	0
Jan-Feb16	3	29	0.093	0.51
Jan-Feb16	7	33	0.015	0.69
Jan-Feb16	9	12	0.394	-0.28
Jan-Feb16	11	5	0.041	-0.60
Jan-Feb16	13	34	0.009	0.74
Mar-Apr16	1	21	0.699	0.18
Mar-Apr16	3	24	0.394	0.28
Mar-Apr16	7	30	0.065	0.56
Mar-Apr16	9	18	1.00	0
Mar-Apr16	11	17	0.937	-0.046
Mar-Apr16	13	34	0.009	0.74
May-Jun16	1	27	0.180	0.42
May-Jun16	9	30	0.065	0.56
May-Jun16	11	32	0.026	0.56
Jul-Aug16	1	18	1.00	0
Jul-Aug16	7	33	0.015	0.69
Jul-Aug16	9	25	0.310	0.32
Jul-Aug16	11	28	0.132	0.46
Sep-Oct16	1	21	0.699	0.18
Sep-Oct16	7	29	0.093	0.51
Sep-Oct16	9	20	0.818	0.09
Sep-Oct16	11	15	0.699	-0.14
Dec16-Jan17	1	18	1.00	0
Dec16-Jan17	7	32	0.026	0.65
Dec16-Jan17	9	31	0.041	0.60
Dec16-Jan17	11	30	0.065	0.56
Feb-Mar17	1	18	1.00	0
Feb-Mar17	9	19	1.00	0.05
Feb-Mar17	11	20	0.818	0.09

The variability in phycocyanin fluorescence intensity between the control culture of S-morphotype of *Arthrospira* and incubated culture of the same morphotype that incubated with water sample from Lake Bogoria over the period of (May15- Mar17). The pigment fluorescence was measured day after day for 13 days. The significant level (α) was adjusted to 0.007.

Table 8.14: Bacteria composition and abundance in Sep 2014 water sample, which constitute 100% of the total.

Kingdom	Phylum	Class	Order	Family	Genus	Species	Strain	%
Bacteria	Proteobacteria	Gammaproteobacteria	Enterobacteriales	Enterobacteriaceae	<i>Serratia</i>	<i>Serratia marcescens</i>	<i>Serratia_marcescens</i> unclassified	89.39
Bacteria	Actinobacteria	Actinobacteria	Actinomycetales	Mycobacteriaceae	<i>Mycobacterium</i>	<i>M.tuberculosis bovis africanum canetti</i>	<i>M.tuberculosis bovis africanum canetti</i> unclassified	10.61

Table 8.15: Bacteria composition and abundance in May 2015 water sample, which constitute 93.28% of the total.

Kingdom	Phylum	Class	Order	Family	Genus	Species	Strain	%
Bacteria	Proteobacteria	Gammaproteobacteria	Enterobacteriales	Enterobacteriaceae	<i>Escherichia</i>	<i>E.coli</i>	<i>Escherichia coli</i> unclassified	4.131
Bacteria	Proteobacteria	Gammaproteobacteria	Oceanospirillales	Halomonadaceae	<i>Halomonas</i>	<i>H.stevensii</i>	GCF 000275 725	73.39
Bacteria	Cyanobacteria	Cyanobacteria nomane	Oscillatoriales	Pharmidiaceae	<i>Arthrospira</i>	<i>Arthrospira</i> unclassified	/	1.769
Bacteria	Actinobacteria	Actinobacteria	Actinomycetales	Dietziaceae	<i>Dietzia</i>	<i>Dietzia</i> unclassified	/	3.61
Bacteria	Actinobacteria	Actinobacteria	Actinomycetales	Brevibacteriaceae	<i>Brevibacterium</i>	<i>Brevibacterium</i> unclassified	/	4.48
Bacteria	Proteobacteria	Gammaproteobacteria	Pseudomonadales	Pseudomonadaceae	<i>Pseudomonas</i>	<i>Pseudomonas</i> unclassified	/	5.91

Table 8.16: Viruses composition and abundance in May 2015 water sample, which constitute 6.72 % of the total.

Order	Family	Genus	Species	Strain	%
Viruses noname	Endornaviridae	Endornavirus	Phytophthora endornavirus 1	PRJNA15418	0.89
Viruses noname	Anelloviridae	Alphatorquevirus	Torque teno virus 12	PRJNA48149	4.61
Viruses noname	Flaviviridae	Flavivirus	Royal Farm virus	/	1.21

Table 8.17: Bacteria composition and abundance in Jul 2015 water sample, which constitute 100% of the total.

Kingdom	Phylum	Class	Order	Family	Genus	Species	Strain	%
Bacteria	Proteobacteria	Alphaproteobacteria	Rhizobiales	Rhizobiaceae	<i>Agrobacterium</i>	<i>A.tumefaciens</i>	<i>A.tumefaciens</i> unclassified	0.09
Bacteria	Proteobacteria	Alphaproteobacteria	Rhizobiales	Rhizobiaceae	<i>Rhizobium</i>	<i>R. lupini</i>	GCF 000304595	0.09
Bacteria	Proteobacteria	Betaproteobacteria	Burkholderiales	Alcaligenaceae	<i>Achromobacter</i>	<i>A.piechaudii</i>	<i>A.piechaudii</i> unclassified	0.21
Bacteria	Proteobacteria	Gammaproteobacteria	Thiotrichales	Piscirickettsiaceae	<i>Methylophaga</i>	<i>M.lonarensis</i>	GCF 000349205	0.31
Bacteria	Proteobacteria	Gammaproteobacteria	Xanthomonadales	Xanthomonadaceae	<i>Stenotrophomonas</i>	<i>S.maltophilia</i>	<i>S.maltophilia</i> unclassified	1.67
Bacteria	Proteobacteria	Gammaproteobacteria	Oceanospirillales	Halomonadaceae	<i>Halomonas</i>	<i>H.stevensii</i>	GCF 000275725	41.95
Bacteria	Proteobacteria	Gammaproteobacteria	Oceanospirillales	Halomonadaceae	<i>Halomonas</i>	<i>Halomonas</i> sp. GFAJ 1	GCF 000236625	52.83
Bacteria	Proteobacteria	Betaproteobacteria	Burkholderiales	Comamonadaceae	<i>Comamonas</i>	<i>Comamonas</i> unclassified	/	0.16
Bacteria	Proteobacteria	Betaproteobacteria	Burkholderiales	Alcaligenaceae	<i>Bordetella</i>	<i>Bordetella</i> unclassified	/	0.21
Bacteria	Cyanobacteria	Cyanobacteria noname	Chroococcales	Chroococcales noname	<i>Cyanobium</i>	<i>Cyanobium</i> unclassified	/	0.29
Bacteria	Proteobacteria	Alphaproteobacteria	Rhodospirillales	Rhodospirillaceae	<i>Rhodospirillum</i>	<i>Rhodospirillum</i> unclassified	/	0.47

Continued on next page.

Chapter 8. Appendices

Table 8.17: continued from previous page.

Kingdom	Phylum	Class	Order	Family	Genus	Species	Strain	%
Bacteria	Proteobacteria	Alphaproteobacteria	Rhizobiales	Rhizobiaceae	<i>Agrobacterium</i>	<i>Agrobacterium</i> unclassified	/	0.69
Bacteria	Proteobacteria	Betaproteobacteria	Burkholderiales	Comamonadaceae	<i>Alicyclophilus</i>	<i>Alicyclophilus</i> unclassified	/	0.84

Table 8.18: Bacteria composition and abundance in Sep 2015 water sample, which constitute 77.53 % of the total.

Kingdom	Phylum	Class	Order	Family	Genus	Species	Strain	%
Bacteria	Proteobacteria	Gammaproteobacteria	Vibrionales	Vibrionaceae	<i>Vibrio</i>	<i>V.metschnikovii</i>	GCF 000176155	0.24
Bacteria	Proteobacteria	Gammaproteobacteria	Thiotrichales	Piscirickettsiaceae	<i>Methylophaga</i>	<i>M.lonarensis</i>	GCF 000349205	1.42
Bacteria	Proteobacteria	Gammaproteobacteria	Oceanospirillales	Halomonadaceae	<i>Halomonas</i>	<i>H.stevensii</i>	GCF 000275725	12.23
Bacteria	Proteobacteria	Gammaproteobacteria	Oceanospirillales	Halomonadaceae	<i>Halomonas</i>	<i>Halomonas</i> sp. GFAJ 1	GCF 000236625	57.29
Bacteria	Proteobacteria	Alphaproteobacteria	Sphingomonadales	Sphingomonadaceae	<i>Sphingopyxis</i>	<i>Sphingopyxis</i> unclassified	/	1.23
Bacteria	Proteobacteria	Gammaproteobacteria	Enterobacteriales	Enterobacteriaceae	<i>Escherichia</i>	<i>Escherichia</i> unclassified	/	1.23
Bacteria	Proteobacteria	Betaproteobacteria	Burkholderiales	Alcaligenaceae	<i>Pusillimonas</i>	<i>Pusillimonas</i> unclassified	/	1.47
Bacteria	Actinobacteri	Actinobacteria	Actinomycetales	Dietziaceae	<i>Dietzia</i>	<i>Dietzia</i> unclassified	/	2.49

Table 8.19: Viruses composition and abundance in Sep 2015 water sample, which constitute 22.47% of the total.

Order	Family	Genus	Species	Strain	%
Viruses noname	Adenoviridae	Mastadenovirus	Human adenovirus D	Human_adenovirus D unclassified	0.39
Viruses noname	Narnaviridae	Narnavirus	Saccharomyces 23S RNA narnavirus	PRJNA14840	3.28
Viruses_noname	Circoviridae	Circoviridae noname	Cyclovirus NGchicken15 NGA 2009	PRJNA61953	5.26
Viruses_noname	Viruses noname	Viruses noname	Chilli leaf curl Multan alphasatellite	PRJNA39933	6.76
Viruses noname	Viruses noname	Viruses noname	Eupatorium yellow vein betasatellite	PRJNA14447	6.83

■ Hits against Virus and Prophage Database ■ Hits against Bacterial Database or GenBank File			
Region 1, unitig_1 quiver, total 11 CDS			
#	CDS Position	BLAST Hit	E-Value
1	complement(516250..517737)	PHAGE_Mycoba_Dori_NC_023703: gp42; PP_02803; phage(gi593775732)	8.59e-95
2	517961..518212	PHAGE_Plankt_PaV_LD_NC_016564: hypothetical protein; PP_02804; phage(gi371496245)	1.49e-10
3	518267..519322	hypothetical; PP_02805	0.0
4	complement(519359..519652)	hypothetical; PP_02806	0.0
5	complement(519666..520775)	PHAGE_Citrob_Margaery_NC_028755: baseplate wedge initiator; PP_02807; phage(gi100178)	1.62e-09
6	complement(521503..521928)	hypothetical; PP_02808	0.0
7	complement(521937..522323)	PHAGE_Phormi_MIS_PhV1B_NC_028998: hypothetical protein; PP_02809; phage(gi100004)	7.64e-09
8	complement(522369..522578)	PHAGE_Prochl_P_SSM2_NC_006883: hypothetical protein; PP_02810; phage(gi61806050)	1.86e-07
9	522959..523630	PHAGE_Acinet_LZ35_NC_031117: hypothetical protein; PP_02811; phage(gi100034)	1.48e-10
10	523743..525410	PHAGE_Salmon_SJ46_NC_031129: hypothetical protein; PP_02812; phage(gi100044)	1.96e-16
11	525524..526135	PHAGE_Staphy_SPbeta_like_NC_029119: tRNA (cmo5U34)-methyltransferase; PP_02813; phage(gi985761180)	2.13e-05

Figure 8.11: Details of incomplete prophage region, which is integrated within the H-morphotype of *Arthrospira* genome from Lake Bogoria.

Chapter 8. Appendices

■ Hits against Virus and Prophage Database ■ Hits against Bacterial Database or GenBank File			
Region 1, unitig_0 quiver, total 12 CDS			
#	CDS Position	BLAST Hit	E-Value
1	801004..801015	attL	0.0
2	801064..801651	PHAGE_Gordon_Twister6_NC_031052: hypothetical protein; PP_03188; phage(gi100049)	1.63e-06
3	complement(801927..802286)	hypothetical; PP_03189	0.0
4	802805..804643	PHAGE_Bacill_SP_15_NC_031245: hypothetical protein; PP_03190; phage(gi100150)	2.53e-15
5	804802..806766	PHAGE_Salmon_SJ46_NC_031129: hypothetical protein; PP_03191; phage(gi100063)	3.36e-05
6	806860..807048	hypothetical; PP_03192	0.0
7	807067..807873	PHAGE_Mycoba_Bactobuster_NC_031279: prohead core protein protease; PP_03193; phage(gi100061)	5.90e-07
8	807925..808782	PHAGE_Natria_PhiCh1_NC_004084: putative plasmid partitioning protein Soj; PP_03194; phage(gi22091150)	1.92e-17
9	808786..809544	PHAGE_Anabae_A_4L_NC_024358: tail protein; PP_03195; phage(gi658310555)	1.56e-05
10	809555..810496	hypothetical; PP_03196	0.0
11	complement(810641..811714)	PHAGE_Citrob_Margaery_NC_028755: baseplate wedge initiator; PP_03197; phage(gi100178)	1.45e-07
12	814810..814821	attR	0.0

Figure 8.12: Details of the first incomplete prophage region that is integrated within the S-morphotype of *Arthrospira* genome from Lake Bogoria.

Region 2, unitig_7 quiver, total 12 CDS			
#	CDS Position	BLAST Hit	E-Value
1	complement(225615..227102)	PHAGE_Mycoba_Dori_NC_023703: gp42; PP_05566; phage(gi593775732)	9.76e-95
2	227326..227577	PHAGE_Plankt_PaV_LD_NC_016564: hypothetical protein; PP_05567; phage(gi371496245)	1.49e-10
3	227632..228687	hypothetical; PP_05568	0.0
4	complement(228724..229017)	hypothetical; PP_05569	0.0
5	complement(229031..230140)	PHAGE_Citrob_Margaery_NC_028755: baseplate wedge initiator; PP_05570; phage(gi100178)	1.60e-09
6	complement(230497..230922)	hypothetical; PP_05571	0.0
7	complement(230931..231317)	PHAGE_Phormi_MIS_PhV1B_NC_028998: hypothetical protein; PP_05572; phage(gi100004)	5.53e-09
8	complement(231363..231572)	PHAGE_Prochl_P_SSM2_NC_006883: hypothetical protein; PP_05573; phage(gi61806050)	1.86e-07
9	231737..231820	hypothetical; PP_05574	0.0
10	231953..232624	PHAGE_Acinet_LZ35_NC_031117: hypothetical protein; PP_05575; phage(gi100034)	1.48e-10
11	232737..234404	PHAGE_Salmon_SJ46_NC_031129: hypothetical protein; PP_05576; phage(gi100044)	1.87e-16
12	234518..235129	PHAGE_Staphy_SPbeta_like_NC_029119: tRNA (cmo5U34)-methyltransferase; PP_05577; phage(gi985761180)	2.13e-05

Figure 8.13: Details of the second incomplete prophage region that is integrated within the S-morphotype of *Arthrospira* genome from Lake Bogoria.

Bibliography

- Abbate, E., Bruni, P., Sagri, M., 2015. Geology of Ethiopia: a review and geomorphological perspectives. In Billi, P. (ed.) *Landscapes and Landforms of Ethiopia*. Springer, Dordrecht.2, 33-64.
- Abedon, S., 2009. Disambiguating bacteriophage pseudolysogeny: an historical analysis of lysogeny, pseudolysogeny, and the phage carrier state. In Adams, H. (ed.) *Contemporary trends in bacteriophage research*. Nova Science Publishers: New York, NY, USA.11, 285-307.
- Ackermann, H.-W., 2006. Classification of bacteriophages. In Calendar, R. (ed.) *The bacteriophages*. Oxford University Press: New York, NY.2, 8-16.
- Ackermann, H., 1987. Bacteriophage taxonomy in 1987. *Microbiological sciences*, **4**, 214-218.
- Ackermann, H. W., 2007. 5500 Phages examined in the electron microscope. *Archives of Virology, Springer*, **152**, 227-243.
- Anon, R., 1992. *Standard Methods of Water and Wastewater Examination*. 18. American Public Health Association: 18th edn. Washintong DC, USA.,
- Arber, W. and Linn, S., 1969. DNA modification and restriction. *Annual review of biochemistry*, **38**, 467-500.
- Arengo, F. and Baldassarre, G. A., 1999. Resource variability and conservation of American Flamingos in coastal wetlands of Yucatan, Mexico. *The Journal of wildlife management*, **63**, 1201-1212.
- Arndt, D., Grant, J. R., Marcu, A., Sajed, T., Pon, A., Liang, Y., Wishart, D. S., 2016. PHASTER: a better, faster version of the PHAST phage search tool. *Nucleic Acids Research*, **44**, 16-21.

- Arumugam, P. and Saranya, R., 2018. Outlier Detection and Missing Value in Seasonal ARIMA Model Using Rainfall Data. *Materials Today: Proceedings*, **5**, 1791-1799.
- Aziz, R. K., Bartels, D., Best, A. A., DeJongh, M., Disz, T., Edwards, R. A., Formsma, K., Gerdes, S., Glass, E. M., Kubal, M., 2008. The RAST Server: rapid annotations using subsystems technology. *BioMed Central (BMC) genomics*, **9**, 75.
- Ballot, A., Dadheech, P. K., Krienitz, L., 2004a. Phylogenetic relationship of *Arthrospira*, *Phormidium*, and *Spirulina* strains. *Algological studies*, **113**, 37-56.
- Ballot, A., Krienitz, L., Kotut, K., Wiegand, C., Metcalf, J. S., Codd, G. A., Pflugmacher, S., 2004b. Cyanobacteria and cyanobacterial toxins in three alkaline Rift Valley lakes of Kenya—Lakes Bogoria, Nakuru and Elmenteita. *Journal of Plankton Research*, **26**, 925-935.
- Ballot, A., Krienitz, L., Kotut, K., Wiegand, C., Pflugmacher, S., 2005. Cyanobacteria and cyanobacterial toxins in the alkaline crater lakes Sonachi and Simbi, Kenya. *Harmful Algae*, **4**, 139-150.
- Barrangou, R., Fremaux, C., Deveau, H., Richards, M., Boyaval, P., Moineau, S., Romero, D. A., Horvath, P., 2007. CRISPR provides acquired resistance against viruses in prokaryotes. *Science*, **315**, 1709-1712.
- Baurain, D., Renquin, L., Grubisic, S., Scheldeman, P., Belay, A., Wilmotte, A., 2002. remarkable conservation of internally transcribed spacer sequences of *Arthrospira* ("*spirulina*") (cyanophyceae, cyanobacteria) strains from four continents and of recent and 30-year-old dried samples from africa¹. *Journal of Phycology*, **38**, 384-393.

- Belay, A., Ota, Y., Miyakawa, K., Shimamatsu, H., 1993. Current knowledge on potential health benefits of *Spirulina*. *Journal of Applied Phycology*, **5**, 235-241.
- Belkin, S. and Boussiba, S., 1991. Resistance of *Spirulina platensis* to ammonia at high pH values. *Plant and cell physiology*, **32**, 953-958.
- Bergner, A., Strecker, M., Trauth, M., Deino, A., Gasse, F., Blisniuk, P., Duhnforth, M., 2009. Tectonic and climatic control on evolution of rift lakes in the Central Kenya Rift, East Africa. *Quaternary Science Reviews*, **28**, 2804-2816.
- Blumwald, E., Mehlhorn, R. J., Packer, L., 1984. Salt adaptation mechanisms in the cyanobacterium *Synechococcus* 6311. In Sybesma, C. (ed.) *Advances in Photosynthesis Research*, Springer, Dordrecht. 627-630.
- Bocci, F., Ferrari, F., Materassi, R., Mannelli, D., 1980. Prime ricerche sulla crescita di *Spirulina platensis* e *Spirulina maxima* in coltura fotolimitata. *Atti XIX Congr Naz Soc Ital Microbiol, Catania (Italy) July*, 5-8.
- Booker, M. and Walsby, A., 1979. The relative form resistance of straight and helical blue-green algal filaments. *British phycological journal*, **14**, 141-150.
- Boyer, S. L., Flechtner, V. R., Johansen, J. R., 2001. Is the 16S–23S rRNA internal transcribed spacer region a good tool for use in molecular systematics and population genetics? A case study in cyanobacteria. *Molecular Biology and Evolution*, **18**, 1057-1069.
- Bratbak, G., Bergh, Ø., Heldal, M., Børsheim, K. Y., 1989. High abundance of viruses found in aquatic environments. *Nature*, **340**, 467-468.
- Brettin, T., Davis, J. J., Disz, T., Edwards, R. A., Gerdes, S., Olsen, G. J., Olson, R., Overbeek, R., Parrello, B., Pusch, G. D., Shukla, M.,

- Thomason Iii, J. A., Stevens, R., Vonstein, V., Wattam, A. R., Xia, F., 2015. RASTtk: A modular and extensible implementation of the RAST algorithm for building custom annotation pipelines and annotating batches of genomes. *Scientific Reports*, **5**, 8365.
- Brezonik, P., Menken, K. D., Bauer, M., 2005. Landsat-based remote sensing of lake water quality characteristics, including chlorophyll and colored dissolved organic matter (CDOM). *Lake and Reservoir Management*, **21**, 373-382.
- Britton, J. R. and Harper, D. M., 2006. Length–weight relationships of fish species in the freshwater rift valley lakes of Kenya. *Journal of Applied Ichthyology*, **22**, 334-336.
- Brussaard, C., Riegman, R., Noordeloos, A., Cadée, G., Witte, H., Kop, A., Nieuwland, G., Van Duyl, F., Bak, R., 1995. Effects of grazing, sedimentation and phytoplankton cell lysis on the structure of a coastal pelagic food web. *Marine ecology progress series*, **123**, 259-271.
- Buck, R., Rondinini, S., Covington, A., Baucke, F., Brett, C. M., Camoes, M., Milton, M., Mussini, T., Naumann, R., Pratt, K., 2002. Measurement of pH. Definition, standards, and procedures (IUPAC Recommendations 2002). *Pure and applied chemistry*, **74**, 2169-2200.
- Burgis, M. and Morris, P., 1987. *The natural history of lakes*. Cambridge University Press, Cambridge, 218.
- Burian, A., Kainz, M., Schagerl, M., Yasindi, A., 2014. The role of rotifers in the food web of the saline-alkaline, hypereutrophic Kenyan Rift Valley Lake Nakuru: a snapshot-analysis of micro-and mesoplankton communities. *Freshwater Biology*, **59**, 1257-1265.

- Burian, A., Schagerl, M., Yasindi, A., 2013. Microzooplankton feeding behaviour: grazing on the microbial and the classical food web of African soda lakes. *Hydrobiologia*, **710**, 61-72.
- Busson, F., 1970. *Spirulina platensis* (Gom.) Geitler et *spirulina geitleri* J. de Toni; cyanophycees alimentaires. Service de Santé, Marseille, France. 138-139.
- Carver, T., Harris, S. R., Berriman, M., Parkhill, J., McQuillan, J. A., 2012. Artemis: an integrated platform for visualization and analysis of high-throughput sequence-based experimental data. *Bioinformatics*, **28**, 464-469.
- Casjens, S., 2003. Prophages and bacterial genomics: what have we learned so far? *Molecular microbiology*, **49**, 277-300.
- Castenholz, R. W., 1982. Motility and Taxes. In Carr, N. G. & Whitton, B. A. (eds.) *The biology of cyanobacteria*. Blackwell Scientific, Oxford.16, 420-439.
- Cebrian, J., 1999. Patterns in the fate of production in plant communities. *The American Naturalist*, **154**, 449-468.
- Cheevadhanarak, S., Paithoonrangarid, K., Prommeenate, P., Kaewngam, W., Musigkain, A., Tragoonrung, S., Tabata, S., Kaneko, T., Chaijaruwanich, J., Sangsrakru, D., Tangphatsornruang, S., Chanprasert, J., Tongsim, S., Kusonmano, K., Jeamton, W., Dulsawat, S., Klanchui, A., Vorapreeda, T., Chumchua, V., Khannapho, C., Thammarongtham, C., Plengvidhya, V., Subudhi, S., Hongsthong, A., Ruengjitchatchawalya, M., Meechai, A., Senachak, J., Tanticharoen, M., 2012. Draft genome sequence of *Arthrospira platensis* C1 (PCC9438). *Stand Genomic Sci*, **6**, 43-53.

- Chen, I. and Dubnau, D., 2004. DNA uptake during bacterial transformation. *Nature Reviews Microbiology*, **2**, 241.
- Childress, B., Hughes, B., Harper, D., Van Den Bossche, W., 2007a. East African flyway and key site network of the Lesser Flamingo (*Phoenicopterus minor*) documented through satellite tracking. *Ostrich*, **78**, 463-468.
- Childress, B., Hughes, B., Harper, D., van den Bossche, W., Berthold, P., Querner, U. 2006. Satellite tracking documents the East African flyway and key site network of the Lesser Flamingo *Phoenicopterus minor*. *Waterbirds around the world: a global overview of the conservation, management and research of the world's waterbird flyways. International conference on waterbirds*. The Stationery Office, Edinburgh, UK, 234-238.
- Childress, B., Nagy, S., Hughes, B. 2007b. *International Single Species Action Plan for the Conservation of the Lesser Flamingo (Phoenicopterus minor)*. CMS Technical Series No. 18, AEWA Technical Series No. 34, p. 59.: Bonn, Germany.
- Ciferri, O., 1981. Let them eat algae. *New Scientist*, **91**, 810-812.
- Ciferri, O., 1983. *Spirulina*, the edible microorganism. *Microbiology and Molecular Biology Reviews*, **47**, 551-578.
- Clark, J. R. and March, J. B., 2006. Bacteriophages and biotechnology: vaccines, gene therapy and antibacterials. *Trends in Biotechnology*, **24**, 212-218.
- Clarke, M. C., 1990. *Geological, Volcanological and Hydrogeological Controls on the Occurrence of Geothermal Activity in the Area Surrounding Lake Naivasha, Kenya: With Coloured 1: 250 000 Geological Maps*. Ministry of Energy, Nairobi, 138.

- Cloern, J. E., 1996. Phytoplankton bloom dynamics in coastal ecosystems: a review with some general lessons from sustained investigation of San Francisco Bay, California. *Reviews of Geophysics*, **34**, 127-168.
- Clough, S. 2015. *A study of the spatial diversity of Arthrospira, and the viruses that infect it, in Lake Bogoria, Kenya*. Ph. D. Bsc Dissertation, Department of Biological Science, University of Leicester, UK.
- Codd, G. A., Metcalf, J. S., Morrison, L. F., Krienitz, L., Ballot, A., Pflugmacher, S., Wiegand, C., Kotut, K., 2003. Susceptibility of flamingos to cyanobacterial toxins via feeding. *Veterinary Record* **152**, 722-723.
- Cohen, Y., Jørgensen, B. B., Revsbech, N. P., Poplawski, R., 1986. Adaptation to hydrogen sulfide of oxygenic and anoxygenic photosynthesis among cyanobacteria. *Appl Environ Microbiol*, **51**, 398-407.
- Cooper, J., Karstad, L., BOUGHTCN, E., 1975. Tuberculosis in lesser flamingoes in Kenya. *Journal of Wildlife Diseases*, **11**, 32-36.
- Cooper, J. E., Deacon, A. E., Nyariki, T., 2014. Post-mortem examination and sampling of African flamingos (*Phoenicopteridae*) under field conditions. *Ostrich*, **85**, 75-83.
- Cornejo, J. and Beale, S. I., 1997. Phycobilin biosynthetic reactions in extracts of cyanobacteria. *Photosynthesis research*, **51**, 223-230.
- Curtis, P. and Adams, H., 1995. Dissolved organic matter quantity and quality from freshwater and saltwater lakes in east-central Alberta. *Biogeochemistry*, **30**, 59-76.
- Cyr, H. and Face, M. L., 1993. Magnitude and patterns of herbivory in aquatic and terrestrial ecosystems. *Nature*, **361**, 148.

- Dadheech, P. K., Ballot, A., Casper, P., Kotut, K., Novelo, E., Lemma, B., Pröschold, T., Krienitz, L., 2010. Phylogenetic relationship and divergence among planktonic strains of *Arthrospira* (Oscillatoriales, Cyanobacteria) of African, Asian and American origin deduced by 16S–23S ITS and phycocyanin operon sequences. *Phycologia*, **49**, 361-372.
- Dadheech, P. K., Krienitz, L., Kotut, K., Ballot, A., Casper, P., 2009. Molecular detection of uncultured cyanobacteria and aminotransferase domains for cyanotoxin production in sediments of different Kenyan lakes. *Federation of European Microbiological Societies (FEMS) Microbiology Ecology*, **68**, 340-350.
- Danesi, E. D. G., Rangel-Yagui, C. O., Sato, S., Carvalho, J. C. M. d., 2011. Growth and content of *Spirulina platensis* biomass chlorophyll cultivated at different values of light intensity and temperature using different nitrogen sources. *Brazilian Journal of Microbiology*, **42**, 362-373.
- Darling, A. E., Treangen, T. J., Messeguer, X., Perna, N. T., 2007. Analyzing patterns of microbial evolution using the mauve genome alignment system. In Bergman, N. H. (ed.) *Comparative Genomics. Methods In Molecular Biology™*, vol 396. Humana Press, 135-152.
- Davies, T., Vincent, C., Beresford, A., 1985. July-August rainfall in West-Central Kenya. *International Journal of Climatology*, **5**, 17-33.
- Dawson, J. B., 2008. *The Gregory rift valley and Neogene-recent volcanoes of northern Tanzania*. Geological Society, London, Memoir, **33**, 3-7.
- De Cort, G., Bessems, I., Keppens, E., Mees, F., Cumming, B., Verschuren, D., 2013. Late-Holocene and recent hydroclimatic variability in the central Kenya Rift Valley: The sediment record of hypersaline lakes Bogoria, Nakuru and Elementeita. *Palaeogeography, Palaeoclimatology, Palaeoecology*, **388**, 69-80.

- Deng, L. I. and Hayes, P. K., 2008. Evidence for cyanophages active against bloom-forming freshwater cyanobacteria. *Freshwater Biology*, **53**, 1240-1252.
- Deocampo, D. M. and Renaut, R. W., 2016. Geochemistry of african soda lakes. In Schagerl, M. (ed.) *Soda Lakes of East Africa*. Springer, Switzerland.4, 77-93.
- Depraetere, O., Pierre, G., Deschoenmaeker, F., Badri, H., Foubert, I., Leys, N., Markou, G., Wattiez, R., Michaud, P., Muylaert, K., 2015. Harvesting carbohydrate-rich *Arthrospira platensis* by spontaneous settling. *Bioresource Technology*, **180**, 16-21.
- Deshnium, P., Paithoonrangsarid, K., Suphatrakul, A., Meesapyodsuk, D., Tanticharoen, M., Cheevadhanarak, S., 2000. Temperature-independent and-dependent expression of desaturase genes in filamentous cyanobacterium *Spirulina platensis* strain C1 (*Arthrospira* sp. PCC 9438). *Federation of European Microbiological Societies (FEMS) microbiology letters*, **184**, 207-213.
- Desikachary, T. and Bai, N. J., 1996. Taxonomic studies in *Spirulina* II. The identification of *Arthrospira* («*Spirulina*») strains and natural samples of different geographical origins. *Algological Studies/Archiv für Hydrobiologie*, **83**, 163-178.
- Dillon, A. and Parry, J. D., 2009. Amoebic grazing of freshwater *Synechococcus* strains rich in phycocyanin. *Federation of European Materials Societies (FEMS) microbiology ecology*, **69**, 106-112.
- Duckworth, D. H., 1976. " Who discovered bacteriophage?". *Bacteriological reviews*, **40**, 793.

- Duggan, P. S., Gottardello, P., Adams, D. G., 2007. Molecular analysis of genes in *Nostoc punctiforme* involved in pilus biogenesis and plant infection. *Journal of Bacteriology*, **189**, 4547-4551.
- Eisenberg, C., 2010. *The wolf's tooth keystone predators, trophic cascades, and biodiversity*. Washington, DC: Island Press/Island Press, 272.
- Espie, G. S., Miller, A. G., Canvin, D. T., 1988. Characterization of the Na⁺-requirement in cyanobacterial photosynthesis. *Plant physiology*, **88**, 757-763.
- Feiner, R., Argov, T., Rabinovich, L., Sigal, N., Borovok, I., Herskovits, A. A., 2015. A new perspective on lysogeny: prophages as active regulatory switches of bacteria. *Nature Reviews Microbiology*, **13**, 641-650.
- Field, C. B., Behrenfeld, M. J., Randerson, J. T., Falkowski, P., 1998. Primary production of the biosphere: integrating terrestrial and oceanic components. *Science*, **281**, 237.
- Fott, B. and Karim, A. G., 1973. *Spirulina* plankton community in a lake in Jebel Marra, Sudan. *Archiv fur Protistenkunde*, **115**, 408-418.
- Fuhrman, J. A., 1999. Marine viruses and their biogeochemical and ecological effects. *Nature*, **399**, 541-548.
- Fuhrman, J. A. and Proctor, L. M., 1990. Viral mortality of marine bacteria and cyanobacteria. *Nature*, **343**, 60-62.
- Fuhs, G., 1973. Cytochemical examination of blue-green algae. In Carr, N. G. & Whitton, B. A. (eds.) *The biology of the blue-green algae*. Blackwell: Oxford, UK. 6, 117-143.

- Fužinato, S., Fodora, A., Subakov-Simić, G., 2010. *Arthrospira fusiformis* (Voronichin) Komárek et Lund (Cyanoprokaryota)—A new species for Europe. *Algological studies*, **134**, 17-24.
- Gao, K., Li, P., Watanabe, T., Walter Helbling, E., 2008. Combined effects of ultraviolet radiation and temperature on morphology, photosynthesis, and DNA of *Arthrospira (Spirulina) platensis* (Cyanophyta). *Journal of Phycology*, **44**, 777-786.
- Garcia-Pichel, F., Belnap, J., Neuer, S., Schanz, F., 2003. Estimates of global cyanobacterial biomass and its distribution. *Algological studies*, **109**, 213-227.
- Ghai, R., Martin-Cuadrado, A.-B., Molto, A. G., Heredia, I. G., Cabrera, R., Martin, J., Verdu, M., Deschamps, P., Moreira, D., López-García, P., 2010. Metagenome of the Mediterranean deep chlorophyll maximum studied by direct and fosmid library 454 pyrosequencing. *The International Society for Microbial Ecology (ISME) journal*, **4**, 1154.
- Giesy, R. M., 1964. A light and electron microscope study of interlamellar polyglucoside bodies in *Oscillatoria chalybia*. *American Journal of Botany*, **51**, 388-396.
- Gomont, M., 1892. Monographie des Oscillariées (Nostocacées Homocystées). Deuxième partie—Lyngbyeées *Annales des Sciences Naturelles Botanique* Série 7:91–264.
- Gons, H. J., Hoogveld, H. L., Simis, S. G., Tijdens, M., 2006. Dynamic modelling of viral impact on cyanobacterial populations in shallow lakes: implications of burst size. *Journal of the Marine Biological Association of the United Kingdom*, **86**, 537-542.
- Greichus, Y. A., Greichus, A., Ammann, B. D., Hopcraft, J., 1978. Insecticides, polychlorinated biphenyls and metals in african lake ecosystems .3. Lake

- Nakuru, Kenya. *Bulletin of Environmental Contamination and Toxicology*, **19**, 454-461.
- Gumbo, R. J., Ross, G., Cloete, E. T., 2008. Biological control of *Microcystis* dominated harmful algal blooms. *African Journal of Biotechnology*, **7**, 4765–4773.
- Hagens, S. and Loessner, M. J., 2007. Bacteriophages of *Listeria*. In Goldfine, H. & Shen, H. (eds.) *Listeria monocytogenes: Pathogenesis and Host Response*. Springer, Boston, MA.13, 265-279.
- Halfen, L. N. and Castenholz, R. W., 1971. Gliding motility in the blue-green alga *Oscillatoria princeps*¹. *Journal of Phycology*, **7**, 133-145.
- Hambly, E., Tétart, F., Desplats, C., Wilson, W. H., Krisch, H. M., Mann, N. H., 2001. A conserved genetic module that encodes the major virion components in both the coliphage T4 and the marine cyanophage S-PM2. *Proceedings of the National Academy of Sciences*, **98**, 11411-11416.
- Hammer, U. T., 1986. *Saline lake ecosystems of the world* Monographiae Biologicae 59: Dr W Junk Publishers, Dordrecht, Netherlands,**59**,616.
- Hanlon, G. W., 2007. Bacteriophages: an appraisal of their role in the treatment of bacterial infections. *International Journal of Antimicrobial Agents*, **30**, 118-128.
- Haq, I. U., Chaudhry, W. N., Akhtar, M. N., Andleeb, S., Qadri, I., 2012. Bacteriophages and their implications on future biotechnology: a review. *Virology journal*, **9**, 9-9.
- Harper, D. M., Childress, R. B., Harper, M. M., Boar, R. R., Hickley, P., Mills, S. C., Otieno, N., Drane, T., Vareschi, E., Nasirwa, O., 2003. Aquatic

- biodiversity and saline lakes: Lake Bogoria National Reserve, Kenya. *Hydrobiologia*, **500**, 259-276.
- Harper, D. M., Morrison, E. H., Macharia, M. M., Mavuti, K. M., Upton, C., 2011. Lake Naivasha, Kenya: ecology, society and future. *Freshwater Reviews*, **4**, 89-114.
- Harper, D. M., Tebbs, E., Bell, O., Robinson, V. J., 2016. Conservation and Management of East Africa's Soda Lakes. In Schagerl, M. (ed.) *Soda Lakes of East Africa*. Springer, Switzerland: 14, 345-364.
- Helbling, E. W., Gao, K., Ai, H., Ma, Z., Villafane, V. E., 2006. Differential responses of *Nostoc sphaeroides* and *Arthrospira platensis* to solar ultraviolet radiation exposure. *Journal of Applied Phycology*, **18**, 57-66.
- Hickel, B., 1982. helical, bloom-forming *Anabaena*-like blue-green alga (Cyanophyta) from hypertrophic lakes. *Archiv fur hydrobiology*, **95**, 115–124.
- Hickley, P., Boar, R. R., Mavuti, K. M., 2003. Bathymetry of Lake Bogoria, Kenya. *Journal of East African Natural History*, **92**, 107-117.
- Hill, L., Bowerman, W., Roos, J., Bridges, W., Anderson, M., 2013. Effects of water quality changes on phytoplankton and lesser flamingo *Phoeniconaias minor* populations at Kamfers Dam, a saline wetland near Kimberley, South Africa. *African Journal of Aquatic Science*, **38**, 287-294.
- Hindák, F., 1985. Morphology of trichomes in *Spirulina fusiformis* Voronichin from Lake Bogoria, Kenya. *Algological Studies/Archiv für Hydrobiologie, Supplement Volumes*, **38/39**, 201-218.
- Hoiczky, E., 1998. Structural and biochemical analysis of the sheath of *Phormidium uncinatum*. *Journal of Bacteriology*, **180**, 3923-3932.

- Jacquet, S., Zhong, X., Parvathi, A., Ram, A. S. P., 2013. First description of a cyanophage infecting the cyanobacterium *Arthrospira platensis* (*Spirulina*). *Journal of Applied Phycology*, **25**, 195-203.
- Jeeji Bai, N., 1985. Competitive exclusion or morphological transformation? A case study with *Spirulina fusiformis*. *Algological Studies/Archiv für Hydrobiologie, Supplement Volumes*, **38/39**, 191-199.
- Jeeji Bai, N. and Seshadri, C., 1980. On coiling and uncoiling of trichomes in the genus *Spirulina*. *Algological Studies/Archiv für Hydrobiologie, Supplement Volumes*, **26**, 32-47.
- Jenkin, P. M., 1957. The filter-feeding and food of flamingoes (*Phoenicopteri*). *Philosophical Transactions of the Royal Society of London B: Biological Sciences*, **240**, 401-493.
- Ji Won, H., Sung-Ho, K., Ho-Sung, Y., 2010. Axenic purification and cultivation of an Arctic cyanobacterium, *Nodularia spumigena* KNUA005, with cold tolerance potential for sustainable production of algae-based biofuel. *Algae*, **25**, 99-104.
- Jiang, S. C. and Paul, J. H., 1996. Occurrence of lysogenic bacteria in marine microbial communities as determined by prophage induction. *Marine ecology progress series*, **142**, 27-38.
- Jirsa, F., Gruber, M., Stojanovic, A., Omondi, S. O., Mader, D., Körner, W., Schagerl, M., 2013. Major and trace element geochemistry of Lake Bogoria and Lake Nakuru, Kenya, during extreme draught. *Chemie der Erde - Geochemistry*, **73**, 275-282.
- John, S. G., Mendez, C. B., Deng, L., Poulos, B., Kauffman, A. K., Kern, S., Brum, J., Polz, M. F., Boyle, E. A., Sullivan, M. B., 2011. A simple and efficient method for concentration of ocean viruses by chemical flocculation. *Environmental Microbiology Reports*, **3**, 195-202.

- John, S. G., Poulos, B., Schirmer, C. 2014. *Iron chloride precipitation of viruses from seawater. Tucson Marine Phage Lab. The Sullivan Lab at the University of Arizona.* [Online]. Available from: <https://www.protocols.io/view/Iron-Chloride-Precipitation-of-Viruses-from-Seawat-c2wyfd> [cited 12/11/2017].
- Johnson, D. W. and Potts, M., 1985. Host range of LPP cyanophages. *International Journal of Systematic and Evolutionary Microbiology*, **35**, 76-78.
- Jones, B. and Grant, W., 2000. Microbial diversity and ecology of alkaline environments. In Seckbach, J. (ed.) *Journey to Diverse Microbial Worlds*. Kluwer Academic Publishers, Dordrecht.13, 177-190.
- Jungblut, A. D., Hawes, I., Mountfort, D., Hitzfeld, B., Dietrich, D. R., Burns, B. P., Neilan, B. A., 2005. Diversity within cyanobacterial mat communities in variable salinity meltwater ponds of McMurdo Ice Shelf, Antarctica. *Environ Microbiol*, **7**, 519-529.
- Kaggwa, M. N., Burian, A., Oduor, S. O., Schagerl, M., 2013a. Ecomorphological variability of *Arthrospira fusiformis* (Cyanoprokaryota) in African soda lakes. *Microbiologyopen*, **2**, 881-891.
- Kaggwa, M. N., Gruber, M., Oduor, S. O., Schagerl, M., 2013b. A detailed time series assessment of the diet of Lesser Flamingos: further explanation for their itinerant behaviour. *Hydrobiologia*, **710**, 83-93.
- Kairu, J. K., 1996. Heavy metal residues in birds of Lake Nakuru, Kenya. *African Journal of Ecology*, **34**, 397-400.
- Kalff, J., 1983. Phosphorus limitation in some tropical African lakes. *Hydrobiologia*, **100**, 101-112.

- Kaliner, G. and Cooper, J., 1973. Dual infection of an African fish eagle with acid-fast *bacilli* and an *Aspergillus* sp. *Journal of Wildlife Diseases*, **9**, 51-55.
- Kearse, M., Moir, R., Wilson, A., Stones-Havas, S., Cheung, M., Sturrock, S., Buxton, S., Cooper, A., Markowitz, S., Duran, C., 2012. Geneious Basic: an integrated and extendable desktop software platform for the organization and analysis of sequence data. *Bioinformatics*, **28**, 1647-1649.
- Kebede, E., 1997. Response of *Spirulina platensis* (*Arthrospira fusiformis*) from Lake Chitu, Ethiopia, to salinity stress from sodium salts. *Journal of Applied Phycology*, **9**, 551-558.
- Kock, N. D., Kock, R. A., Wambua, J., Kamau, G. J., Mohan, K., 1999. *Mycobacterium avium*-related epizootic in free-ranging lesser flamingos in Kenya. *Journal of Wildlife Diseases*, **35**, 297-300.
- Koeman, J., Pennings, J., De Goeij, J., Tjioe, P., Olindo, P., Hopcraft, J., 1972. A preliminary survey of the possible contamination of Lake Nakuru in Kenya with some metals and chlorinated hydrocarbon pesticides. *Journal of Applied Ecology*, **9**, 411-416.
- Komárek, J. and Anagnostidis, K., 2005. Cyanoprokaryota Part 2. Oscillatoriales. In Büdel, B., Krienitz, L., Gärtner, G. & Schagerl, M. (eds.) *Süßwasserflora von Mitteleuropa*. Elsevier Spektrum Akademischer Verlag: München, Germany, 1-759.
- Komarek, J. and Hauer, T., 2011. CyanoDB. cz-On-line database of cyanobacterial genera. *Word-wide electronic publication, Univ. of South Bohemia & Inst. of Botany, Academy of Sciences of the Czech Republic*, <http://www.cyanodb.cz>.

- Komárek, J., Kaštovský, J., Mareš, J., Johansen, J. R., 2014. Taxonomic classification of cyanoprokaryotes (cyanobacterial genera) 2014, using a polyphasic approach. *Preslia*, **86**, 295-335.
- Komárek, J. and Lund, J. W., 1990. What is «*Spirulina platensis*» in fact? *Algological Studies/Archiv für Hydrobiologie*, **58**, 1-13.
- Koren, S., Walenz, B. P., Berlin, K., Miller, J. R., Phillippy, A. M., 2017. Canu: scalable and accurate long-read assembly via adaptive k-mer weighting and repeat separation. *Genome Research*, **27**, 722-736.
- Krienitz, L., Ballot, A., Casper, P., Codd, G. A., Kotut, K., Metcalf, J. S., Morrison, L. F., Pflugmacher, S., Wiegand, C., 2005a. Contribution of toxic cyanobacteria to massive deaths of Lesser Flamingos at saline-alkaline lakes of Kenya. *Internationale Vereinigung für theoretische und angewandte Limnologie: Verhandlungen*, **29**, 783-786.
- Krienitz, L., Ballot, A., Casper, P., Kotut, K., Wiegand, C., Pflugmacher, S., 2005b. Cyanobacteria in hot springs of East Africa and their potential toxicity. *Algological studies*, **117**, 297-306.
- Krienitz, L., Ballot, A., Kotut, K., Wiegand, C., Pütz, S., Metcalf, J. S., Codd, G. A., Stephan, P., 2003. Contribution of hot spring cyanobacteria to the mysterious deaths of Lesser Flamingos at Lake Bogoria, Kenya. *Federation of European Microbiological Societies (FEMS)*, **43**, 141-148.
- Krienitz, L., Dapheech, P. K., Kotut, K., 2013. Mass developments of a small sized ecotype of *Arthrospira fusiformis* in Lake Oloidien, Kenya, a new feeding ground for Lesser Flamingos in East Africa. *Fottea*, **13**, 215-225.
- Krienitz, L. and Kotut, K., 2010. Fluctuating algal food populations and the occurrence of lesser flamingos (*phoeniconaias minor*) in three kenyan rift valley lakes¹. *Journal of Phycology*, **46**, 1088-1096.

- Krienitz, L., Krienitz, D., Dadheech, P., Hübener, T., Kotut, K., Luo, W., Teubner, K., Versfeld, W., 2016a. Food algae for Lesser Flamingos: a stocktaking. *Hydrobiologia*, **775**, 21-50.
- Krienitz, L., Mañhnert, B., Schagerl, M., 2016b. Lesser Flamingo as a Central Element of the East African Avifauna. In Schagerl, M. (ed.) *Soda Lakes of East Africa* Springer, Switzerland. 10, 259-284.
- Krienitz, L. and Schagerl, M., 2016. Tiny and Tough: Microphytes of East African Soda Lakes. In Schagerl, M. (ed.) *Soda Lakes of East Africa* Springer, Switzerland. 6, 155-159.
- Krzywinski, M. I., Schein, J. E., Birol, I., Connors, J., Gascoyne, R., Horsman, D., Jones, S. J., Marra, M. A., 2009. Circos: an information aesthetic for comparative genomics. *Genome Research*, **19**, 1639–1645.
- Kumar, S., Stecher, G., Tamura, K., 2016. MEGA7: molecular evolutionary genetics analysis version 7.0 for bigger datasets. *Molecular Biology and Evolution*, **33**, 1870-1874.
- Kutser, T., 2004. Quantitative detection of chlorophyll in cyanobacterial blooms by satellite remote sensing. *Limnology and Oceanography*, **49**, 2179-2189.
- Kutser, T., Metsamaa, L., Strömbeck, N., Vahtmäe, E., 2006. Monitoring cyanobacterial blooms by satellite remote sensing. *Estuarine, Coastal and Shelf Science*, **67**, 303-312.
- Labrie, S. J., Samson, J. E., Moineau, S., 2010. Bacteriophage resistance mechanisms. *Nature Reviews Microbiology*, **8**, 317.
- LaVigne, M. and Ashley, G. 2001. *Climatology and Rainfall Patterns: Lake Bogoria National Reserve (1976–2001)*. Rutgers University, New Brunswick, NJ, USA, unpublished report.

- Lecina, M., Sanchez, B., Solà, C., Prat, J., Roldán, M., Hernández, M., Bragós, R., Paredes, C. J., Cairó, J. J., 2017. Structural changes of *Arthrospira* sp. after low energy sonication treatment for microalgae harvesting: Elucidating key parameters to detect the rupture of gas vesicles. *Bioresource Technology*, **223**, 98-104.
- Lefort, F., Calmin, G., Crovadore, J., Falquet, J., Hurni, J.-P., Osteras, M., Haldemann, F., Farinelli, L., 2014. Whole-genome shotgun sequence of *Arthrospira platensis* strain Paraca, a cultivated and edible cyanobacterium. *Genome announcements*, **2**, 1-2.
- Levin, B. R. and Bull, J. J., 2004. Population and evolutionary dynamics of phage therapy. *Nature Reviews Microbiology*, **2**, 166-173.
- Li, R. H., Debella, H. J., Carmichael, W. W., 2001. Isolates identifiable as *Arthrospira maxima* and *Arthrospira fusiformis* (Oscillatoriales, Cyanobacteria) appear identical on the basis of a morphological study in culture and 16S rRNA gene sequences. *Phycologia*, **40**, 367-371.
- Lu, C. and Vonshak, A., 2002. Effects of salinity stress on photosystem II function in cyanobacterial *Spirulina platensis* cells. *Physiologia plantarum*, **114**, 405-413.
- Ludwig, W. and Schleifer, K., 1994. Bacterial phylogeny based on 16S and 23S rRNA sequence analysis. *Federation of European Microbiological Societies (FEMS) reviews*, **15**, 155-173.
- Lugomela, C., Pratap, H. B., Mgaya, Y. D., 2006. Cyanobacteria blooms—A possible cause of mass mortality of Lesser Flamingos in Lake Manyara and Lake Big Momela, Tanzania. *Harmful Algae*, **5**, 534-541.
- Lv, J., Wu, H., Chen, M., 2011. Effects of nitrogen and phosphorus on phytoplankton composition and biomass in 15 subtropical, urban shallow

- lakes in Wuhan, China. *Limnologica-Ecology and Management of Inland Waters*, **41**, 48-56.
- Lyra, C., Halme, T., Torsti, A. M., Tenkanen, T., Sivonen, K., 2000. Site-specific restriction endonucleases in cyanobacteria. *Journal of applied microbiology*, **89**, 979-991.
- MacIntyre, S. and Melack, J. M., 1982. Meromixis in an equatorial African soda lake. *Limnology and Oceanography*, **27**, 595-609.
- Manage, P. M., Kawabata, Z. i., Nakano, S.-i., 2001. Dynamics of cyanophage-like particles and algicidal bacteria causing *Microcystis aeruginosa* mortality. *Limnology*, **2**, 73-78.
- Manen, J.-F. and Falquet, J., 2002. The *cpcB-cpcA* locus as a tool for the genetic characterization of the genus *Arthrospira* (Cyanobacteria): evidence for horizontal transfer. *International Journal of Systematic and Evolutionary Microbiology*, **52**, 861-867.
- Mann, N. H., 2003. Phages of the marine cyanobacterial picophytoplankton. *Federation of European Microbiological Societies (FEMS)*, **27**, 17-34.
- Mann, N. H. and Clokie, M. R. J., 2012. Cyanophages. In Whitton, B. A. (ed.) *Ecology of Cyanobacteria II*. London: Springer.21, 535-552.
- Masuda, T., Mochimaru, M., Takaichi, S., Awai, K., Sekine, M., Horikawa, H., Yashiro, I., Omata, S., Takarada, H., Katano, Y., 2010. Genomic Structure of an Economically Important Cyanobacterium. *DNA Research*, **17**, 85-103.
- Matagi, S. V., 2004. A biodiversity assessment of the Flamingo Lakes of eastern Africa. *Biodiversity*, **5**, 13-26.

- Matthews, M. W., Bernard, S., Winter, K., 2010. Remote sensing of cyanobacteria-dominant algal blooms and water quality parameters in Zeekoevlei, a small hypertrophic lake, using MERIS. *Remote Sensing of Environment*, **114**, 2070-2087.
- Mayo, M., Gitelson, A., Yacobi, Y., Ben-Avraham, Z., 1995. Chlorophyll distribution in lake kinneret determined from Landsat Thematic Mapper data. *Remote Sensing*, **16**, 175-182.
- McCall, J., 2010. Lake Bogoria, Kenya: Hot and warm springs, geysers and Holocene stromatolites. *Earth-Science Reviews*, **103**, 71-79.
- Melack, J., 1996. Saline and freshwater lakes of the Kenyan Rift Valley. In McClanahan, T. R. & Young, T. P. (eds.) *East African Ecosystems and Their Conservation*. 7, 171-182.
- Melack, J. M. 1977. *Limnology and dynamics of phytoplankton in equatorial African lakes*. Ph. D. Duke University, USA.
- Melack, J. M., 1979. Photosynthesis and growth of *Spirulina platensis* (Cyanophyta) in an equatorial lake (Lake Simbi, Kenya). *Limnology and Oceanography*, **24**, 753-760.
- Melack, J. M., 1981. 7. Photosynthetic activity of phytoplankton in tropical African soda lakes. *Hydrobiologia*, **81**, 71-85.
- Melack, J. M., 1988. Primary producer dynamics associated with evaporative concentration in a shallow, equatorial soda lake (Lake Elmenteita, Kenya). *Hydrobiologia*, **158**, 1-14.
- Melack, J. M., 2009. Diel variability and community metabolism in African soda lakes. *Natural Resources and Environmental Issues*, **15**, 153.

- Melack, J. M. and Kilham, P., 1974. Photosynthetic rates of phytoplankton in East African alkaline, saline lakes1. *Limnology and Oceanography*, **19**, 743-755.
- Metcalf, J. S., Banack, S. A., Kotut, K., Krienitz, L., Codd, G. A., 2013. Amino acid neurotoxins in feathers of the Lesser Flamingo, *Phoeniconaias minor*. *Chemosphere*, **90**, 835-839.
- Millard, A. D., 2009. Isolation of Cyanophages from Aquatic Environments. In Clokie, M. R. J. & Kropinski, A. M. (eds.) *Bacteriophages: methods and protocols*. New York: Humana Press.4, 33-54.
- Miller, A. G., Turpin, D. H., Canvin, D. T., 1984. Na⁺ requirement for growth, photosynthesis, and pH regulation in the alkalotolerant cyanobacterium *Synechococcus leopoliensis*. *Journal of Bacteriology*, **159**, 100-106.
- Miyake, K., Abe, K., Ferri, S., Nakajima, M., Nakamura, M., Yoshida, W., Kojima, K., Ikebukuro, K., Sode, K., 2014. A green-light inducible lytic system for cyanobacterial cells. *Biotechnology for Biofuels*, **7**, 56.
- Mohanty, P., Srivatava, M., Krishna, K., 1997. The Photosynthetic Apparatus of *Spirulina*: Electron transport and Energy transfer In Vonshak, A. (ed.) *Spirulina Platensis Arthrospira : Physiology, Cell-Biology and Biotechnology*. 1 ed.: Taylor & Francis, London.2, 17-43.
- Moore, R., Richards, G., Story, A., 2008. Electrical conductivity as an indicator of water chemistry and hydrologic process. *Streamline Watershed Management Bulletin*, **11**, 25-29.
- Muhling, M. 2000. *Characterization of Arthrospira (Spirulina) strains*. Ph. D. Durham theses, Durham University.

- Mühling, M., Harris, N., Belay, A., Whitton, B. A., 2003. Reversal of helix orientation in the cyanobacterium *Arthrospira*¹. *Journal of Phycology*, **39**, 360-367.
- Mühling, M., Somerfield, P. J., Harris, N., Belay, A., Whitton, B. A., 2006. Phenotypic analysis of *Arthrospira* (*Spirulina*) strains (cyanobacteria). *Phycologia*, **45**, 148-157.
- Mungoma, S., 1990. The alkaline, saline lakes of Uganda: a review. *Hydrobiologia*, **208**, 75-80.
- Mussagy, A., Annadotter, H., Cronberg, G., Biologiska, i., Naturvetenskap, Science, Aquatic, E., Lunds, u., Department of, B., Akvatisk, E., Lund, U., 2006. An experimental study of toxin production in *Arthrospira fusiformis* (Cyanophyceae) isolated from African waters. *Toxicon*, **48**, 1027-1034.
- Muthulakshmi, M., Saranya, A., Sudha, M., Selvakumar, G., 2012. Extraction, partial purification, and antibacterial activity of phycocyanin from *Spirulina* isolated from fresh water body against various human pathogens. *Algal Biomass Utilization*, **3**, 7-11.
- Mwatha, W. E. 1991. *Microbial ecology of Kenyan soda lakes*. Ph. D. University of Leicester, UK.
- NanoSight, 2012. NanoSight NTA 2.3 Analytical Software, Operating Manual. *NanoSight Ltd., Minton Park, Amesbury, Wiltshire SP4 7RT, UK*.
- Ndetei, R. and Muhandiki, V. S., 2005. Mortalities of lesser flamingos in Kenyan Rift Valley saline lakes and the implications for sustainable management of the lakes. *Lakes & Reservoirs: Research & Management*, **10**, 51-58.
- Nelissen, B., Wilmotte, A., Neefs, J.-M., De Wachter, R., 1994. Phylogenetic relationships among filamentous helical cyanobacteria investigated on

the basis of 16S ribosomal RNA gene sequence analysis. *Systematic and Applied Microbiology*, **17**, 206-210.

Nomsawai, P., de Marsac, N. T., Thomas, J. C., Tanticharoen, M., Cheevadhanarak, S., 1999. Light regulation of phycobilisome structure and gene expression in *Spirulina platensis* C1 (*Arthrospira* sp. PCC 9438). *Plant and cell physiology*, **40**, 1194-1202.

Oaks, J., Walsh, T., Bradway, D., Davis, M., Harper, D., 2006. Septic arthritis and disseminated infections caused by *Mycobacterium avium* in Lesser Flamingos, Lake Bogoria, Kenya. *Flamingo*, **14**, 30-32.

Ochieng, E. Z., Lalah, J. O., Wandiga, S. O., 2007. Analysis of Heavy Metals in Water and Surface Sediment in Five Rift Valley Lakes in Kenya for Assessment of Recent Increase in Anthropogenic Activities. *Bulletin of Environmental Contamination and Toxicology, Springer*, **79**, 570-576.

Oduor, S. O. and Kotut, K., 2016. Soda Lakes of the East African Rift System: The Past, the Present and the Future. In Schagerl, M. (ed.) *Soda Lakes of East Africa*. Springer, Switzerland.15, 365-373.

Oduor, S. O. and Schagerl, M., 2007a. Phytoplankton primary productivity characteristics in response to photosynthetically active radiation in three Kenyan Rift Valley saline-alkaline lakes. *Journal of Plankton Research*, **29**, 1041-1050.

Oduor, S. O. and Schagerl, M., 2007b. Temporal trends of ion contents and nutrients in three Kenyan Rift Valley saline-alkaline lakes and their influence on phytoplankton biomass. *Hydrobiologia*, **584**, 59-68.

Ogato, T. and Kifle, D., 2014. Morphological variability of *Arthrospira* (*Spirulina*) *fusiformis* (Cyanophyta) in relation to environmental variables in the tropical soda lake Chitu, Ethiopia. *Hydrobiologia*, **738**, 21-33.

- Olago, D., Opere, A., Barongo, J., 2009. Holocene palaeohydrology, groundwater and climate change in the lake basins of the Central Kenya Rift. *Hydrological Sciences Journal*, **54**, 765-780.
- Olaka, L., Odada, E., Trauth, M., Olago, D., 2010. The sensitivity of East African rift lakes to climate fluctuations. *Journal of Paleolimnology*, **44**, 629-644.
- Oliver, R. L. and Ganf, G. G., 2000. Freshwater blooms. In Whitton, B. A. & Potts, M. (eds.) *The ecology of cyanobacteria*. Kluwer Academic Publishers, Dordrecht, NL: 6, 149-194.
- Ondov, B. D., Bergman, N. H., Phillippy, A. M., 2011. Interactive metagenomic visualization in a Web browser. *BioMed Central (BMC) bioinformatics*, **12**, 385.
- Oren, A., 2004. A proposal for further integration of the cyanobacteria under the Bacteriological Code. *International Journal of Systematic and Evolutionary Microbiology*, **54**, 1895-1902.
- Owino, A., Oyugi, J., Nasirwa, O., Bennun, L., 2001. Patterns of variation in waterbird numbers on four Rift Valley lakes in Kenya, 1991–1999. *Hydrobiologia*, **458**, 45-53.
- Ozaki, K., Ohta, A., Iwata, C., Horikawa, A., Tsuji, K., Ito, E., Ikai, Y., Harada, K.-i., 2008. Lysis of cyanobacteria with volatile organic compounds. *Chemosphere*, **71**, 1531-1538.
- Padisák, J., Soróczki-Pintér, É., Rezner, Z., 2003. Sinking properties of some phytoplankton shapes and the relation of form resistance to morphological diversity of plankton—an experimental study. *Hydrobiologia*, **500**, 243-257.
- Paerl, H., 2008. Nutrient and other environmental controls of harmful cyanobacterial blooms along the freshwater–marine continuum. In

- Lajtha, A., Paoletti, R. & Hudnell, H. K. (eds.) *Cyanobacterial harmful algal blooms: state of the science and research needs, vol 619*. Springer, New York, NY.10, 217-237.
- Paerl, H. W., 1996. A comparison of cyanobacterial bloom dynamics in freshwater, estuarine and marine environments. *Phycologia*, **35**, 25-35.
- Page, A. J., Cummins, C. A., Hunt, M., Wong, V. K., Reuter, S., Holden, M. T. G., Fookes, M., Falush, D., Keane, J. A., Parkhill, J., 2015. Roary: rapid large-scale prokaryote pan genome analysis. *Bioinformatics*, **31**, 3691-3693.
- Palinska, K. A. and Marquardt, J., 2008. Genotypic and phenotypic analysis of strains assigned to the widespread cyanobacterial morphospecies *Phormidium autumnale* (Oscillatoriales). *Archives of Microbiology*, **189**, 325-335.
- Patel, A., Noble, R. T., Steele, J. A., Schwalbach, M. S., Hewson, I., Fuhrman, J. A., 2007. Virus and prokaryote enumeration from planktonic aquatic environments by epifluorescence microscopy with SYBR Green I. *Nature Protocols*, **2**, 269-276.
- Peduzzi, P., Gruber, M., Gruber, M., Schagerl, M., 2014. The virus's tooth: cyanophages affect an African flamingo population in a bottom-up cascade. *International Society for Microbial Ecology (ISME)*, **8**, 1346-1351.
- Perkins, D. N., Pappin, D. J., Creasy, D. M., Cottrell, J. S., 1999. Probability-based protein identification by searching sequence databases using mass spectrometry data. *ELECTROPHORESIS: An International Journal*, **20**, 3551-3567.
- Philip-Heinemann, 1991. Atlas. Relief Map of Kenya.

- Pollard, P. C. and Young, L. M., 2010. Lake viruses lyse cyanobacteria, *Cylindrospermopsis raciborskii*, enhances filamentous-host dispersal in Australia. *Acta oecologica*, **36**, 114-119.
- Price, M. N., Dehal, P. S., Arkin, A. P., 2010. FastTree 2—approximately maximum-likelihood trees for large alignments. *Public Library of Science (PloS) one*, **5**, e9490, Available from: <http://www.microbesonline.org>.
- Proteau, P., Gerwick, W., Garcia-Pichel, F., Castenholz, R., 1993. The structure of scytonemin, an ultraviolet sunscreen pigment from the sheaths of cyanobacteria. *Experientia*, **49**, 825-829.
- Quail, M. A., Smith, M., Coupland, P., Otto, T. D., Harris, S. R., Connor, T. R., Bertoni, A., Swerdlow, H. P., Gu, Y., 2012. A tale of three next generation sequencing platforms: comparison of Ion Torrent, Pacific Biosciences and Illumina MiSeq sequencers. *BioMedCentral (BMC) Genomics*, **13**, 341.
- Redhead, K. and Wright, S., 1980. Lysis of the cyanobacterium *Anabaena flos-aquae* by antibiotic-producing fungi. *Microbiology*, **119**, 95-101.
- Renaut, R., Owen, R., Ego, J., 2008. Recent changes in geyser activity at Loburu, Lake Bogoria, Kenya rift valley. *GOSA Translation*, **10**, 4-14.
- Renaut, R. W. and Tiercelin, J.-J., 1994. Lake Bogoria, Kenya rift valley—a sedimentological overview. In Renaut, R. W. & Last, W. M. (eds.) *Sedimentology and geochemistry of modern and ancient saline lakes*. SEPM (Society for Sedimentary Geology) Special Publication. 50, 101-123.
- Rhoads, A. and Au, K. F., 2015. PacBio sequencing and its applications. *Genomics, proteomics & bioinformatics*, **13**, 278-289.

- Ridley, M., Moss, B., Percy, R., 1955. The food of flamingoes in Kenya Colony. *Journal of the East Africa Natural History Society*, **22**, 147-158.
- Roberts, R. J., Belfort, M., Bestor, T., Bhagwat, A. S., Bickle, T. A., Bitinaite, J., Blumenthal, R. M., Degtyarev, S. K., Dryden, D. T., Dybvig, K., 2003. A nomenclature for restriction enzymes, DNA methyltransferases, homing endonucleases and their genes. *Nucleic Acids Research*, **31**, 1805-1812.
- Robinson, V. J. 2015. *The ecology of East African soda lakes: implications for lesser flamingo (Phoeniconaias minor) feeding behaviours*. Ph. D. University of Leicester, UK.
- Rodda, K. M. 1996. *Temporal and spatial dynamics of Synechococcus spp. and Micromonas pusilla host-viral systems*. Ph. D. University of Texas at Austin.
- Rogerson, A. and Hauer, G., 2002. Naked amoebae (protozoa) of the Salton Sea, California. In D.A, B., J.F, E., D, S. & M, F. (eds.) *The Salton Sea*. Developments in Hydrobiology, vol 161. Springer, Dordrecht., 161-177.
- Rohwer, F., Prangishvili, D., Lindell, D., 2009. Roles of viruses in the environment. *Environ Microbiol*, **11**, 2771-2774.
- Rout, N. P., Khandual, S., Gutierrez-Mora, A., Ibarra-Montoya, J. L., Vega-Valero, G., 2015. Divergence in three newly identified *Arthrospira* species from Mexico. *World Journal of Microbiology and Biotechnology*, **31**, 1157-1165.
- Ryther, J. H. and Dunstan, W. M., 1971. Nitrogen, phosphorus, and eutrophication in the coastal marine environment 1008-1013. *Science*, **171**, 1008-1013.
- Safferman, R. S. and Morris, M.-E., 1963. Algal virus: isolation. *Science*, **140**, 679-680.

- Safferman, R. S. and Morris, M.-E., 1964. Growth characteristics of the blue-green algal virus LPP-1. *Journal of Bacteriology*, **88**, 771-775.
- Sahl, J. W., Caporaso, J. G., Rasko, D. A., Keim, P., 2014. The large-scale blast score ratio (LS-BSR) pipeline: a method to rapidly compare genetic content between bacterial genomes. *PeerJ*, **2**, e332.
- Salmaso, N. and Padisák, J., 2007. Morpho-functional groups and phytoplankton development in two deep lakes (Lake Garda, Italy and Lake Stechlin, Germany). *Hydrobiologia*, **578**, 97-112.
- Schadt, E. E., Turner, S., Kasarskis, A., 2010. A window into third-generation sequencing. *Human molecular genetics*, **19**, R227-R240.
- Schagerl, M., Burian, A., Gruber-Dorninger, M., Oduor, S. O., Kaggwa, M. N., 2015. Algal communities of Kenyan soda lakes with a special focus on *Arthrospira fusiformis*. *Fottea*, **15**, 245-257.
- Schagerl, M. and Oduor, S. O., 2008. Phytoplankton community relationship to environmental variables in three Kenyan Rift Valley saline-alkaline lakes. *Marine and Freshwater Research*, **59**, 125-136.
- Schagerl, M. and Renaut, W. R., 2016. Dipping into the Soda Lakes of East Africa. In Michael, S. (ed.) *Soda Lakes East Africa*. Springer, Switzerland.1, 3-20.
- Scheer, H., 2006. An overview of chlorophylls and bacteriochlorophylls: biochemistry, biophysics, functions and applications. In B, G., R.J, P., W, R. & H, S. (eds.) *Chlorophylls and Bacteriochlorophylls. Advances in Photosynthesis and Respiration, vol 25*. Springer, Dordrecht., 1-26.
- Scheldeman, P., Baurain, D., Bouhy, R., Scott, M., Mühling, M., Whitton, B. A., Belay, A., Wilmotte, A., 1999. *Arthrospira* ('*Spirulina*') strains from four

- continents are resolved into only two clusters, based on amplified ribosomal DNA restriction analysis of the internally transcribed spacer. *Federation of European Microbiological Societies (FEMS) microbiology letters*, **172**, 213-222.
- Schlesinger, P., Belkin, S., Boussiba, S., 1996. Sodium deprivation under alkaline conditions causes rapid death of the filamentous cyanobacterium *Spirulina platensis*¹ *Journal of Phycology*, **32**, 608-613.
- Schlüter, T., 1997. *Geology of East Africa*. Gebrüder Borntraeger: Stuttgart, Germany, **27**, 21-39.
- Schneider, I., Diener, T., Safferman, R. S., 1964. Blue-green algal virus LPP-1: purification and partial characterization. *Science*, **144**, 1127-1130.
- Schopf, J. W., 2000. The Fossil Record: Tracing the Roots of the Cyanobacterial Lineage. In Whitton, B. A. & Potts, M. (eds.) *The Ecology of Cyanobacteria*. Springer, Dordrecht, **2**, 13-35.
- Seemann, T., 2014. Prokka: rapid prokaryotic genome annotation. *Bioinformatics*, **30**, 2068-2069.
- Sena, L., Rojas, D., Montiel, E., González, H., Moret, J., Naranjo, L., 2011. A strategy to obtain axenic cultures of *Arthrospira* spp. cyanobacteria. *World Journal of Microbiology and Biotechnology*, **27**, 1045-1053.
- Shilo, M., 1967. Formation and mode of action of algal toxins. *Bacteriological reviews*, **31**, 180.
- Shiraishi, H., 2016. Cryopreservation of the edible alkalophilic cyanobacterium *Arthrospira platensis*. *Bioscience, biotechnology, and biochemistry*, **80**, 2051-2057.

- Shurin, J. B., Borer, E. T., Seabloom, E. W., Anderson, K., Blanchette, C. A., Broitman, B., Cooper, S. D., Halpern, B. S., 2002. A cross-ecosystem comparison of the strength of trophic cascades. *Ecology letters*, **5**, 785-791.
- Sileo, L., Grootenhuis, J., Tuite, C., Hopcraft, J., 1979. Mycobacteriosis in the lesser flamingos of Lake Nakuru, Kenya. *Journal of Wildlife Diseases*, **15**, 387-389.
- Sili, C., Torzillo, G., Vonshak, A., 2012. *Arthrospira (Spirulina)*. In Whitton, B. A. (ed.) *Ecology of Cyanobacteria II*. Springer, Dordrecht.25, 677-706.
- Simis, S. G., Tijdens, M., Hoogveld, H. L., Gons, H. J., 2007. Optical signatures of the filamentous cyanobacterium *Leptolyngbya boryana* during mass viral lysis. *Limnology and Oceanography*, **52**, 184-197.
- Singh, S. P., Rastogi, R. P., Häder, D.-P., Sinha, R. P., 2011. An improved method for genomic DNA extraction from cyanobacteria. *World Journal of Microbiology and Biotechnology*, **27**, 1225-1230.
- Soper, B. W. and Reddy, K., 1994. Identification of a nuclease and host restriction-modification in the unicellular, aerobic nitrogen-fixing cyanobacterium *Cyanothece* sp. *Journal of Bacteriology*, **176**, 5565-5570.
- Sorek, R., Lawrence, C. M., Wiedenheft, B., 2013. CRISPR-mediated adaptive immune systems in bacteria and archaea. *Annual review of biochemistry*, **82**, 237-266.
- Stamatakis, A., 2014. RAxML version 8: a tool for phylogenetic analysis and post-analysis of large phylogenies. *Bioinformatics*, **30**, 1312-1313.
- Statistics, S., 2012. Statistical package for the social sciences. *SPSS Statistics*. Chicago, USA.

- Stern, A., Mick, E., Tirosh, I., Sagy, O., Sorek, R., 2012. CRISPR targeting reveals a reservoir of common phages associated with the human gut microbiome. *Genome Research*, **22**, 1985-1994.
- Stewart, F. M. and Levin, B. R., 1984. The population biology of bacterial viruses: why be temperate. *Theoretical population biology*, **26**, 93-117.
- Stizenberger, E., 1852. *Spirulina* and *Arthrospira Hedwigia*, **1**, 32-34.
- Straubinger-Gansberger, N., Gruber, M., Kaggwa, M. N., Lawton, L., Oduor, S. O., Schagerl, M., 2014. Sudden flamingo deaths in Kenyan Rift Valley lakes. *Wildlife Biology*, **20**, 185-189.
- Street-Perrott, F. A. and Roberts, N., 1983. Fluctuations in closed-basin lakes as an indicator of past atmospheric circulation patterns. In A, S.-P., M, B. & R, R. (eds.) *Variations in the global water budget*. Springer, Dordrecht, 331-345.
- Stucken, K., Koch, R., Dagan, T., 2013. Cyanobacterial defense mechanisms against foreign DNA transfer and their impact on genetic engineering. *Biological Research*, **46**, 373-382.
- Suttle, C. A., 2005. Viruses in the sea. *Nature*, **437**, 356-361.
- Suttle, C. A., 2007a. Cyanophages and their role in the ecology of cyanobacteria. In Whitton, B. A. & Potts, M. (eds.) *Ecology of Cyanobacteria : Their Diversity in Time and Space*. Springer, Dordrecht. 20, 563-589.
- Suttle, C. A., 2007b. Marine viruses [mdash] major players in the global ecosystem. *Nature Reviews Microbiology*, **5**, 801-812.

- Takahashi, I., Hayano, D., Asayama, M., Masahiro, F., Watahiki, M., Shirai, M., 1996. Restriction barrier composed of an extracellular nuclease and restriction endonuclease in the unicellular cyanobacterium *Microcystis* sp. *Federation of European Microbiological Societies (FEMS) microbiology letters*, **145**, 107-111.
- Takaichi, S. and Mochimaru, M., 2007. Carotenoids and carotenogenesis in cyanobacteria: unique ketocarotenoids and carotenoid glycosides. *Cellular and molecular life sciences*, **64**, 2607.
- Talling, J. and Driver, D. 1963. Some problems in the estimation of chlorophyll-a in phytoplankton. *Proceedings of the Conference of Primary Productivity Measurement, Marine and Freshwater*. University of Hawaii, Honolulu, Atomic Energy Commission TID-7633, 142-146.,
- Talling, J. and Talling, I. B., 1965. The chemical composition of African lake waters. *International Review of Hydrobiology*, **50**, 421-463.
- Talling, J. F., Wood, R. B., Prosser, M. V., Baxter, R. M., 1973. The upper limit of photosynthetic productivity by phytoplankton: evidence from Ethiopian soda lakes. *Freshwater Biology*, **3**, 53-76.
- Taylor, R. 2014. *Influences of biotic and abiotic factors on the cyanobacteria abundance of an African soda lake, Bogoria, Kenya*. Ph. D. Bsc Dissertation, Department of Biological Science, University of Leicester, UK.
- Team, R. C. 2013. *R: A language and environment for statistical computing*. [Online]. Available from: <http://www.R-project.org/> 2018].
- Tebbs, E., Remedios, J., Harper, D., 2013. Remote sensing of chlorophyll-a as a measure of cyanobacterial biomass in Lake Bogoria, a hypertrophic, saline-alkaline, flamingo lake, using Landsat ETM+. *Remote Sensing of Environment*, **135**, 92-106.

- Tebbs, E. J. 2014. *Remote sensing for the study of ecohydrology in East African Rift lakes*. Ph. D. Department of Physics and Astronomy, University of Leicester, UK.
- The UniProt Consortium 2017. *UniProt: the universal protein knowledgebase*. [Online]. Available from: <http://dx.doi.org/10.1093/nar/gkw1099> [2018].
- Tiercelin, J.-J. and Lezzar, K.-E., 2002. A 300 million years history of rift lakes in Central and East Africa: an updated broad review. In Odada, E. O. & Olago, D. O. (eds.) *The East African great lakes: limnology, palaeolimnology and biodiversity*. Advances in Global Change Research, vol 12. Springer, Dordrecht.1, 3-60.
- Tijdens, M., Hoogveld, H. L., Kamst-van Agterveld, M. P., Simis, S. G., Baudoux, A.-C., Laanbroek, H. J., Gons, H. J., 2008a. Population dynamics and diversity of viruses, bacteria and phytoplankton in a shallow eutrophic lake. *Microb Ecol*, **56**, 29-42.
- Tijdens, M., Van de Waal, D. B., Slovackova, H., Hoogveld, H. L., Gons, H. J., 2008b. Estimates of bacterial and phytoplankton mortality caused by viral lysis and microzooplankton grazing in a shallow eutrophic lake. *Freshwater Biology*, **53**, 1126-1141.
- Tokarz-Deptuła, B., Sliwa-Dominiak, J., Adamiak, M., Deptuła, T., Nowak, M., Deptuła, W., 2011. Application of bacteriophages - Selected data. *Central European Journal of Immunology*, **36**, 87-91.
- Tomaselli, L., 1997. Morphology, Ultrastructure and Taxonomy of *Arthrospira* (*Spirulina*) *maxima* and *Arthrospira* (*Spirulina*) *platensis*. In Vonshak, A. (ed.) *Spirulina Platensis Arthrospira : Physiology, Cell-Biology And Biotechnology*. Taylor & Francis 48396-0, London.1, 1-17.

- Tomaselli, L., Giovannetti, L., Margheri, M., 1981. On the mechanism of trichome breakage in *Spirulina platensis* and *Spirulina maxima*. *Ann. Microbiol*, **31**, 27–34.
- Torzillo, G. and Vonshak, A., 1994. Effect of light and temperature on the photosynthetic activity of the cyanobacterium *Spirulina platensis*. *Biomass and Bioenergy*, **6**, 399-403.
- Trauth, M. H., Maslin, M. A., Deino, A., Strecker, M. R., 2005. Late Cenozoic moisture history of East Africa. *Science (New York, N.Y.)*, **309**, 2051.
- Truong, D. T., Franzosa, E. A., Tickle, T. L., Scholz, M., Weingart, G., Pasolli, E., Tett, A., Huttenhower, C., Segata, N., 2015. MetaPhlan2 for enhanced metagenomic taxonomic profiling. *Nature methods*, **12-10**, 902-903.
- Tucker, S. and Pollard, P., 2005. Identification of Cyanophage Ma-LBP and Infection of the Cyanobacterium *Microcystis aeruginosa* from an Australian Subtropical Lake by the Virus. *Appl Environ Microbiol*, **71**, 629-635.
- Tuite, C., 1981. Standing crop densities and distribution of *Spirulina* and benthic diatoms in East African alkaline saline lakes. *Freshwater Biology*, **11**, 345-360.
- Tuite, C. H., 1979. Population Size, Distribution and Biomass Density of the Lesser Flamingo in the Eastern Rift Valley, 1974-76. *Journal of Applied Ecology*, **16**, 765-775.
- Tuite, C. H., 2000. The distribution and density of Lesser Flamingos in East Africa in relation to food availability and productivity. *Waterbirds*, **23**, 52-63.

- Urmeneta, J., Navarrete, A., Huete, J., Guerrero, R., 2003. Isolation and characterization of cyanobacteria from microbial mats of the Ebro Delta, Spain. *Current microbiology*, **46**, 0199-0204.
- Vaara, T., Vaara, M., Niemelä, S., 1979. Two improved methods for obtaining axenic cultures of cyanobacteria. *Appl Environ Microbiol*, **38**, 1011-1014.
- Van Boekel, W., Hansen, F., Riegman, R., Bak, R., 1992. Lysis-induced decline of a Phaeocystis spring bloom and coupling with the microbial foodweb. *Marine ecology progress series*, **81**, 269-276.
- Van Eykelenburg, C., 1979. The ultrastructure of *Spirulina platensis* in relation to temperature and light intensity. *Antonie van Leeuwenhoek*, **45**, 369-390.
- Van Eykelenburg, C. and Fuchs, A., 1980. Rapid reversible macromorphological changes in *Spirulina platensis*. *Naturwissenschaften*, **67**, 200-201.
- Van Eykelenburg, C., Fuchs, A., Schmidt, G., 1980. Some theoretical considerations on the in vitro shape of the cross-walls in *Spirulina* spp. *Journal of theoretical biology*, **82**, 271-282.
- Van Hannen, E. J., Zwart, G., van Agterveld, M. P., Gons, H. J., Ebert, J., Laanbroek, H. J., 1999. Changes in bacterial and eukaryotic community structure after mass lysis of filamentous cyanobacteria associated with viruses. *Appl Environ Microbiol*, **65**, 795-801.
- van Regenmortel, M. H., Fauquet, C., Bishop, D., Carstens, E., Estes, M., Lemon, S., Maniloff, J., Mayo, M., McGeoch, D., Pringle, C., 2000. *Virus taxonomy: classification and nomenclature of viruses. Seventh report of the International Committee on Taxonomy of Viruses*. Academic Press, San Diego, USA.,

- Van Wichelen, J., Van Gremberghe, I., Vanormelingen, P., Debeer, A. E., Leporcq, B., Menzel, D., Codd, G. A., Descy, J. P., Vyverman, W., 2010. Strong effects of amoebae grazing on the biomass and genetic structure of a *Microcystis* bloom (Cyanobacteria). *Environ Microbiol*, **12**, 2797-2813.
- Vareschi, E., 1978. The Ecology of Lake Nakuru (Kenya). I. Abundance and Feeding of the Lesser Flamingo. *Oecologia*, **32**, 11-35.
- Vareschi, E., 1982. The ecology of Lake Nakuru (Kenya). III. Abiotic factors and primary production. *Springer & International Association for Ecology*, **55**, 81-101.
- Vass, I. Z., Kos, P. B., Sass, L., Nagy, C. I., Vass, I., 2013. The ability of cyanobacterial cells to restore UV-B radiation induced damage to Photosystem II is influenced by photolyase dependent DNA repair. *Photochemistry and Photobiology*, **89**, 384-390.
- Vasu, K. and Nagaraja, V., 2013. Diverse functions of restriction-modification systems in addition to cellular defense. *Microbiology and Molecular Biology Reviews*, **77**, 53-72.
- Vonshak, A. and Novoplansky, N., 2008. Acclimation to low temperature of two *Arthrospira platensis* (cyanobacteria) strains involves down-regulation of psii and improved resistance to photoinhibition¹. *Journal of Phycology*, **44**, 1071-1079.
- Vonshak, A. and Tomaselli, L., 2000. *Arthrospira (Spirulina)*: systematics and ecophysiology. In Whitton, A. & M, P. (eds.) *The ecology of cyanobacteria* The Netherlands: Springer, Dordrecht., 502-522.
- Walsh, E. 2015. *Dynamics of the zooplankton of Lake Bogoria*. Ph. D. Bsc Dissertation, Department of Biological Science, University of Leicester, UK.

- Weinbauer, M. G., 2004. Ecology of prokaryotic viruses. *European Microbiological Societies (FEMS) microbiology reviews*, **28**, 127-181.
- Whittaker, R. H. and Likens, G. E., 1973. Primary production: the biosphere and man. *Human Ecology*, **1**, 357-369.
- Wiggins, B. A. and Alexander, M., 1985. Minimum bacterial density for bacteriophage replication: implications for significance of bacteriophages in natural ecosystems. *Appl Environ Microbiol*, **49**, 19-23.
- Wilhelm, S. W., Carberry, M. J., Eldridge, M. L., Poorvin, L., Saxton, M. A., Doblin, M. A., 2006. Marine and freshwater cyanophages in a Laurentian Great Lake: evidence from infectivity assays and molecular analyses of g20 genes. *Appl Environ Microbiol*, **72**, 4957-4963.
- Wilhelm, S. W. and Poorvin, L., 2001. Quantification of Algal Viruses in Marine Samples. In Paul, J. H. (ed.) *Marine Microbiology*. Academic Press, New York, NY.4, 53-65.
- William, S., Feil, H., Copeland, A., 2012. Bacterial genomic DNA isolation using CTAB. *Sigma*, **50**, 6876.
- Williams, W., 1986. Conductivity and salinity of Australian salt lakes. *Marine and Freshwater Research*, **37**, 177-182.
- Williams, W. and Sherwood, J., 1994. Definition and measurement of salinity in salt lakes. *International Journal of Salt Lake Research*, **3**, 53-63.
- Wilson, W. H., Carr, N. G., Mann, N. H., 1996. The effect of phosphate status on the kinetics of cyanophage infection in the oceanic cyanobacterium *Synechococcus* sp. WH7803. *Journal of Phycology*, **32**, 506-516.

- Wittrock, V. and Nordstedt, C., 1884. *Algae aquae dulcia exiccata. Fasc, 14, 679:59.*
- Wolk, C. P. and Kraus, J., 1982. Two approaches to obtaining low, extracellular deoxyribonuclease activity in cultures of heterocyst-forming cyanobacteria. *Archives of Microbiology*, **131**, 302-307.
- Wu, H., Gao, K., Villafañe, V. E., Watanabe, T., Helbling, E. W., 2005. Effects of solar UV radiation on morphology and photosynthesis of filamentous cyanobacterium *Arthrospira platensis*. *Appl Environ Microbiol*, **71**, 5004-5013.
- Xu, T., Qin, S., Hu, Y., Song, Z., Ying, J., Li, P., Dong, W., Zhao, F., Yang, H., Bao, Q., 2016. Whole genomic DNA sequencing and comparative genomic analysis of *Arthrospira platensis*: high genome plasticity and genetic diversity. *DNA Research*, **23**, 325-338.
- Yin, C., Daoust, K., Young, A., Tebbs, E., Harper, D., 2017. Tackling community undernutrition at Lake Bogoria, Kenya: The potential of *Spirulina (Arthrospira fusiformis)* As a food supplement. *African Journal of Food, Agriculture, Nutrition and Development*, **17**, 11603-11615.
- Yoshihara, S. and Ikeuchi, M., 2004. Phototactic motility in the unicellular cyanobacterium *Synechocystis* sp. PCC 6803. *Photochemical & Photobiological Sciences*, **3**, 512-518.
- Zaccara, S., Crosa, G., Vanetti, I., Binelli, G., Childress, B., McCulloch, G., Harper, D. M., 2011. Lesser Flamingo *Phoeniconaias minor* as a nomadic species in African shallow alkaline lakes and pans: genetic structure and future perspectives. *The Ostrich*, **82**, 95-100.
- Zarrouk, C. 1966. *Contribution à l'étude d'une cyanophycée. Influence de divers facteurs physiques et chimiques sur la croissance et la*

Bibliography

photosynthèse de Spirulina maxima (Setchell et Gardner) Geitler. Ph. D. University of Paris, France.

Zeng, M.-T. and Vonshak, A., 1998. Adaptation of *Spirulina platensis* to salinity-stress. *Comparative Biochemistry and Physiology Part A: Molecular & Integrative Physiology*, **120**, 113-118.